Development of macrophages in the intestine

Antonio Alberto Bravo Blas

MVZ, M en C.

A thesis submitted to the College of Medicine, Veterinary and Life Sciences, University of Glasgow in fulfilment of the requirements for the degree of Doctor of Philosophy.

July 2014

Institute of Infection, Immunity and Inflammation
University of Glasgow
120 University Place Glasgow
G128TA

Acknowledgements

First I would like to thank my supervisor, Professor Allan Mowat. Thank you very much for having me in your lab for all this time, for your guidance during my project and the patience during the reading my thesis drafts over and over and over again.

I am also very thankful with the groups I collaborated with during my project: Professor Frederic Geissmann and Dr Elisa Gomez in King's College, London, many thanks for having me in London and for all the mice provided. And thanks also to Dr David Artis and Dr Lisa Osborne in the University of Pennsylvania, not only for the mice but especially for the most rewarding experience I had during my PhD.

Another massive thank you to Calum Bain. You were always in the lab/office, willing to provide advice, assistance, out-of-hours cell sorting troubleshooting and in general making science look a little bit easier. People are right when say that good things come in small packages.

Obviously I have also benefited immensely from the day-to-day routine with the rest of the Mowlings, especially Charlie Scott (and your never ending supply of cookies), Tamsin Zangerle Murray and Pamela Wright for taking some time to do the proofreading of my thesis chapters. Also big thanks to Aude Aumeunier for all the assistance during the first half of my PhD, and all the other side of the office, Vuk Cerovic (and the random evening conversations), Stephanie Houston, Lotta Utriainen and Simon Milling. Thank you very much, I learned loads from all of you!

Another huge thank you must go to the CRF people, Tony, Sandra and Joanne, who helped me so much with my breeding mice. Also I am very grateful to Diane Vaughan, from the FACS facility.

I would particularly like to signal my deep gratitude to the López Murillo family. Karla, Ivonne, Roberto, haberlos conocido fue un parteaguas en mi vida personal y profesional. Esta tesis es fruto de la confianza que depositaron en mi.

Thanks are also due to my new family in Scotland who supported me immensely: my wife Justyna and Rita, the dog. You are a couple of stars, simply the best, I love you both. Thank you for bearing with me and being by my side, especially during the thesis writing season. Also a big thank you to my family and friends in Mexico.

Last but not least, I would like to thank the Consejo Nacional de Ciencia y Tecnología, Banco de México and Tenovus Scotland. Their support is fully acknowledged.

Table of Contents

List of Figures and tables

Author's declaration

I declare that all the experimental data contained in this thesis is the result of my own work with the exception of the experiments using Csf1r$^{mer\text{-}iCre\text{-}Mer}$; Rosa$^{LSL\text{-}YFP}$ and Flt3-Cre; Rosa26-YFP, which were carried out in collaboration with Dr Elisa Gómez-Perdiguero, from Professor Frederic Geissmann's group in King's College London, UK. The experiments using germ free mice were carried out in collaboration with Dr Lisa Osborne, from Dr David Artis' group in the University of Pennsylvania, USA.

Signature…….

Printed name Antonio Alberto Bravo Blas

Publication

Bain, CC*, Bravo-Blas, A*, Scott, CL, Gomez Perdiguero, E, Geissmann, F, Henri, S, Malissen, B, Osborne, LC, Artis, D and Mowat. AM. 2014. Constant Replenishment from Circulating Monocytes Maintains the Macrophage Pool in Adult Intestine. *Nat. Immunol.* In press.
*Equally contributing authors.

List of Abbreviations

AAD	Aminoactinomycin D
ABX	Antibiotics
AGM	Aorta gonad mesonephros
APC	Allophycocyanin
BM	Bone marrow
BMM	Bone marrow macrophage
BSA	Bovine serum albumin
CD	Crohn's disease
CDP	Common dendritic cell progenitor
CMP	Common myeloid progenitor
CNV	Conventional
CO2	Carbon dioxide
CSF	Colony stimulating factor
CT	Cholera toxin
DC	Dendritic cell
DEPC	Diethylpyrocarbonate
DNA	Deoxyribonucleic acid
dNTP	Deoxyribonucleotide triphosphate
dpc	Days post-coitus
DSS	Dextran sulphate sodium
EDTA	Ethylenediaminetetraacetic acid
ELISA	Enzyme-linked immunosorbent assay
FACS	Fluorescence-activated cell sorting
FAE	Follicle-associated epithelium
FCS	Foetal calf serum
FITC	Fluorescein isothiocyanate
FL	Foetal liver
FLT3	*Fms*-like tyrosine kinase 3 ligand
g	Gravity
GF	Germ free
GFP	Green fluorescence protein
GMP	Granulocyte-macrophage progenitor
h	Hour
HBSS	Hank's balanced salt solution

HEK	Human embryonic kidney
HSC	Haematopoietic stem cells
IBD	Inflammatory bowel disease
IEL	Intraepithelial lymphocyte
IFN	Interferon
Ig	Immunoglobulin
ILC	Innate lymphoid cells
ILF	Isolated lymphoid follicle
INOS	Inducible nitric oxide synthase
IRF	Interferon regulatory transcription factor
kDa	Kilo Daltons
KDR	Kinase insert domain receptor
kg	Kilogram
KO	Knock out
LFA	Lymphocyte function-associated antigen 1
LN	Lymph node
LP	Lamina propria
LPS	Lypopolysaccharide
LRR	Leucine-rich repeat
LTI	Lymphoid tissue inducer
M-CSF	Macrophage colony stimulating factor
MADCAM	Mucosal vascular addressin cell adhesion molecule
MCP	Monocyte chemoattractant protein
MDP	Macrophage-dendritic cell progenitor
MEP	Megakaryocyte-erythroid progenitor
MER	Mammalian estrogen receptor
MFI	Mean fluorescene intensity
MHC	Major histocompatibility complex
MLN	Mesenteric lymph node
mRNA	Messenger ribonucleic acid
MyD88	Myeloid differentiation primary response gene 88
NK	Natural killer
NLR	Nod like receptor
NO	Nitric oxide
NOD	Nucleotide-binding oligomerisation domain
OVA	Ovalbumin

PAMP	Pathogen-associated molecular patterns
PBS	Phosphate buffered saline
PCR	Polymerase chain reaction
PE	Phycoerythrin
PECAM	Platelet endothelial cell adhesion molecule
PFA	Paraformaldehyde
PP	Peyer's patch
PRR	Patter recognition receptor
PSGL1	P-selectin glycoprotein ligand-1
RNA	Ribonucleic acid
ROR	RAR-related orphan receptor
RPMI	Roswell Park Memorial Institute
RT	Reverse transcriptase
SCF	Stem cell factor
SFB	Segmented filamentous bacteria
SPF	Specific pathogen free
SSC	Side scatter
TACE	Tumor necrosis factor-α-converting enzyme
TED	Transepithelial dendrites
TGF	Transforming growth factor
TLR	Toll-like receptor
TMB	Tetramethylbenzidine
TNBS	Trinitrobenzenesulphonic acid
TNF	Tumour necrosis factor
TRAM	TNF receptor associated factors
TRIF	TIR-domain-containing adapter-inducing interferon-ß
UC	Ulcerative colitis
VEGF	Vascular endothelial growth factor
WT	Wild type
YFP	Yellow fluorescence protein
YS	Yolk sac

Summary

Macrophages (mϕ) are one the most numerous leukocytes present in the healthy gut and contribute to both harmful and beneficial immune reactions. In the colon, mϕ are exposed continuously to large amounts of material from the environment, including harmful agents such as invasive bacteria, viruses and parasites, as well as harmless materials such as food proteins and the commensal bacteria which inhabit the healthy intestine. As a result, mϕ play an important role in helping defend the intestine against harmful invaders. However if these cells make similar reactions to harmless food proteins or commensal bacteria, it would be both wasteful and detrimental, likely leading to inflammatory diseases such as coeliac disease and Crohn's disease. Several genes, which underlie susceptibility to Crohn's disease are involved in controlling how macrophages respond to the microbiota, with considerable evidence indicating that this reflects a loss of the normal unresponsiveness that characterises intestinal macrophages in the healthy intestine. One of the most significant aspects of the epidemiology of Crohn's disease is a particularly rapid increase in its incidence in childhood, suggesting that the first encounters between the microbiota and intestinal macrophages may be of critical importance in determining disease susceptibility. Given this link, it is essential that we elucidate the processes controlling macrophage seeding and development in the intestine and this was an aim of this thesis.

In the adult healthy colon, two main mϕ subsets can be identified: A dominant and homogenous one, made up of mature mϕ, which express high levels of F4/80, MHC II, CX3CR1, are $CD11b^{int/+}$, highly phagocytic and produce high amounts of IL10. The second mϕ group is relatively smaller and is much more heterogeneous. These cells express intermediate levels of F4/80 and CX3CR1, are $CD11b^{+}$ and can be divided into 3 subsets based on their levels of Ly6C and MHC II. These subsets represent a maturation continuum towards the mature mϕ phenotype. Recent reports have suggested that resident macrophages in healthy tissues may be derived from yolk-sac and/or foetal liver precursors that seed tissues during development and subsequently self-renew locally. In contrast, it is proposed that macrophages in inflammation are generated by recruitment of blood monocytes, raising the possibility that these different origins could be exploited in therapy.

However none of these studies have examined macrophages in the intestine and recent work in our laboratory has suggested that monocytes may be the precursors of macrophages in both healthy and inflamed gut of adult mice.

Therefore, the aims of this thesis were to investigate the development of murine colonic mϕ from birth until adulthood, examining the relative roles of the yolk sac, foetal liver and bone marrow monocytes, exploring their functions and comparing them with the well-characterised adult mϕ. In addition, I also examined how mϕ phenotype and functions are influenced by the microbiota using broad-spectrum antibiotics and germ free mice. Lastly, I examined the role of fractalkine and its receptor CX3CR1 in defining the development and functions of intestinal macrophages.

Development of macrophages in early life

The initial characterisation and comparison of colonic mϕ subsets is included in Chapter 3. In this chapter, I describe a series of experiments adapting existing protocols and techniques used for examining the adult murine intestine in order to analyse the origin, phenotype and functions of murine colonic macrophages from late foetal life through to adulthood. These studies found that intestinal mϕ are present before birth, with similar levels of phagocytic ability and IL10, TNFα and CD163 mRNA expression to the adult. However, the numbers and phenotype of mϕ in the intestine do not reach the adult level until the 3rd week of postnatal life. This phenomenon appears to reflect the *de novo* recruitment of blood monocytes in a CCR2-dependent fashion at this time and throughout adult life, but not at early stages of life.

In the colon of newborn mice, two macrophage populations can be observed and are clearly differentiated based on their F4/80 and CD11b expression: F4/80^{hi} CD11b$^{int/+}$ and F4/80^{lo} CD11b^{+}. Interestingly, unlike adult colonic F4/80^{hi} mϕ, the majority of F4/80^{hi} neonatal cells do not express MHC II, however they gradually express this molecule as they age. In addition to acquiring MHC II expression, the two populations in the newborn colon gradually merge and from the 3rd week of life it is difficult to discriminate them reliably. My experiments show that both mϕ subsets proliferate actively during the first 2 weeks of life, but this is later reduced and maintained at

low levels indicating that there is no self-renewal of mature mϕ. Moreover, fate-mapping analysis carried out in collaboration with Professor Frederic Geissmann, showed that yolk sac-derived precursors contribute only minimally to the pool of colonic mϕ, even at early life stages. Conversely, additional fate mapping studies suggested that most intestinal macrophages are derived from $Flt3^{+}$ progenitors. Taken together, the results in this chapter demonstrate that blood monocytes are vital in replenishing the intestinal macrophage pool in the steady state, setting them apart from other tissue macrophages, which derive from primitive progenitors.

Investigating the effect of the microbiota on intestinal macrophage subsets

In Chapter 4, I assessed the effects of the commensal microbiota on intestinal mϕ, using two different approaches: First, I assessed the function and gene expression of colonic macrophages following administration of broad-spectrum antibiotics. My results showed that this did not alter the numbers, phenotype, intracellular cytokine production or mRNA expression by macrophages. Several reasons may account for this, including dose/nature of antibiotics, length of administration or lifespan of macrophages. To overcome these issues, I compared the phenotype of colonic mϕ in germ free (GF) and conventionally (CNV) reared mice of different ages in collaboration with Dr David Artis. Absolute absence of microbiota in GF mice severely impacted $Ly6C^{hi}$ monocyte recruitment to the colon, suggesting that constant recruitment of monocytes to the gut is at least in part due to the microbial burden. The biggest differences between GF and CNV mice were evident at 3 weeks of age, when GF mice had a much lower number and frequency of monocyte-derived cells than their CNV counterparts. By 12 weeks of age, $Ly6C^{hi}$ mϕ populations from GF mice were partially restored, although the expression of MHC II by $F4/80^{hi}$ mϕ remained reduced. Additionally, I FACS-purified $F4/80^{hi}$ cells from GF and CNV adults and sent RNA for microarray analysis, the results of which we are waiting to receive. This data will provide further information regarding how GF intestinal mϕ differ from those found in conventional animals.

Role of the CX3CL1-CX3CR1 axis in mϕ development and function

As mature colonic mϕ express high levels of the chemokine receptor CX3CR1 (fractalkine), finally, in Chapter 5 I went on to investigate the role of CX3CL1-CX3CR1 axis in colonic lamina propria. In addition to the high expression of CX3CR1 by colonic mϕ, its ligand, CX3CL1 has been reported to be expressed at high levels by the intestinal epithelium. Furthermore, as there is strong evidence that the CX3CL1-CX3CR1 axis may be involved in inflammation in several tissues, we hypothesised this axis might play a role in mϕ function in the gut. To this end, I examined mϕ phenotype, activation status and survival following *in vitro* co-culture of WT or CX3CR1-deficient bone marrow-derived mϕ with an epithelial cell line modified to express either the soluble or membrane-bound forms of CX3CL1. I also examined the development of chemically induced colitis in CX3CR1-deficient mice. Finally, since it has been reported by the lab of Oliver Pabst, that the lack of CX3CR1 results in reduced IL10 production by intestinal mϕ, I compared the ability of WT and CX3CR1-deficient mice to prime T cells after being fed with ovalbumin together with an adjuvant. The results from this chapter failed to show any definitive role of the CX3CL1-CX3CR1 axis in mϕ function in either the steady state or in the setting of inflammation.

My *in vitro* studies did not show any significant difference between WT and CX3CR1 deficient intestinal mϕ in terms of survival, or co-stimulatory molecule expression, nor did bone marrow mϕ (BMM) from CX3CR1 KO mice show differences in co-stimulatory molecules and pro-inflammatory cytokine production with or without stimulation by LPS. Moreover, the responses of wild type BMM were not altered by exposure to exogenous CX3CL1 either in soluble form, or when expressed as a transmembrane form by epithelial cells.

The *in vivo* assessment of CX3CR1 during inflammation, Ly6C^{hi} CX3CR1^{int} cells increased after 4 days on DSS, however, the lack of CX3CR1 failed to confer protection from colitis in a consistent manner, suggesting that there may be more factors responsible for colonic inflammation apart from the CX3CL1-CX3CR1 axis.

Taken together, the results of this thesis highlight that important cellular changes take place during the development of mϕ in the intestine. In addition, the presence or absence of microbiota plays a crucial role in this development with acquisition of MHC II depending at least in part on the presence of microbes. Microarray data obtained from purified F4/80^{hi} mϕ populations of GF and CNV mice may reveal interesting differences and suggest how mϕ phenotype and function may be regulated by the microbiota. Finally, I have shown that the CX3CL1-CX3CR1 axis plays a redundant role in the regulation of intestinal mϕ phenotype and function with mϕ from CX3CR1-deficient animals appearing to function normally in both health and disease.

Chapter 1
General introduction

1.1 The intestinal immune system

The mucosal surfaces that comprise the gastrointestinal, reproductive and respiratory tracts have a unique immune system whose properties are determined by their anatomical location and function they execute (Maldonado-Contreras and McCormick, 2011). The intestine has a massive surface area and is in intimate contact with a vast array of foreign antigens such as bacteria, food proteins and potential pathogens. As a result, the intestine is the largest compartment of the immune system and it has to discriminate between harmless and harmful antigens (Artis, 2008; Mowat, 2003). While adaptive immunity has to be induced against pathogens, similar responses against harmless materials such as commensal bacteria or foods are dangerous, as they can lead to inflammatory bowel disease (IBD) or coeliac disease, respectively (Bain and Mowat, 2011; Gujral et al., 2012). Thus, a complex and sophisticated series of processes have evolved to ensure appropriate immune responses in the intestine.

1.2 Adaptive immune responses in the intestine

The intestinal immune system comprises both organised lymphoid tissues and populations of scattered effector cells. The organised lymphoid tissues are the sites where immune responses are initiated and they comprise the Peyer's patches and isolated lymphoid follicles (ILF) found in the intestinal wall, together with the draining mesenteric lymph nodes (MLN) (Bailey and Haverson, 2006; Mowat, 2003).

Peyer's patches are macroscopic structures located along the small intestine containing several large B cell follicles with germinal centres and smaller T cell areas between the follicles. The scattered ILFs are similar in structure to PP, but are much smaller and are found throughout the small and large intestines (Jung et al., 2010). They are mainly composed of B cells, with a low proportion of T cells and only develop after birth in response to bacterial colonisation (Bouskra et al., 2008). Both the PP and ILFs also contain DCs and macrophages (mϕ). The PP are covered by a single layer of follicle associated epithelium (FAE), containing specialised epithelial cells known as microfold (M) cells that take up bacteria and other antigens from the lumen and pass

them on to DCs in the dome region underlying the FAE. DCs can then present the antigen either to T and B lymphocytes in the PP themselves, or migrate through lymphatics to the MLN to interact with lymphocytes there. The MLNs are the largest lymph nodes in the body and are essential for all immune responses in the intestine. Lymphocytes which are primed in the PP or MLN acquire homing molecules which ensure the activated lymphocytes return specifically to the intestinal mucosa as effector cells via the efferent lymph and bloodstream. These molecules are $\alpha4\beta7$ integrin, that binds to MADCAM-1 on the vascular endothelium of mucosal blood vessels and in the small intestine, CCR9, the receptor for the CCL25 chemokine produced selectively by epithelial cells in the small intestine. The mechanisms responsible for driving lymphocyte recirculation to the large intestine are not yet known, but may include CCR10 and its ligand CCL28 (Jung et al., 2010; Mowat, 2003).

The lamina propria (LP) is the layer of loose connective tissue beneath the epithelium and contains large numbers of $CD4^+$ and $CD8^+$ T cells, as well as IgA producing plasma cells, mϕ, DCs, occasional eosinophils and mast cells. The majority of T cells in the LP have a memory/effector phenotype, consistent with them being the product of primed naïve T cells; $CD4^+$ T cells outnumber $CD8^+$ T cells by ~2:1 (MacDonald et al., 2011). $CD4^+$ T cells producing IFNγ or IL17 or expressing Foxp3 are all readily detectable in the LP even under steady state conditions, emphasising the constant stimulation present in this tissue (Shale et al., 2013). The epithelium also contains many lymphocytes but these are virtually all $CD8^+$ T cells, which again have a memory/effector phenotype and are capable of constitute functions such as cytotoxicity and cytokine production. Many intraepithelial lymphocytes (IEL) also express the unusual homodimeric α-α form of the CD8 molecule and appear to be related to cells of the innate immune system, rather than being conventional $CD8^+$ T cells. $\gamma\delta$ T cells are also present in the epithelium, where they again have an activated phenotype and innate-like properties (Mowat, 2003; van Wijk and Cheroutre, 2009).

Humoral immunity in the intestine is characterised by the selective production of IgA antibodies that are transported across the epithelial cells into the lumen. The production of IgA is dependent on selective switching of

B cells under control of TGFβ, and is driven by T cells primed by antigen in the PP or MLN (Cerutti and Rescigno, 2008).

1.3 Innate immunity in the intestine

As in other parts of the body, innate immune responses are triggered in a very short time, but do not generate memory responses or show antigen-specificity (Medzhitov and Janeway, 2000). Despite these limitations, the local innate immune response can deal efficiently with most challenges and it was this aspect of immune function my project focused on.

The first layer of innate immunity comprises physiological factors such as the low pH of the stomach, digestive enzymes and the peristaltic movement of fluid through the lumen. The epithelium then presents an important mechanical barrier, dependent both on passive and active mechanisms that contribute to innate defence. The tight junctions between epithelial cells prevent influx of materials across the barrier, while the goblet cells within the epithelium produce mucus which forms an additional physical barrier and has antimicrobial properties (Abreu, 2010; van der Flier and Clevers, 2009). Paneth cells are a further kind of epithelial cell found in the crypts of the small intestine, which in response to microbial products, secrete antimicrobial mediators, such as α-defensins, cryptdins, C-type lectins and RegIIIγ. Their production is also enhanced by IL22 produced by local $CD4^+$ T cells and innate lymphoid cells (ILC). Together, these small proteins play an important part in intestinal defence by disrupting the membranes of bacteria, fungi and viral envelopes. Paneth cells also produce phospholipase A_2, which kills bacteria by hydrolising phospholipids in the cell membrane (Clevers and Bevins, 2013; Ganz, 2003; Reddy et al., 2004). A further important characteristic of gut epithelial cells is their very high turnover rate which means they are replaced every 4-5 days, allowing removal of attached or invading organisms (van der Flier and Clevers, 2009).

1.4 TLRs and NLRs

Epithelial cells and many leukocytes found in the intestinal mucosa express germline-encoded pattern recognition receptors (PRRs) that recognise

conserved features on microbes, which are not found in mammalian cells and are known as pathogen-associated molecular patterns (PAMPs). PAMPs are carbohydrate, lipid or nucleic acid structures essential for the survival of microbes, and thus are ideal targets for the innate immune system (Raetz and Whitfield, 2002).

The best known PRRs are the Toll-like receptors (TLRs), of which 13 have been described in the mouse and 10 in humans (Bryant and Monie, 2012; Oldenburg et al., 2012). As shown in Table 1.1, different TLRs recognise a variety of microbial products including nucleic acids, membrane components, LPS and flagellin. TLRs are single-pass transmembrane proteins with an extracellular region composed of leucine-rich repeats (LRR) creating a protein scaffold that forms the basis of ligand binding. Mammalian TLRs are activated when binding of a ligand induces them to form dimers or oligodimers and they are found either on the cell surface, in endosomes or in the cytoplasm (Bryant and Monie, 2012; Murphy, 2012; Testro and Visvanathan, 2009).

TLR ligation triggers a signalling cascade of NF-κB and interferon regulatory factor (IRF) mediated intracellular responses, which result in the production of proinflammatory mediators such as TNFα, IL6, chemokines, antimicrobial peptides, as well as interferons (Cario, 2010). These mediators also attract and activate innate effector cells such as neutrophils, monocytes, eosinophils and DCs. Additionally, TLR signalling involves a number of adaptor molecules such as myeloid differentiation factor 88 (MyD88), which is a universal adaptor used by almost all the TLRs except for TLR3 (Gay et al., 2011). TIR domain-containing adaptor-inducing IFN-β (TRIF) and TRIF-related adaptor molecule (TRAM) on the other hand are responsible for activation of MyD88-independent genes after stimulation with TLR4 and TLR3 ligands (Brasier, 2006; Paun and Pitha, 2007; Yamamoto et al., 2003).

Other innate sensors displayed by epithelial and haematopoietic cells are the nucleotide-binding oligomerisation domain proteins NOD1 and NOD2. These PRRs are related to TLRs, but are exclusively intracellular and recognise components of the peptidoglycans found in bacterial cell walls (Cario, 2010; Franchi et al., 2009).

TLR	Ligand that binds to	Cellular distribution
TLR1:TLR2 heterodimer	Lipomannans (Diacyl/triacyl lipopeptides)	Monocytes, DCs, mϕ, mast cells, neutrophils, eosinophils, basophils
TLR2:TLR6 heteromdimer	Lipoteichoic acids Cell wall β-glucans Zymosan	
TLR3	Double-stranded RNA	NK cells, $CD8^+$ DCs, $CD103^+$ DCs, mϕ
TLR4 (plus MD-2 and CD14)	Bacterial LPS Lipoteichoic acids	$CD103^-$ $CD11b^+$ DCs, mϕ, mast cells, neutrophils, eosinophils
TLR5	Flagellin	DCs, mϕ, neutrophils, intestinal epithelium
TLR7	Single-stranded RNA	NK cells, mϕ plasmacytoid DCs, neutrophils, eosinophils, B cells
TLR8	Single-stranded RNA	NK cells, mϕ, DCs, neutrophils
TLR9	DNA with unmethylated CpG	NK cells, mϕ, plasmacytoid DCs, neutrophils, eosinophils, B cells, basophils

TLR10	Unknown	Plasmacytoid DCs, neutrophils, eosinophils, B cells, basophils
TLR11 (mouse only)	Flagellin Profilin	$CD8^+$ DCs, mϕ
TLR12	Profilin	$CD8^+$ DCs, mϕ, neurons
TLR13	Bacterial ribosomal RNA sequence "CGGAAAGACC"	$CD8^+$ DCs, mϕ and monocytes

Table 1.1. Innate immune recognition by Toll-like receptors. Adapted from Mishra 2008, Murphy, 2012 and Rosenberg, 2003.

1.5 Effector cells of the intestinal innate immune system

The cellular arm of the innate immune system is found mostly in the LP and comprises natural killer (NK) cells, innate lymphoid cells, granulocytes (basophils and eosinophils), DCs, monocytes and mϕ.

Natural killer (NK) cells. Are cytotoxic non-B, non-T lymphocytes that are not antigen specific, but are stimulated by cytokines and molecules present on stressed cells, tumour cells or infected cells. In addition, they express inhibitory receptors that recognise MHC I and which prevent their activation, unless MHC I has been downregulated. NK cells act through the release of cytotoxic granules containing perforin and granzymes, and by producing cytokines such as IFNγ (Vivier et al., 2011; Vivier et al., 2008). Currently, NK cells are seen as part of a wider range of innate lymphoid cells and classified amongst Group 1 ILCs (Hwang and McKenzie, 2013).

Innate lymphoid cells (ILC). These newly identified members of the lymphoid lineage comprise a number of non-antigen specific, non-T, non-B cells that are related to lymphoid tissue inducer (LTI) cells. So far, 3 groups of ILCs have been identified based on their signature cytokines and their dependence on different growth factors and transcription factors. As mentioned above, ILC1 include NK cells and are characterised by their production of IFNγ and TNFα in response to IL15. They are dependent on the Th1 cell-associated transcription factor T-bet. ILC2, previously known as natural helper cells and "nuocytes", produce IL5, IL9 and IL13 in response to IL25 and IL33 and are controlled by the retinoic acid receptor-related orphan receptorα (RORα) and GATA-binding protein 3 (GATA3). ILC3 produce IL17 and IL22 in response to IL23 and are dependent on the transcription factor RORγt. A subset of ILC3 produces both IFNγ and IL17 and has been associated with intestinal inflammation. These subsets of ILCs are believed to be the innate equivalent of the various subsets of effector T cells that play distinct roles in immunity against viruses and intracellular bacteria (ILC1), parasites and allergens (ILC2) and extracellular bacteria and fungi (ILC3) (Pearson et al., 2012; Spits et al., 2013; Walker et al., 2013).

Granulocytes. Despite their usual association with parasite infections, allergic reactions and asthma, eosinophils are found at surprisingly high frequencies in the steady state LP, where they may play a role in tissue repair and remodelling of the epithelial barrier (Mowat, 2010; Rothenberg and Hogan, 2006). Eosinophils also make important contributions to defence against helminths in the intestine and express several TLRs, such as TLR1, TLR2, TLR4, TLR6, TLR7, TLR9 and TLR10. Finally, basophils are rare in the normal intestine, but increase in numbers during helminth infections (Anthony et al., 2007; Kvarnhammar and Cardell, 2012; Suurmond et al., 2013). Granulocytes can be divided into neutrophils, eosinophils and basophils based on the content of their granules and their staining with haematoxylin and eosin. Although they are rare in the steady state LP, neutrophils are the first cells to accumulate during acute inflammation of the intestine, where they are phagocytic, have a microbicidal role and produce proinflammatory cytokines (Rosenberg, 2003).

Dendritic cells (DCs). These myeloid cells received their name from Ralph Steinman in the early 1970s and form a crucial link between the innate and adaptive immune systems (Steinman and Cohn, 1973). They are defined by their morphology and by their ability to sample antigens in tissues, before migrating in afferent lymph to draining lymph nodes, where they have a unique ability to prime naïve T cells and initiate adaptive immune responses (Banchereau and Steinman, 1998). These properties are dependent on the ability of DCs to respond to TLR ligands and their PAMPs in the tissues, which stimulate locomotor activity, antigen processing, expression of the LN homing chemokine receptor CCR7 and of the costimulatory molecules CD40, CD80 and CD86 needed for T cell priming (Hammer and Ma, 2013).

DC development is dependent on Fms-like kinase 3 (Flt3) and these cells begin as committed DC precursors in the BM, before migrating via the bloodstream into lymphoid and non-lymphoid tissues, where they divide and differentiate into mature DCs (Bogunovic et al., 2009; McKenna et al., 2000; Onai et al., 2007). Two major families of conventional DCs have been defined in humans and mice, which can be defined by their mutually exclusive expression of SIRPα and XCR1. In mice, the former population expresses CD11b, but not CD8α, whereas the latter is C11b^{-} CD8α^{+} (Turnbull et al.,

2005). CD8α^+ (XCR1$^+$) DCs have a specialised ability to cross-present exogenous antigens to CD8$^+$ T cells and they are found particularly in the T cell dependent areas of secondary lymphoid tissues (Bachem et al., 2012). However like SIRPα^+ DCs, they can also be found in non-lymphoid tissues and can migrate to lymph nodes to prime CD4$^+$ T cells (Cerovic et al., 2013). Plasmacytoid DCs are a further lineage of DCs, but these do not migrate from tissues to LN and their ability to present antigen to T cells is controversial. Their main role in the immune system is the production of type 1 interferons in response to virus infections (Yrlid et al., 2006).

DCs are abundant both in the organised lymphoid tissues of the intestine such as the PP and MLN, as well as in the LP. Recent studies in our own and other laboratories have identified 4 main subsets of DCs in intestinal LP that can migrate in lymph to the MLN, based on their expression of CD103 and CD11b (Cerovic et al., 2013). These are CD103$^+$ CD11b$^-$, CD103$^+$ CD11b$^+$, CD103$^-$ CD11b$^+$ and CD103$^-$ CD11b$^-$. All are *bona fide* DCs as shown by their dependency on Flt3 and expression of the DC specific transcription factor zbtb46 (Satpathy et al., 2012) (Scott, unpublished data). The exact functions of these individual subsets are still being defined, but previous work has shown that CD103$^+$ DCs from the intestine are characterised by a unique ability to imprint the expression of the gut markers CCR9 and $\alpha4\beta7$ on interacting naïve T and B cells and may selectively generate FoxP3 expressing regulatory T cells; these properties reflect the production of retinoic acid from dietary vitamin A (Engberg et al., 2010; Johansson-Lindbom et al., 2005; Scott et al., 2011). In addition, CD103$^+$ DCs express the TGFβ activating integrin $\alpha v\beta8$ and indoleamine 2-3 dioxygenase (IDO), which collectively inhibit the generation of effector T cells and favour the differentiation of Treg cells (Paidassi et al., 2012). For these reasons, it is proposed that CD103$^+$ DCs play the critical role in the development of tolerance to food proteins and commensals in the intestine (Pabst and Mowat, 2012; Persson et al., 2013). Conversely, it is thought that CD103$^-$ CD11b$^+$ DCs may be responsible for Th17 cell differentiation through production of pro-inflammatory mediators such as IL6 or IL23 (Cerovic et al., 2013; Siddiqui et al., 2010). However it has to be noted that TLR activated CD103$^+$ DCs can produce IL12 and drive Th1 differentiation (Fujimoto et al., 2012) and that CD103$^+$ DCs are the principal cells carrying *Salmonella* to MLN (Farache et al.,

2013). Furthermore, recent work shows that loss of IRF4 or Notch 2 leads to a selective defect in $CD103^-$ $CD11b^+$ DC which is associated with absence of Th17 cells in the LP (Schlitzer et al., 2013). Therefore there may be functional plasticity within the individual DC subsets.

1.6 Intestinal macrophages

1.6.1 What is an intestinal macrophage and why are they important?

Phagocytosis was first reported in starfish over a century ago by the zoologist Elie Metchnikoff (Gordon, 2007; Metchnikoff, 1989). This early discovery led to the description of the cells later known to comprise the reticuloendothelial system and they were eventually classified as macrophages (mϕ) in the early 1970's by van Furth (Lichanska and Hume, 2000; van Furth R, 1972). Mϕ are found throughout the body, with the single largest population being in the intestine and they act as innate effector cells ingesting and killing microbes, as well as having important homeostatic functions, such as the clearance of debris and apoptotic cells, and the production of growth factors. At the same time however, activated mϕ produce a wide variety of proinflammatory mediators which can contribute to tissue damage (Wynn et al., 2013).

Intestinal mϕ are found in the lamina propria, just underneath the epithelial surface all along the length of the intestinal tract. There are more mϕ in the colon than the small intestine, which correlates with the microbial load in these sites. Being adjacent to the epithelium puts mϕ in an ideal position to clear away dying epithelial cells and to assist the tissue remodelling needed in such a rapidly dividing tissue (Hopkinson-Woolley et al., 1994; Hume et al., 1995; Mantovani et al., 2013; van der Flier and Clevers, 2009). Additionally, they can act as sentinels for any microbes that may have breached the epithelium. Mϕ can express a wide range of TLRs and normally, the interaction between TLRs and PAMPs would trigger the synthesis of mediators of inflammation such as nitric oxide (NO), reactive oxygen species, IL6 and TNFα (Medzhitov and Janeway, 2000; Raetz and Whitfield, 2002). However this is not the case with intestinal mϕ, which even though they express TLRs, they do not respond to TLR ligation or other stimuli in a classical manner by

producing such mediators. Instead they produce high levels of IL10 constitutively. However, intestinal mϕ are not entirely inert, as in addition to producing IL10, they are highly phagocytic, express high levels of MHC II and produce some TNFα constitutively (Bain et al., 2013; Platt and Mowat, 2008; Smith et al., 2011; Ueda et al., 2010). This suggests that mϕ are partially activated *in situ,* but are held in check by IL10.

Intestinal mϕ have several unusual phenotypic features. As well as expressing classical mϕ markers such as F4/80, CD68, CD64 and CD11b, they also express intermediate to high levels of CD11c and most express very high levels of the fractalkine receptor CX3CR1 (Bain and Mowat, 2011; Platt and Mowat, 2008; Smythies et al., 2005; Tamoutounour et al., 2012). Consistent with their position and functions, they also express receptors that assist the phagocytosis of microbes and cells, such as the scavenger receptor CD163 and the mannose receptor CD206 (Bain and Mowat, 2011; Bain et al., 2013; Platt et al., 2010). Interestingly, the realisation that CX3CR1 is a mϕ marker has revised opinion on the nature of the MHC II^+ $CX3CR1^+$ cells that form transepithelial dendrites (TEDs) and capture bacteria from the lumen. Originally believed to be DCs, it seems likely that they are resident mϕ (Niess, 2010; Niess and Adler, 2010; Niess et al., 2005; Zigmond and Jung, 2013).

1.6.2 Origins and development of intestinal macrophages

Mϕ first appear early in embryogenesis, when they develop from primitive mesenchymal precursors in the yolk sac (YS), around day 8 in mice. The purpose of this primitive production of $CSF1R^+$ cells is to facilitate tissue oxygenation in the rapidly growing embryo (Ginhoux et al., 2010; Hume et al., 1995; Orkin and Zon, 2008; Schulz et al., 2012) and is quickly replaced by $CSF1R^+$ cells that have seeded the FL from the aorta gonad mesonephros (AGM) around embryonic day 10.5. Finally, the BM takes over haematopoiesis during the perinatal period (Gekas et al., 2005; Muller et al., 1994; Pixley and Stanley, 2004).

In the adult BM, haematopoietic stem cells (HSC) give rise to common myeloid progenitors (CMP), which then differentiate into the myeloid,

megakaryocytic or erythroid lineages (Figure 1.1). Next, granulocyte/macrophage progenitors (GMP) give rise to granulocytes and to the mϕ and DC precursor (MDP), which then generates the common DC precursors (CDP) of conventional and plasmacytoid DCs, as well as the monoblasts that are the precursors of pro-monocytes that give rise to monocytes that are released into the bloodstream and mature into mϕ after entry into tissues (Geissmann et al., 2010; Hettinger et al., 2013; Mouchemore and Pixley, 2012). All these stages of mϕ differentiation are controlled by a range of growth factors and transcription factors (Figure 1.1), such as Notch homolog 1 (Notch1) and runt related transcription factor 1 (*Runx1*), which regulate the earliest phase of HSC differentiation in the AGM, while the transcription factor PU.1 is required for the earliest steps of myeloid lineage commitment and regulates the genes encoding the macrophage colony-stimulating factor (M-CSF or CSF-1) (Anderson et al., 1998; Lichanska et al., 1999; Orkin and Zon, 2008). The CSF1R, (also known as c-fms, M-CSFR and CD115), along with the stem cell factor (c-kit ligand) and IL3 are critical for the survival and early differentiation of myeloid cells. CSF1 deficient mice (*op*/*op*) lack virtually all mϕ including intestinal mϕ (Bartelmez et al., 1989; Cecchini et al., 1994; Mouchemore and Pixley, 2012; Pixley and Stanley, 2004; Yoshida et al., 1990).

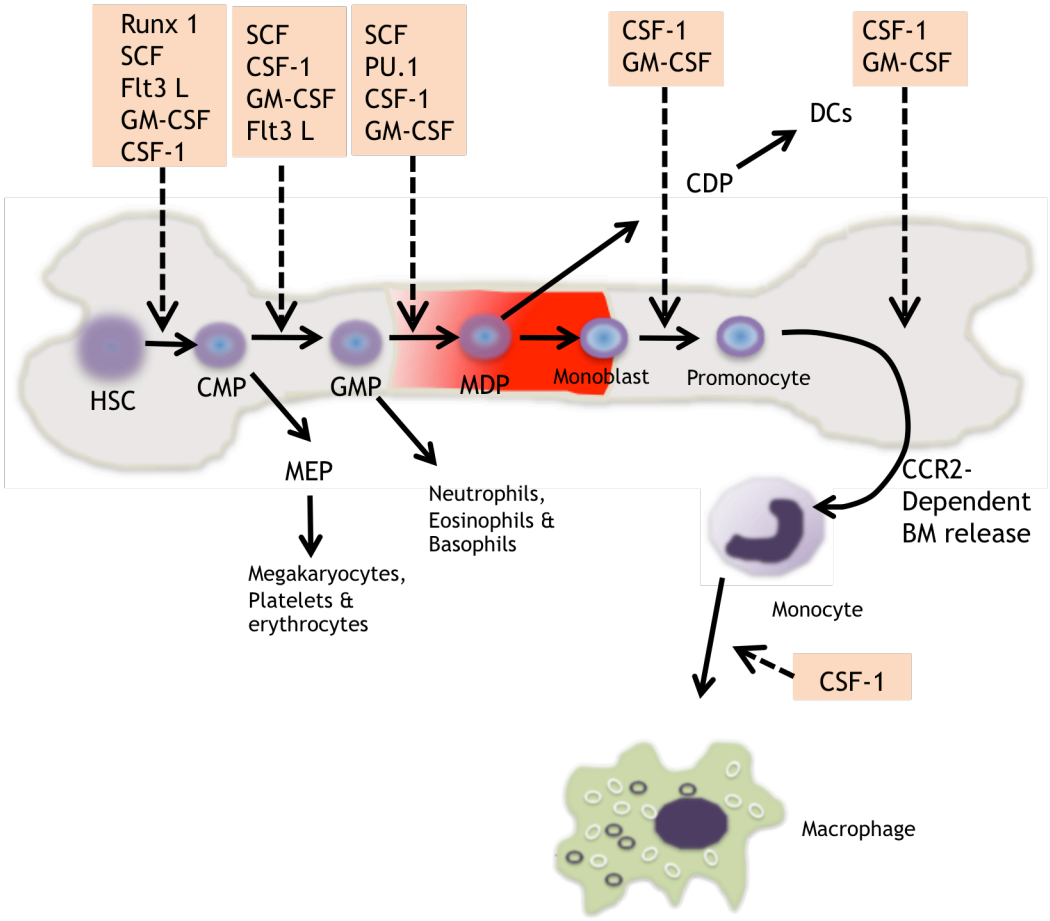

Figure 1.1. Schematic differentiation of macrophages from haematopoietic stem cells (HSC) in the adult bone marrow. CMP, common myeloid progenitor; GMP, granulocyte-macrophage progenitor; MEP, megakaryocyte-erythroid progenitor; MDP, macrophage-dendritic cell progenitor; DC, dendritic cell; CDP, common dendritic cell progenitor; Runx1, runt related transcription factor 1; SCF, stem cell factor; Flt3 L, Flt3 ligand; GM-CSF, granulocyte/macrophage colony stimulation factor; CSF-1, colony stimulation factor. Adapted from Mouchemore and Pixley, 2012, Orkin and Zon, 2008.

Until recently, it was believed that tissue mϕ were derived from blood monocytes and two populations of $CD115^{+}$ blood monocytes have been described in mice and humans. In mice, one of these groups expresses high levels of Ly6C, GR1 and CCR2, together with low levels of CX3CR1, while the other is $GR1^{lo}$ $Ly6C^{lo}$ $CCR2^{-}$ and $CX3CR1^{+}$ (Auffray et al., 2009; van Furth and Cohn, 1968; Varol et al., 2009b). Initially, it was suggested that $Ly6C^{hi}$ monocytes only gave rise to mϕ in inflamed tissues, whereas the $Ly6C^{lo}$ subset was thought to generate mϕ in steady state tissues. Although supported by some studies on lung parenchyma (Landsman et al., 2007; Yona, 2009), this idea has gone out of fashion in recent years, as it has been very difficult to show $Ly6C^{lo}$ monocytes migrating into tissues. Rather, it is now believed that these are a more mature form of $Ly6C^{hi}$ monocytes and that they have a specialised role in patrolling the vasculature by crawling along the endothelium (Auffray et al., 2007; Auffray et al., 2009; Geissmann et al., 2003; Gordon and Taylor, 2005; Varol et al., 2009b).

After circulating in the bloodstream, monocytes extravasate into tissues using adhesion molecules such as L-selectin (CD62L), P-selectin glycoprotein ligand 1 (PSGL1), lymphocyte function-associated antigen 1 (LFA1) and platelet endothelial cell adhesion molecule (PECAM1) (Ley et al., 2007; Shi and Pamer, 2011), together with chemotactic factors such as CSF1 and the chemokines CX3CL1 and CXCL12. Once in tissues, monocytes differentiate into mϕ under control of CSF1 (Auffray et al., 2009; Fong et al., 1998; Pixley and Stanley, 2004).

This view of mϕ development has been challenged recently by the idea that conventional haematopoiesis in the bone marrow may not be the principal source of the resident mϕ pool and that they may be derived from precursors that enter the tissues in foetal life, before self-renewing throughout adult life (Chorro et al., 2009; Ginhoux et al., 2010; Schulz et al., 2012). Using *Csf1r*$^{mer\text{-}iCre\text{-}mer}$ reporter gene mice, Schulz and collaborators proposed that mϕ in skin, brain, lung, liver and pancreas are derived exclusively from YS-derived precursors that self renew in tissues under control of the CSF1R ligands IL34 or CSF1 (Greter et al., 2012). In this model, pregnant dams receive a low dose of tamoxifen at 8.5 days post coitus (dpc) and only those cells expressing the CSF1R at that time will react to tamoxifen, due to their

expression of the mammalian oestrogen receptor (mer) under control of the CSF1R promoter. The mer in turn is linked to cre recombinase and after crossing to ROSA-STOP reporter mice, in which YFP has been inserted into the ROSA locus, with its expression normally prevented by an upstream lox P-flanked (floxed) STOP codon. Therefore, by driving excision of the STOP codon, tamoxifen induces irreversible YFP expression by CSF1R bearing cells in the progeny of these mice. Although these findings have been challenged by evidence that the Langerhans cell precursors are derived from foetal liver (FL) rather than the yolk sac (YS), the overall conclusion remains that blood monocytes do not appear to contribute to the ontogeny of many tissue mϕ such as Kupffer cells in the liver, microglia of the CNS and alveolar mϕ (Geissmann et al., 2010; Ginhoux et al., 2010; Hoeffel et al., 2012; Schulz et al., 2012; Wang et al., 2012). Importantly however, none of these studies have examined intestinal mϕ and indeed very little is known about their development or precursors.

When I began my project, a PhD student in the laboratory had found that steady state mϕ in mouse colon were derived via local differentiation of BM derived Ly6C^{hi} monocytes (Bain et al., 2013). This process can be followed phenotypically, revealing individual stages based on their expression of CX3CR1, Ly6C and MHC II. When they first arrive in the intestine, the cells are identical to blood monocytes, being Ly6C^{hi} MHC II^{-} CX3CR1^{int} and are referred to as P1. These then acquire MHC II expression (P2), before losing MHC II (P3) and finally becoming CX3CR1^{hi} Ly6C^{-} MHC II^{+} resident mϕ (P4). Importantly, these phenotypic changes are accompanied by functional maturation. Recently arrived cells in P1 and P2 are fully responsive to TLR stimulation and produce TNFα, but have very little IL10 production or phagocytic activity. However these properties are acquired progressively as the mϕ differentiate, together with expression of CD163 and CD206 and loss of TLR responsiveness (Bain et al., 2013). That this process needs to be maintained throughout life is suggested by the fact that there are reduced numbers of intestinal mϕ in mice lacking CCR2, the chemokine receptors needed for egress of Ly6C^{hi} monocytes from BM to tissues (Serbina and Pamer, 2006; Si et al., 2010). Together those findings have suggested that intestinal mϕ may differ from those in other tissues by being derived from continuous replenishment by blood borne monocytes. However when and how this process becomes

established, or whether foetal precursors make any contribution to the intestinal mϕ pool is unknown. Exploring these ideas were major aims of my project.

1.6.3 Monocytes and macrophages in intestinal inflammation

Intestinal mϕ populations alter dramatically during infection or inflammation, such as that found in IBD (Serbina et al., 2008; Shi and Pamer, 2011; Si et al., 2010). Under these conditions, there is an accumulation of proinflammatory monocytes and immature mϕ, which retain TLR responsiveness and produce mediators such as IL1, IL6 and TNFα, as well as iNOS (Smith et al., 2011). These cells are crucial for killing microbes and for causing damage, as is shown by the success of targeting mϕ products like TNFα and IL6 in human Crohn's disease (Bain et al., 2013; Kaser et al., 2010; Maloy and Powrie, 2011). Thus it would be important to understand the factors responsible for driving the steady state differentiation of monocytes into non-inflammatory mϕ and how these processes are disrupted in inflammation.

1.6.4 Is it a macrophage or a DC?

A topic of much recent debate in the field of myeloid cell biology has been the relationship between mϕ and DCs. This is particularly the case in the intestine due to the shared expression of several surface markers such as CD11b, CD11c and MHC II (Bain et al., 2013; Shortman and Liu, 2002). Initial studies assumed that all MHC II^+ $CD11c^+$ mononuclear phagocytes (MPs) were DCs, leading to considerable confusion about the relative roles of these cells in intestinal immune responses, as well as to the idea that $Ly6C^{hi}$ monocytes may give rise to both intestinal DCs and mϕ (Bogunovic et al., 2009; Persson et al., 2013; Varol et al., 2007; Varol et al., 2009a).

Distinguishing between mϕ and DCs is important, as despite their phenotypic similarities, they play quite different roles in the intestinal immune response. Whereas DCs migrate to LN and prime T cells, LP mϕ are sessile and cannot prime T cells, with their main role being as local scavenger cells (Johansson-Lindbom et al., 2005; Schulz et al., 2009). For a time it was proposed that the mutually exclusive expression of CD103 and CX3CR1 could be used to

identify intestinal DCs and mϕ respectively (Schulz et al., 2009). However as discussed above, it is now known that there is a populations of $CD103^-$ DCs that are $CX3CR1^{int}$, meaning that additional markers are needed to be used (Cerovic et al., 2013). As part of ongoing work in our and other laboratories, a multiparametric strategy has been developed to do this, which is based on the expression of F4/80 and CD64 by mϕ but not DCs (Bain et al., 2013; De Calisto et al., 2012; Persson et al., 2013; Tamoutounour et al., 2012). By allowing these cells to be identified precisely, this approach can be applied to characterising mononuclear phagocytes in new models and different mouse strains, as I will do here in neonatal and germ free mice.

1.7 The intestinal microbiota

Prenatal development takes place in a sterile environment, but at birth the newborn animal comes into direct contact with the maternal flora. This leads to the progressive establishment of a complex intestinal microbiota and to a host-bacterial mutualism (Kosiewicz et al., 2011; Macpherson and Harris, 2004; Reading and Kasper, 2011; Round and Mazmanian, 2009). The density of bacteria increases going down the length of the gastrointestinal tract, with the stomach and proximal small intestine containing few organisms (10^1-10^3 CFU/ml), whereas the colon contains up to 10^{12} microbes/ml of luminal contents (Figure 1.2) (Langhendries, 2005; Sartor, 2008). The exact number of intestinal bacteria and their species are not yet clear, as most are non-culturable, but modern molecular biological techniques estimate that there may be 10 times more commensal bacteria as the number of cells in the human body, comprising of several hundred species. The majority of these are obligate anaerobes, with the Bacteriodetes phylum dominating, followed by Firmicutes (Figure 1.2) (Kosiewicz et al., 2011; Kuwahara et al., 2011; Langhendries, 2005).

The result of this enormous colonisation is a symbiotic mutualism which benefits both the host and the bacteria (Inman et al., 2010a; Molloy et al., 2012; Mulder et al., 2011). In addition to metabolising indigestible food compounds such as complex carbohydrates and producing vitamins (Hooper and Gordon, 2001; Round and Mazmanian, 2009), the commensal bacteria provide an important defence against pathogens by competing for nutrients,

space and surface receptors (Atarashi et al., 2011; Ewaschuk et al., 2008; Fagundes et al., 2011; Hans et al., 2000; Lamouse-Smith et al., 2011; Macpherson and Harris, 2004; Mazmanian et al., 2008; Ochoa-Reparaz et al., 2010; Reading and Kasper, 2011; Seth et al., 2008; Smith et al., 2007).

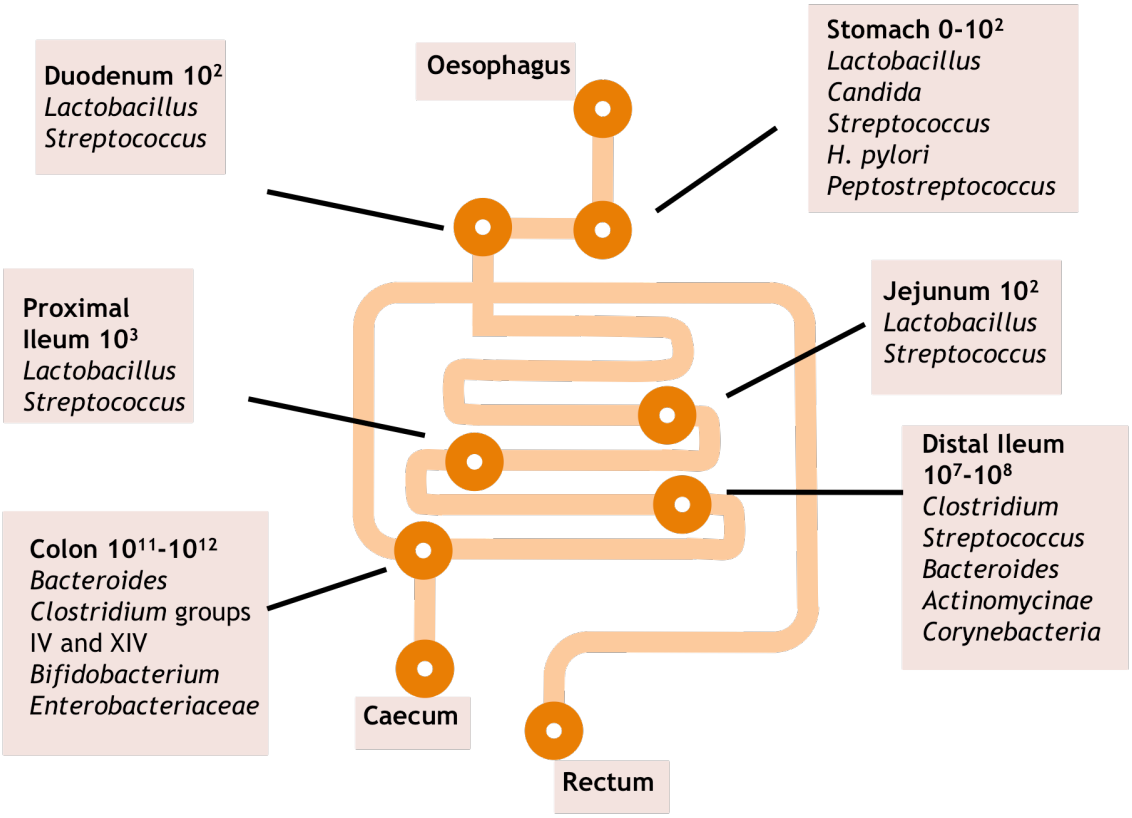

Figure 1.2. Composition of dominant microbial species in various regions of the human gastrointestinal tract. Adapted from Sartor, 2008.

As well as being beneficial for normal health, commensal bacteria are also potentially harmful, producing sepsis if they gain access to the mucosa and systemic tissues (Madan et al., 2012). Furthermore, all experimental models of IBD are entirely dependent on the presence of the microbiota (Elson et al., 2005). Because so many bacteria are separated from the intestinal environment by only a single layer of epithelium, the host has evolved a sophisticated array of mechanisms to maintain the microbiota at arm's length and prevent inappropriate immune responses (Artis, 2008; Dahan et al., 2007; Sonnenberg et al., 2012). These include many of the innate immune mechanisms discussed above, such as mucus production, epithelial tight junctions and antimicrobial peptides, as well as antigen specific mechanisms involving regulatory T cells and IL10, and immunity mediated by IL22 and Th17 cells (Atarashi et al., 2011; Hadis et al., 2011; Ivanov et al., 2009; Natividad et al., 2012; Ostman et al., 2006; Pearson and Brownlee, 2010; Ueda et al., 2010; Wu et al., 2010). Importantly, defects in all these processes have been associated with susceptibility to IBD under experimental conditions.

1.8 Tonic effects of the microbiota on intestinal function

Although germ free (GF) animals can be maintained for long periods, this has severe effects on many aspects of metabolism and immune function (Sartor, 2008; Tlaskalova-Hogenova et al., 2011). GF mice have decreased cellularity in Peyer's patches, delayed or absent maturation of isolated lymphoid follicles (ILFs), immaturity of epithelial cells and slower epithelial turnover rates (Abrams et al., 1963; Bouskra et al., 2008; Macpherson and Harris, 2004). Additionally, the normal maturation of the mucosal immune system is dependent on the presence of microbiota and colostrum, with germ free mice showing a general paucity of lymphocytes, with fewer IgA producing plasma cells in both systemic and intestinal lymphoid tissues, as well as low serum immunoglobulins (Atarashi et al., 2008; Bauer et al., 1963; Benveniste et al., 1971; Macpherson and Harris, 2004).

Administration of broad-spectrum antibiotics reproduces many of the effects of the GF state, including amelioration of colitis (Cummings et al., 2003;

Guarner and Malagelada, 2003; Hans et al., 2000; Videla et al., 1994), impairment of IFN dependent mϕ activation, NK cell priming and mϕ activation during virus infection (Abt et al., 2012; Ganal et al., 2012). There are also decreased numbers of Th17 cells in the LP and a concomitant increase in $Foxp3^+$ Treg cells. Antibiotic treatment also decreases Paneth cell function and MHC II expression in the small intestine (Ivanov et al., 2008; Schumann et al., 2005). Interestingly, a recent report has suggested that modulation of the intestinal microbiota by antibiotic treatment of pregnant mice can have longterm effects on the offspring, impairing their antibody production (Lamouse-Smith et al., 2011).

Interestingly it has also been reported that colonic $CD11b^+$ $CD11c^-$ MPs from GF mice produce less IL10 than their conventional counterparts and are fully responsive to LPS stimulation, although the exact nature of these cells was not defined precisely (Ueda et al., 2010). Furthermore, these effects are only partial and subsequent work suggested that they were not dependent on the TLR signalling adapter MyD88, making these effects difficult to interpret mechanistically (Rivollier et al., 2012). Although all those defects caused by lack of the microbiota can be reversed by colonisation with normal commensal bacteria, it has been suggested that this must occur within a narrow time window after birth, as reconstitution of GF mice can restore innate immune responses when given during the first week of age, but not at 5 weeks of age.

1.9 Modulation of immune responses by the microbiota

The wider impact of commensal microbes in health and disease is highlighted by the hygiene hypothesis. First put forward by Strachan, this proposes that the reduced number of microbes found in the cleaner environment of industrialised countries, together with the wider use of antibiotics has led to an over-reactive immune system (Strachan, 1989). This theory is supported by evidence that the incidence of allergy, IBD and autoimmune diseases has increased dramatically in industrialised countries in the last 50 years. The immune response of newborns is characterised by a bias towards a T-helper-2 (Th2) cytokine profile (Rowe et al., 2000), the kind of response which causes allergic diseases, such as asthma and atopic dermatitis. However, once the

newborn gut has been colonised with commensals and has been in contact with bacterial and food antigens, the cytokine profile normally reaches a more balanced Th1/Th2 state (Romagnani, 2004; Strachan, 1989). Consistent with the hygiene hypothesis, a number of reports highlight the proinflammatory effect of being brought up in a clean environment, as shown by delayed epithelial maturation, accumulation of DCs, Th17 cells and $CD4^+$ $CD25^+$ T cells, along with a concomitant decrease in $Foxp3^+$ Tregs. Additionally, animals reared in high hygiene conditions produced more type I IFN, IL22, and IL23 (Inman et al., 2010a; Lewis et al., 2012; Mulder et al., 2011). It is for this reason that abnormal microbial colonisation (dysbiosis) has been proposed to be a predisposing factor in atopic disease and it is assumed that analogous processes may be involved in susceptibility to Th1/Th17 driven inflammatory diseases such as IBD, rheumatoid arthritis and others (Seiderer et al., 2008; Siddiqui et al., 2010; Wu et al., 2010).

Not surprisingly, many of the immunomodulatory effects of the microbiota have been described in the intestine itself. These include decreased responsiveness to TLR ligands in LP mϕ, increased regulatory T cell development and skewed production of antibodies towards secretory IgA rather than IgG antibodies. More distally, it is now clear that the microbiota can impact on the immune response throughout the body, influencing the outcome of diabetes, atherosclerosis and viral infections (Abraham and Medzhitov, 2011; Abt et al., 2012; Sartor, 2008; Tlaskalova-Hogenova et al., 2011). Although the precise mechanisms that link individual bacterial species to different aspects of health and disease are mostly unclear, a well-known example is segmented filamentous bacteria (SFB). These were first discovered in studies of IgA production in mouse intestine (Jiang et al., 2004), but have received attention recently after studies showing that the numbers of Th17 cells in the intestine between mice from different suppliers correlated with the presence or absence of SFB (Denning et al., 2011; Ivanov et al., 2009). In accordance with this, monocolonisation of GF mice with SFB was then shown to produce an expansion of IL17 and IL22 producing $CD4^+$ T cells in the LP, as well as stimulating the production of secretory IgA. SFB driven expansion of Th17 cells and auto-antibodies has also been related to autoimmune arthritis (Chappert et al., 2013; Gaboriau-Routhiau et al., 2009; Wu et al., 2010). The specific mechanisms involved in these effects of SFB

are still to be defined, but have been associated with the production of serum amyloid A, which in turn may induce intestinal DCs to promote a Th17 cell environment (Ivanov et al., 2009). On the other hand, the administration of capsular polysaccharide A (PSA) derived from *Bacteroides fragilis* induces IL10 production together with reduction of IL17 and TNFα production by $CD4^+$ T cells (Mazmanian et al., 2008). Other studies have also shown that certain *Clostridia* species can induce the development of $Foxp3^+$ cells in mouse intestine (Atarashi et al., 2011) and more recently, similar organisms have been isolated from human intestine, generating Treg, IL10 production through TGFβ dependent mechanisms (Atarashi et al., 2013).

Other examples of organisms of this kind remain to be identified and although there are now several diseases which have been associated with dysbiosis of the microbiota, the role of individual organisms remains mostly unproven. There is evidence that patients with active IBD have imbalances in their commensal bacterial populations, with increased proportions of *Proteobacteria* and *Actinobacteria* and decreases in Firmicutes and Bacteroidetes (Frank et al., 2007). Whether these changes are cause or effect remains to be established. Some specific organisms that have been associated with Crohn's disease include *Mycobacterium paratuberculosis* and more recently, enteroadhesive *E. coli*, which has been shown to colonise the ileum of Crohn's disease patients (Barnich and Darfeuille-Michaud, 2007; Chiodini, 1989; Frank et al., 2007; Sartor, 2005). Additionally, deficiency of a member of the Firmicutes family *Faecalibacterium prautsnitzii* has been associated with higher risk of recurrence of ileal CD and this is consistent with *F. prautsnitzii* normally favouring IL10 production and reducing IL12 and IFNγ production by blood mononuclear cells. Finally, oral adiminstration of *F. prautsnitzii* reduces severity of TNBS (2,4,6-tinitrobenzene sulfonic acid) colitis (Sokol et al., 2008).

In all these cases, it has been difficult to prove whether the relevant organisms are acting as pathogens or simply reflect altered balance within the overall microbiota, or if their presence is a cause or an effect of the disease.

In summary, colonisation of the intestine is initiated at birth and has a profound influence on intestinal and systemic immune responses. However, the cellular mechanisms are still being explored and interestingly, little is known about how the microbiota affects intestinal mϕ behaviour, despite the proximity of these cells to the lumen and their clear role in dealing with local bacteria. Therefore one aim of my project was to use our refined analysis protocols to explore the influence of microbiota on mϕ development.

1.10 Chemokines

Chemokines are a family of small proteins (8-14 kDa) that coordinate leukocyte trafficking, adhesion and homing (Zimmerman et al., 2008; Zlotnik and Yoshie, 2000). Even though all chemokines share structural similarities, they can be classified into four subgroups according to the number and spacing of the first two cysteines in a conserved cysteine structural motif (C, CC, CXC and CX3C). They signal through G-protein-coupled receptors to stimulate a number of cellular responses, but are best known for their ability to induce migration of cells, which may be directional if a gradient is present (D'Haese et al., 2010). Originally, chemokines were described as attractants for leukocytes, therefore regarded as proinflammatory. However other chemokines were constitutively expressed in lymphoid and mucosal tissues and increasing evidence suggests chemokines may also be important in development and homeostasis (Kunkel et al., 2003; Nishimura et al., 2009).

Homeostatic chemokines are expressed constitutively in normal tissues and mediate migration of leukocytes in steady state, whilst inflammatory chemokines are upregulated in response to inflammation. In practice however, there may be overlap between these groups, with some chemokines having both homeostatic and inflammatory roles (Le et al., 2004). Chemokines play two roles in the extravasation of leukocytes from the bloodstream. First, chemokines presented on the surface of vascular endothelial cells induce increased affinity of leukocyte integrins on leukocytes, allowing them to bind more strongly to endothelial adhesion molecules inducing the cells to stop. Secondly, chemokines present in the tissue parenchyma attract leukocytes to move through the vascular endothelium into the tissues (Butcher and Picker, 1996; Johnson et al., 2005; MacDermott et al., 1998; Zlotnik and Yoshie, 2000).

Apart from the functions mentioned above, chemokines and their receptors can play an important role in mucosal immunity, influencing particularly the cell migration, or homing of effector/memory cells from regional lymph nodes to the mucosal-associated sites (Bono et al., 2007; Forster et al., 2008; Le et al., 2004). Several chemokines and their receptors have been associated with the promotion/regulation of homing mechanisms, examples

being CCR9-CCL25 (Rivera-Nieves et al., 2006), CCR10-CCL28 (Pan et al., 2000) and less gut homing specific, such as CCL5 and CCR7 (Thomas and Baumgart, 2011; Zimmerman et al., 2008). Amongst the chemokine receptors studied, it has been previously reported that CCR2 (CCL2 receptor) plays a key role in monocyte recruitment during inflammation and work from our lab has confirmed that this also happens in the intestine (Bain et al., 2013; Serbina and Pamer, 2006). Additionally it has been described that colonic mϕ express high levels of CX3CR1 (the CX3CL1 receptor), although more detailed information about the specific role of these chemokines in the intestine is required. Therefore my project focused on these two particular chemokine receptors

1.10.1 CCR2

CCR2 is a member of the CC chemokine family that is expressed as a cell surface G-protein linked receptor. The known ligands for CCR2 are CCL2 (MCP1), CCL7 (MCP3), CCL8 and CCL12, which can be produced by epithelial cells, endothelial cells and mesenchymal cells in response to activation by proinflammatory cytokines or stimulation via innate immune receptors (Rollins and Pober, 1991; Serbina et al., 2012; Struyf et al., 1998; Tsou et al., 2007; Tsuboi et al., 2002). The best known role for CCR2 is in the accumulation of the $Ly6C^{hi}$ subset of monocytes at sites of inflammation, although the exact role of CCR2 in the entry of monocytes into tissues can be difficult to determine because CCR2 plays a crucial role in the egress of these monocytes from BM (Boring et al., 1997; Engel et al., 2008; Serbina et al., 2008; Si et al., 2010). CCR2 has also been shown to be required for recruitment of inflammatory monocytes to the intestine during *T. gondii*, *Listeria monocytogenes* infection and experimental colitis (Platt et al., 2010; Serbina et al., 2008; Serbina and Pamer, 2006). As noted above, the idea that CCR2 dependent accumulation of monocytes is only important in intestinal inflammation has been challenged by the recent work in our laboratory which indicates that $CCR2^{+}$ $Ly6C^{hi}$ monocytes appear to replenish steady state intestinal mϕ (Bain et al., 2013). This is supported by other work showing that the accumulation of IL10 producing intestinal mϕ in normal intestine is dependent on CCR2 and its ligand CCL2 (Feterowski et al., 2004). More recently it has also been suggested that CCR2 dependent monocytes actually

play a protective role in the intestinal inflammation associated with *T. gondii* infection, by encouraging tissue repair and inhibiting pathogenic neutrophil activity (Grainger et al., 2013). Thus the role of CCR2 in regulating intestinal mϕ recruitment and function remains uncertain. Furthermore it is unknown if CCR2 plays a role throughout life, or if the possible involvement of non BM-derived precursors in early tissue mϕ development might overcome a need for CCR2. Finally other receptors such as CCR1 and CCR5 have been implicated in monocyte recruitment (Lebre et al., 2011; Tokuyama et al., 2005). The effects of CCR2 or other mechanisms have never been examined in neonatal intestine and this was one of the aims of my project.

1.10.2 CX3CR1

The CX3CL1/CX3CR1 axis has been implicated in a number of models of inflammation, pain, cancer, neurodegenerative diseases, pancreatic disease, fibrogenesis and even mood disorders (D'Haese et al., 2010; D'Haese et al., 2012).

CX3CR1 is the only member of the CX3CR family and its ligand is CX3CL1 (fractalkine). CX3CL1 can be produced as a membrane-bound chemokine, in which a chemokine/mucin hybrid domain is linked to a transmembrane domain, or as a soluble molecule following its cleavage from the cell surface by ADAM10 and ADAM17/TACE (tumour-necrosis factor alpha converting enzyme) during inflammation (Andrzejewski et al., 2010; Bazan et al., 1997; Garton et al., 2001; Hundhausen et al., 2003; Pan et al., 1997; Tsou et al., 2001). The membrane-bound form of CX3CL1 is expressed by epithelial cells in the lung, bronchus and intestine, as well as by tubular and glomerular epithelial cells in the kidney and by vascular endothelial cells (Durkan et al., 2007). Its production by epithelia can be increased by stimulation with pro-inflammatory cytokines, such as TNFα (D'Haese et al., 2010; Fong et al., 1998; Sans et al., 2007).

Regarding mucosal immunity, it is believed that membrane-bound CX3CL1 acts as an adhesion molecule, promoting the local retention of receptor bearing leukocytes and the formation of TEDs by intestinal mϕ (Ancuta et al., 2003; Imaizumi et al., 2004; Muehlhoefer et al., 2000; Niess et al., 2005;

Owlasiuk et al., 2009). Additionally, reports suggest that inflammation can enhance the expression of the membrane bound form of CX3CL1. *In vitro* stimulation of human intestinal microvascular endothelial cells with TNFα and IFNγ enhances CX3CL1 expression and clinical studies have shown that increased CX3CL1 mRNA expression in inflamed lesions of Crohn´s disease (Nishimura et al., 2009; Sans et al., 2007) and IL8 induces increased expression of mRNA for CX3CL1 by a colonic epithelial cell line (Brand et al., 2006).

Conversely, the functions of the shed isoform of CX3CL1 remain poorly defined, especially in regard to mϕ or its role in mucosal immunity. However it is thought to induce chemotaxis of $CX3CR1^{+}$ leukocytes and is also associated with myositis (Suzuki et al., 2012). It may promote survival of $Ly6C^{lo}$ blood monocytes (Kim, 2011; Landsman et al., 2009) and it has recently been reported to be necessary for neuroprotection in a model of Parkinson's disease, while its presence has been associated with mild to moderate Alzheimer's disease (Kim, 2011; Kim et al., 2008; Morganti et al., 2012).

CX3CR1 is considered to be a myeloid specific marker, being present no only on monocytes or intestinal macrophages, but also in microglia in the central nervous system, some DCs and NK cells (Fong et al., 1998; Imai et al., 1997; Kim, 2011). Very interestingly, one of the most characteristic features of mature intestinal mϕ is their expression of very high levels of CX3CR1 (Bain et al., 2013; Cerovic et al., 2013; Hamann et al., 2011; Kim, 2011; Mionnet et al., 2010), although its precise role in the intestine has yet to be defined. The presence of $CX3CR1^{+}$ cells correlates with increased risk of relapse in breast cancer patients (Andre et al., 2006) and expression of CX3CL1 by local vascular cells may promote tumour development by inducing angiogenesis via a VEGF-A/KDR (kinase insert domain receptor)- dependent pathway (D'Haese et al., 2010; Ryu et al., 2008).

Despite the high expression of CX3CR1 by steady state intestinal LP mϕ, little is known about its role in the function of these cells. Most evidence from models of colitis suggests that the CX3CL1-CX3CR1 axis plays a proinflammatory role in the intestine (Kayama et al., 2012; Kostadinova et

al., 2010; Niess and Adler, 2010). However, conflicting data has shown that CX3CR1 KO mice are actually more susceptible to colitis (Kim, 2011; Medina-Contreras et al., 2011), and these mice are also resistant to the induction of oral tolerance secondary to a failure of LP mϕ to produce IL10, needed for the secondary expansion of $Foxp3^+$ Tregs in the mucosa (Hadis et al., 2011). In view of this lack of information and contradictory findings, one of my project aims was to examine how CX3CR1 influenced mϕ populations in the intestine and to investigate the effects of CX3CL1 on mϕ function.

1.11 Thesis aims

It is clear that although the development and functions of intestinal macrophages depend on a wide array of local factors, much remains to be determined about their origin and the regulatory mechanisms involved.

Thus, the central aim of this thesis was to gain knowledge about colonic macrophage development, by following their numbers, phenotype and functions from just before birth until adulthood. In order to do this, the experiments shown in Chapter 3 adapted techniques which had been established in the laboratory for isolating and characterising mϕ from adult intestine and analysed neonatal mϕ using multi parametric flow cytometry and real time quantitative PCR. In addition, I examined the relative contributions of foetal precursors and classical monocytes to the origin of intestinal mϕ, using fate mapping models and CCR2 deficient mice. In Chapter 4, I then explored how colonic macrophages were influenced by the microbiota, first by treating adult mice with broad-spectrum antibiotics, and then using germ free mice. Finally in Chapter 5, I investigated the role of CX3CL1 and its receptor on macrophage function during steady state and inflammatory conditions. I also performed *in vitro* analysis of bone marrow-derived macrophages co-cultured with cell lines expressing either the soluble or membrane bound form of CX3CL1 to assess how the chemokine influenced the activation status of macrophages.

Chapter 2
Materials and methods

2.1 Mice

All the mice used were on C57/Bl6 background unless stated otherwise. All experiments were carried out according to UK Home Office regulations.

$CX3CR1^{GFP/GFP}$ mice (Jung et al., 2000) were originally obtained from Professor William Agace (Lund University, Sweden), bred and kept at the University of Glasgow Veterinary Research Facility or the Central Research Facility and maintained on conventional diet until use.

CCR2 null mice (Boring et al., 1997) were kindly provided by Dr Robert Nibbs (University of Glasgow) and originally obtained from Jackson Laboratories (Maine, USA). 6-8-week-old WT mice for the oral priming experiments were purchased from Harlan UK (Bicester, Oxfordshire).

For studies on foetal or neonate animals, $CX3CR1^{GFP/+}$ litters were obtained after mating a $CX3CR1^{GFP/GFP}$ male with C57/Bl6 females. For timed pregnancies, mice were mated in harem system and presence of vaginal plug was considered as gestation day 0.5.

$Csf1r^{mer\text{-}iCre\text{-}Mer}$; $Rosa^{LSL\text{-}YFP}$ and Flt3-Cre; Rosa26-YFP mice were kindly provided by Professor Frederic Geissmann's lab (King's College London, UK).

Germ free mice and their conventional counterparts were all in the C57/Bl6 background with the exception of one set of 3-week-old mice, which were on a Rag-deficient background. All animals were kindly provided by Dr David Artis' lab (University of Pennsylvania, USA).

2.2 Treatment of mice with antibiotics

For the simple antibiotics scheme mice received 50mg/kg Meropenem and Vancomycin (both from Hospira, UK Limited) plus artificial sweetener (Sweetex, Reckitt Benckiser Household, UK) in drinking water for different periods of between 10 and 22 days. For the broader scheme, 500mg/kg ampicillin, gentamicin, metronidazole, neomycin (Roche) and vancomycin

(250mg/kg) were administered to mice for either 10 or 21 days. Control mice received sweetened water only. Antibiotic solutions were made up immediately before giving use and were replaced every other day.

2.3 Isolation of colonic lamina propria cells

Mice were culled by cervical dislocation (or with CO_2 overdose when blood was collected), colons were carefully removed and soaked in non-sterile PBS. Residual fat and faeces were removed, the colons opened longitudinally and washed in Hank's Balanced Salt Solution (HBSS) 2% FCS (Sigma) and ~5mm segments cut. The segments were placed in 10ml of HBSS 2% FCS at 4ºC for storage, before being shaken vigorously and supernatants discarded by passing them through nitex mesh (Cadisch, London). The pieces of colon were then incubated in 10-15ml of HBSS 1mM EDTA in a shaking incubator at 37ºC for 15 min. After incubation, the supernatants were discarded, the samples were rinsed with pre-warmed HBSS and then incubated further 30 min. Next, the colon pieces were rinsed again before being incubated in complete RPMI 1640 (2mM L-glutamine, 100µg/ml penicillin, 100µg/ml streptomycin, 1.25µg/ml fungizone, and 10% FCS) containing 0.85mg/ml collagenase V (Sigma), 1.25mg/ml collagenase D (Roche), 1mg/ml Dispase (Gibco) and 30µg/ml Dnase (Roche) for another 25-45 min with constant observation. To ensure complete digestion, the samples were shaken vigorously every 5-10 min and the resulting cells were passed through a 40µm cell strainer (BD, Biosciences), centrifuged at 400*g* at 4ºC for 5 min, resuspended in FACS buffer, counted and kept at 4ºC until use. If necessary, the enzymatic digestion step was repeated in order to achieve proper tissue disruption. For isolation of LP cells from 7-day-old or younger mice, the guts were not opened nor emptied before digestion due to their size and fragility.

2.4 Generation of bone marrow-derived macrophages (BMM)

Bone marrow (BM) was flushed out of the femurs and tibiae of healthy adult mice in RPMI 1640 (Gibco BRL, Paisley, Scotland) using a syringe and a 26G needle. The BM cells were transferred into a sterile 15ml tube and counted using a haemocytometer and phase contrast microscope. In some cases, erythrocytes were removed using red blood cell lysis buffer (Sigma). Next,

1ml of cell suspension containing $3x10^6$ cells was transferred into 90cm Petri dishes (Sterilin, UK) and cultured in complete RPMI 1640 medium, plus 10% M-CSF (supernatant from the L929 fibroblast cell line) at 37ºC in 5% CO_2. After three days, the medium was supplemented with 5ml of CRPMI plus 2ml of M-CSF and incubated for 3 more days. On day 6, non-adherent cells were discarded and adherent cells were harvested by adding 1mM EDTA/PBS for 5 min and then displacing them with cell scrapers (Costar). The resulting cells were then washed before use and were tested for viability and presence of F4/80 and CD11b by flow cytometry.

2.5 CX3CL1-expressing HEK cells

Human embryonic kidney cell lines (HEK293) modified to express either membrane-bound or soluble CX3CL1, as well as wild type HEK cells were kindly provided by Professor Andreas Ludwig (Aachen University, Germany) (Andrzejewski et al., 2010). Due to their original transfection with lipofectamin, the presence of 500µg/ml geneticin (Gibco, UK) in DMEM 10% FCS selects only cells with stable expression CX3CL1 and cells cultures had to be allowed to grow for at least two weeks before working with each newly-defrosted aliquot.

2.6 Culture of BMM with LPS and FKN

BMM suspensions at $1x10^5$ or $1x10^6$ cells/ml of CRPMI were cultured in ultra-low attachment 24-well plates (Costar) in the presence of different concentrations of recombinant fractalkine (rCX3CL1; R&D Systems) and *S. tyhpimurium* LPS (Sigma), for varying times before being harvested and assessed for viability and expression of CD40, CD80, CD86, MHC II and CX3CR1 by flow cytometry. Culture supernatants were collected and stored at -20ºC until used for measurement of cytokines by ELISA.

2.7 Co-culture of BMM with CX3CL1-expressing HEK cells

HEK cells were used at decreasing concentrations, starting at $1x10^6$. Conventional or CX3CL1 expressing HEK cells were cultured in 24-well low-adherence plate overnight before BMM were added and incubated for a

further 24h. Next, 100ng/ml of LPS was added to each well for a final period of 24h and the BMM analysed for viability, phenotype and cytokine production as described above.

2.8 Measurement of antigen-specific proliferative and cytokine responses *in vitro*

Single cell suspensions were obtained by mashing spleen and MLN through sterile nitex mesh in RPMI 1640 medium. After washing by centrifugation at 400*g* for 5 min at 4ºC, the cells were resuspended in CRPMI, counted, adjusted to $1x10^6$ cells/ml and 200µl added in triplicate to 96-well round-bottomed plates in the presence or absence of 500µg/ml OVA (Sigma) or 1µg/ml anti-CD3 and anti-CD28 (both from BD, Biosciences). After 48h culture at 37ºC, ~200µl supernatant was collected and stored at -20ºC for measurement of cytokines by ELISA and the medium was replaced. To measure proliferative activity, cells were cultured for a total of 96 hr with 1µCi tritiated thymidine (3H-TdR) (Western Infirmary radionucleotide dispensary) being added for the final 18 hours of culture. Cellular DNA was then harvested onto glass fibre filter mats (Wallac, Perkin Elmer, UK) and thymidine uptake was measured using a scintillation counter.

2.9 Measurement of cytokines by ELISA

Immulon 4 plates (Corning) were pre-coated with 1µg/ml purified anti-IL-6 or 2µg/ml anti-TNF-α (both from BD Biosciences, Table 2.1) capture antibodies in carbonate-bicarbonate coating buffer (Sigma) and incubated at 4°C overnight. The plates were washed three times with PBS/0.05% Tween 20 (Sigma), 200µl of blocking buffer (PBS/10% FCS) was added to each well and the plates incubated for 1h at 37°C. After three more washes, serial dilutions of standards and samples were incubated for 2h at 37°C, before the plates were washed again and incubated with 50µl of biotinylated anti IL-6 (1µg/ml) and anti TNF-α (2µg/ml) detection antibodies (BD Biosciences, Table 2.1) for 1h at 37°C. The plates were then washed and incubated with 1:1000 dilution of extravidin-peroxidase (Sigma) for 40 min. After washing, the plates were developed using 50µl of tetramethylbenzidine (TMB) substrate (KPL) and

stopped by adding 1N sulphuric acid. Optical densities were then obtained using a Dynex MRX TC Microplate reader at 450nm wavelength.

2.10 Measurement of OVA-specific antibodies and total immunoglobulins in serum by ELISA

Blood samples were centrifuged at 13000*g* at 4ºC for 20 min, serum collected and stored at -20ºC until use. To measure OVA specific antibodies by ELISA, flat-bottomed Immulon 96-well plates were coated with 10µg/ml OVA in 50µl PBS coating buffer overnight at 4ºC. For detection of total IgG and IgA, plates were coated with appropriate coating antibodies (Table 2.1). The plates were then washed with PBS Tween (0.05%) and blocked with PBS 3% BSA for 1 hour, before being washed again and doubling dilutions of serum samples added, followed by double serial dilutions. After incubating overnight at 4ºC, the plates were washed and 75µl biotin-conjugated detection antibodies were added at the appropriate concentration (Table 2.1) and incubated at 37ºC for one more hour. After washing, 50µl of 1:1000 extravidin peroxidase (Sigma) were added to each well for 45-60 min at 37ºC. Finally, plates were washed and developed by adding 50µl TMB, followed by 50µl 1N sulphuric to stop the reaction and the plates were read at 630nm using the microplate reader (Dynex).

2.11 Measurement of OVA-specific and total IgA in faeces

Faeces were removed from colon into ice-cold protease inhibitor cocktail (complete mini, Roche Diagnostics, Germany) PBS 50mM EDTA. After centrifugation at 1500*g* for 10 min, the supernatants were transferred to fresh 1.5ml tubes and 10µl of 100mM phenylmethylsulfonyl (PMSF; Sigma) in 95% ethanol was added followed by centrifugation at 14000*g* for 30min at 4ºC. Finally, 10µl PMSF solution, 10µl of 1% sodium azide (Sigma) and 50µl FCS were added to the resulting supernatants and were stored at -20ºC until used. Total and OVA specific IgA levels were measured by ELISA as described above.

Table 2.1. Antibodies used for measurement of antibodies in serum and faeces

Use	Antibody	Capture/detection	Working concentration	Source
Total **IgG**	Anti mouse IgG (Fc specific) Alkaline phosphatase ab	Capture	1:40000	Sigma
Total & OVA specific **IgG**	Anti mouse IgG (Fab specific) biotin ab (produced in goat)	Detection	1:200000	Sigma
Total **IgA**	Purified rat anti mouse IgA	Capture	1:500	BD Biosciences
Total & OVA specific **IgA**	Biotin rat anti-mouse IgA	Detection	1:500	BD Biosciences
OVA specific **IgG1**	Biotin rat anti mouse IgG1	Detection	1:16000	BD Biosciences
OVA specific **IgG2a**	Biotin rat anti mouse IgG2a	Detection	1:1000	BD Biosciences

Use	Antibody	Capture/detection	Working concentration	Source
IL6	Purified rat anti mouse IL6	Capture	1:25000	BD Pharmigen
IL6	Biotin rat anti mouse IL6	Detection	1:25000	BD Pharmigen
TNF α	Purified hamster anti mouse	Capture	1:12500	BD Biosciences
TNF α	Biotin human anti mouse	Detection	1:12500	BD Pharmigen

2.12 Induction of DSS colitis

Mice were fed 2% DSS in their drinking water for up to 8 days and the disease progression monitored by measuring weight loss, clinical score (Table 2.2) and colon length. In accordance with the Home Office regulations, mice were sacrificed if they lost >20% of their original body weight.

Table 2.2. Points system for evaluation of DSS induced colitis severity

Score	% Weight loss compared to steady state	Rectal bleeding	Stool
0	No weight loss	None	Well formed pellets
1	1-5	Blood traces in faeces	Well formed pellets
2	5-10	Blood stains in bedding and cage	Softer pellets
3	10-15	Blood stains around anus	Pasty faeces adhered to anus
4	15-20	Gross bleeding	Diarrhoea

2.13 Flow cytometry

Surface staining. 1-5x10^6 cells were added to FACS tubes and Fc receptors blocked by incubating with a 1:200 dilution of purified anti-mouse CD16/CD32 (Fc block, BD Biosciences) and incubated for 20 min at 4ºC. Next, cells were washed with FACS buffer, and the incubated for 20 min at 4ºC with relevant fluorochrome-conjugated antibodies, as detailed in Table 2.3. Cells were then washed in FACS buffer twice before be acquired on LSRII or AriaI (BD Bioscience).

Intracellular staining. For assessment of intracellular cytokine production, 4x10^6 cells in 1ml were incubated in sterile FACS tubes with 1μM monensin (Biolegend) and 10μg/ml Brefeldin A (Sigma) at 37ºC for 4.5 hrs. After washing with PBS, the cells were then incubated with 1:1000 dilution of violet viability dye (Molecular Probes; Life Technologies) or fixable viability dye eFluor 780 (eBioscience) in PBS in the dark at 4ºC for 30 min, washed in FACS buffer, blocked with Fc block and stained for surface markers as above, except that PBS was used instead of FACS buffer. After a further wash, the cells were fixed with 1% paraformaldehyde (or 4% if cells were obtained from CX3CR1$^{gfp/+}$ reporter mice) for 10 min, washed once in FACS buffer and once in Perm wash (PBS 0.1% NaN3 0.1% BSA 0.2% FCS 0.1% saponin). These cells were then blocked again with 1:200 Fc block in Perm stain buffer (PBS 0.1% NaN3 0.1% BSA 1% FCS 0.1% saponin) for 20 min at 4ºC, washed in Perm wash and stained for intracellular cytokines in 1:100 dilution Perm stain buffer. Finally, the cells were washed in Perm wash, resuspended in FACS buffer and analysed by flow cytometry.

For the assessment of Ki67 expression by colonic isolates, 3-4x10^6 cell suspensions were incubated with fixable viability and stained for the appropriate surface markers as described above. Next, cells were resuspended in 200μl of Foxp3 fixation/permeabilisation working solution and incubated overnight at 4ºC. Next, cells were washed in PermWash, Fc blocked for 15 min and then incubated with Ki67 fluorochrome-conjugated antibody for further 30min. Finally, cells suspensions were washed and resuspended in FACS buffer before acquisition.

Table 2.3. List of antibodies for surface and intracellular FACS analysis. Primary antibodies were conjugated to either FTIC, PE, PerCP-Cy5.5, PE-Cy7, APC, APC-Cy7, Alexa Fluor 700, BD Horizon V450, V500 or biotinylated and conjugated to Streptavidin Q-dot 605 (Molecular probes, Invitrogen UK).

Cellular marker	Working concentration	Isotype	Clone	Source
CD3α	1:200	Armenian hamster IgG1	15-2C11	BD biosciences
CD11b	1:200	Rat IgG2b	M1/70	BD biosciences
CD11c	1:200	Armenian hamster IgG1	HL3	BD biosciences
CD19	1:200	Rat IgG2a	1D3	BD biosciences
CD40	1:200	Rat IgG2a	3/23	BD biosciences
CD45	1:200	Rat IgG2a	30-F11	BD biosciences
CD45.2	1:200	Mu IgG2a	104	BD biosciences

Cellular marker	Working concentration	Isotype	Clone	Source
CD49b	1:200	Rat IgM	DX5	BD biosciences
CD64	1:200	Rat IgG1	X54-5/7.1	Biolegend
CD80	1:200	Armenian hamster IgG2	16-10A1	BD biosciences
CD86	1:200	Rat IgG2a	GL1	BD biosciences
F4/80	1:200	Rat IgG2a	BM8	BD biosciences
IL-10 (intracellular)	1:100	Rat IgG2b	JES5-16E3	BD biosciences
Ly6C	1:200	Rat IgM	AL-21	BD biosciences
Ly6G	1:200	Rat IgG2a	1A8	BD biosciences
MHC II	1:600	Rat IgG2b	M5/114.15.2	BD biosciences
Siglec F	1:200	Rat IgG2a	E50-2440	BD biosciences

2.14 Phagocytosis assay

The phagocytic activity of colonic isolates was assessed using pHrodo *E.coli* bioparticles (Molecular Probes, Life Technologies), with adaptations made to the manufacturer's instructions. Briefly, LP cells from neonate or adult CX3CR1$^{GFP/+}$ mice were stained for surface markers as described above, washed in FACS buffer and resuspended in 100µl CRPMI. After 15 min incubation on ice, 10µl of pHrodo *E. coli* bioparticles was added to each sample. For each biological replicate there were two conditions: one tube was left on ice (negative control), while the other was incubated at 37ºC for 15 min. Finally all samples were washed, resuspended and acquired in ice cold buffer C.

2.15 FACS purification of colonic CX3CR1^{hi} subpopulations

Neonate colonic LP cells were stained as described above in sterile conditions. CX3CR1 subsets were sorted using FACSAria I (BD Biosciences) on the basis of viable CD45^{+} Siglec F^{-} Ly6G^{-}, F4/80, CD11b and GFP expression.

2.16 Oral priming of mice

Mice were fed 10mg OVA with or without 10µg *Vibrio cholerae* toxin (CT; both from Sigma) by gavage curved shed tube on three occasions 7 days apart. Control mice were fed PBS alone. 7 days after the last feed, the mice were killed and blood collected by cardiac puncture and stored in Eppendorf tubes. Faecal samples were taken directly from the colon, and MLN and spleen were isolated.

2.17 DNA extraction

DNA was obtained from tail tips and extracted using DNeasy blood & tissue kit (Qiagen) following manufacturer's spin-column protocol. Briefly, 0.5cm collected tail segments received 180µl ATL buffer, 20µl proteinase K, mixed by vortexing and incubated overnight at 56ºC followed by adding 200µl buffer AL and further vortexing, samples then received 200µl absolute ethanol,

mixed, transferred into the DNeasy mini spin column and washed by centrifugation at 6000*g*. Samples in the column then received 500µl buffer AW2 before being centrifuged at 20000*g* for 3 min to get rid of the ethanol. Finally, columns were placed in a 1.5 ml collection tube 200µl elution buffer was added and incubated at room temperature for 1 min before centrifuging at 6000*g*. Flow through was then stored at -20ºC until use.

PCR was carried out using T professional thermocycler (Biometra, Denmark), adding 1µl 1:2 DNA to 0.4µl 10µM primers mix, 4µl 5X reaction buffer, 0.4µl dNTPs, 0.1µl Taq polymerase and 14.1µl nuclease free water (all from New England Biolabs). DNA amplification needed 94ºC 5min plus 35 cycles at 94ºC 30sec, 50ºC 30sec and 72ºC 1min, followed by 72ºC 10min and held at 4ºC.

PCR products were then run on a 2% agarose gel (Gibco) containing 100µg ethidium bromide (Sigma) in 1x TBE buffer in a gel tank, gel run for 45 min at 90V and analysed using the Gel Logic 200 imaging system.

2.18 RNA extraction

RNA was obtained from sorted CX3CR1^{hi} cells using the RNeasy Micro kit (Qiagen). Briefly, after cell suspensions were spun, cell pellets were loosened by flicking the collection tubes and 75µl of RLT buffer was added, mixed and homogenised by passing samples through a Qiashredder column and centrifuged for 2 min at full speed. Next, 75µl 70% ethanol was added, mixed and transferred to an RNeasy MinElute column placed in a fresh collection tube for a further centrifugation at 8000*g*, followed by washing with 350µl buffer RW1 plus further centrifugation at 8000*g*. Elute columns then received 10µl DNase I in 70µl buffer RDD and incubated at room temperature for 15min and washed with 350µl buffer RW1, centrifuged then washed again with 500µl buffer RPE and a final wash with 500µl 80% ethanol. Finally columns were dried by 5min centrifugation full speed and RNA eluted by adding 14µl of RNase-free water, spun at full speed for 1min and flow-through was collected. RNA concentration and purity were measured using Nanodrop 3300 (Thermo Scientific) and stored at -20ºC until use.

2.19 cDNA synthesis

cDNA was reverse transcribed from DNase-treated RNA using Superscript II Reverse Transcriptase (RT) (Invitrogen) according to the manufacturer's instructions on the T professional thermocycler. Briefly, RNA was added to 1µl 10mM dNTP mix, 1µl 10µM primer mix, and DEPC treated water in a nuclease-free microcentrifuge tube in a total volume of 10µl. RNA/primer mixture was then incubated at 65ºC 5min followed by chilling at 4ºC for at least 1 minute before adding a mixture of 2µl 10x RT buffer, 4µl 25mM $MgCl_2$, 2µl 0.1M DTT and 1µl 40U/µl RNaseOUT to make up to a total of 19µl and incubated at 42ºC 2min. Then 1µl of Superscript II RT was added to each tube, incubated at 42ºC for 50min, increased to 72ºC for 15min, before 1µl of RNase H was added for the final incubation at 37ºC for 20min. Samples were stored at -20ºC until use.

2.20 Quantitative real time PCR

Gene expression was measured by quantitative reverse transcription PCR using specific primers (Table 2.4) and Brilliant III Ultra Fast SYBR qPCR master mix (Agilent Technologies) and run on the 7500HT Real Time Fast system (Applied Biosystems). Each assay was performed with technical replicates, gene expression was normalised to Cyclophilin A (CPA) and the mean relative quantification was calculated using $2^{-\Delta\Delta CT}$. Melting curves were estimated to confirm the specificity of the amplification.

2.21 Analysis of CSF1r/YFP and Flt3/YFP reporter mice

Sample collection, CLP isolation and cell-surface staining were performed as described above at the Centre of Molecular & Cellular Biology of Inflammation, King's College London. FACS analysis was using a BD LSR II and a BD LSR Fortessa (both BD Biosciences). Both mice strains were generated and kept as described previously (Schulz et al., 2012).

2.22 Analysis of germ free mice

All experiments done on germ free mice were performed at David Artis' lab at the Perelman School of Medicine, University of Pennsylvania, USA. In order to assess the germ free (GF) status, in-house testing of fecal pellets from GF mice for culturable aerobic and anaerobic bacteria was performed every two weeks and quarterly testing at Charles River Animal Diagnostics (USA). FACS analysis was using a BD FACS Aria II (BD Biosciences).

2.23 Statistical analysis

Results are shown as means ±1 standard deviation (SD) unless stated otherwise and groups were compared using a Student's unpaired two-tailed t test. When comparing multiple groups, two-way ANOVA was performed, followed by a Bonferroni multiple comparison test. P values <0.05 were considered to be statistically significant.

Table 2.4. List of primers used for PCR and qPCR

Gene	Sense	Anti-sense	Reaction
CCR2	CTT GGG TGG AGA GGC TAT TC	AGG TGA GAT GAC AGG AGA TC	End point PCR
CD163	CCT TGG AAA CAG AGA CAG GC	TCC ACA CGT CCA GAA CAG TC	Q PCR
Cyclophilin A	GTG GTC TTT GGG AAG GTG AA	TTA CAG GAC ATT GCG AGC AG	Q PCR
IL-10	GCT CTT ACT GAC TGG CAT GAG	CGC AGC TCT AGG AGC ATG TG	Q PCR
TNF-α	ACC CTC ACACTC AGA TCA TCT TC	TGG TGGTTT GCT ACG ACG T	Q PCR

Chapter 3
Development of intestinal macrophages in early life

3.1 Introduction

The vast majority of studies of intestinal mϕ have focused on adult mice and little is known about these cells during development in early life. Given the recent interest in how the intestinal microbiota can influence immune responses and the fact that it becomes established soon after birth, it would seem important to know how the local mϕ population behaves during this period. One study has suggested anti-inflammatory mϕ are already present in human foetal intestine, but this has not been examined in mice (Maheshwari et al., 2011). Recent work in other tissues in mice has lead to the idea that there are two mutually exclusive mϕ populations with distinct origins. The majority comprise "resident" mϕ, which populate target tissues very early during development, self-renew after birth and are derived from prenatal precursors either in the yolk sac (YS) or foetal liver (FL) (Ginhoux et al., 2010; Schulz et al., 2012). A second pool of "inflammatory" mϕ derived from BM monocytes may be recruited into tissues in response to infection or tissue damage (Geissmann et al., 2010). None of these studies defining the prenatal origin of mϕ had examined the gastrointestinal compartment, and as discussed earlier, work going on in the lab when I started my project was suggesting that BM monocytes made a major contribution to the intestinal mϕ pool, even in steady state. Therefore I designed a series of experiments aimed at exploring mϕ ontogeny and behaviour early in life. In the first experiments, I examined if mϕ were already present in the newborn intestine and investigated how the populations changed during the process of natural colonisation with microbiota after birth and through weaning. I then went on to study directly the possibility that YS and/or FL derived precursors might contribute to the intestinal mϕ pool. When I began this work no methods were available to isolate and characterise intestinal mϕ in neonatal mice and therefore, in the first experiments, I had to optimise protocols for obtaining sufficient cells to do this reproducibly.

3.2 Intestinal mϕ populations can be found from before birth onwards

Because of the size of the neonatal mice and their colons (Figure 3.1), I had to adapt the isolation technique used in adults in terms of general tissue

handling, as well as the volumes and concentrations of reagents used. Having done this, I then combined the gating strategy routinely used in our laboratory (Bain et al., 2013) with one reported previously (Schulz et al., 2012), in which mϕ of YS or FL origin can be discriminated on the basis of their F4/80 and CD11b expression.

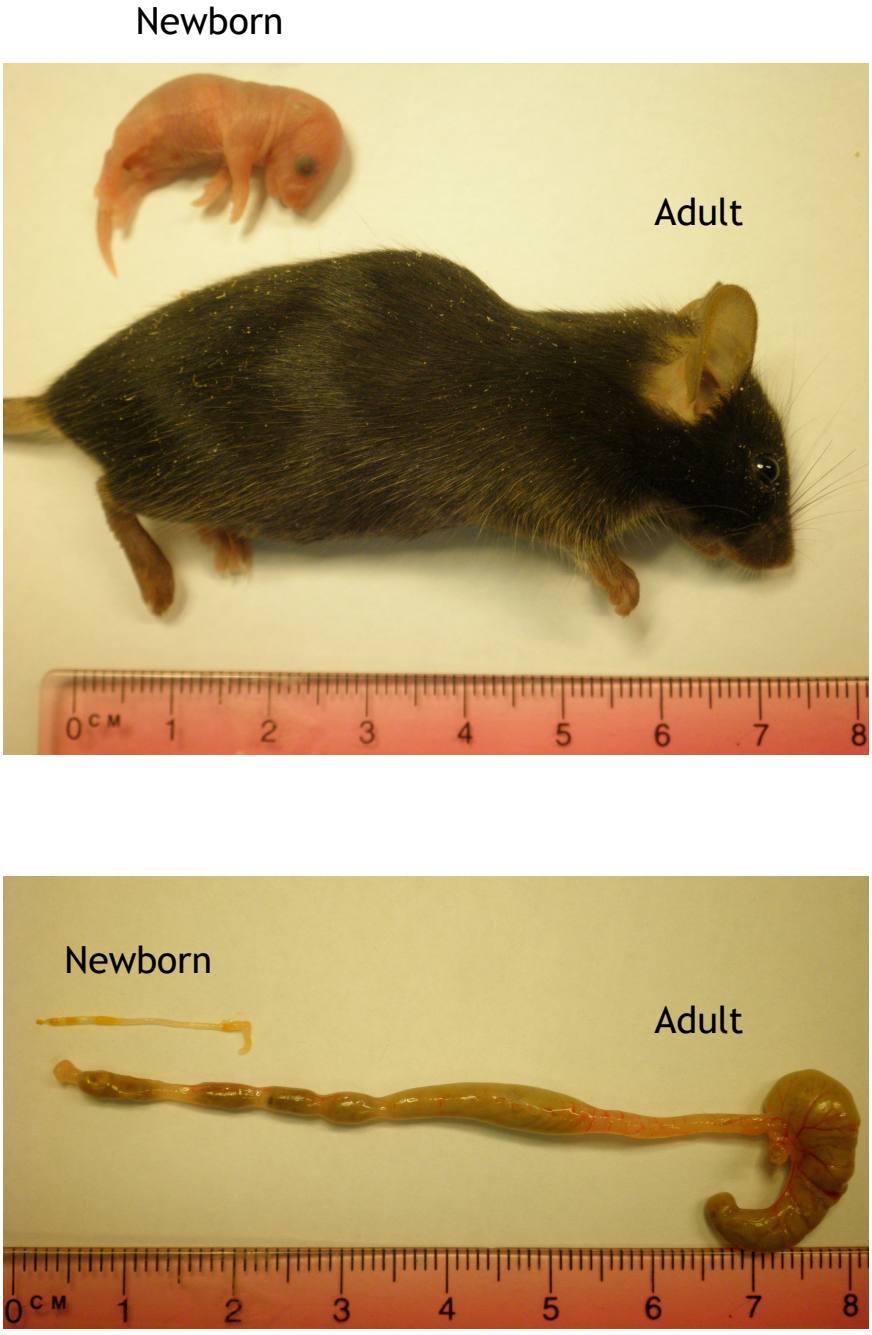

Figure 3.1. Representative appearance of newborn and adult mice (top panels), together with their large intestines (bottom panels).

First, using adult mice, I set out to establish the procedures. I selected single cells, followed by identification of live (7-AAD$^-$) CD45$^+$ leukocytes, and then excluded Ly6G$^+$ neutrophils Siglec F$^+$ eosinophils and F4/80^{lo} CD11c$^+$ DCs (Figure 3.2 A). This allowed me to identify two distinct populations of CD11b$^+$ putative mϕ lineage cells: F4/80^{hi} CD11b^{int} and F4/80^{lo} CD11b$^+$ (Figure 3.2 B). Consistent with previous work in our lab (Bain et al., 2013), the F4/80^{hi} CD11b^{int} populations in adults was homogenously Ly6C$^-$ MHC II$^+$, whereas the F4/80^{lo} CD11b$^+$ population was made up of 3 subpopulations: Ly6C^{hi} MHC II$^-$, Ly6C^{hi} MHC II$^+$ and Ly6C$^-$ MHC II$^+$, referred to as P1, P2 and P3 respectively (Figure 3.2 C). By using CX3CR1$^{GFP/GFP}$ mice, I could show that the F4/80^{hi} CD11b^{int} cells also expressed uniformly high levels of CX3CR1, consistent with them being mature mϕ, while F4/80^{lo} CD11b$^+$ were mostly CX3CR1^{int}, consistent with them being maturing monocytes/mϕ (Bain et al., 2013). There was also a small number of CX3CR1$^-$ cells whose nature is unclear (Figure 3.2 D).

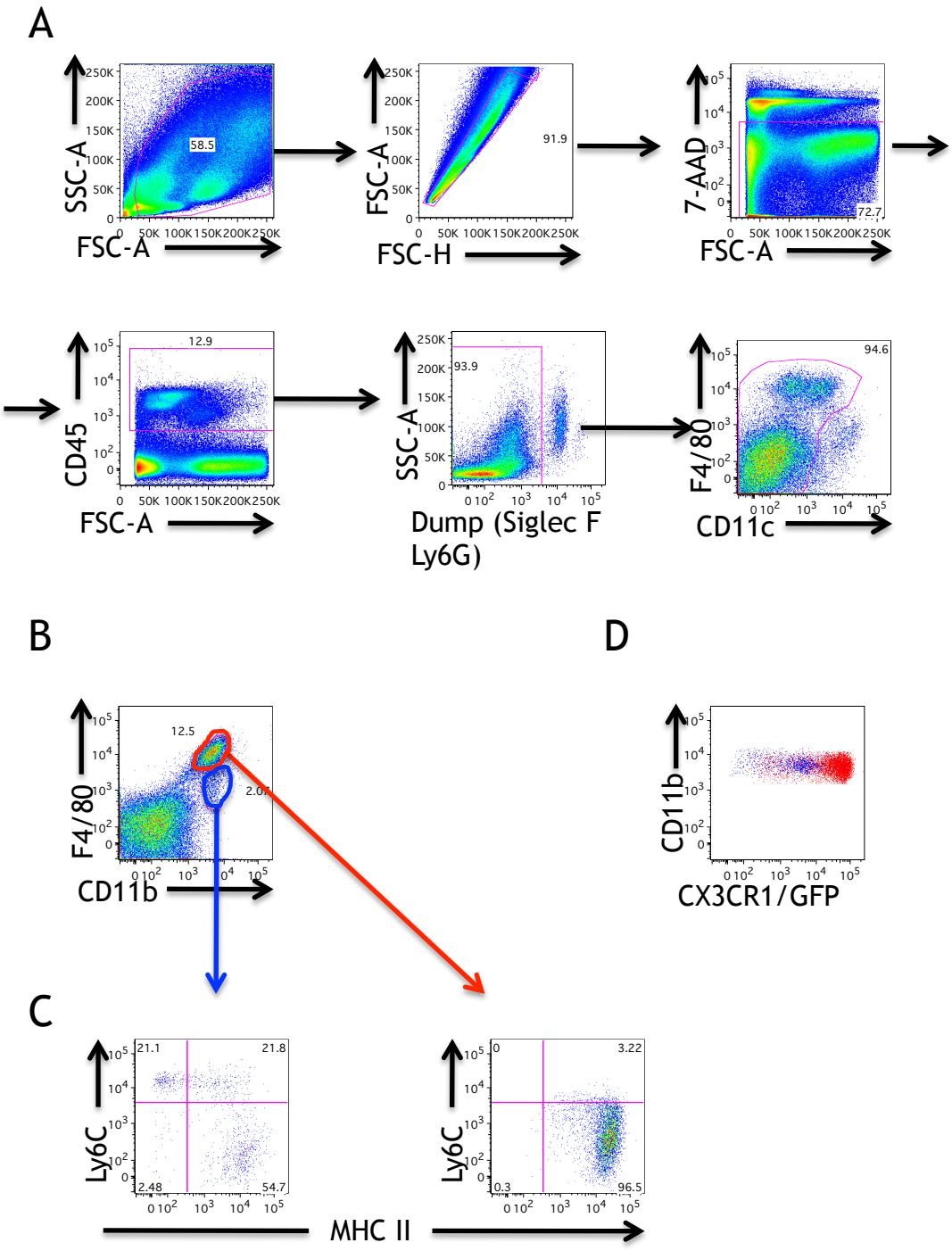

Figure 3.2. Characterisation of colonic macrophages in adult mice. A) Colonic lamina propria cells were isolated from the colon of CX3CR1$^{GFP/+}$ mice and single viable leukocytes (7-AAD^{-} CD45^{+}) were identified. After excluding granulocytes (Ly6G^{+} neutrophils and Siglec F^{+} eosinophils) and F4/80$^{lo/-}$ CD11c^{+} DCs, CD11b^{+} cells could be separated into F4/80^{hi} CD11b^{int} and F4/80^{lo} CD11b^{+} subsets (B). (C) Expression of Ly6C and MHC II by F4/80^{lo} (blue arrow) and F4/80^{hi} cells (red arrow). (D) In CX3CR1$^{GFP/+}$ mice, the F4/80^{hi} CD11b^{int} cells were mostly CX3CR1^{hi} (red), while the F4/80^{lo} cells were predominantly CX3CR1^{int}, plus a few CX3CR1^{-} cells.

3.3 Detailed comparison of adult and newborn colonic mϕ subsets

Having shown that I could define appropriate subsets of monocytes and mϕ in the adult intestine, I went on to analyse neonatal mice. I obtained an average of just over 1 million cells per gut from 1 day old (D1) CX3CR1$^{GFP/+}$ mice and as expected, the absolute numbers of leukocytes were considerably lower than in adults, and these made up a much lower frequency of the total yield. It was immediately obvious that the F4/80^{hi} CD11b^{int} and F4/80^{lo} CD11b^{+} subsets were much more distinct than in the adult, mainly due to the appearance of a clear population of F4/80^{hi} cells expressing intermediate levels of CD11b (Figure 3.3 A). As in the adult, the F4/80^{hi} cells were all CX3CR1^{hi}, while the F4/80^{lo} CD11b^{+} cells were mostly CX3CR1^{int} and again, this marker revealed a more clearly defined population in the neonate (Figure 3.3 C). However, unlike the adult intestine, ~70% of the neonatal F4/80^{hi} CD11b^{int} cells were MHC II^{-}, although they were mostly Ly6C$^{lo/-}$. A further major difference from the adult was that the F4/80^{lo} CD11b^{+} subset contained lower proportions of the Ly6C^{hi} MHC II^{+} and Ly6C^{-} MHC II^{+} subsets, while in parallel there were more Ly6C^{hi} MHC II^{-} and Ly6C^{-} MHC II^{-} amongst the F4/80^{lo} population in the neonate (Figure 3.3 B). Interestingly some of these subsets were present before birth, as shown by the analysis of 18.5-day foetal intestine, where there was already a small population of MHC II^{+} F4/80^{hi} mϕ (Figure 3.4). Thus cells with the phenotype of mϕ are present in the intestine even at birth, but they have some differences compared to what is seen in adults, such as a relative absence of MHC II and a population with lower levels of CD11b. Therefore I went on to explore when these cells acquired the adult characteristics.

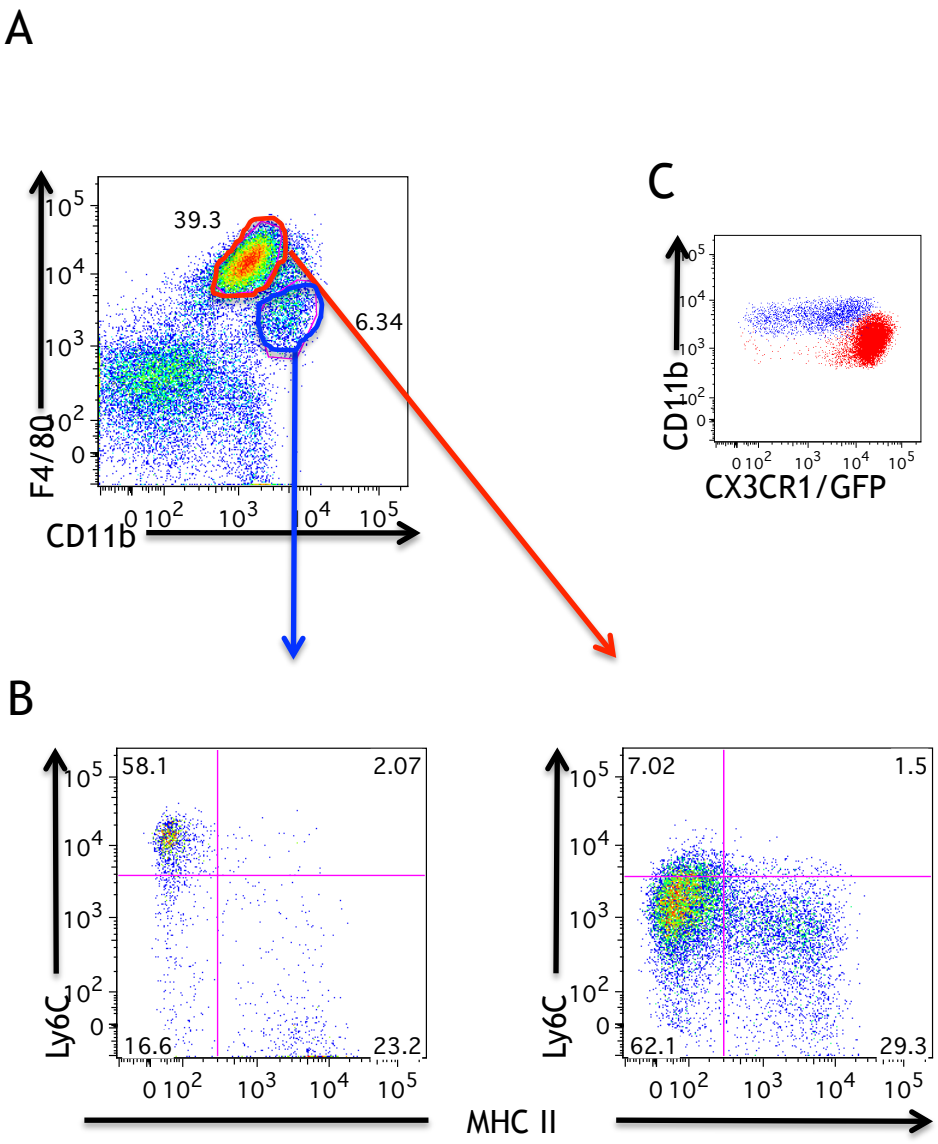

Figure 3.3. Characterisation of colonic macrophages in newborn mice. A) Colonic lamina propria cells were isolated from the colon of CX3CR1$^{GFP/+}$ newborn mice and single viable leukocytes (7-AAD^{-} CD45^{+}) were identified. After excluding granulocytes (Ly6G^{+} neutrophils and Siglec F^{+} eosinophils) and F4/80$^{lo/-}$ CD11c^{+} DCs, CD11b^{+} cells could be separated into F4/80^{hi} CD11b^{int} and F4/80^{lo} CD11b^{+} subsets. (B) Expression of Ly6C and MHC II by F4/80^{lo} (blue arrow) and F4/80^{hi} (red arrow) subsets. (C) In newborn CX3CR1$^{GFP/+}$ mice, all the F4/80^{hi} CD11b^{int} cells were CX3CR1^{hi} Ly6C^{-} with different levels of MHC II (red), while the F4/80^{lo} cells were predominantly CX3CR1^{int}, plus a few CX3CR1^{-} cells.

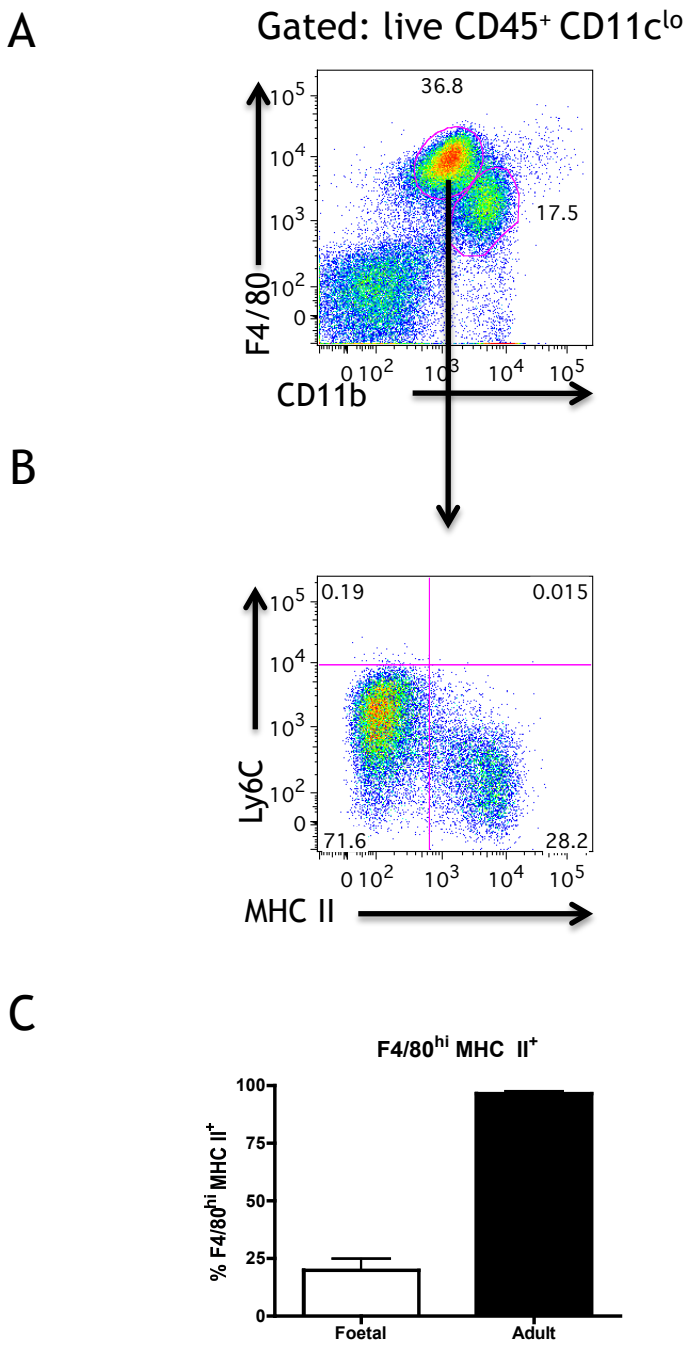

Figure 3.4. Characterisation of colonic macrophages in foetal mice. A) Colonic lamina propria cells were isolated from the colon of embryonic day 18.5 CX3CR1$^{GFP/+}$ mice and after selecting single viable leukocytes (7-AAD^{-} CD45^{+}) and excluding F4/80$^{lo/-}$ CD11c^{+} DCs, CD11b^{+} cells were separated into F4/80^{hi} CD11b^{int} and F4/80^{lo} CD11b^{+} subsets. (B) Representative FACS plot showing expression of Ly6C and MHC II by F4/80^{hi} cells. (C) Comparison of MHC II expression from F4/80^{hi} CD11b^{int} cells from intestine of foetal and adult mice.

3.4 Development of colonic mϕ during the neonatal period

To do this, I carried out an analysis of mϕ populations from birth until adulthood at 7 weeks of age. Although the total cell numbers I could isolate from each sample increased steadily throughout the period of the experiment, the proportion of $CD45^+$ leukocytes reached adult levels by 14 days of age (Figure 3.5 A & B). This translated into there being no major changes in the absolute numbers of leukocytes after a progressive increase from birth until the 3rd week of life (Figure 3.5 C). On the other hand, while the proportions of total $Ly6G^-$ Siglec F^- $CD11b^+$ cells declined gradually with age, the total numbers of these cells increased slightly during the 1st and again during the 2nd week of life, before increasing markedly to attain adult levels by 21 days of age (Figure 3.5 D & E). As noted earlier, newborn $CD11b^+$ cells divided clearly into $F4/80^{hi}$ $CD11b^{int}$ and $F4/80^{lo}$ $CD11b^+$ populations and these could be seen until adulthood (Figures 3.6 & 3.7). $F4/80^{hi}$ $CD11b^{int}$ cell numbers increased steadily with age, even though their proportions fluctuated on each time point (Figure 3.7 A). Notably, the separation between $F4/80^{hi}$ $CD11b^{int}$ and $F4/80^{lo}$ $CD11b^+$ populations became less distinct by 21 days, at which time the $F4/80^{hi}$ subset had also acquired the higher levels of CD11b seen in the adult (Figure 3.6 histogram). The $F4/80^{lo}$ subset was also present throughout, but fell in proportions during the 1st and 2nd weeks of life, before increasing back to adult proportions on day 21 (Figure 3.6 & 3.7 B).

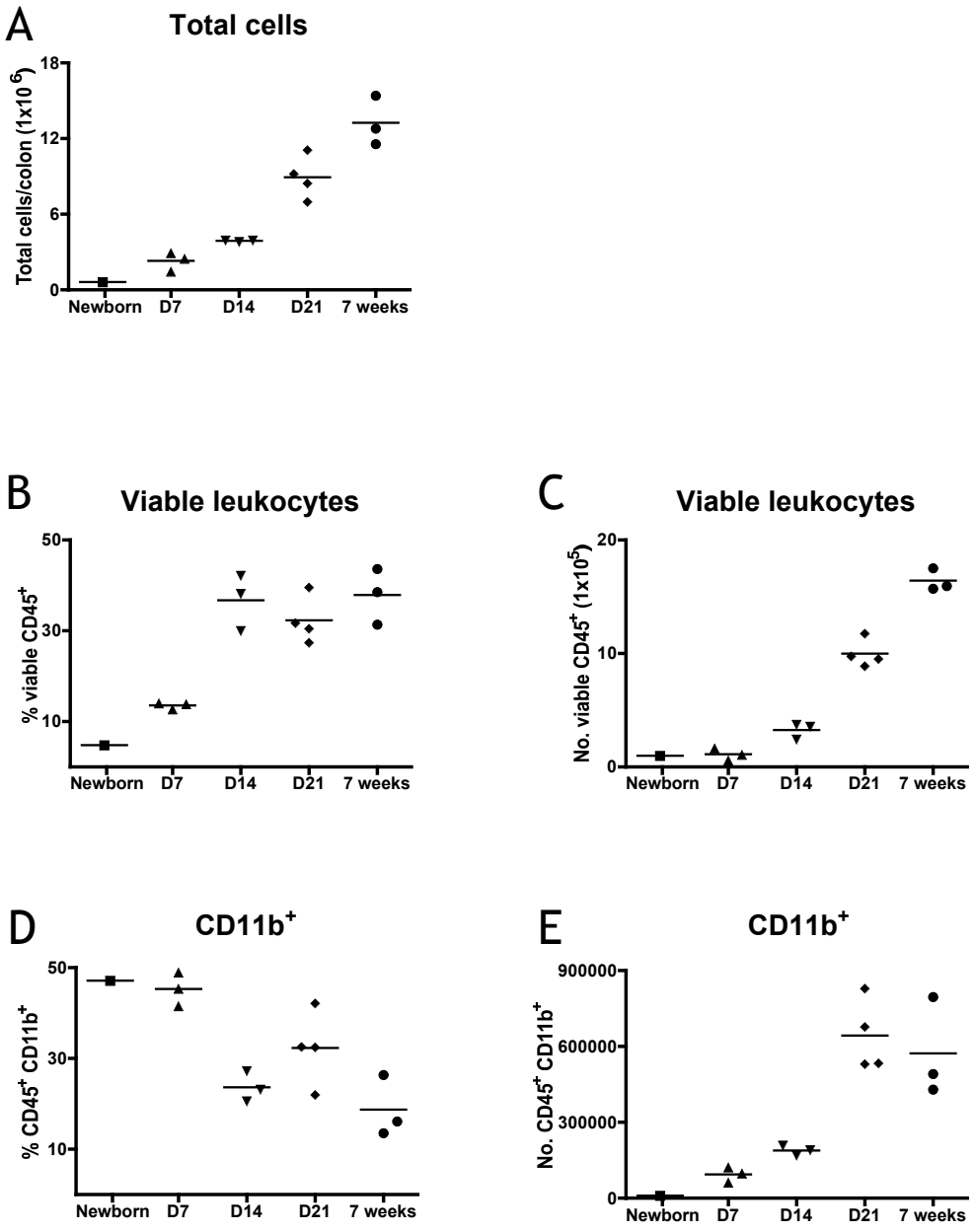

Figure 3.5. Development of leukocytes in colonic lamina propria. Total cell numbers (A), frequencies (B) and absolute numbers (C) of $CD45^+$ leukocytes from the colonic lamina propria of $CX3CR1^{GFP/+}$ mice of different ages from the day of birth until adulthood (7 weeks). (D) Proportions and numbers (E) of $CD11b^+$ cells amongst live leukocytes. Results are representative of at least 3 independent experiments.

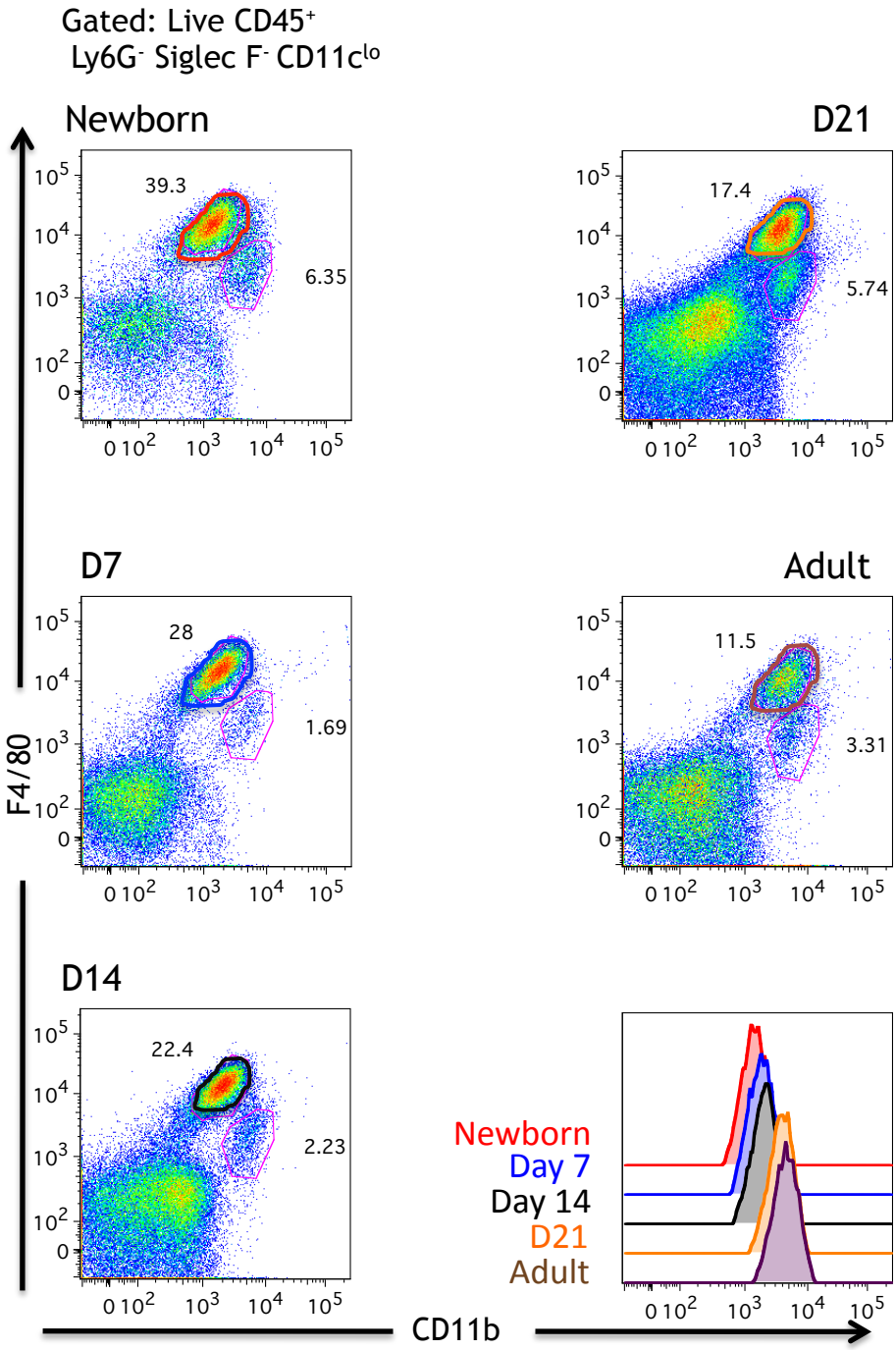

Figure 3.6. Development of macrophages in colonic lamina propria. Expression of CD11b and F4/80 by live gated CD45$^+$, excluding F4/80$^{lo/-}$ CD11c$^+$ DCs and Ly6G$^+$ Siglec F$^+$ granulocytes from the colon of CX3CR1$^{GFP/+}$ mice at different ages up until adulthood (7 weeks). Numbers show proportions of F4/80^{hi} CD11b^{int} and F4/80^{lo} CD11b$^+$ cells amongst total CD11b$^+$ cells, while the histogram shows the expression of CD11b on the F4/80^{hi} population at different ages. Results are representative of at least 3 independent experiments.

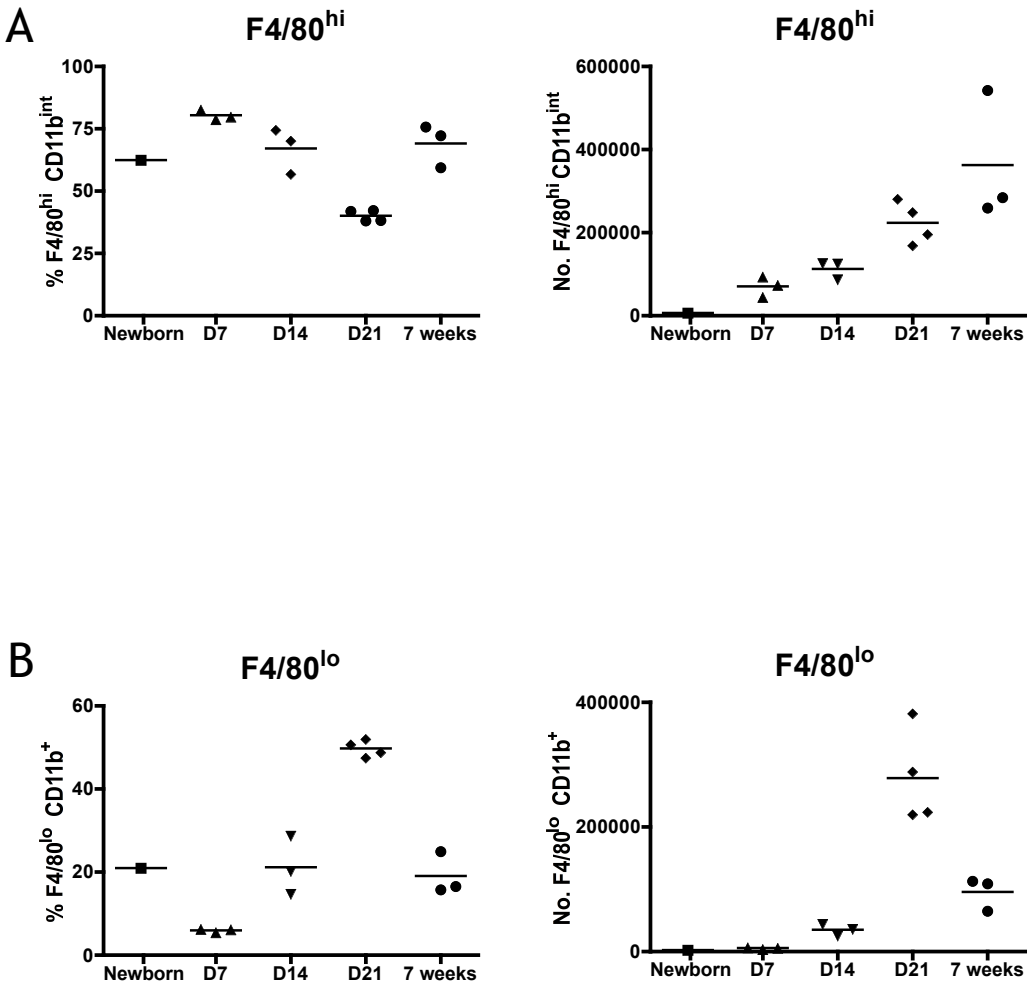

Figure 3.7. Development of macrophages in colonic lamina propria. Proportions (left panels) and absolute numbers (right panels) of F4/80^{hi} CD11b^{int} (A), and F4/80^{lo} CD11b^{+} (B) cells. Both F4/80 subsets were gated from live CD45^{+} CD11b^{+}, excluding F4/80$^{lo/-}$ CD11c^{+} DCs and Ly6G^{+} Siglec F^{+} granulocytes from colonic lamina propria of CX3CR1$^{GFP/+}$ mice of different ages up until adulthood (7 weeks). Results are representative of at least 3 independent experiments.

Next I assessed the age-related changes in more detail by analysing the mϕ subsets based on their expression of Ly6C and MHC II. As mentioned earlier, at birth the F4/80^{hi} (CX3CR1^{hi}) subset was Ly6C$^{lo/-}$ in newborn mice and only ~30% were MHC II^{+}. However, the proportion and absolute numbers of MHC II^{+} cells increased gradually from birth onwards and Ly6C expression was lost completely (Figure 3.8 and 3.10 D). In parallel, the proportions of Ly6C^{-} MHC II^{-} cells amongst this population decreased gradually, although their absolute numbers increased until 14 days of age before falling again (Figure 3.10 E). The F4/80^{lo} CD11b^{+} CX3CR1^{int} cells were mostly Ly6C^{hi} MHC II^{-}, with some Ly6C^{-} MHC II^{+} cells at birth (Figure 3.9) and there was a sharp drop in the proportions of Ly6C^{hi} MHC II^{-} cells at one week of age (Figure 3.10 A left). However the proportions of Ly6C^{hi} MHC II^{+} cells had increased again by 14 days of age, and reached their highest proportion at 21 days (Figure 3.10 B left). The size of the Ly6C^{-} MHC II^{+} cell subset also fluctuated from week to week, but it was the biggest cell fraction amongst F4/80^{lo} cells from the 2nd week onwards (Figure 3.9 and 3.10 C left). All the subsets of F4/80^{lo} CD11b^{+} cells showed a peak in their absolute numbers at 21 days of age, before falling again by 7 weeks of age (Figure 3.10 B-C right).

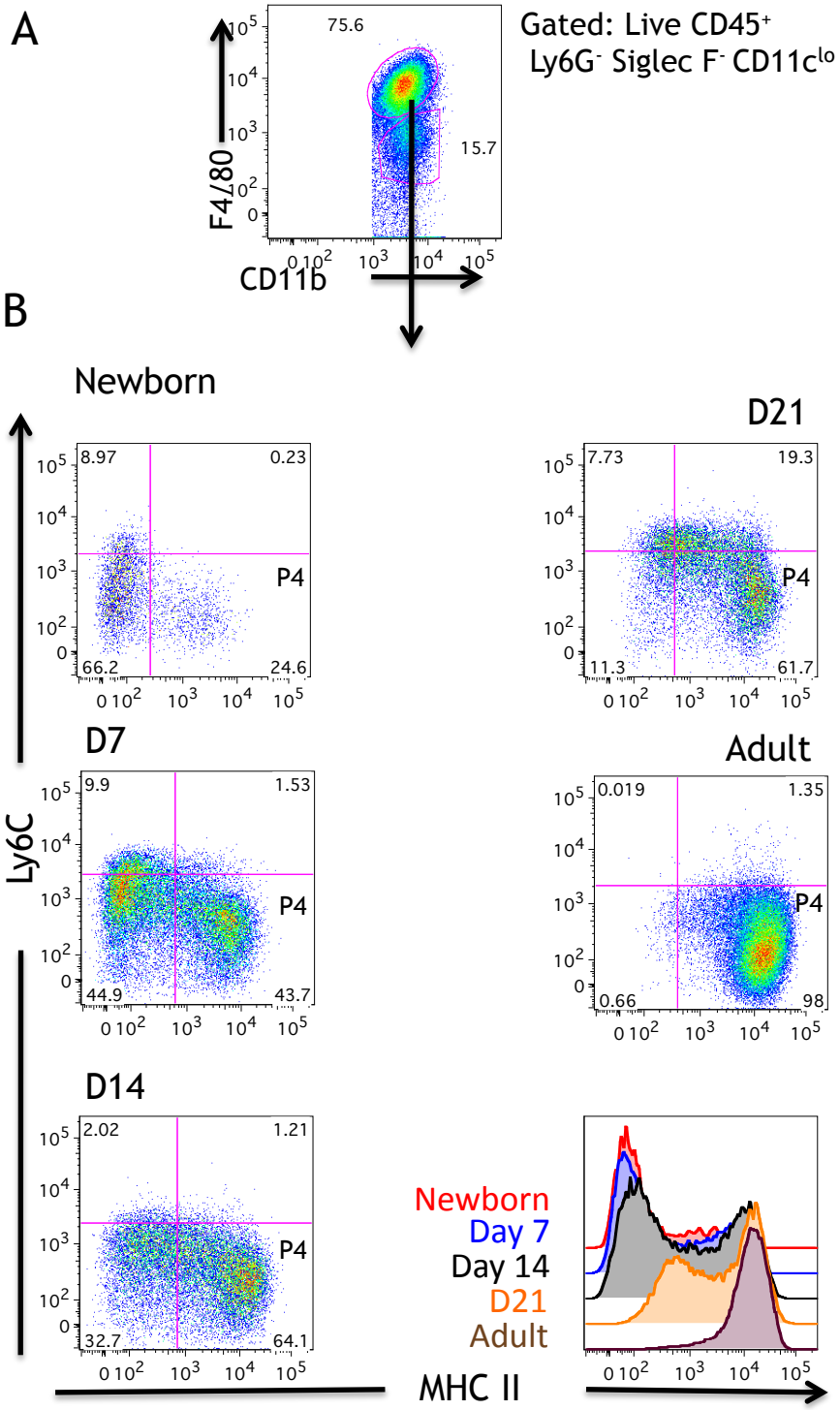

Figure 3.8. Development of macrophages in colonic lamina propria. Expression of Ly6C and MHC II by F4/80^{hi} CD11b$^{int/+}$ cells amongst live CD45^{+} CD11b^{+}, excluding F4/80$^{lo/-}$ CD11c^{+} DCs and Ly6G^{+} Siglec F^{+} granulocytes from colonic lamina propria of CX3CR1$^{GFP/+}$ mice of different ages up until adulthood (7 weeks). (A) Representative FACS plot from adult CLP. Numbers in FACS plots are the proportion of cells in Ly6C^{hi} MHC II^{-}, Ly6C^{hi} MHC II^{+}, Ly6C^{-} MHC^{+} (P4) and Ly6C^{-} MHC^{-} gates. Histogram shows expression of MHC II in the F4/80^{hi} CD11b^{int} subset at different ages. Data are representative of at least 3 independent experiments.

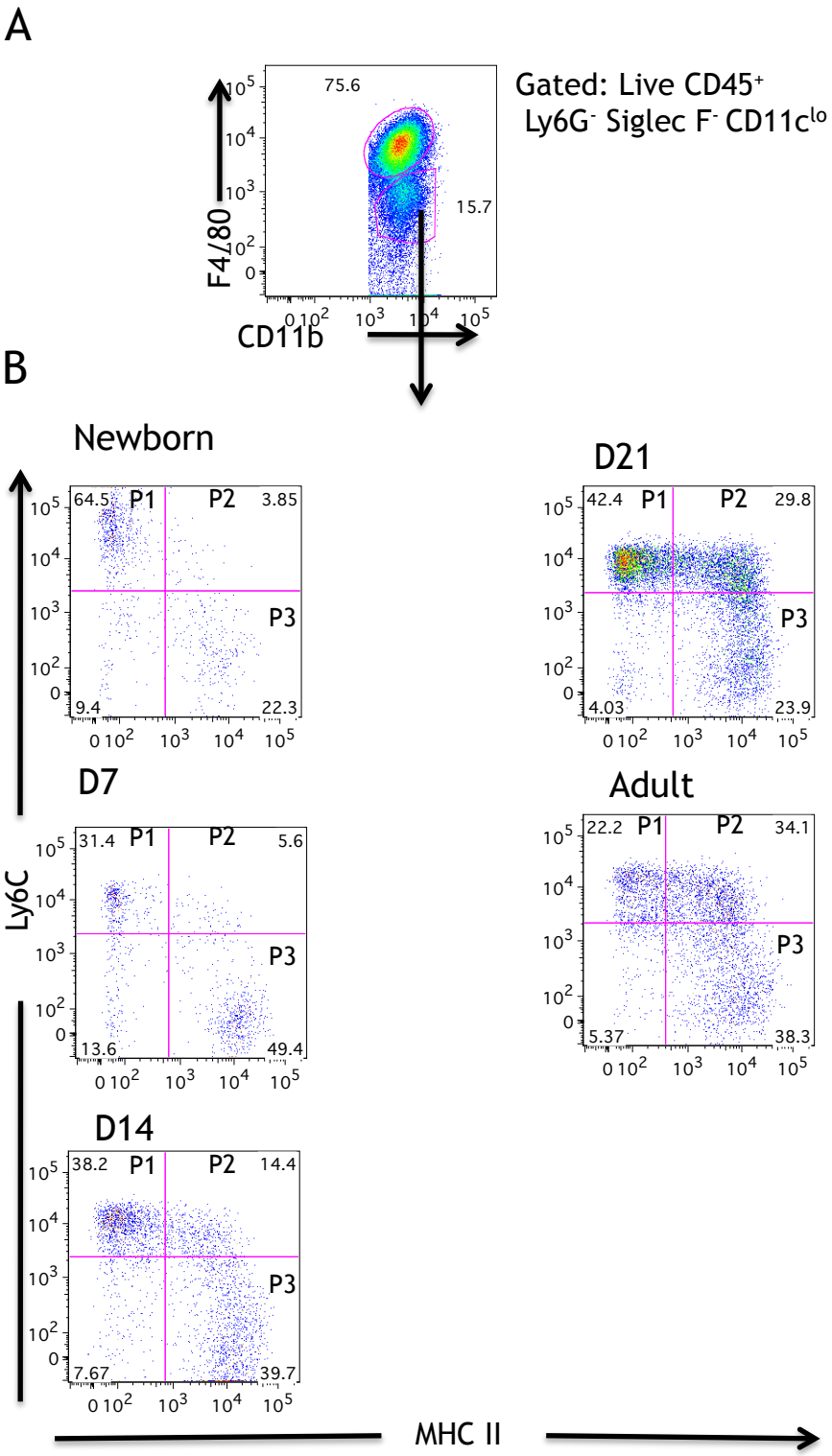

Figure 3.9. Development of macrophages in colonic lamina propria. Expression of Ly6C and MHC II by F4/80^{lo} CD11b^{+} cells amongst live CD45^{+} CD11b^{+} excluding F4/80$^{lo/-}$ CD11c^{+} DCs and Ly6G^{+} Siglec F^{+} granulocytes from colonic lamina propria of CX3CR1$^{GFP/+}$ mice of different ages up until adulthood (7 weeks). (A) Representative FACS plot from adult CLP. (B) Numbers in FACS plots are the proportion of cells in Ly6C^{hi} MHC II^{-} (P1), Ly6C^{hi} MHC II^{+} (P2) and Ly6C^{-} MHC^{+} (P3) gates. Data are representative of at least 3 independent experiments.

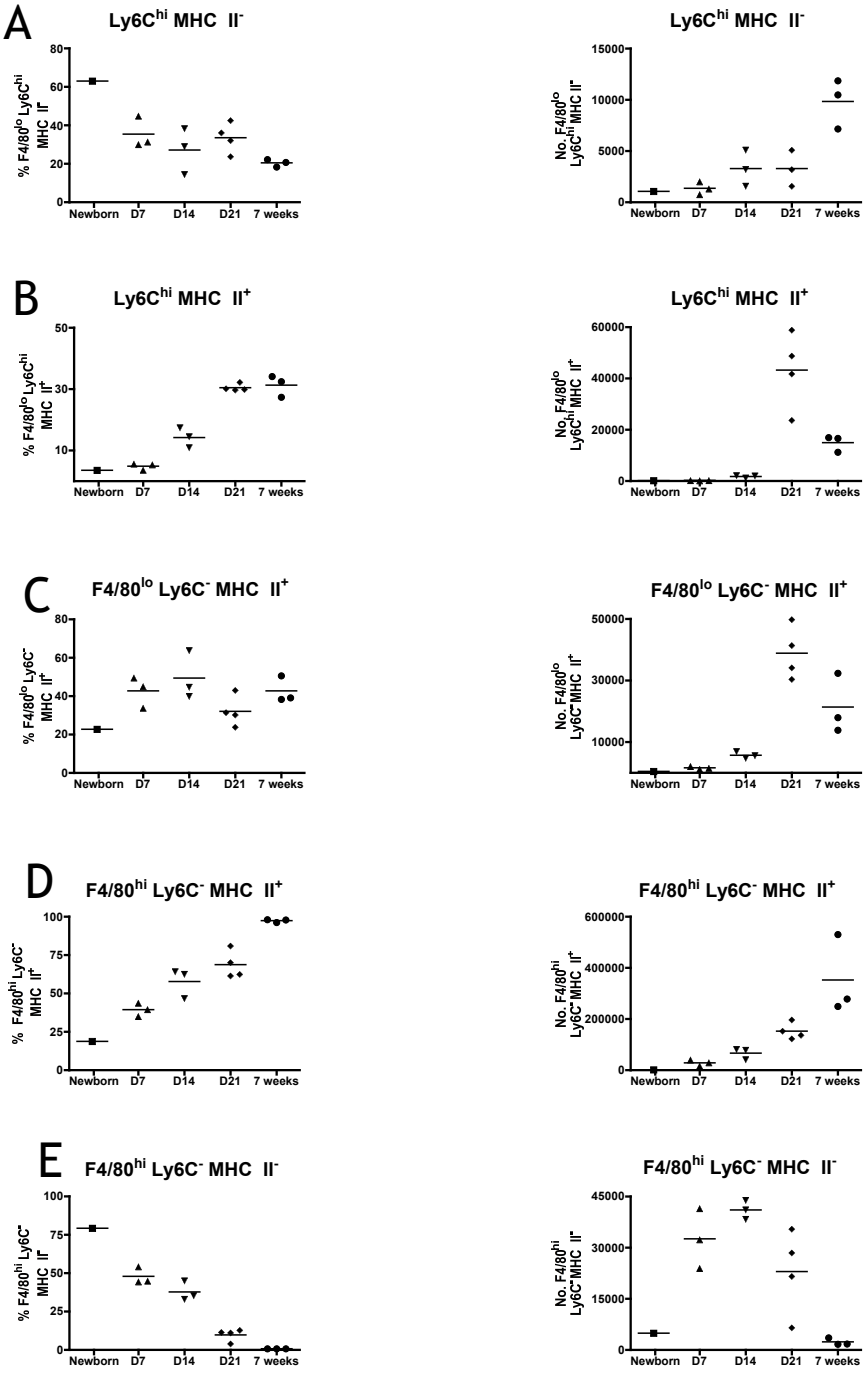

Figure 3.10. Development of macrophages in colonic lamina propria. Proportions (left panels) and absolute numbers (right panels) of Ly6C^{hi} MHC II^{-} (P1, A), Ly6C^{hi} MHC II^{+} (P2, B) and Ly6C^{-} MHC II^{+} (P3, C) cells within the F4/80^{lo} CD11b^{+} subset. D, E) Ly6C^{-} MHC II^{+} (P4) and Ly6C^{-} MHC II^{-} cells within the F4/80^{hi} CD11b^{int} population. Both F4/80 subsets were gated from live CD45^{+} CD11b^{+}, excluding F4/80$^{lo/-}$ CD11c^{+} DCs and Ly6G^{+} Siglec F^{+} granulocytes from colonic lamina propria of CX3CR1$^{GFP/+}$ mice of different ages up until adulthood (7 weeks). Results are representative of at least 3 independent experiments.

3.5 Contribution of self renewing foetal-derived precursors to the intestinal pool of intestinal mϕ

These results showed that macrophages were present in the intestine from before birth and recent reports suggest that the majority of tissue macrophages may be derived from YS and/or FL precursors that seed tissues during development and subsequently self-renew locally (Schulz et al., 2012). Although none of these studies have examined the intestine, the F4/80^{hi} CD11b^{int} and F4/80^{lo} CD11b^{+} subsets I found in newborn mice are phenotypically similar to what has been described for YS and FL derived mϕ respectively in other tissues. To examine this more directly, we initiated a collaboration with Professor Frederic Geissmann to investigate intestinal mϕ in CSF1R$^{mer\text{-}icre\text{-}mer}$;Rosa$^{LSL\text{-}YFP}$ mice, in which cells expressing the CSF1R will be responsive to tamoxifen due to expression of the mammalian oestrogen receptor (mer). The mer in turn is linked to the cre recombinase. After crossing to ROSA reporter mice, in which YFP has been inserted into the ROSA locus but expression prevented by an upstream lox P-flanked (floxed) STOP codon. Administration of low dose tamoxifen results in deletion of the STOP codon and irreversible YFP expression by CSF1R bearing cells in the progeny of these mice. In my experiments, pregnant mice were given tamoxifen at 8.5 days post-coitus (dpc), a time at which the YS is the only source of mϕ precursors (Figure 3.11 A). At 9 days of age, 2% of the F4/80^{hi} compartment of CD11b^{+} Ly6G^{-} Siglec F^{-} colonic mϕ were YFP^{+}, but no YFP^{+} cells were seen amongst the F4/80^{lo} population (Figure 3.11 AB and 3.12 A & B). This could be consistent with a YS origin for at least some of the F4/80^{hi} mϕ, whereas F4/80^{lo} mϕ may be derived from FL. I then examined YFP expression by colonic mϕ from 7-week-old mice. As shown in Figures 3.11 C and 3.12 A & C, a very small population of YFP^{+} F4/80^{hi} cells could be found at this time (0.1-0.2%). However, this was much lower than the YFP expression amongst F4/80^{hi} microglial mϕ in the adult brain where ~30% were YFP^{+}, confirming the large contribution of YS to this population throughout life (Figure 3.12 B & C). As reported by the Geissmann group (Schulz et al., 2012), other tissues such as liver, pancreas and epidermis also contained significantly more YFP^{+} F4/80^{hi} mϕ than the colon, while kidney mϕ were more similar to colon. YFP^{+}

cells were not seen amongst the F4/80^{lo} population in any tissue from adult mice, again confirming previous work from the Geissmann lab.

Together these results suggest that although YS derived mϕ are present in the intestine at birth, these do not make a major contribution to the adult pool.

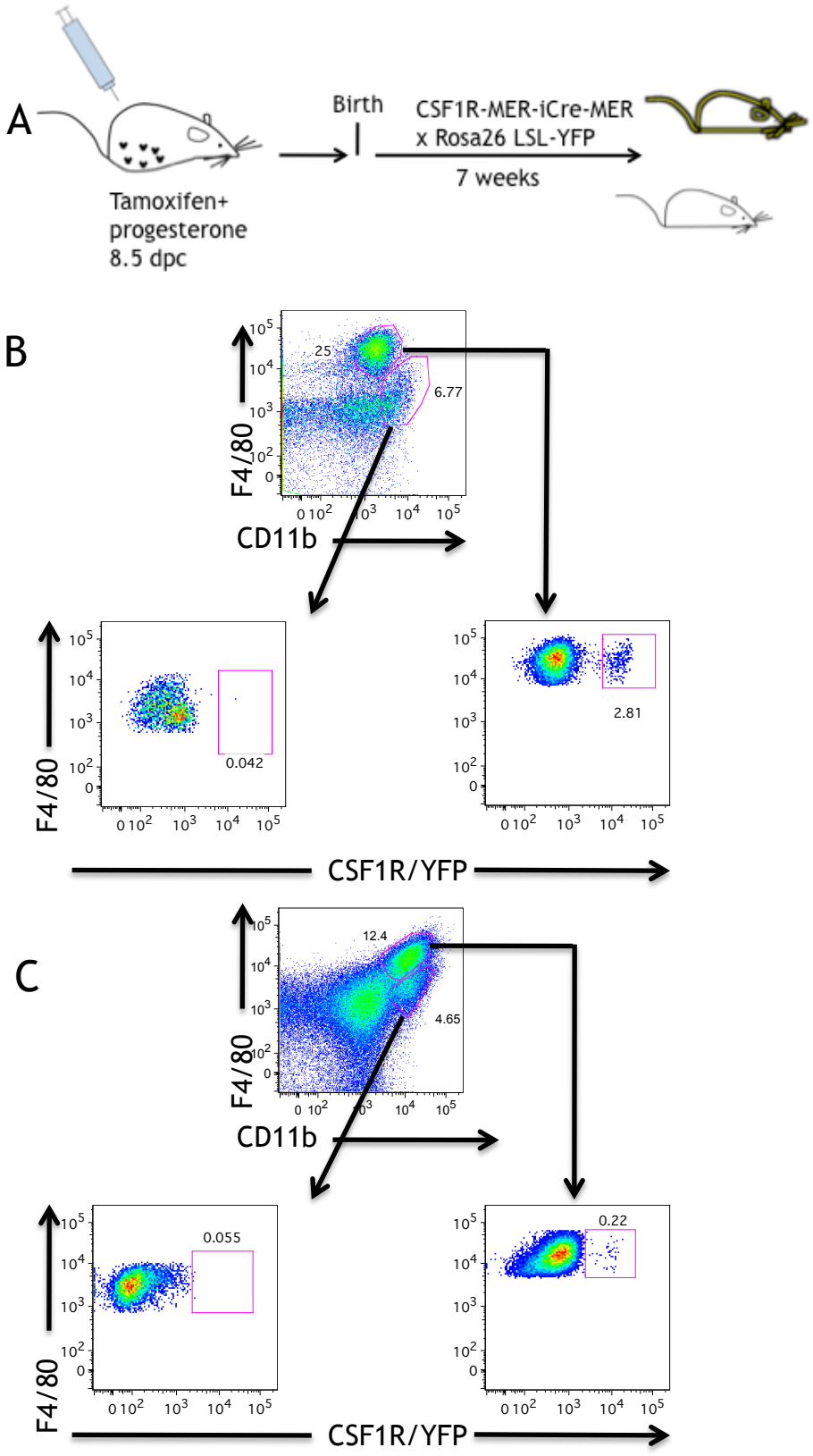

Figure 3.11. Identification of yolk sac-derived macrophages in colonic lamina propria. (A) Pregnant CSF1R$^{mer\text{-}icre\text{-}mer}$;Rosa$^{LSL\text{-}YFP}$ mice were injected with tamoxifen at gestational day 8.5 and the colonic lamina propria was analysed in pups at 9 days (B) or 7 weeks of age (C). The plots show the proportions of CSF1R/YFP^{+} cells amongst live CD45^{+} F4/80^{hi} CD11b^{int} Ly6G^{-} Siglec F^{-} and F4/80^{lo} CD11b^{+} Ly6G^{-} Siglec F^{-} mφ. Representative FACS plots from 2 experiments with at least 3 mice/group.

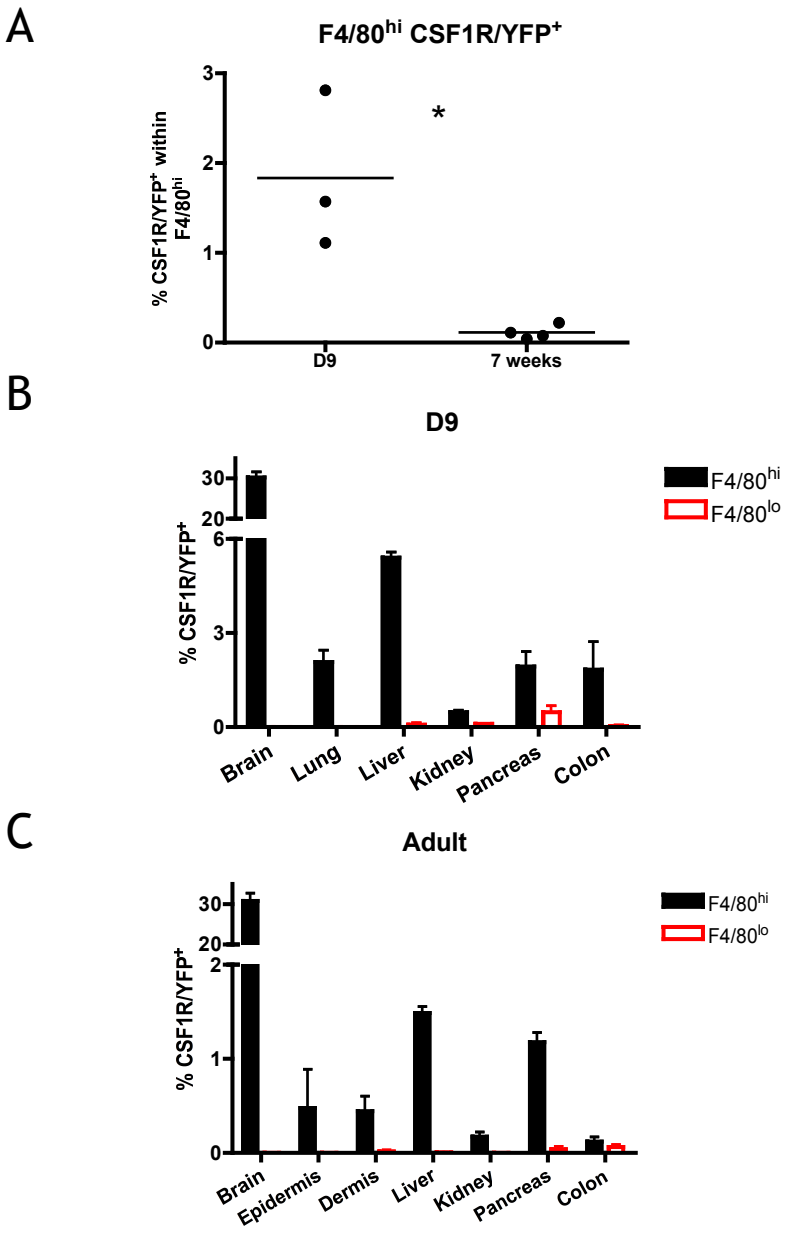

Figure 3.12. Identification of yolk sac-derived macrophages in colonic lamina propria. A) Pregnant CSF1R$^{mer\text{-}icre\text{-}mer}$;Rosa$^{LSL\text{-}YFP}$ mice were injected with tamoxifen at gestational day 8.5 and the colonic lamina propria was analysed for CSF1R/YFP^{+} cells within F4/80^{hi} CD11b^{int} amongst live CD45^{+} Ly6G^{-} Siglec F^{-} cells in pups at 9 days or 7 weeks of age. Frequencies of CSF1R/YFP^{+} cells within F4/80^{hi} CD11b^{int} and F4/80^{lo} CD11b^{+} populations compared with other tissues at 9 days (B) and 7 weeks of age (C). Results are means for 3 individual mice/ group +1SD and represent two independent experiments. *p<0.05. Student's t-test.

3.6 Contribution of local proliferation to the developing pool of colonic mϕ

My results show that small numbers of foetal derived mϕ are present from birth until two weeks of life, but that there is a large expansion in mϕ numbers around the time of weaning in the 3rd week. I thought it was important to explore how this might take place and first I examined whether it was due to local expansion of the pre-existing mϕ populations. To do this, I used Ki67 staining to assess cell division *in situ*. This showed that ~30% of F4/80^{hi} mϕ were actively dividing in the colon of newborn and 2 week old mice, with slightly fewer in the 3 week old colon, when there was also greater variability within the group. In contrast, very few dividing mϕ could be observed in 5 or 9-week old adult mice. Similar proportions of dividing cells were found amongst the F4/80^{lo} subset in newborn intestine, but these levels fell progressively thereafter, unlike the F4/80^{hi} mϕ, which maintained high levels for longer. However, slightly more F4/80^{lo} mϕ were Ki67^{+} than their F4/80^{hi} counterparts in the adult intestine (Figure 3.13 A & B and 3.14). In contrast to these marked age dependent differences in the mϕ populations, the F4/80^{-} CD11c^{+} MHC II^{+} DC showed high levels of Ki67^{+} cells throughout, consistent with other work in the laboratory which has found that a substantial proportion of mature DC in the intestine are dividing *in situ* (Figure 3.13 B) (Scott C, submitted for publication). As a negative control, I examined Ki67 expression by eosinophils and these showed little or no proliferation at any timepoint (Figure 3.13 C and 3.14).

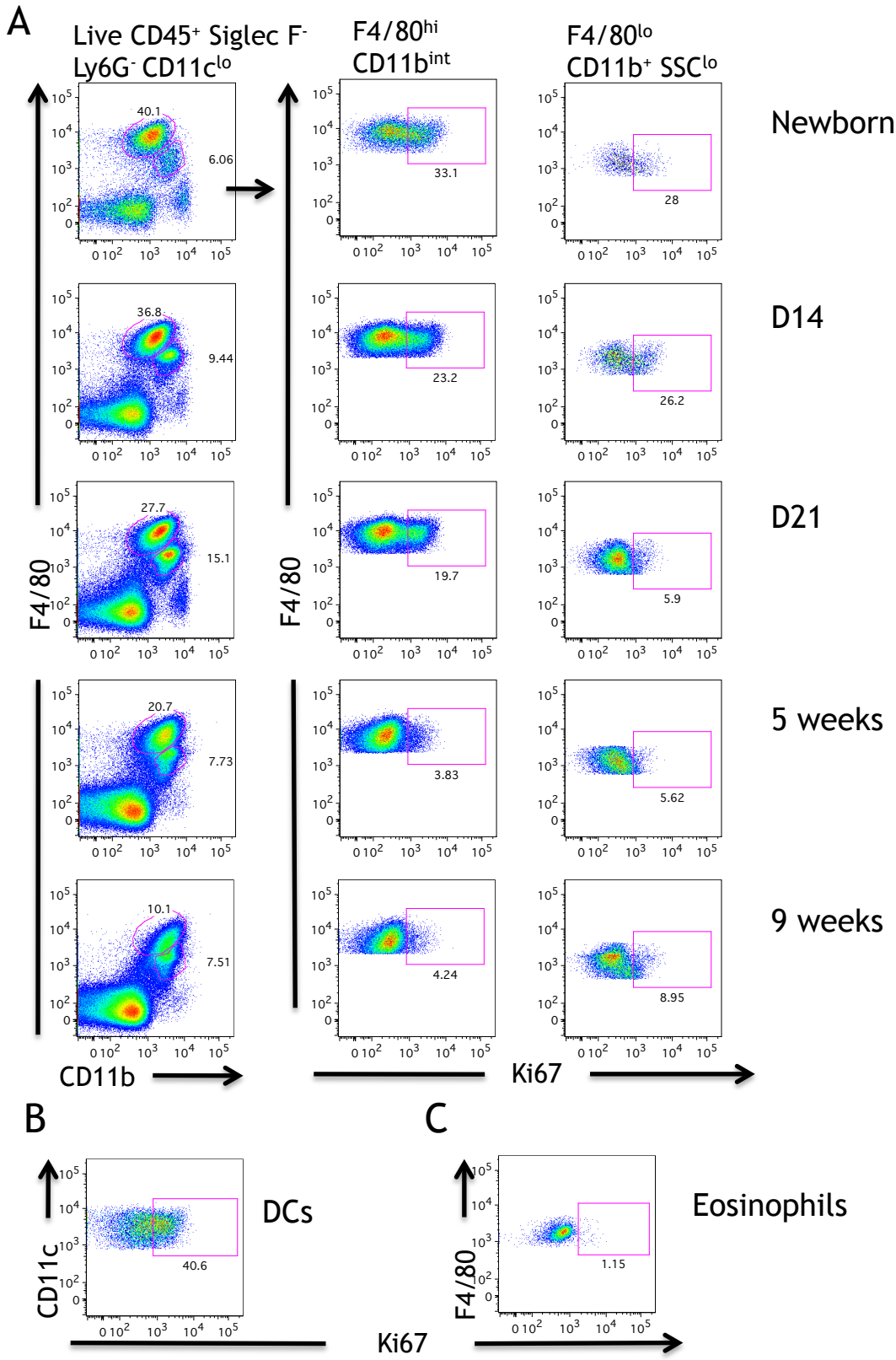

Figure 3.13. *In situ* proliferation of leukocytes in colonic lamina propria. (A) F4/80^{hi} CD11b^{int} and F4/80^{lo} CD11b^{+} SSC^{lo} mφ were identified amongst live CD45^{+} cells, excluding F4/80$^{lo/-}$ CD11c^{+} DCs and Ly6G^{+} Siglec F^{+} granulocytes from CX3CR1$^{GFP/+}$ mice of different ages and Ki67 expression was assessed. B, C) Ki67 expression by F4/80^{-} CD11c^{+} MHC II^{+} DC and F4/80^{lo} SSC^{hi} eosinophils (C) from adult colon as positive and negative controls respectively. Data are representative of 2 independent experiments with at least 3 mice.

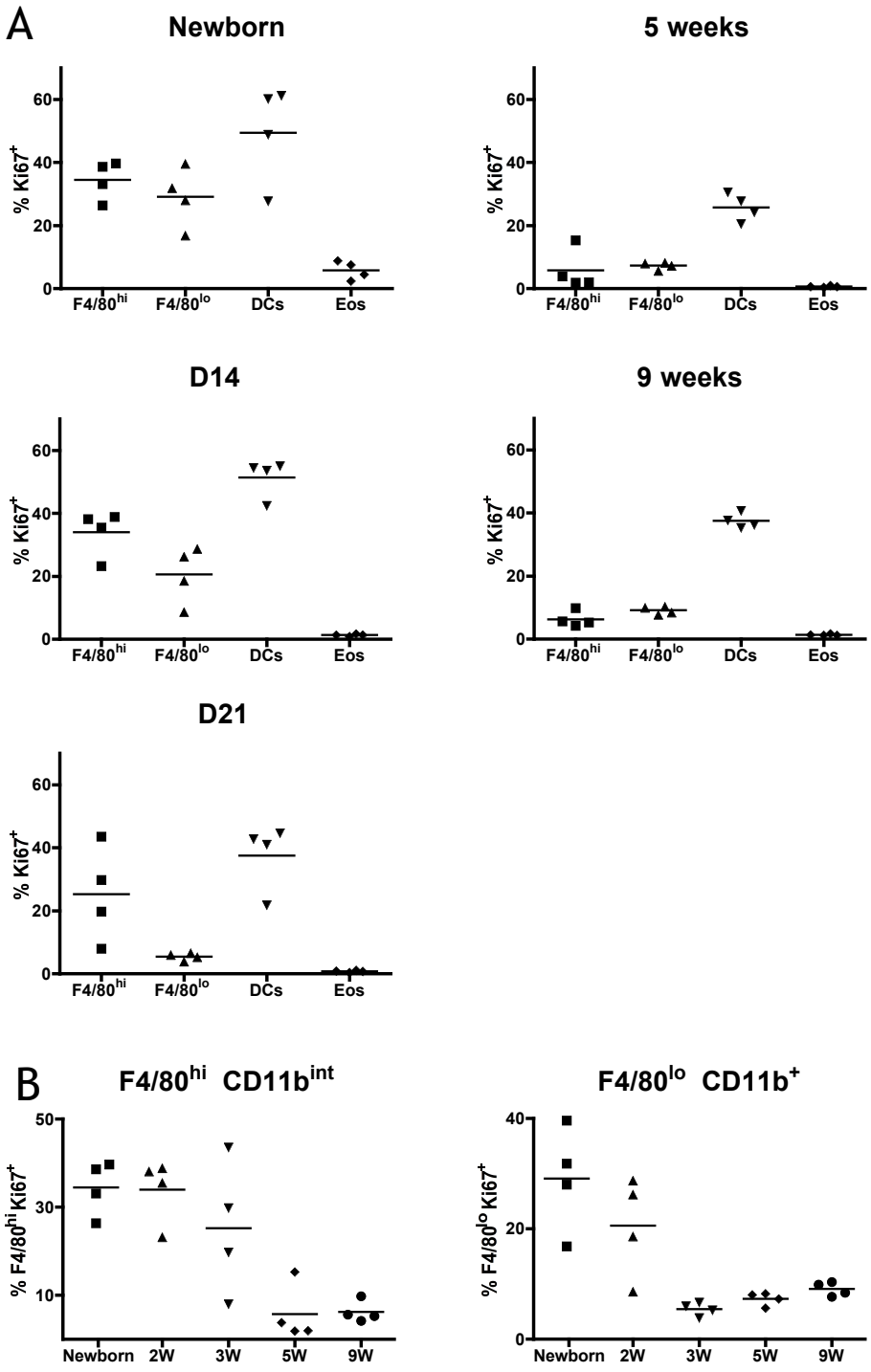

Figure 3.14. *In situ* proliferation of leukocytes in colonic lamina propria. (A) Proportions of Ki67^{+} cells amongst F4/80^{hi} CD11b^{int} and F4/80^{lo} CD11b^{+} mφ, F4/80^{-} CD11c^{+} MHC II^{+} DC and F4/80^{lo} SSC^{high} eosinophils amongst live CD45^{+} cells, excluding F4/80$^{lo/-}$ CD11c^{+} DCs and Ly6G^{+} Siglec F^{+} granulocytes from colonic lamina propria of CX3CR1$^{GFP/+}$ mice at different ages. (B) Time course of Ki67 expression by F4/80^{hi} CD11b^{int} and F4/80^{lo} CD11b^{+} mφ at different ages. Results shown are representative of 2 independent experiments.

3.7 Generation of intestinal mϕ from Flt3 dependent monocytes

My findings of relatively high cell division in neonatal colonic mϕ could be consistent with those from other tissues, where it is suggested that foetal precursor-derived mϕ populate the adult pool by self-renewal *in situ*. However, the highest levels of cell division I found occurred some time before the large expansion in mϕ populations around weaning, and indeed were falling by that time, suggesting that the two processes might not be linked. As ongoing studies in the lab had suggested that Ly6C^{hi} monocytes replenish colonic mϕ in adults, I therefore went on to investigate whether an influx of monocytes might be responsible for the expansion of mϕ around weaning.

To do this, I first used Flt3-Cre; Rosa26-YFP mice, again in collaboration with Professor Geissmann's laboratory. In these mice, YFP is expressed permanently on all cells which have ever expressed the fms-like tyrosine kinase (Flt3) during development, as the active Flt3 promoter drives cre-recombinase mediated excision of the STOP codon in the ROSA locus (Figure 3.15 A). As Flt3 is expressed only by hematopoietic progenitors (including blood monocytes) but not by foetal mϕ precursors, expression of YFP is restricted to cells derived from conventional haematopoietic precursors. Using this approach, ~50% of Ly6C^{hi} monocytes in the blood of adult mice were YFP^{+}, although this was significantly less than the frequency amongst the total blood CD45^{+} leukocyte population (Figure 3.15 A right & B). The proportions of YFP^{+} cells seen amongst both the F4/80^{lo} and F4/80^{hi} populations of adult mϕ were identical to that seen with blood Ly6C^{hi} monocytes, supporting the idea that adult mϕ originate from conventional monocytes (Figure 3.15 C).

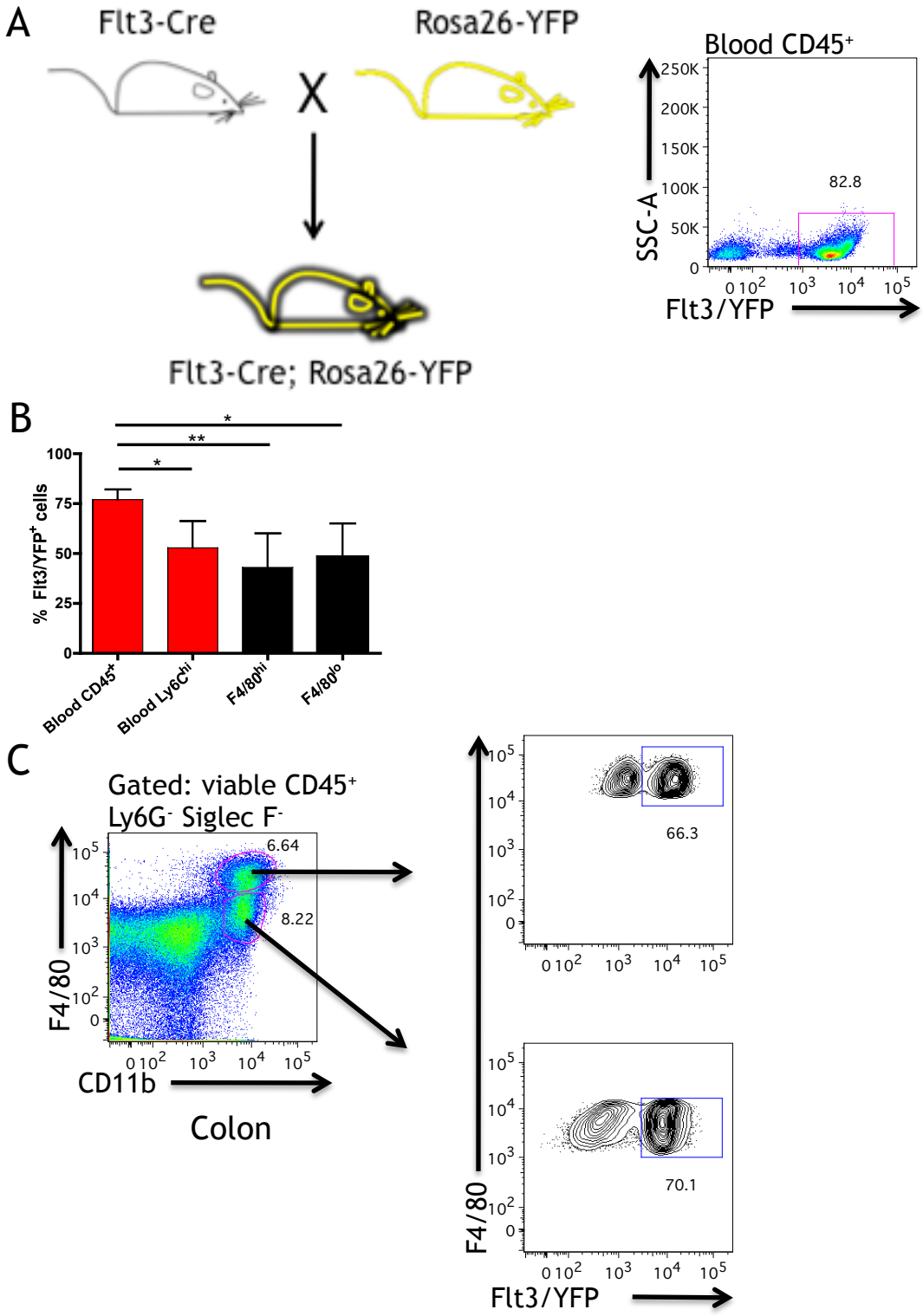

Figure 3.15. Generation of intestinal macrophages from Flt3 dependent monocytes. A) Haematopoietic progenitors from Flt3-Cre; Rosa26-YFP mice were identified in the blood and (B, C) the proportions of Flt3/YFP^{+} cells amongst blood CD45^{+} leukocytes, blood Ly6C^{hi} monocytes, F4/80^{hi} and F4/80^{lo} subsets amongst live CD45^{+} F4/80^{hi} CD11b^{int} Ly6G^{-} Siglec F^{-} cells in the colon of 8 week old mice. Results are means +1 SD for 3 mice/group from a single experiment. *p<0.05. Student's t-test.

3.8 Role of CCR2 in mϕ accumulation in developing mice

Together these results suggest that although a small number of mϕ that are derived from foetal precursors are present in the neonatal intestine, this population is diluted out considerably around weaning by cells derived from conventional Ly6C^{hi} monocytes. These conventional monocytes then appear to account for the great majority of adult mϕ. To test this hypothesis further, I examined the development of mϕ in CCR2 deficient mice, which lack Ly6C^{hi} monocytes in blood and other tissues due to a block in their egress from BM (Bain et al., 2013; Kurihara et al., 1997; Serbina and Pamer, 2006).

As I found previously, the total cell number in the colon of the CX3CR1$^{GFP/+}$ mice (that were used as WT controls in this experiment) increased in a stepwise fashion from birth up to D14, followed by a slight decrease at D18, after which adult levels were attained (Figure 3.16 A). Similar patterns of total cell number were seen in CCR2 null mice, although these mice had a significantly smaller number of total cells than in controls at 3 weeks of age. Although the proportions of CD45^{+} leukocytes were more variable in the WT mice of different ages, their absolute numbers increased gradually in the first 3 weeks of life, followed by a much more marked increase at 3 weeks of age. The proportions and numbers of CD45^{+} in CCR2 null mice were generally similar to those in the control colon, apart from an unexplained significant increase in the proportion above controls on day 18 (Figure 3.16 B & C).

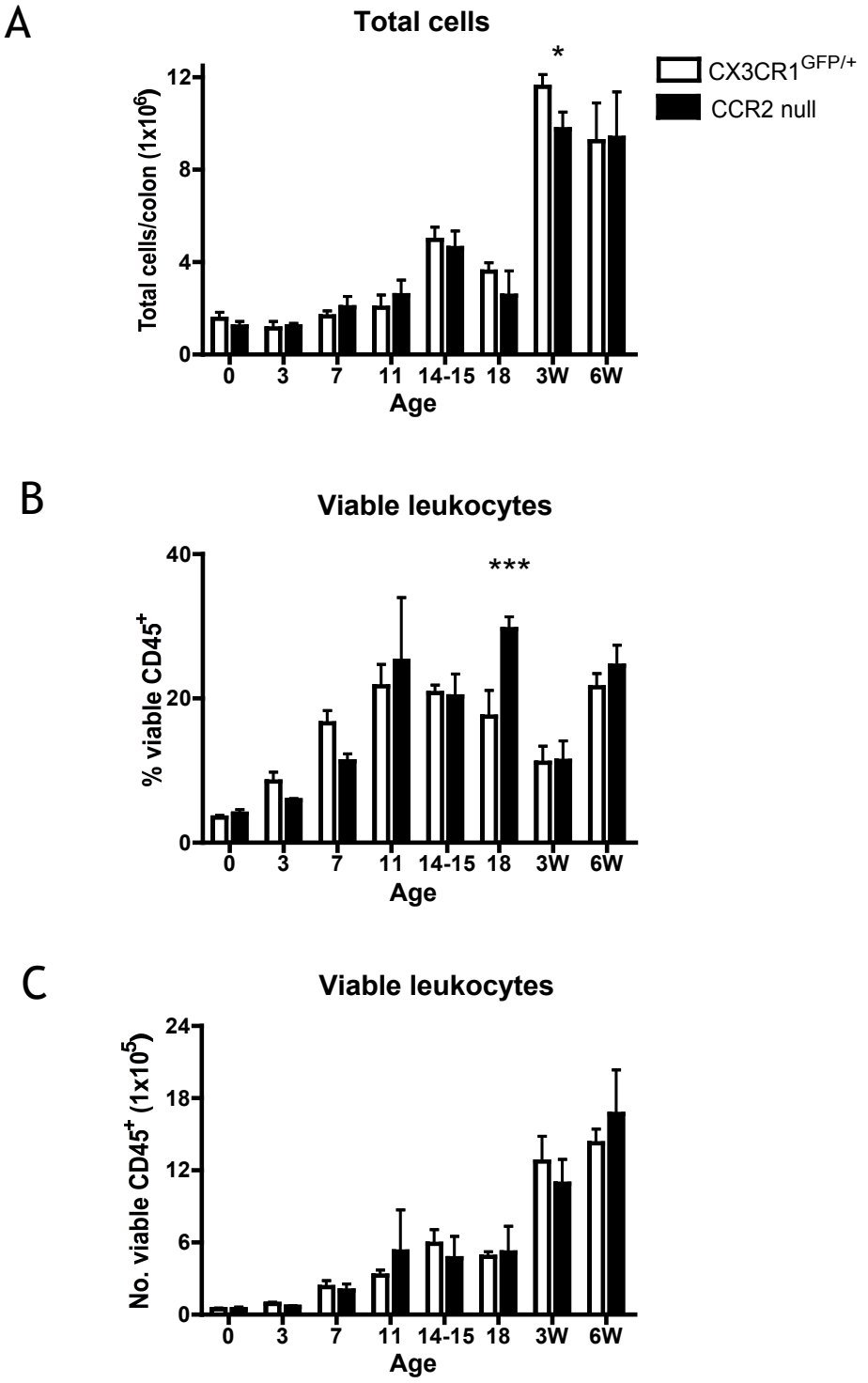

Figure 3.16. Role of CCR2 in development of intestinal macrophages. Colonic lamina propria cells were isolated from age matched CX3CR1$^{GFP/+}$ (open bars) and CCR2 null (black bars) mice at different ages up until adulthood (6 weeks). (A) Total number of cells/colon, B) proportions and (C) total numbers of live CD45^{+} leukocytes/colon. Results are means +1 SD for 3 mice/group and are representative of at least 3 independent experiments. *p<0.05, ***p<0.001 vs CX3CR1$^{GFP/+}$. Two way ANOVA followed by Bonferroni's post-test.

When the different populations F4/80^{+} cells were analysed, I found that the frequencies of F4/80^{lo} mϕ were very variable in each timepoint, however they remained relatively similar in CX3CR1$^{GFP/+}$ and CCR2 null colon throughout, apart from a slight deficiency in CCR2 null colon at 18 days (Figure 3.17 A left). On the other hand, F4/80^{lo} mϕ numbers from CX3CR1$^{GFP/+}$ mice showed little increase in the first two weeks of life, followed by highly variable numbers, showing an apparent drop at 18 days, a massive expansion by 3 weeks and a final decrease by half at 6 weeks of age. Importantly, CCR2 null mice showed significantly fewer cells at 3 and 6 weeks of age (Figure 3.17 A right).

In both strains, the proportion of Ly6C^{hi} MHC II^{-} monocytes (P1) within the F4/80^{lo} population changed at every timepoint. This population decreased from birth to 3 days and apart from a transient increase at day 7, fell gradually thereafter, until increasing to adult levels at 3 and 6 weeks. A similar pattern was seen for the proportions of Ly6C^{hi} MHC II^{-} cells amongst the F4/80^{lo} population in CCR2 null mice up to 3 weeks of age, but their proportions did not recover at later times (Figure 3.17 B left). These changes were mirrored by a marked expansion in the absolute numbers of this subset in CX3CR1$^{GFP/+}$ mice, which were less marked than in CCR2 null mice (and somewhat more variable) at 3 and 6 weeks of age (Figure 3.16 B right). At most timepoints the proportion of Ly6C^{hi} MHC II^{+} cells (P2) were lower in CCR2 null colon but there was an expansion in their numbers at 3 weeks. However from this age and by 6 weeks of age, the number of Ly6C^{hi} MHC II^{+} cells was much lower than in WT colon, paralleling the behaviour of Ly6C^{hi} MHC II^{-} cells at these time points (Figure 3.17 C). The frequency of Ly6C^{-} MHC II^{+} cells was much more variable in WT colon, but again there was an increase after 2 weeks of age, which was reflected by a large expansion in numbers at 3 weeks of age. In comparison, although the proportions of Ly6C^{-} MHC II^{+} F4/80^{lo} cells increased normally at the later timepoints and although this population expanded after 3 weeks of age, this was significantly less than seen in WT colon at the same times (Figure 3.17 D).

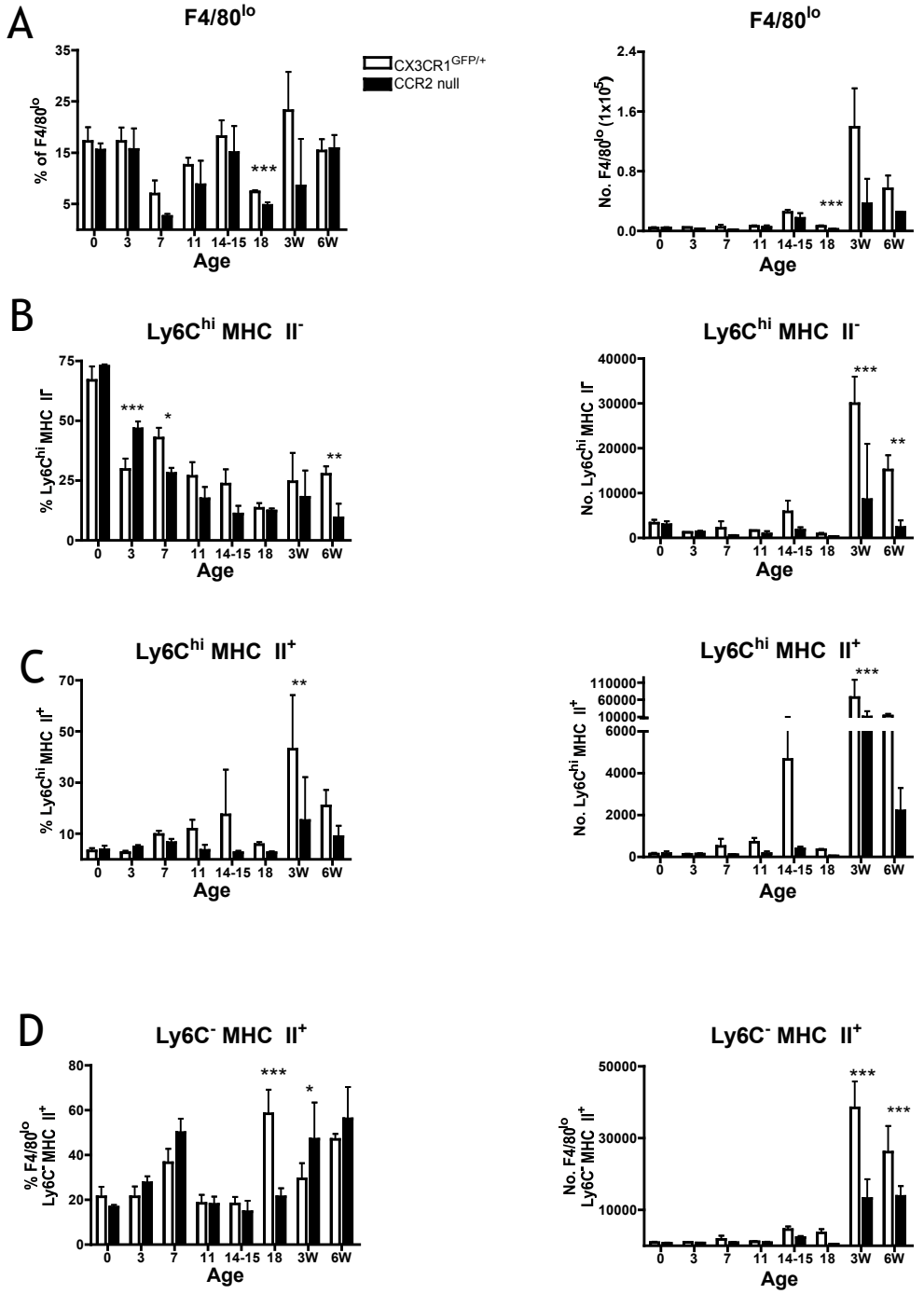

Figure 3.17. Role of CCR2 in development of intestinal macrophages. Colonic lamina propria cells were isolated from age matched CX3CR1$^{GFP/+}$ (open bars) and CCR2 null (black bars) mice at different ages up until adulthood (6 weeks). A) Proportions (left panels) and absolute numbers (right panels) of F4/80^{lo} CD11b^{+}, Ly6C^{hi} MHC II^{-} (P1, B), Ly6C^{hi} MHC II^{+} (P2, C) and Ly6C^{-} MHC II^{+} (P3, D) cells amongst amongst live CD45^{+} CD11b^{+} cells excluding F4/80$^{lo/-}$ CD11c^{+} DCs and Ly6G^{+} Siglec F^{+} granulocytes. Results are means +1 SD for 3 mice/group and are representative of at least 3 independent experiments. *p<0.05, **p<0.01 ***p<0.001 vs CX3CR1$^{GFP/+}$. Two way ANOVA followed by Bonferroni's post-test.

As expected from my previous experiments, the proportions of F4/80^{hi} cells in WT colon showed discrete changes throughout the experiment, and both strains showed a similar pattern to that seen in the CCR2 null colon, with a significant decrease by 6 weeks (Figure 3.18 A). There was a progressive increase in the proportion of F4/80^{hi} cells expressing MHC II (P4) after birth until virtually all were MHC II^{+} by 3 weeks of age in both strains (Figure 3.18 B). Again the absolute numbers of F4/80^{hi} MHC II^{+} mϕ were increased most dramatically at 3 weeks and this was identical in WT and CCR2 null colon. However by 6 weeks of age, a large defect had appeared in CCR2 null mice. This was not simply due to a failure of cells to express MHC II, as MHC II^{-} F4/80^{hi} cells were virtually absent in both strains of mice at 6 weeks of age (Figure 3.18 C).

Thus, this set of results suggests that there may be a number of Ly6C^{hi} monocytes early in life. This population is CCR2 independent and slowly disappears to be replaced by BM derived monocytes which take over as the exclusive haematopoietic organ by 3 weeks of age onwards. This may be the reason CCR2 null mice show a significant cell defect as they approach adulthood.

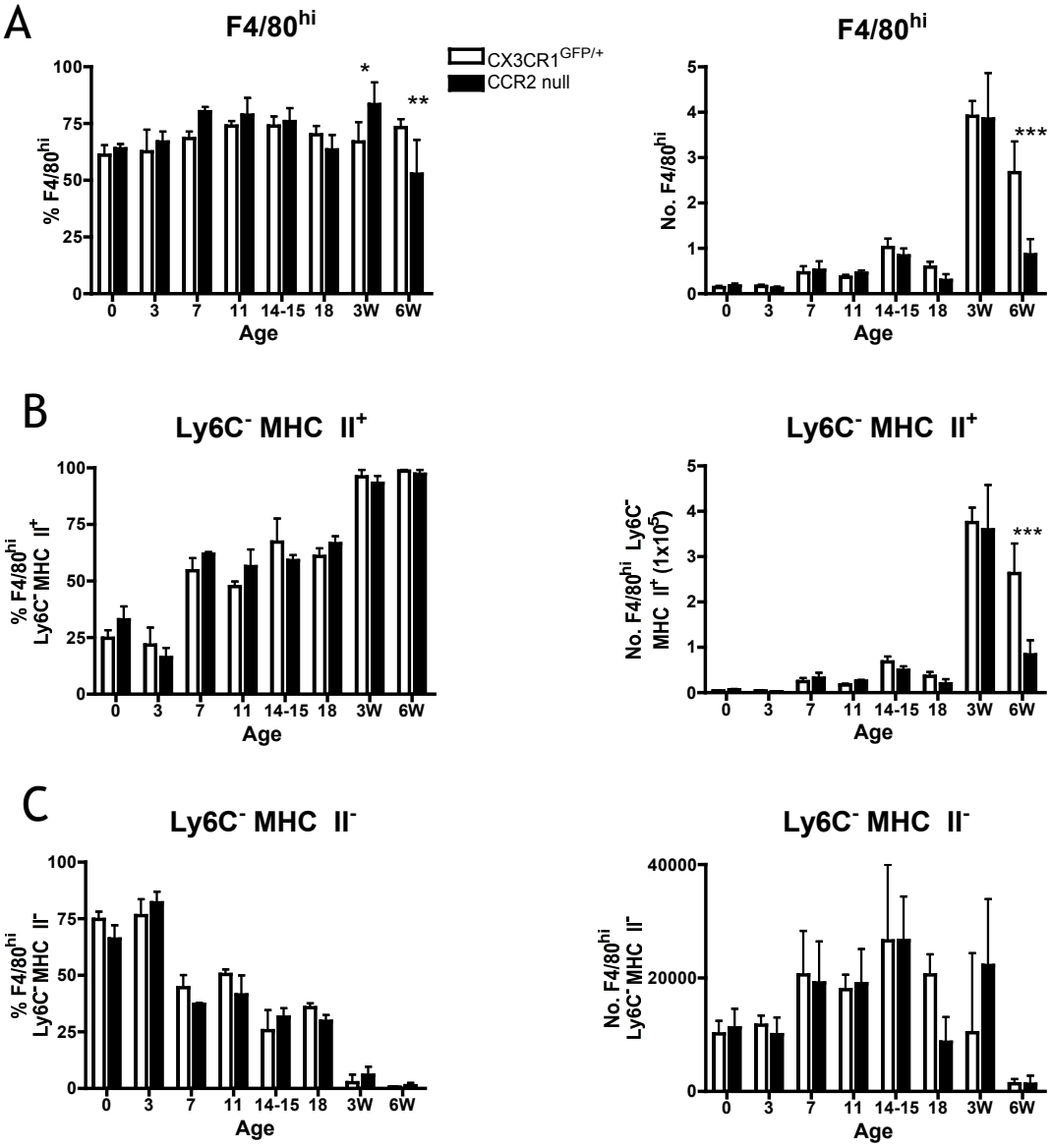

Figure 3.18. Role of CCR2 in development of intestinal macrophages. Colonic lamina propria cells were isolated from age matched CX3CR1$^{GFP/+}$ (open bars) and CCR2 null (black bars) mice at different ages up until adulthood (6 weeks). A) Proportions (left panels) and absolute numbers (right panels) of F4/80hi CD11b^{int}, Ly6C^{-} MHC II^{+} (P4, B) and Ly6C^{-} MHC II^{-} (C) cells amongst live CD45^{+} CD11b^{+} cells excluding F4/80$^{lo/-}$ CD11c^{+} DCs and Ly6G^{+} Siglec F^{+} granulocytes. Results are means +1 SD for 3 mice/group and are representative of at least 3 independent experiments. ***p<0.001 vs CX3CR1$^{GFP/+}$. Two way ANOVA followed by Bonferroni's post-test.

3.9 Functional comparison of adult and newborn colonic mϕ

I also investigated whether newborn mϕ had similar functions to their adult counterparts. I started by assessing their phagocytic ability, which is a characteristic property of mature resident mϕ. To do this I used the pHrodo assay, in which pH-sensitive *E. coli* particles fluoresce after uptake into acidified vesicles. F4/80^{hi} mϕ from adult colon showed high activity in this assay, as did their counterparts in newborn mice (Figure 3.19). However although F4/80^{lo} mϕ from adult mice had similar levels of phagocytic activity to F4/80^{hi} mϕ, neonatal F4/80^{lo} mϕ had little or no ability to phagocytose *E. coli* particles.

Among the other characteristic functions of adult mature mϕ are the constitutive production of IL10, low but significant constitutive TNFα production and expression of scavenger receptors such as CD163 (Bain et al., 2013). To assess these parameters in neonatal mice, I sorted F4/80^{hi} CD11b^{int} mϕ from newborn and adult CX3CR1$^{GFP/+}$ mice (Figure 3.20 A). qPCR analysis showed that, as expected, F4/80^{hi} mϕ from adult colon expressed greater amounts of mRNA for IL10, CD163 and TNFα than the CSF1 generated BM mϕ, which were used as controls. Identical mRNA levels of TNFα and CD163 were found in adult and neonatal F4/80^{hi} CD11b^{int} mϕ. Interestingly, there was a trend suggesting that adult F4/80^{hi} CD11b^{int} mϕ produced more mRNA for IL10 than their neonatal counterparts (Figure 3.20 B) and this was further supported by an apparently lower IL10 production by neonatal CX3CR1^{hi} mϕ, shown by intracellular staining (Figure 3.21).

Finally I wanted to assess the responsiveness of neonatal mϕ to LPS stimulation. This was with the purpose of comparing them with adult colonic mϕ, which are known for being hyporesponsive. My results show that whilst none of the adult or neonatal F4/80^{hi} CD11b^{int} mϕ produced extra TNFα after LPS stimulation, there was a significantly higher proportion of neonatal F4/80^{hi} mϕ producing TNFα during steady state (Figure 3.22 A & B left). In contrast, the F4/80^{lo} CD11b^{+} mϕ from both age groups were fully responsive

to LPS stimulation, although no significant differences were found during steady state (Figure 3.22 A & B right).

Thus intestinal mϕ from newborn mice have most of the characteristics of their counterparts in adult mice, although they produce more TNFα than their adult counterparts at steady state, whilst they may produce less IL10.

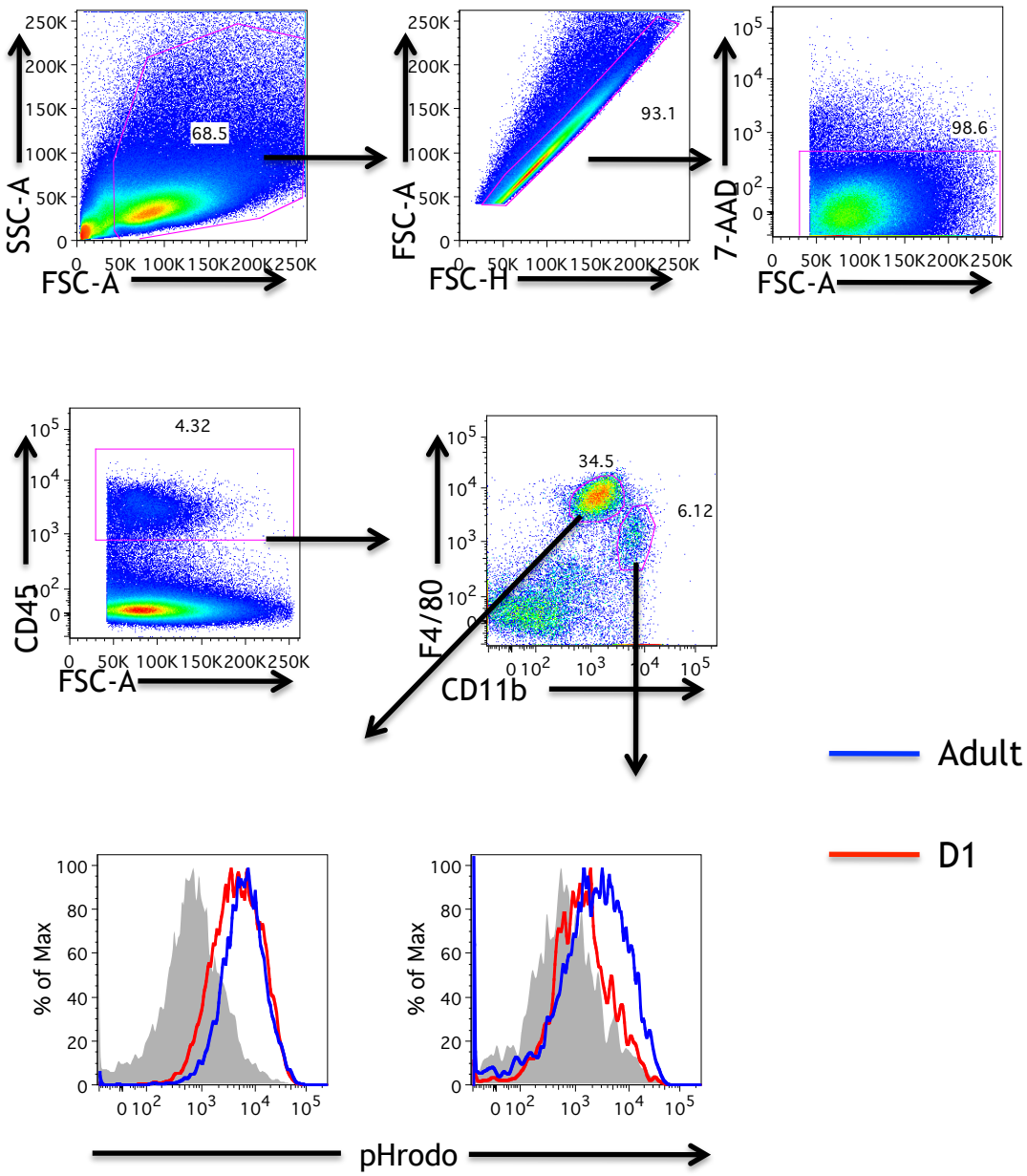

Figure 3.19. Phagocytic activity of newborn and adult intestinal macrophages. Colonic lamina propria cells from the colon of newborn and adult CX3CR1$^{GFP/+}$ mice were incubated with pH-sensitive (pHrodo) *E. Coli* at 37ºC for 15 minutes and analysed by flow cytometry. Results show the pHrodo fluorescence of live CD45^{+} F4/80^{hi} CD11b^{int} Ly6G^{-} Siglec F^{-} mφ from adult (blue line) or newborn mice (red line) compared with staining at 4ºC as a negative control (filled grey). Representative FACS plots from at least 2 independent experiments with 3 mice/group.

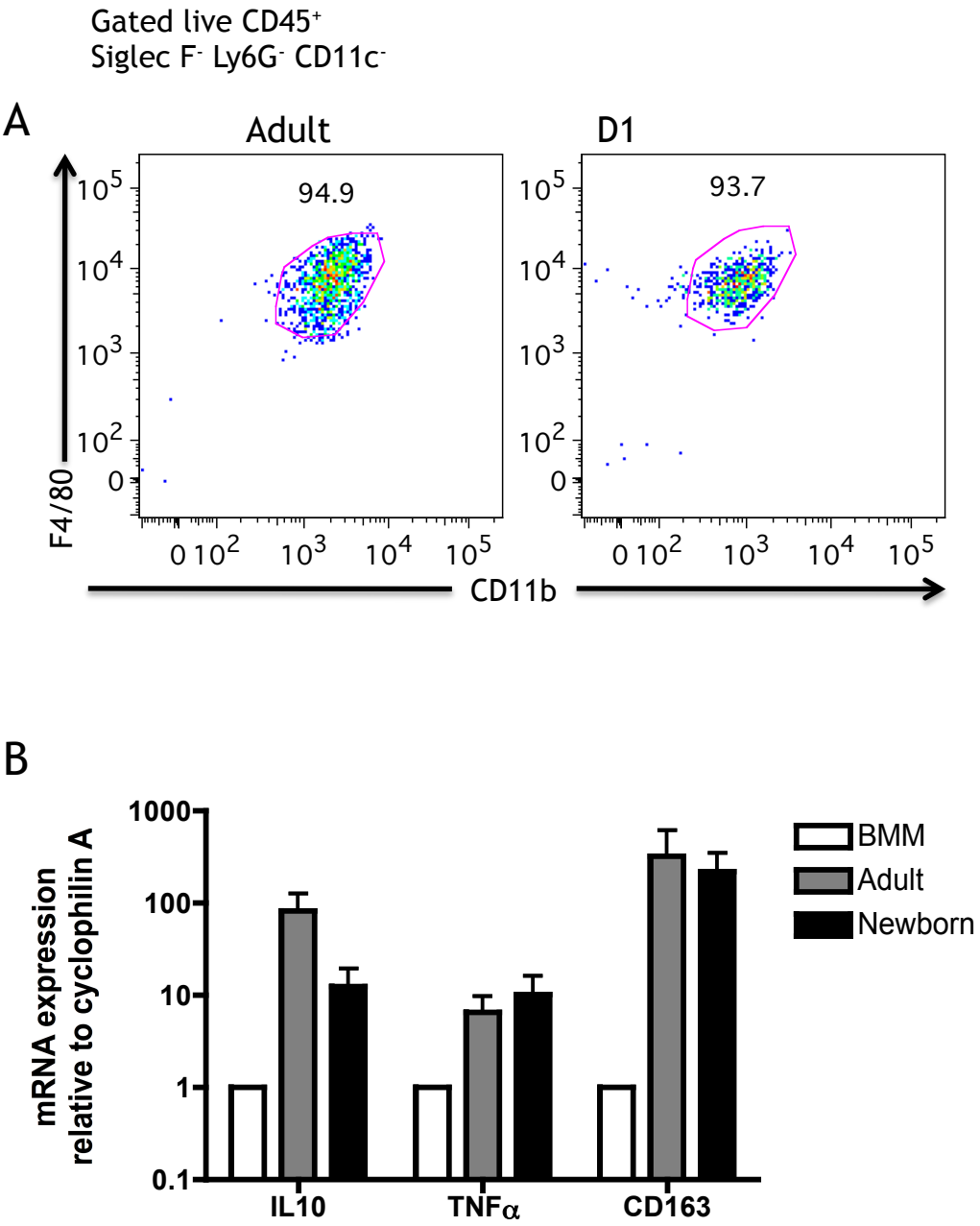

Figure 3.20. Expression of functional molecules by neonatal and adult mφ. (A, B) F4/80^{hi} CD11b^{int} mφ amongst live CD45^{+} cells, excluding F4/80$^{lo/-}$ CD11c^{-} DCs and Ly6G^{-} Siglec F^{-} eosinophils were sorted from 0-2 day old (newborn) and adult CX3CR1$^{GFP/+}$ mice. (C) mRNA from sorted cells was analysed for expression of IL10, TNFα and CD163 by Q-PCR with CSF-1 generated BM mφ set to 1. Results shown are mean expression relative to cyclophilin A (CPA) using the $2^{-\Delta C(t)}$ method. The mean was obtained from (3-4) pooled pups and individual adults with 3 biological replicates. Data are representative of at least 3 independent experiments.

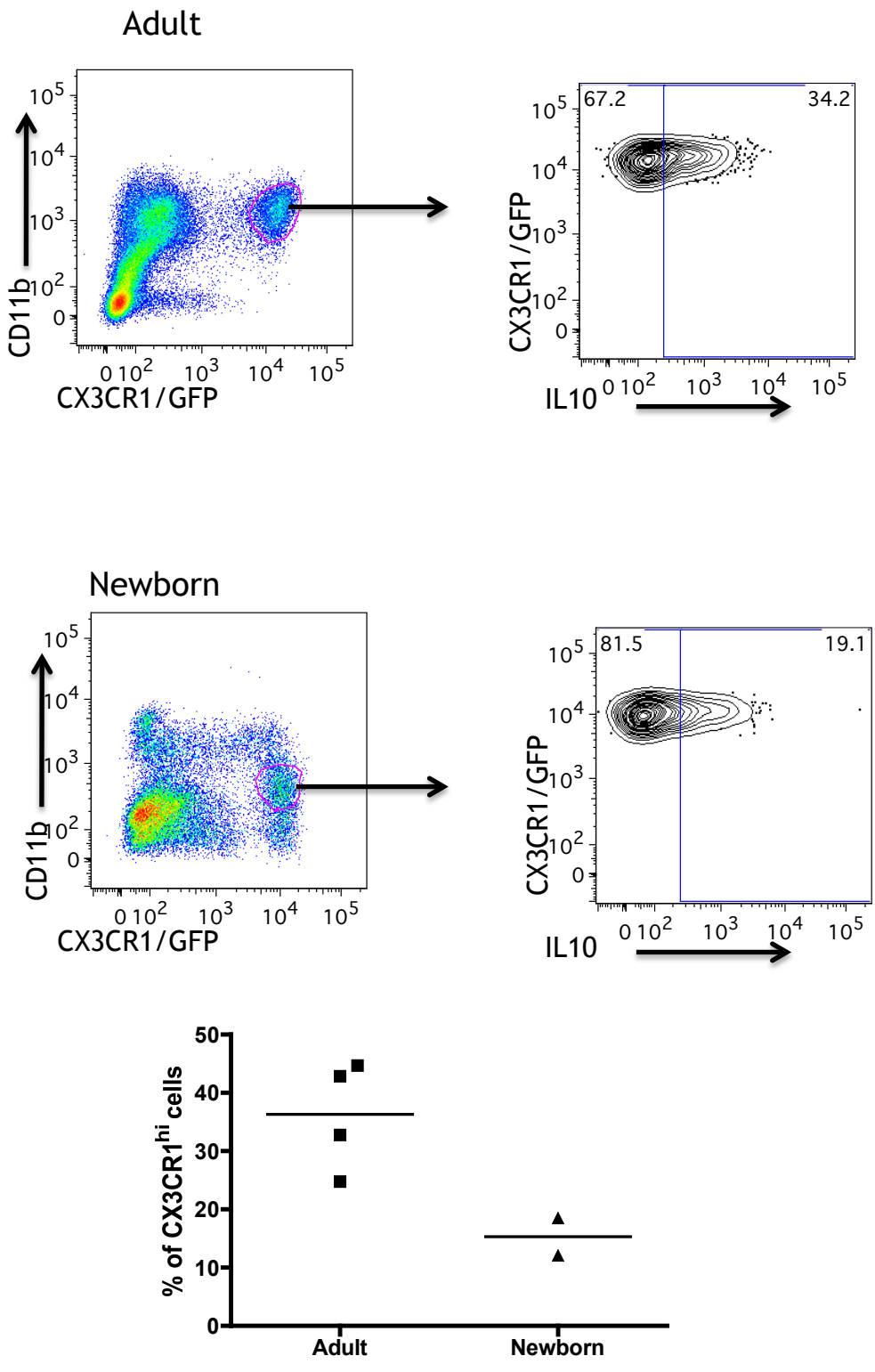

Figure 3.21. IL10 production by intestinal macrophages. Live CD45^{+} CD3^{-} CD19^{-} CD8α^{-} cells from adult and newborn CX3CR1$^{GFP/+}$ colon were analysed for expression of CX3CR1 and CD11b. Intracellular IL10 production by CX3CR1^{hi} cells was then analysed by intracellular staining. Data shown are pooled results from two experiments using 2 adults and one sample of pooled cells from at least 8 neonates/ experiment.

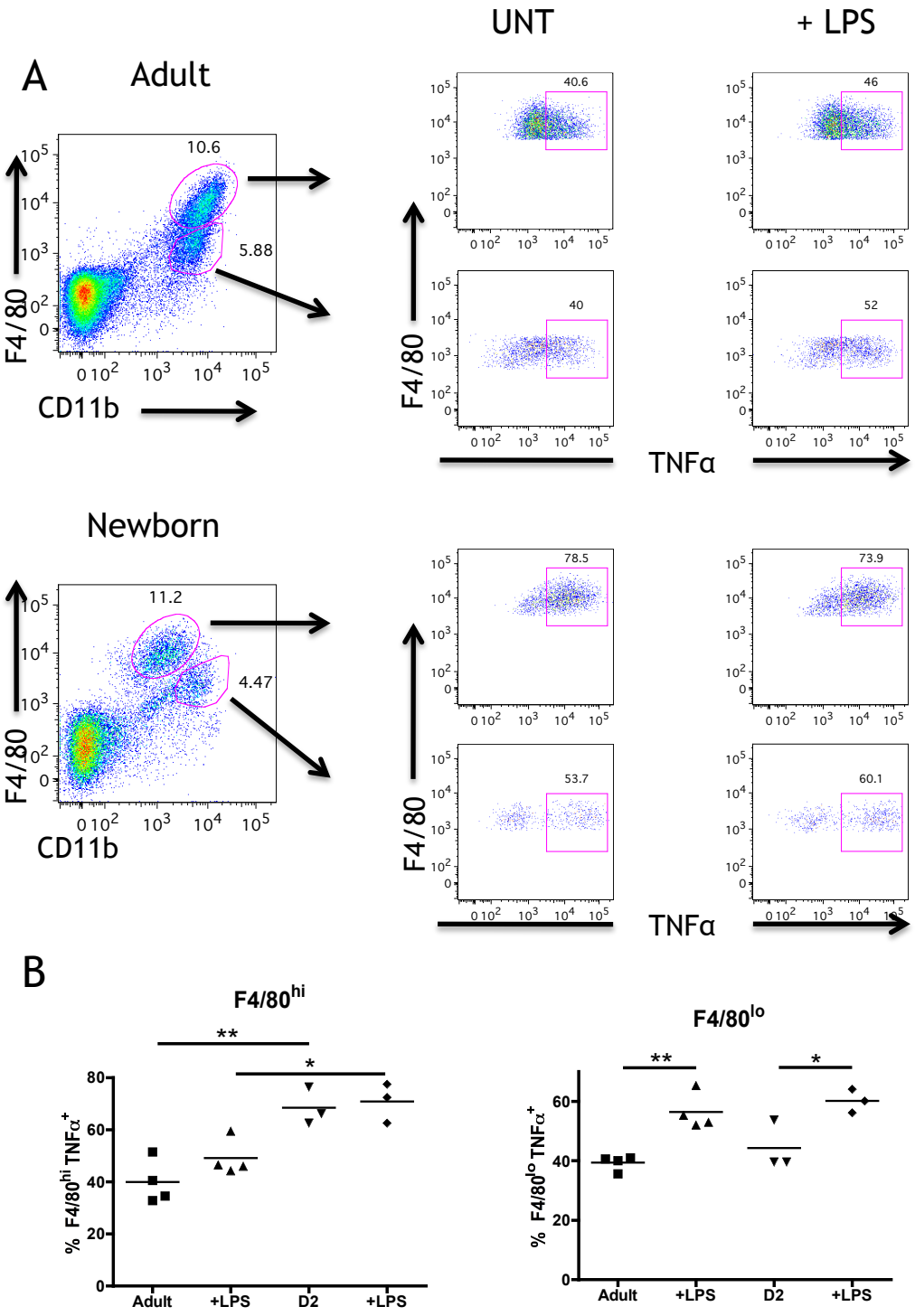

Figure 3.22. TNFα production by intestinal macrophages after LPS stimulation. A & B) F4/80^{hi} CD11b^{int} and F4/80^{lo} CD11b^{+} cells from adult and 2-day-old CX3CR1$^{GFP/+}$ colon were stimulated with 100ng/ml LPS in presence of brefeldin A and monensin for 4.5 hours, followed by analysis for expression of intracellular TNFα production. Both mφ subsets were selected amongst live CD45^{+} cells, excluding F4/80$^{lo/-}$ CD11c^{+} DCs and SSC^{hi} cells. Results are means for individual adult mice/group and 2-3 pooled pups and are representative of two independent experiments. *p<0.05, **p<0.01. Student's t-test.

3.10 Summary

In this chapter, I explored intestinal mϕ development from late foetal life up to adults of 6-7 weeks. My results show that colonic mϕ can be reliably isolated even from late foetal life and that two clearly defined populations of F4/80^{hi} CD11b^{int} and F4/80^{lo} CD11b^{+} mϕ can be identified. However these merge gradually from the 3rd week onwards. In early life, the majority of F4/80^{hi} mϕ do not express MHC II, but acquire it progressively as mice mature. As I found that the resident mϕ were proliferating actively in the first 2 weeks of life, I tested the hypothesis that self-renewal of a foetal derived precursor could account for this increase in mϕ at weaning. The F4/80^{hi} and CD11b^{hi} populations seemed to correspond to YS and FL derived mϕ in other tissues and fate mapping studies showed the presence of some YS derived mϕ in 2 week old intestine. However, there were very few of these in the adult intestine, and the *in situ* proliferation I observed did not correlate with the expression at weaning. Rather, this phenomenon was associated with an influx of Ly6C^{hi} monocytes, which could be shown to express the haematopoietic growth factor receptor Flt3. Unlike the adult mϕ pool, this influx of monocytes at weaning was not entirely CCR2 dependent, indicating that other mechanisms may be involved in recruiting these cells at different ages. However my results show clearly that the vast majority of intestinal mϕ are monocyte-derived from weaning onwards, and non-haematopoietic precursors made little or no contribution. Interestingly despite their different origins, newborn mϕ share many of the functional properties of adult mϕ, including phagocytic activity, expression of scavenger receptor and hyporesponsiveness to LPS stimulation. However, cytokine production shows that TNFα is remarkably high in the newborn intestine, whereas IL10 appears to be lower than in adults.

Chapter 4
Effect of microbiota on intestinal macrophages

4.1 Introduction

Reports suggesting an important influence of the microbiota on the intestinal physiology and structure date back to the late 1960's (Savage and Dubos, 1968; Savage and McAllister, 1971) and its effects on general immune function are also well characterised. However in recent years, more detailed, immunologically-focused work has highlighted how commensal microbes play an important role in tuning individual aspects of intestinal immune responses. The presence of certain *Clostridium* species and *B. fragilis*-derived polysaccharide A have been shown to correlate with increased numbers of colonic Treg cells (Atarashi et al., 2011; Mazmanian et al., 2008), while segmented filamentous bacteria (SFB) drive Th17 responses in the ileum (Denning et al., 2011; Fagundes et al., 2011; Ivanov et al., 2009; Ivanov et al., 2008; Ostman et al., 2006). Given these intricate relationships and the age-related changes I observed in my experiments using neonatal mice, I next sought to investigate whether the intestinal microbiota would affect colonic mϕ distribution in the lamina propria. The initial experiments in this chapter evaluated the effects of treating adult mice with two different gut-sterilising antibiotic schedules whilst the second part involved analysing colonic macrophage populations under germ-free conditions.

4.2 Analysis of colonic mϕ in CX3CR1$^{GFP/+}$ mice

In the previous chapter, I analysed mϕ populations based on their expression of F4/80 and CD11b. However as mentioned in that chapter, much of the other work ongoing in our laboratory used CX3CR1$^{GFP/+}$ mice to analyse mϕ populations and I was able to use them for the experiments assessing antibiotic treatment. The advantage of this mouse strain over non-GFP animals is that it allows a much clearer discrimination between mϕ subsets and the gating strategy used in these mice is depicted in figure 4.1. After discarding doublet cells, 7-AAD$^-$ CD45$^+$ cells are selected, followed by selection of total CD11b$^+$ cells, in which 3 main populations can be identified on the basis of their CX3CR1 expression. First, there is a CX3CR1$^-$ population, composed mainly of eosinophils and a few neutrophils (Bain et al., 2013), which I did not analyse any further. The remaining 2 subsets consist of a dominant CD11b$^+$ CX3CR1^{hi} population that is also homogenously Ly6C$^-$ MHC II$^+$

and has been shown previously to represent a population of mature resident mϕ (designated P4) (Bain et al., 2013). Finally, there is a less numerous $CD11b^{+}$ $CX3CR1^{int}$ population, which is heterogeneous in terms of Ly6C, MHC II, F4/80 and CD11c expression, identifying the $Ly6C^{hi}$ MHC II^{-} (P1) and $Ly6C^{hi}$ MHC II^{+} (P2) subsets of monocytes as well as a $Ly6C^{-}$ MHC II^{+} subset that can be split up further into a subset of semi-mature $F4/80^{hi}$ $Ly6C^{-}$ MHC II^{+} $CX3CR1^{int}$ mϕ (P3) and some $F4/80^{-}$ $CD11c^{+}$ MHC II^{+} DCs (P5) (Bain et al., 2013).

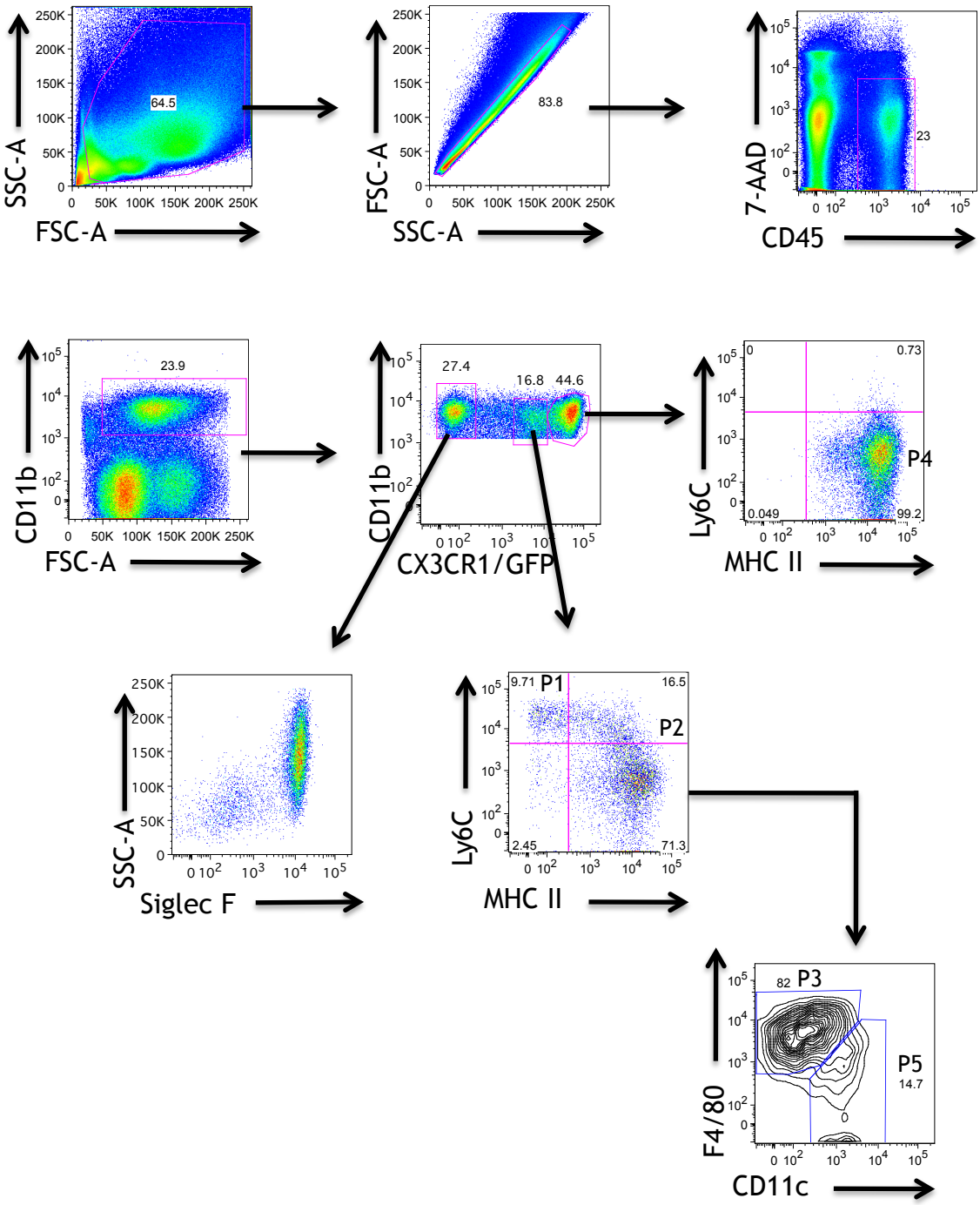

Figure 4.1. Gating strategy for evaluating the effect of antibiotic treatment on colonic lamina propria macrophages. After pre-gating single 7-AAD^{-} CD45^{+} cells from CX3CR1$^{GFP/+}$ adult mice, 3 CD11b^{+} populations could be found: CD11b^{+} CX3CR1^{-}, composed mainly of Siglec F^{+} eosinophils; a CD11b^{+} CX3CR1^{int} subset composed of Ly6C^{hi} MHC II^{-} (P1), Ly6C^{+} MHC II^{+} (P2) and Ly6C^{-} MHC II^{+} cells. The CX3CR1^{int} Ly6C^{-} MHC II^{+} cells can be subdivided into F4/80^{+} CD11c^{-} mφ (P3) and F4/80^{-} CD11c^{+} DCs (P5). The large population of CX3CR1^{hi} Ly6C^{-} MHC II^{+} F4/80^{+} cells is a homogeneous group of mature mφ (P4).

4.3 Effects of antibiotics on intestinal macrophages

In the first experiment I used these indices mentioned above to assess the effects of a relatively simple mixture of antibiotics (ABX) in the drinking water, which was 50mg/kg meropenem and vancomycin. After 22 days of treatment, I analysed the colonic mϕ subsets. This antibiotic regime was adapted from previous published work where imipenem and vancomycin were used to reduce colitis in HLA-B27 transgenic rats as well as BALB/c mice (Rath et al., 2001). There were few clear effects of our regime on the subsets of colonic mϕ in CX3CR1-GFP mice, with no additional changes to the frequencies or absolute numbers of viable leukocytes, total $CD11b^{+}$ cells, or granulocytes (Figure 4.2). Although there was a significant increase in the frequency of $CX3CR1^{hi}$ mϕ in ABX treated mice, this was extremely small and there was no significant difference in the number of these cells (Figure 4.2 D). I then examined the individual populations within the $CX3CR1^{int}$ subset (Figure 4.3 A-C), as well as the $CX3CR1^{hi}$ fraction (Figure 4.3 D). Again the proportions and absolute numbers of all these subsets were not affected by the antibiotic treatment.

It occurred to us that intestinal mϕ, especially the $CX3CR1^{hi}$ subset, may have a lifespan longer than the duration of the ABX treatment. Thus even if cellular changes had started to take place, these might be at a more subtle level that could be detected by enumerating cells by flow cytometry. To explore this possibility, I reduced the ABX treatment to 10 days and looked for changes in intracellular production of IL10 and TNFα by $CX3CR1^{hi}$ mϕ (Figure 4.4), together with qPCR analysis for IL10, TNFα and CD163 expression by FACS sorted $CX3CR1^{int}$ and $CX3CR1^{hi}$ populations. However, none of these parameters were affected by the ABX treatment (Figure 4.5).

As I thought this lack of effect might be due to the antibiotics I used, I decided to investigate whether a broader spectrum antibiotic cocktail might reveal more significant effects.

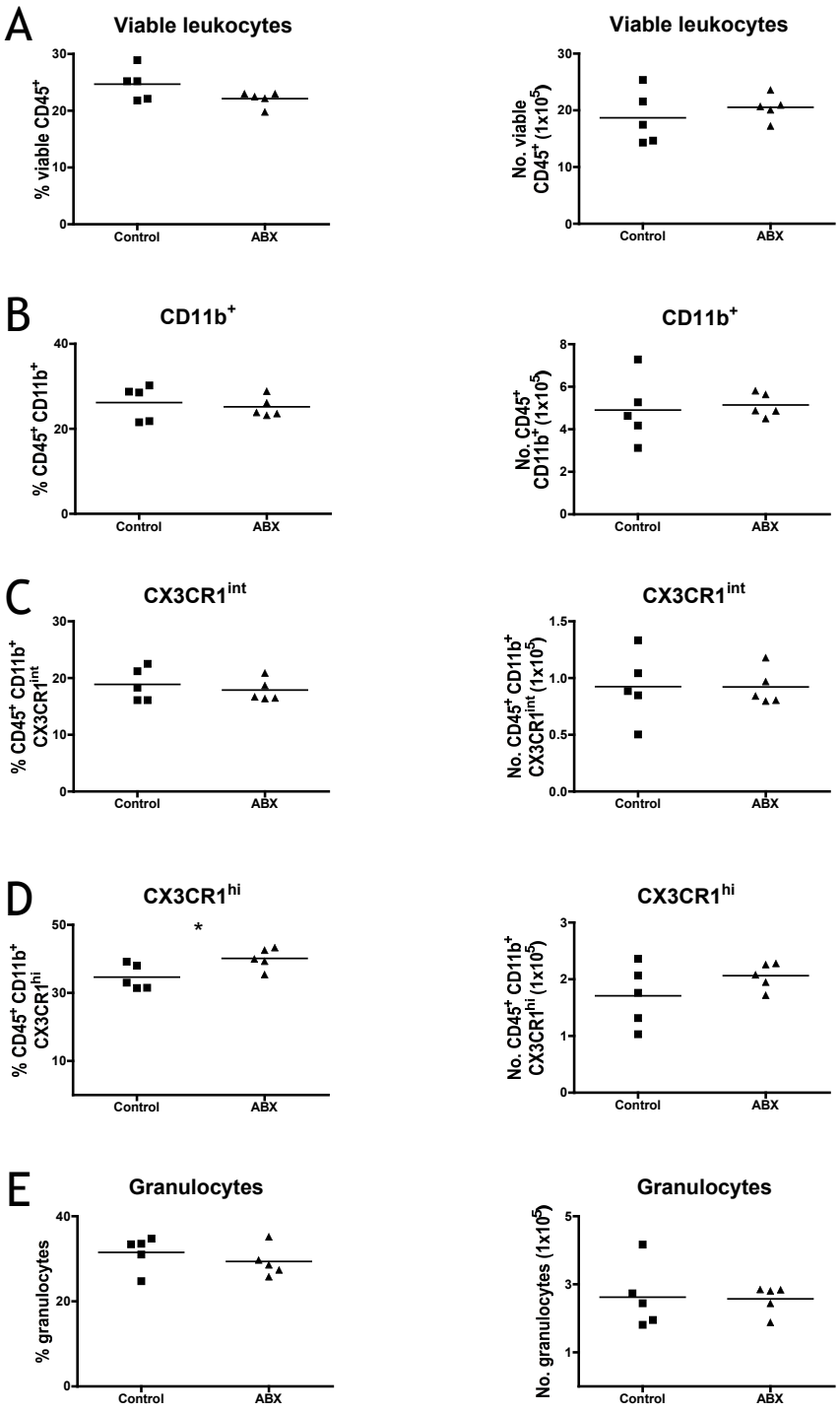

Figure 4.2. Effects of antibiotic treatment on intestinal macrophages. Frequencies (left) and absolute numbers (right) of (A) viable CD45$^+$ leukocytes, (B) CD11b$^+$ CX3CR1^{int} cells (C), CD11b$^+$ CX3CR1^{hi} cells (D) and granulocytes (E) in colon of adult CX3CR1$^{GFP/+}$ mice receiving 50mg/kg vancomycin and 50mg/kg meropenem in drinking water for 22 days and the controls receiving sweetened water. The data shown are from 5 individual mice/group and are representative of 2 independent experiments.

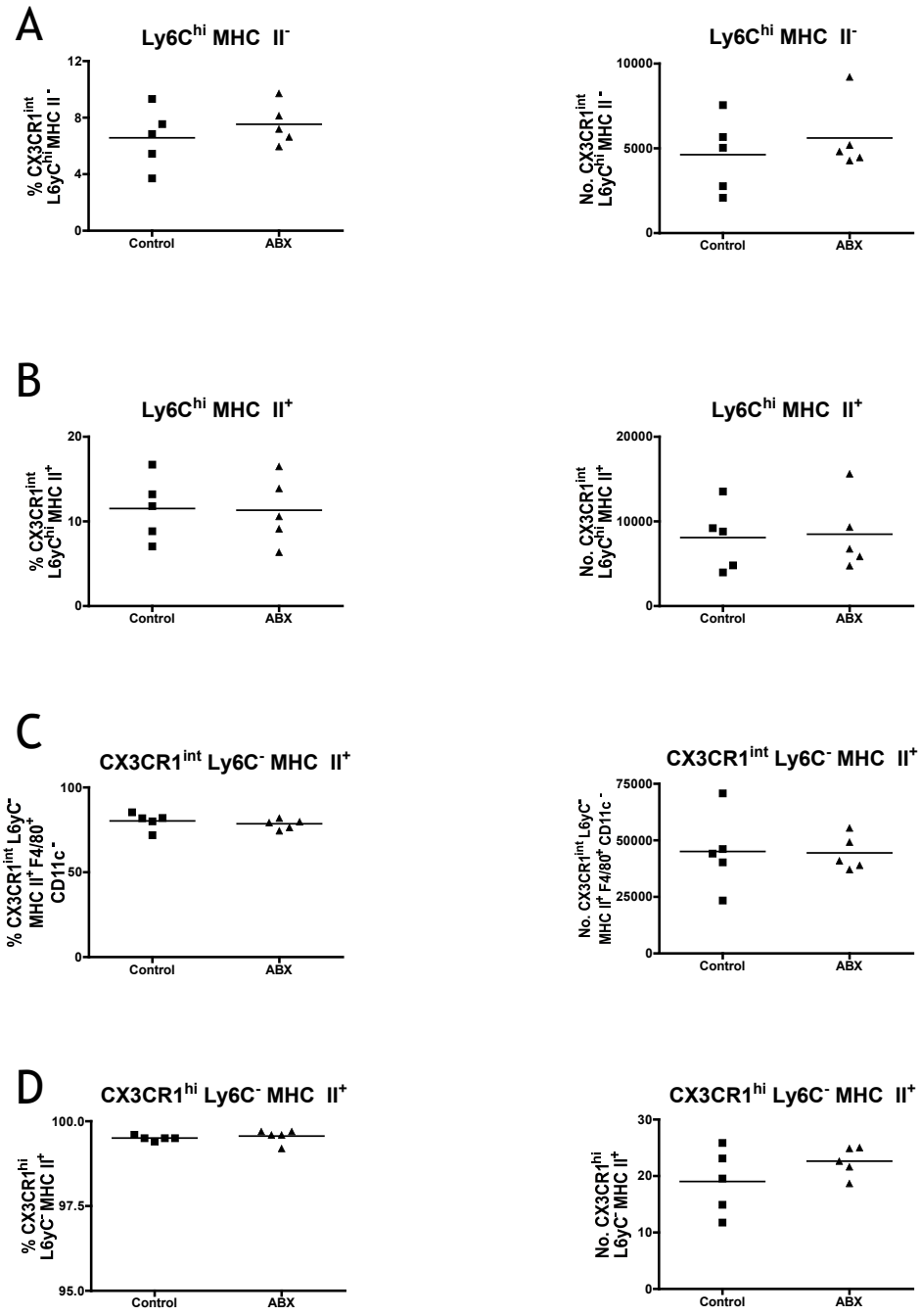

Figure 4.3. Effects of antibiotic treatment on intestinal macrophages. Frequencies (left) and absolute numbers (right) of CX3CR1^{int} Ly6C^{hi} MHC II^{-} (P1, A), CX3CR1^{int} Ly6C^{hi} MHC II^{+} (P2, B), CX3CR1^{int} Ly6C^{-} MHC II^{+} F4/80^{+} CD11c^{-} (P3, C) and CX3CR1^{hi} Ly6C^{-} MHC II^{+} (P4, D) subsets after receiving 50mg/kg vancomycin and 50mg/kg meropenem in drinking water for 22 days. The data shown are from 5 individual mice/group and are representative of 2 independent experiments.

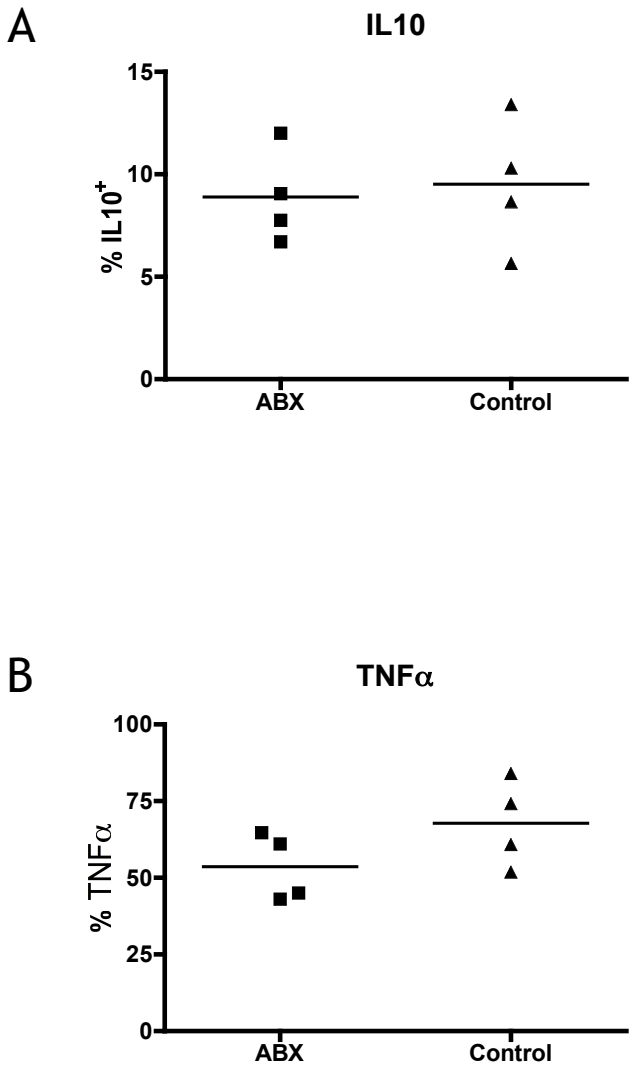

Figure 4.4. Effects of antibiotic treatment on cytokine production by intestinal macrophages. Intracellular IL10 (A) and TNFα (B) expression by CX3CR1^{hi} mφ from mice receiving 50mg/kg vancomycin and 50mg/kg meropenem in drinking water for 10 days. Results shown are % of CX3CR1^{hi} cells expressing each cytokine after 4.5 hour culture with brefeldin A and monensin. The data shown are from at least 4 individual mice/group and are representative of one experiment.

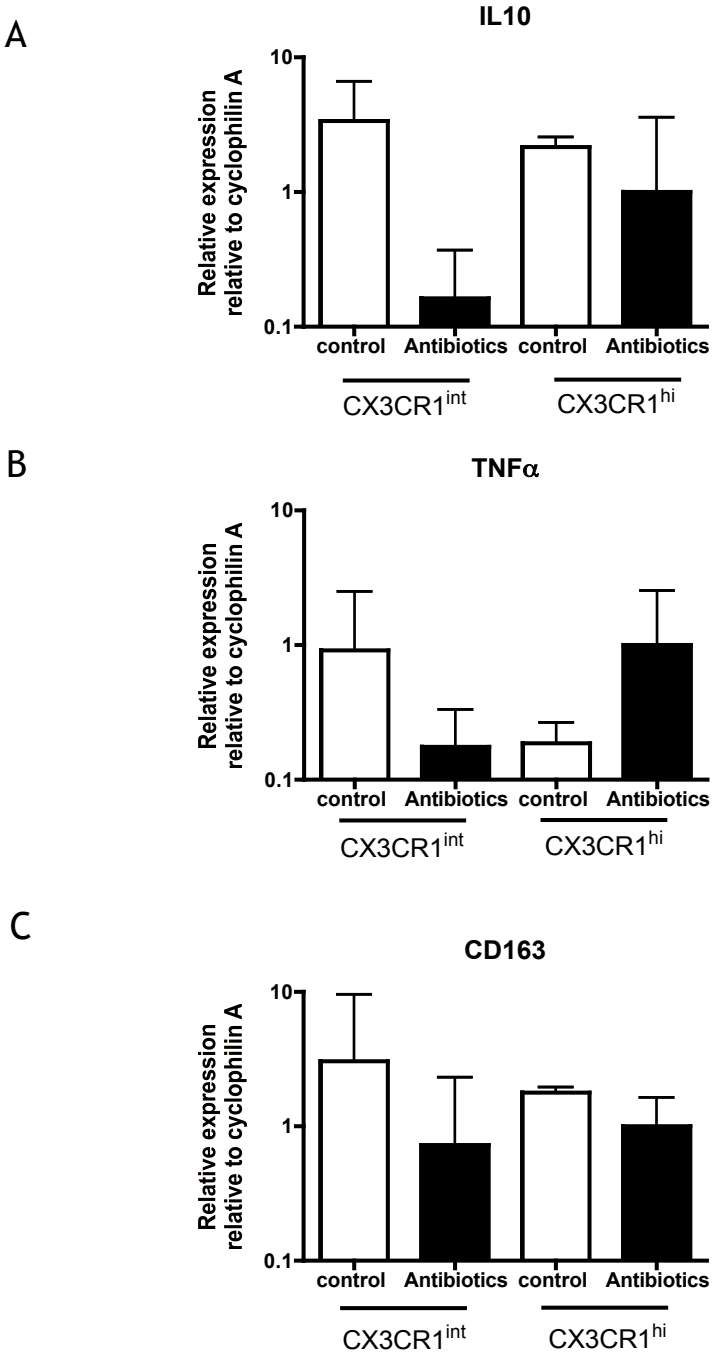

Figure 4.5. Effects of antibiotic treatment on intestinal macrophages. CX3CR1^{int} and CX3CR1^{hi} mφ amongst live CD45^{+} Ly6G^{-} Siglec F^{-} cells were sorted from mice treated with 50mg/kg vancomycin and 50mg/kg meropenem for 10 days and from sweetened water-fed controls. mRNA from sorted cells was analysed for expression of IL10 (A), TNFα (B) and CD163 (C) by qPCR. Results shown are mean expression relative to cyclophilin A (CPA) using the $2^{-\Delta C(t)}$ method. The mean was obtained from 2-3 pooled samples with technical replicates. Data are representative of one experiment.

4.4 Effects of broad spectrum antibiotic treatment on intestinal macrophages

Based on work by Abt and colleagues, which had shown marked effects on intestinal immune responses, I switched to a cocktail containing ampicillin, gentamicin, metronidazole, neomycin and vancomycin administered for 21 days in the drinking water (Abt et al., 2012). This regime would act on Gram+ve, Gram-ve, aerobic and anaerobic bacteria, and is also poorly absorbed from the intestine, maximising its effects on local bacteria. This regime produced small, but significant increases in the frequency and number of total $CD11b^{+}$ cells and a higher number of granulocytes compared with controls (Figure 4.6 B & E). However the frequencies and absolute numbers of viable leukocytes, total $CX3CR1^{int}$ and $CX3CR1^{hi}$ mϕ were not altered by the ABX (Figure 4.6 A, C & D). Although there was a decrease in the proportion of $Ly6C^{hi}$ MHC II^{-} (P1) cells amongst the $CX3CR1^{int}$ population, together with a significant increase in the number of $Ly6C^{-}$ MHC II^{+} $CX3CR1^{int}$ mϕ in ABX treated mice (Figure 4.7 A & C), these changes were generally small and of unclear significance (Figure 4.7). Finally I measured mRNA levels for IL10 and TNFα in $CX3CR1^{hi}$ mϕ sorted from ABX treated and control colon. This experiment detected few differences apart from a trend towards higher expression of TNFα by $CX3CR1^{hi}$ cells from ABX treated mice (Figure 4.8), which interestingly was similar to what I found using the simple ABX regime (Figure 4.5 B).

As these findings revealed few consistent effects, I decided not to pursue any further experiments involving antibiotic manipulation of the intestinal environment.

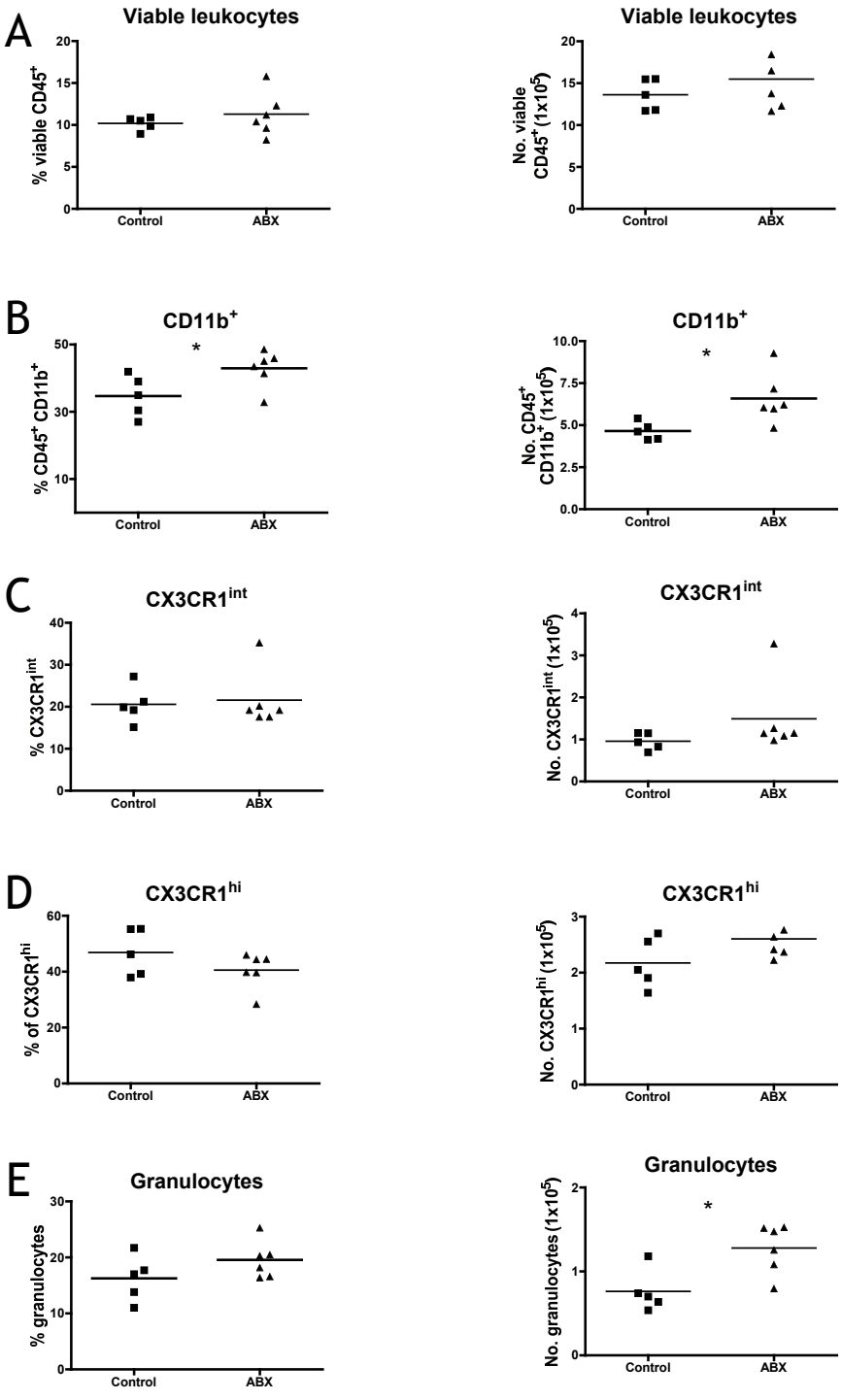

Figure 4.6. Effects of broad spectrum antibiotics on intestinal macrophages. Frequencies (left) and absolute numbers (right) of (A) viable leukocytes, (B) CD11b$^+$ cells, (C) CX3CR1^{int}, (D) CX3CR1^{hi} mφ and granulocytes (E) in colon of adult CX3CR1$^{GFP/+}$ mice after receiving ampicillin, neomycin, gentamycin, metronidazole and vancomycin in drinking water for 21 days. Data shown are from 5 individual mice/group and are representative of at least 2 independent experiments. *$p<0.05$. Student's t test.

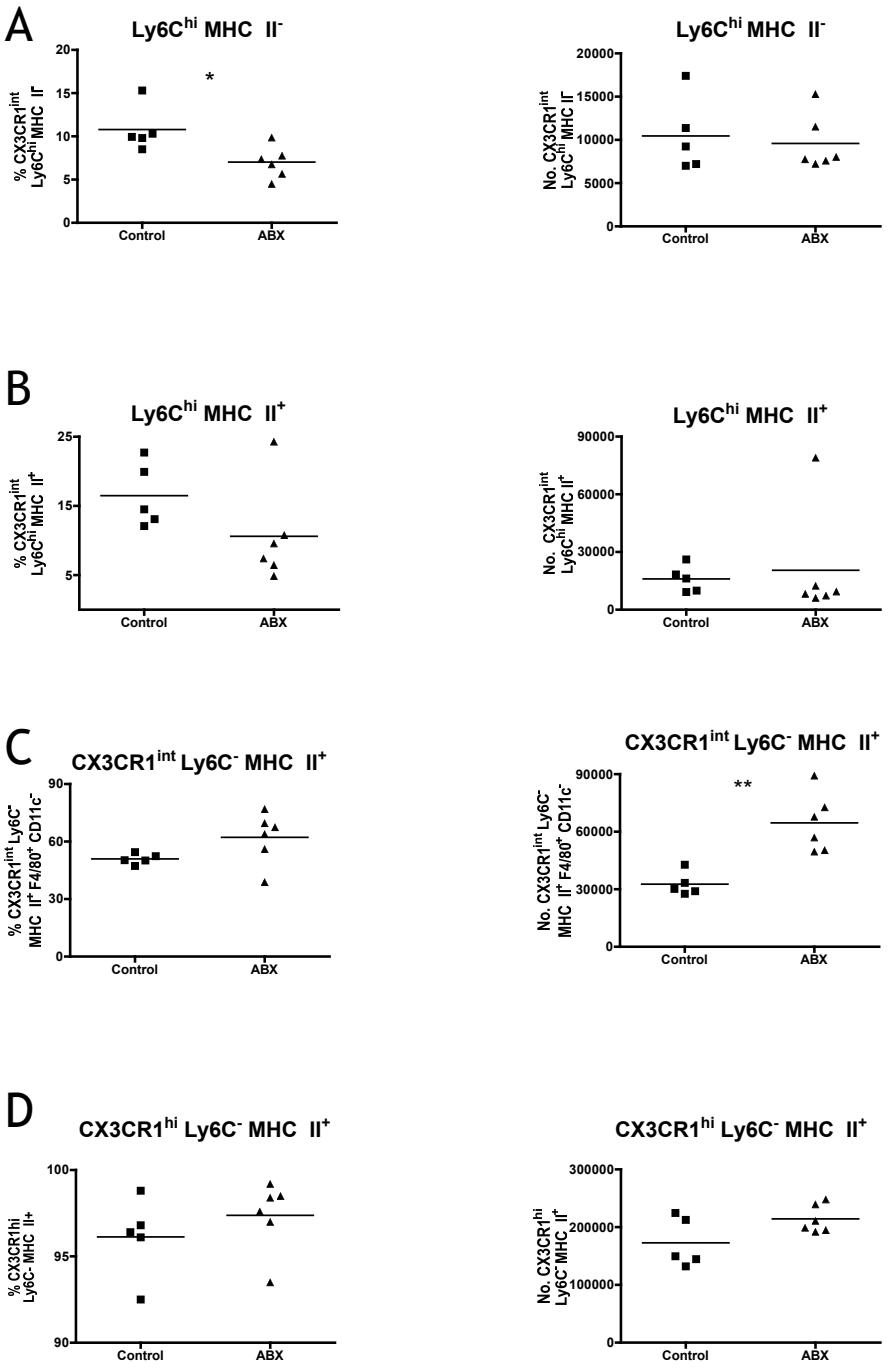

Figure 4.7. Effects of broad spectrum antibiotics on intestinal macrophages. Frequencies (left) and absolute numbers (right) of CX3CR1^{int} Ly6C^{hi} MHC II^{-} (P1, A), CX3CR1^{int} Ly6C^{hi} MHC II^{+} (P2, B), CX3CR1^{int} Ly6C^{-} MHC II^{+} F4/80^{+} CD11c^{-} (P3, C) and CX3CR1^{hi} Ly6C^{-} MHC II^{+} (P4, D) subsets after receiving ampicillin, neomycin, gentamycin, metronidazole and vancomycin in drinking water for 21 days. Data shown are from 5 individual mice/group and are representative of at least 2 independent experiments. *p<0.05. Student's t test. *p<0.05, **p<0.01. Student's t test.

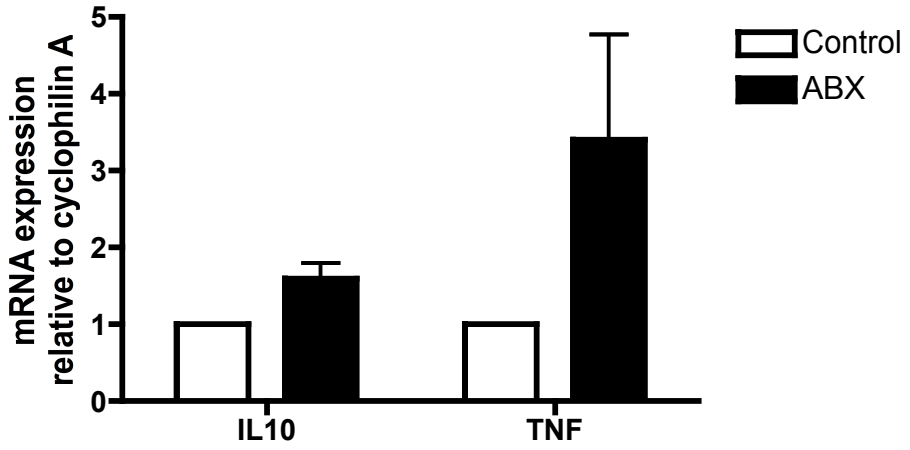

Figure 4.8. Effects of broad spectrum antibiotics on intestinal macrophages. F4/80^{hi} CD11b^{int} mφ amongst live CD45+ Ly6G- Siglec F- CD11c^{lo} cells were sorted from CX3CR1$^{GFP/+}$ mice receiving ampicillin, neomycin, gentamycin, metronidazole and vancomycin in drinking water for 21 days. mRNA from sorted cells was analysed for expression of IL10 and TNFα by qPCR. Results shown are mean expression relative to cyclophilin A (CPA) using the $2^{-\Delta C(t)}$ method. The mean was obtained from 2-3 pooled samples with biological replicates for the ABX treated group. Data are from one experiment.

4.5 Development of intestinal macrophage populations in germ free mice

Because the effects of antibiotic treatment were small and inconsistent, I decided to use a more definitive approach, in which all microbiota were absent. Thanks to collaboration with Dr David Artis, I was able to visit his laboratory in the University of Pennsylvania, to study mice in his germ-free (GF) facility. There I compared the mϕ populations present in the colon of GF mice with those from age-matched conventionally raised (CNV) animals at three different time points: 7-days-old, 3-weeks-old and 12-week-old adults.

4.5.1 Adult germ free mice

First I analysed adult mice and found that these mice had markedly enlarged caeca compared with CNV mice (Figures 4.9 A & B), together with a modest but significant increase colon length, thus confirming their GF status (Figures 4.7 B & C). However this was not reflected in a difference in the total number of cells obtained following enzymatic digestion of the colon (Figure 4.9 D).

For flow cytometric analysis, I used the same gating strategy I developed for identification of mϕ subsets in non-CX3CR$^{GFP/+}$ mice described in Chapter 3. Thus, total CD11b^{+} cells were identified amongst 7-AAD^{-} CD45^{+} Siglec F^{-} Ly6G^{-} CD11c^{lo} cells and separated into F4/80^{hi} and F4/80^{lo} subsets for assessment of their expression of Ly6C and MHC II (Figure 4.10 A). This revealed a trend towards reduced proportions and a significantly reduced absolute number of F4/80^{hi} cells in GF colon compared with CNV colon (Figure 4.10 B). Interestingly, when I looked in more detail within the F4/80^{hi} population I found that the lack of microbiota had significant effects on the proportions and absolute numbers of cells expressing MHC II in this subset (Figures 4.10 C & D). Thus, whereas virtually all F4/80^{hi} mϕ in CNV colon were Ly6C^{-} MHC II^{+} there were many more Ly6C^{-} MHC II^{-} cells within this population in GF mice.

In parallel there was a trend towards an increased frequency of F4/80^{lo} cells in GF colon. Although their absolute numbers showed a trend towards being

lower than in CNV intestine (Figures 4.11 A & B), the proportions and numbers of Ly6C^{hi} MHC II^{-} (P1) and Ly6C^{hi} MHC II^{+} (P2) cells were significantly reduced in the GF colon (Figure 4.11 C & D). The more mature subset of Ly6C^{-} MHC II^{+} (P3-P4) did not exhibit any significant difference between GF and CNV mice (Figure 4.11 E). Thus these cell subsets appear to be show generalised reduction in the proportions and number of mϕ in the adult GF colon, which affects the early stages of monocyte development acquisition of MHC II.

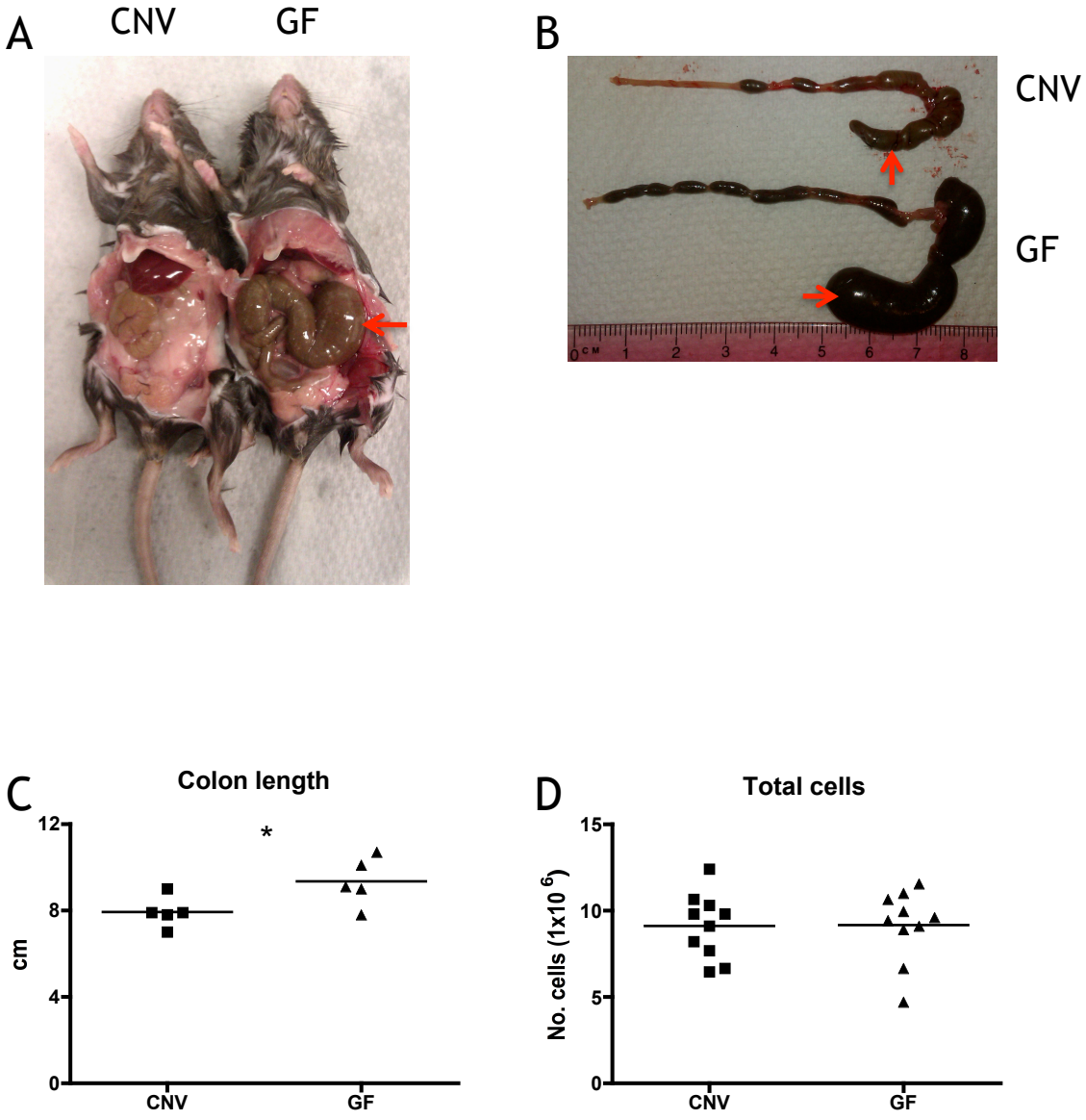

Figure 4.9. Effects of the germ free state on the large intestine. Adult germ-free (GF) mice have a much larger caecum than conventional (CNV) mice (A & B, arrows), as well as increased colon length (B & C). D) Total cells per colon from 12 week old GF and CNV mice. Data shown from 5 mice/group and are representative of two independent experiments. *p<0.05. Student's t test.

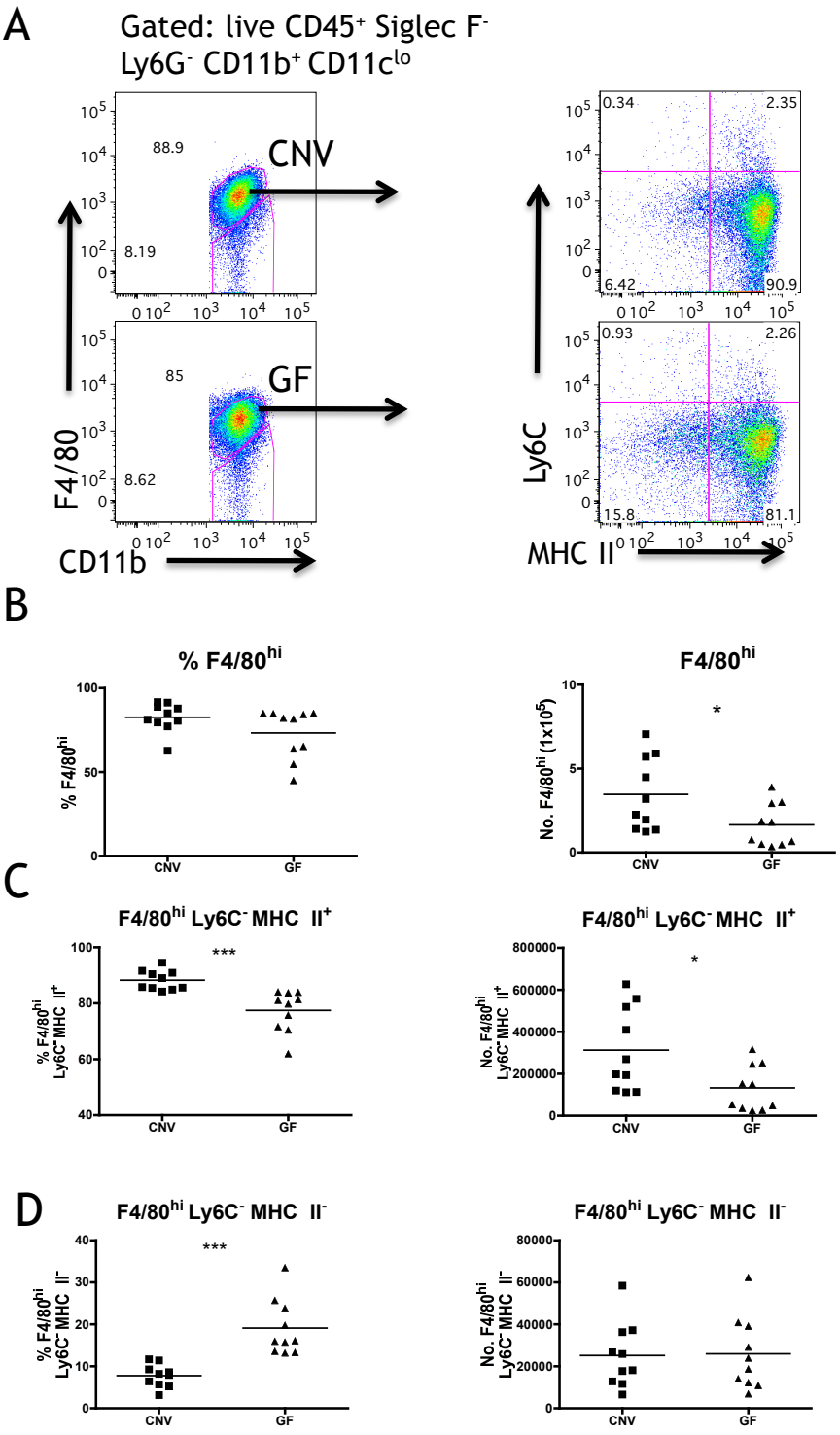

Figure 4.10. Effects of germ free state on intestinal macrophages in adult mice. Colonic LP cells were isolated from 12 week old GF or CNV B6 mice and live CD45^{+} Siglec F^{-} Ly6G^{-} CD11b^{+} CD11c^{lo} cells were analysed. F4/80^{hi} CD11b^{int} mφ were assessed for expression of Ly6C and MHC II (A). Proportions (left) and absolute numbers (right) of F4/80^{hi} CD11b^{int} mφ (B) Ly6C^{-} MHC II^{+} (P4, C) and Ly6C^{-} MHC II^{-} (D) cells within this population. Data are pooled from two independent experiments with 5 mice/group/experiment. *p<0.05, ***p<0.001. Student's t test.

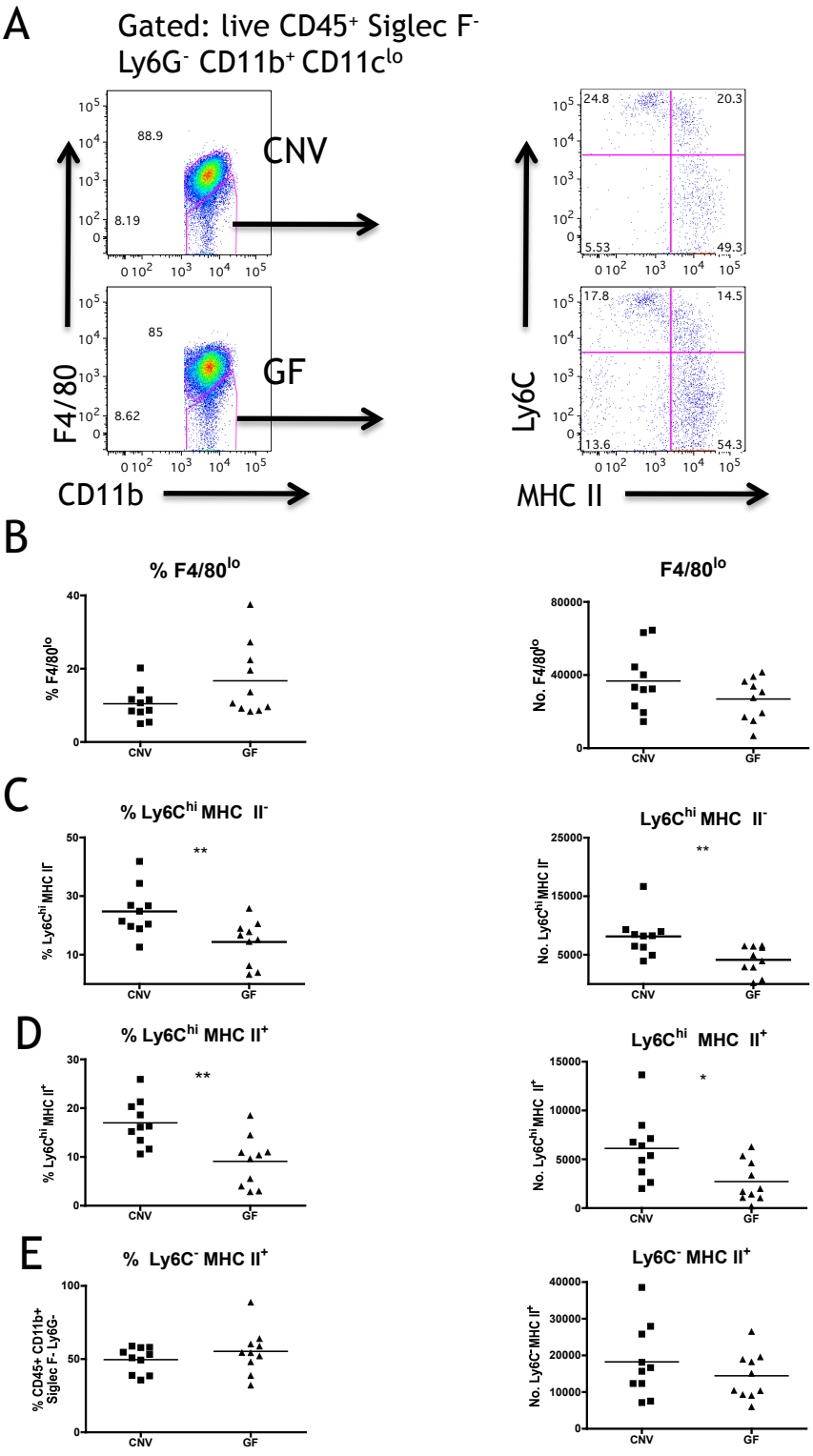

Figure 4.11. Effects of germ free state on intestinal macrophages in adult mice. Colonic LP cells were isolated from 12 week old GF or CNV B6 mice and live CD45$^+$ Siglec F$^-$ Ly6G$^-$ CD11b$^+$ CD11c^{lo} cells were analysed for F4/80^{lo} CD11b$^+$ mφ and their expression of Ly6C and MHC II (A). Proportions (left) and absolute numbers (right) of F4/80^{lo} CD11b$^+$ mφ (B), Ly6C^{hi} MHC II$^-$ (P1, C), Ly6C^{hi} MHC II$^+$ (P2, D) and Ly6C$^-$ MHC II$^+$ (P3, E) cells amongst F4/80^{lo} CD11b$^+$ mφ. Data are pooled from two independent experiments with 5 mice/group/ experiment. *p<0.05, **p<0.01. Student's t test.

4.5.2 3 week old germ free mice

As results in my previous chapter indicated that a large influx of mϕ around the time of weaning might be involved in establishing the adult pool, I thought it was important to determine if this process was dependent on the presence of the microbiota. To do this I compared GF and CNV mice at 21 days of age, around the time when the weaning-related influx occurred. As I found in the previous chapter, there was a much better defined population of F4/80^{lo} cells in CNV mice at this age (Figure 4.12 A left). Although the total numbers of F4/80^{hi} cells were not different between GF and CNV mice, GF mice had significantly higher proportions (Figure 4.12 A & B). Both proportions and numbers of Ly6C^{-} MHC II^{+} cells were significantly reduced in GF mice together with parallel increased proportions and numbers of Ly6C^{-} MHC II^{-} cells (Figure 4.12 C & D). Interestingly, these changes appeared despite the fact that the total numbers of F4/80^{hi} mϕ were similar between groups and GF mice had a significantly higher proportion of F4/80^{hi} cells in comparison to their CNV counterparts (Figure 4.12 A & B) and this probably reflected the fact that these GF mice had fewer F4/80^{lo} cells than the controls (Figure 4.13 A left & B). The most dramatic difference with this population was seen in regards to the Ly6C^{hi} MHC II^{+} subset (P2), which was virtually absent in GF mice (Figure 4.13 A right & D). Additionally, the proportions and numbers of Ly6C^{hi} MHC II^{-} monocytes (P1) were also significantly reduced in GF mice (Figure 4.13 A right & C). Finally, the proportions of Ly6C^{-} MHC II^{+} (P3) cells amongst the F4/80^{lo} subset were significantly increased in GF mice, but these numbers tended to be lower than the CNV colons (Figure 4.13 E). Thus there appears to be a pronounced defect in the recruitment of mϕ precursors in GF mice at weaning.

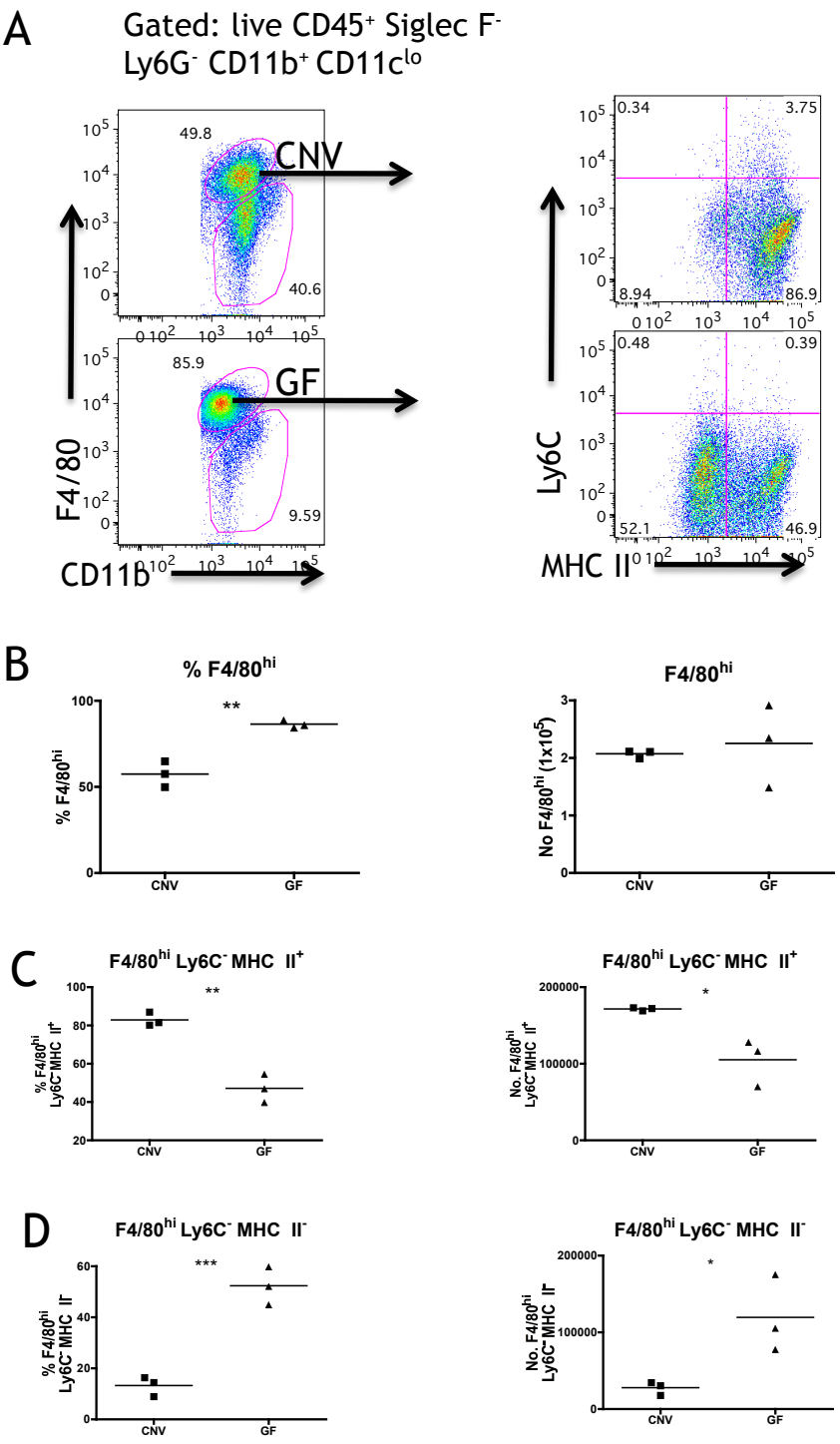

Figure 4.12. Effects of germ free state on intestinal macrophages in 3 week old mice. Colonic LP cells were isolated from 3 week old GF or CNV B6 mice and live CD45$^+$ Siglec F$^-$ Ly6G$^-$ CD11b$^+$ CD11c^{lo} cells were analysed. F4/80^{hi} CD11b^{int} mφ were assessed for expression of Ly6C and MHC II (A). Proportions (left) and absolute numbers (right) of F4/80^{hi} CD11b^{int} mφ (B) Ly6C$^-$ MHC II$^+$ (P4, C) and Ly6C$^-$ MHC II$^-$ (D) cells within this population. Data are from 1 experiment with 3 mice/group. *p<0.05, **p<0.01, ***p<0.01. Student's t test.

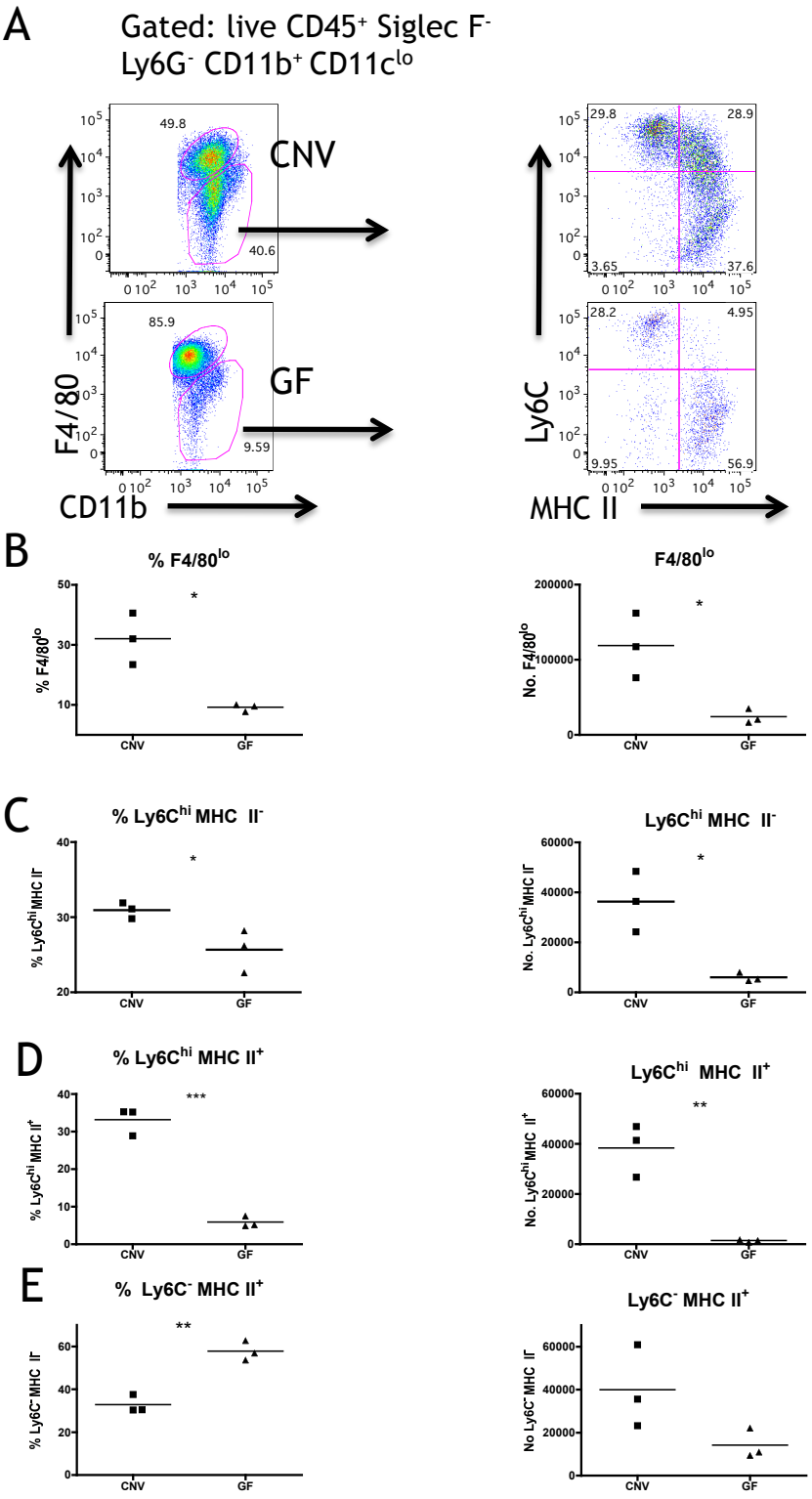

Figure 4.13. Effects of germ free state on intestinal macrophages in 3 week old mice. Colonic LP cells were isolated from 3 week old GF or CNV B6 mice and live CD45$^+$ Siglec F$^-$ Ly6G$^-$ CD11b$^+$ CD11c^{lo} cells were analysed for F4/80^{lo} CD11b$^+$ mφ and their expression of Ly6C and MHC II (A). Proportions (left) and absolute numbers (right) of F4/80^{lo} CD11b$^+$ mφ (B), Ly6C^{hi} MHC II$^-$ (P1, C), Ly6C^{hi} MHC II$^+$ (P2, D) and Ly6C$^-$ MHC II$^+$ (P3, E) cells amongst F4/80^{lo} CD11b$^+$ mφ. Data are from 1 experiment with 3 mice/group. *p<0.05, **p<0.01, ***p<0.001. Student's t test.

4.5.3 7 day old germ free mice

Finally, I compared 7 day old GF and CNV mice to gain some insight into how early mϕ development might be altered in GF conditions at the time when the microbiota would normally begin to establish. As expected, there was a clear distinction between F4/80^{hi} and F4/80^{lo} subsets at this time and this was not dependent on the presence of the microbiota (Figure 4.14 A). Similar to adult mice, there were significant reductions in the frequency and absolute number of F4/80^{hi} cells in GF mice (Figure 4.14 B) and this appeared to be due to a reduced number Ly6C^{-} MHC II^{-} cells (Figure 4.14 A right, C & D).

No differences were seen in the number or frequency of the entire F4/80^{lo} subset between GF and CNV intestine (Figure 4.15 A left & B). However as I found in older mice, 7 day old GF had a very marked reduction in numbers and proportions of the Ly6C^{hi} MHC II^{+} (P2) cells in this subset (Figure 4.15 A right & D). There was also a trend towards fewer Ly6C^{-} MHC II^{+} F4/80^{lo} cells in GF mice (P3) (Figure 4.15 E), also consistent with what I found at previous age time points (Figures 4.13 E & 4.11 E).

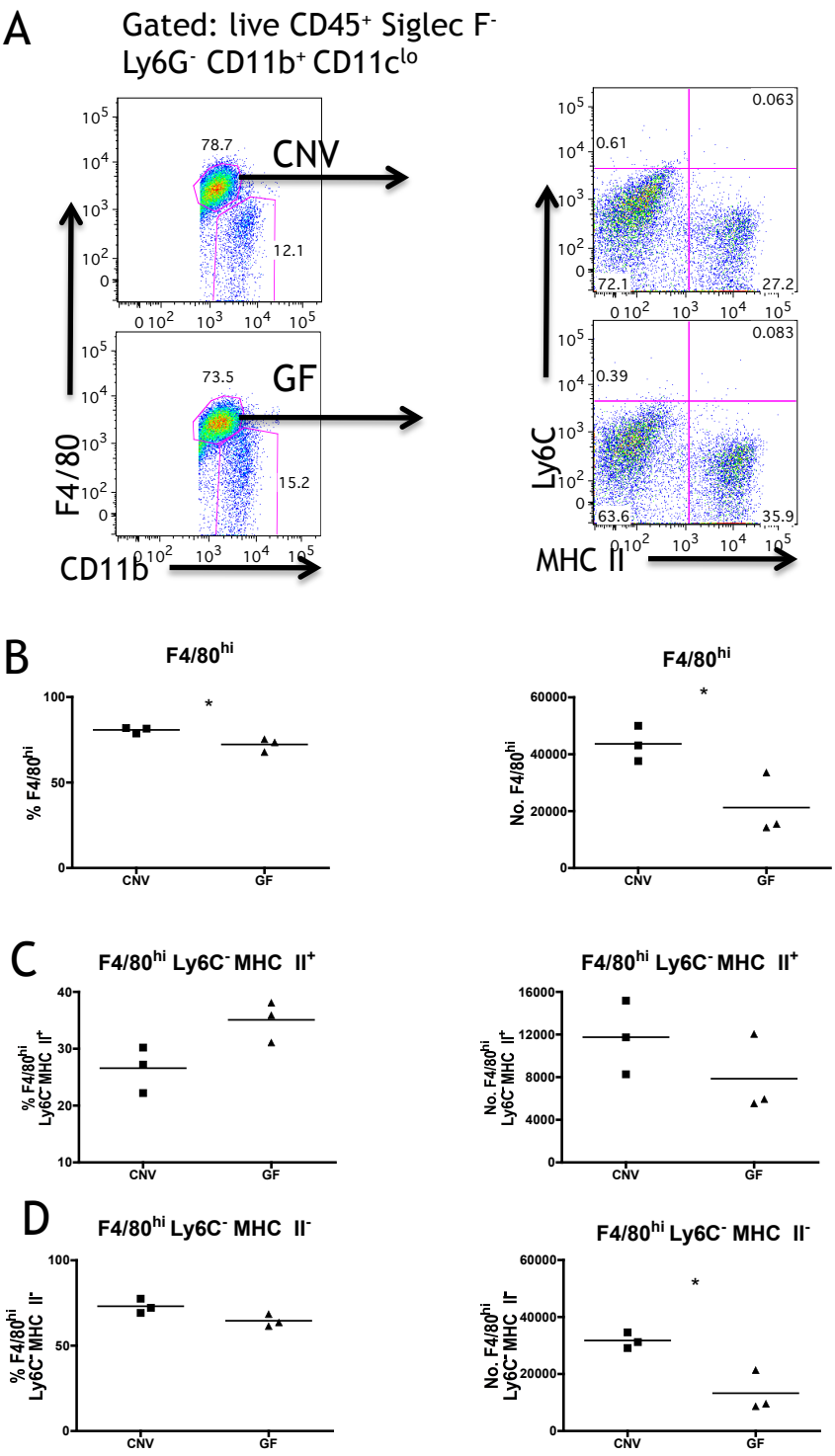

Figure 4.14. Effects of germ free state on intestinal macrophages in 7 day old mice. Colonic LP cells were isolated from 7 day old GF or CNV B6 mice and live CD45$^+$ Siglec F$^-$ Ly6G$^-$ CD11b$^+$ CD11c^{lo} cells were analysed. F4/80^{hi} CD11b^{int} mφ were assessed for expression of Ly6C and MHC II (A). Proportions (left) and absolute numbers (right) of F4/80^{hi} CD11b^{int} mφ (B) Ly6C$^-$ MHC II$^+$ (P4, C) and Ly6C$^-$ MHC II$^-$ (D) cells within this population. Data are from 1 experiment with 3 sets of 2 pooled mice/group. *p<0.05. Student's t test.

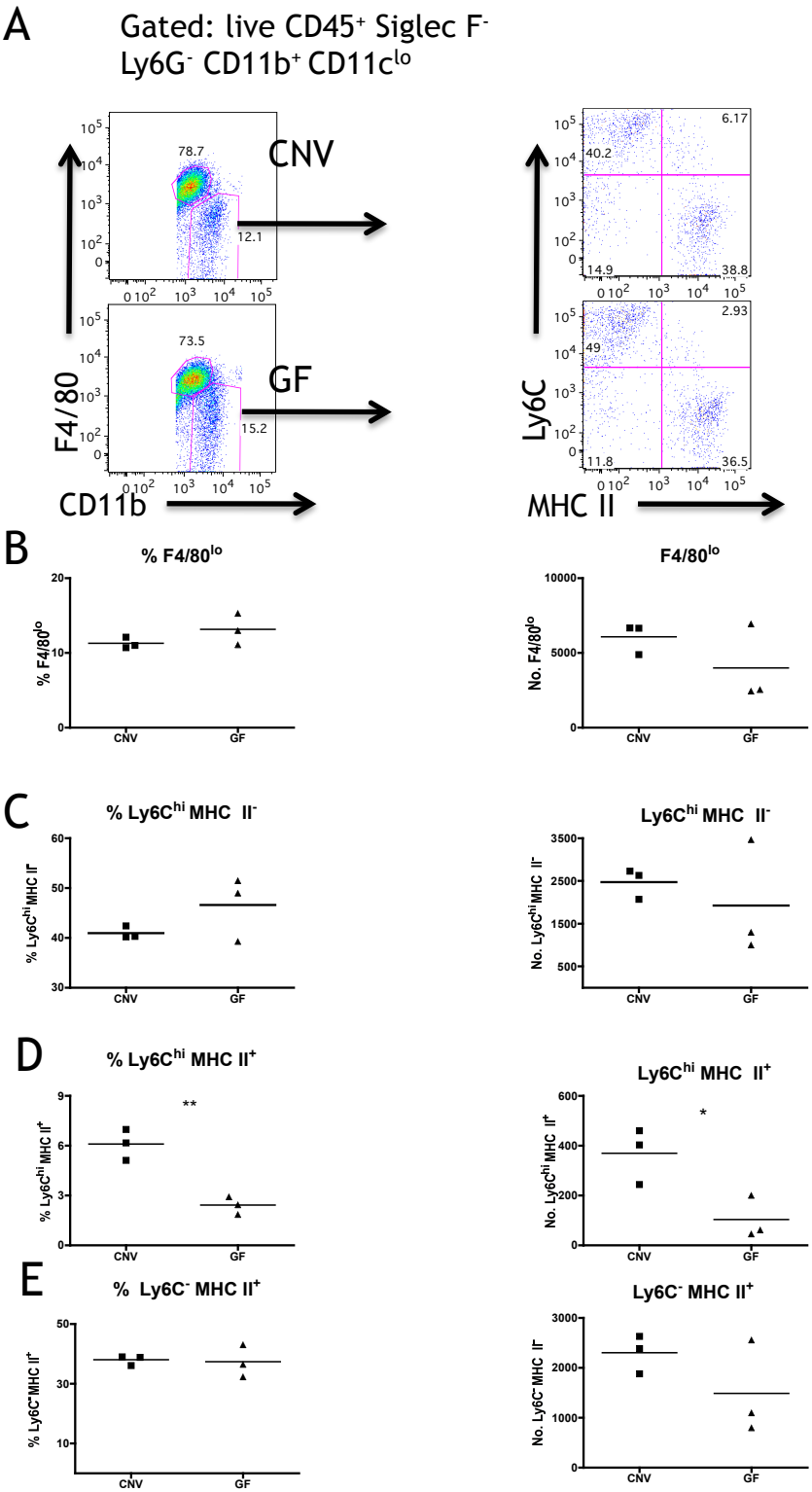

Figure 4.15. Effects of germ free state on intestinal macrophages in 7 day old mice. Colonic LP cells were isolated from 7 day old GF or CNV B6 mice and live CD45$^+$ Siglec F$^-$ Ly6G$^-$ CD11b$^+$ CD11c^{lo} cells were analysed for F4/80^{lo} CD11b$^+$ mφ and their expression of Ly6C and MHC II (A). Proportions (left) and absolute numbers (right) of F4/80^{lo} CD11b$^+$ mφ (B), Ly6C^{hi} MHC II$^-$ (P1, C), Ly6C^{hi} MHC II$^+$ (P2, D) and Ly6C$^-$ MHC II$^+$ (P3, E) cells amongst F4/80^{lo} CD11b$^+$ mφ. Data are from 1 experiment with 3 sets of 2 pooled mice/group. *p<0.05, **p<0.01. Student's t test.

4.6 Summary

In this chapter I examined the role of the commensal microbiota on the development of colonic mϕ. To do this, I first tried to decrease the bacterial load using two different oral antibiotic regimes. My results suggest that short term administration of broad-spectrum antibiotics may not be sufficient to generate significant changes in colonic mϕ in terms of numbers, cell surface markers, intracellular cytokine production or mRNA expression from FACS-purified cells.

Because these studies were unsuccessful, I went on to compare colonic lamina propria mϕ populations in GF and SPF mice at 7 days of age, weaning and adulthood. Interestingly, at 7 days of age GF mice had a defect in the frequency and numbers of the F4/80^{hi} mϕ, thought to be derived from foetal YS precursors, principally affecting the Ly6C^{-} MHC II^{-} subset. This could suggest a crucial role for commensal microbiota in driving the recruitment of primitive mϕ precursors into the developing colonic lamina propria. At 3 weeks of age, GF mice showed a dramatic decrease in the frequency and absolute numbers of the Ly6C^{hi} MHC II^{-} and Ly6C^{hi} MHC II^{+} subsets of F4/80^{lo} cells that represent monocytes and immature mϕ respectively. There was also a relative increase in the number of the Ly6C^{-} MHC II^{-} subset of F4/80^{hi} mϕ in GF mice. Together these results suggest there may be deficient recruitment of monocytes into the GF intestine, as well as delayed maturation with respect to MHC II expression. Although adult GF mice also had fewer F4/80^{hi} cells and decreased numbers of Ly6C^{hi} MHC II^{-}, Ly6C^{hi} MHC II^{+} and Ly6C^{-} MHC II^{+} cells in addition to a higher proportion of Ly6C^{-} MHC II^{-} cells compared with CNV controls, these changes were generally less marked than at weaning, suggesting that although the microbiota play a prominent role in the recruitment and maturation of monocytes at weaning, these defects can be overcome by other mechanisms later in life.

Chapter 5
Role of the CX3CL1-CX3CR1 axis in macrophage function *in vitro* and *in vivo*

5.1 Introduction

The final aim of my thesis was to explore the role of the CX3CL1-CX3CR1 axis in the development and function of intestinal macrophages. As I have shown in the previous chapters, resident intestinal mϕ express very high levels of CX3CR1 and its ligand CX3CL1 is produced by intestinal epithelial cells (Kim, 2011). Additionally, a significant increase in CX3CL1 mRNA expression in inflamed lesions from the intestine of patients with Crohn's disease compared with non-inflamed colonic mucosa has been reported. Furthermore, CX3CR1 deficient mice have been reported to have a defect in mononuclear phagocyte uptake of bacteria from the intestinal lumen (D'Haese et al., 2010; Niess et al., 2005), be resistant to experimental colitis (Kostadinova et al., 2010) and have a defect in oral tolerance induced by feeding protein antigen (Hadis et al., 2011). Taken together, these findings suggest that the CX3CR1-CX3CL1 axis may play an important role in driving active immunity in the intestine (Blaschke et al., 2003; Durkan et al., 2007; Kasama et al., 2010; Lesnik et al., 2003; Staniland et al., 2010; Suzuki et al., 2005). However, contrary to the above there are some reports that actually suggest an anti-inflammatory role for CX3CR1, including models of autoimmune uveitis and DSS colitis (Dagkalis et al., 2009; Medina-Contreras et al., 2011). As high levels of CX3CR1 characterise intestinal mϕ from embryonic life, I thought it would be important to define how CX3CR1 and CX3CL1 might regulate intestinal mϕ populations in steady state and during inflammation. I then went on to investigate the role of CX3CR1 in priming of mice by feeding ovalbumin together with a mucosal adjuvant. Finally, I examined the role of this interaction in the activation of bone marrow-derived macrophages by the TLR agonist LPS *in vitro*.

5.2 Role of the CX3CR1-CX3CL1 axis in DSS colitis

To examine how the lack of CX3CR1 might affect intestinal inflammation, I used a model in which $CX3CR1^{GFP/GFP}$ (KO) mice received 2% DSS in their drinking water for 8 days. In the first experiment, C57/Bl6 (WT) mice were used as controls and as expected, they showed progressive weight loss from day 5 onwards, which was accompanied by colon shortening and signs of clinical disease such as rectal bleeding and diarrhoea (Figure 5.1 A). In this

experiment, the CX3CR1 KO mice showed protection from disease, with no significant weight loss or clinical disease and much less colon shortening than WT mice, confirming previous studies in this model (Brand et al., 2006; Kostadinova et al., 2010; Nishimura et al., 2009). However, this protective effect was not seen consistently when I repeated the experiment. Thus when CX3CR1 KO mice were compared with B6 WT mice on a second occasion, both strains lost weight, had colon shortening and developed clinical disease, with only a small degree of protection being seen for the clinical scores in KO mice compared with WT (Figure 5.1 B). In the last experiment, I used CX3CR1$^{GFP/+}$ mice as controls and on this occasion both strains developed equivalent disease as assessed by all the parameters (Figure 5.1 C).

A

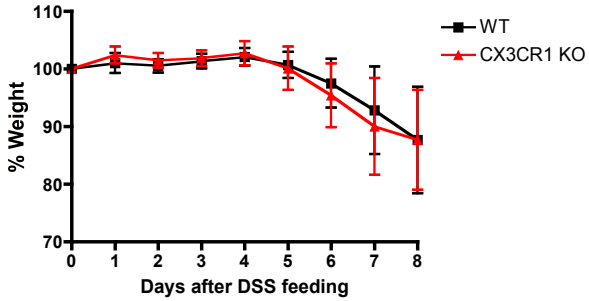

B

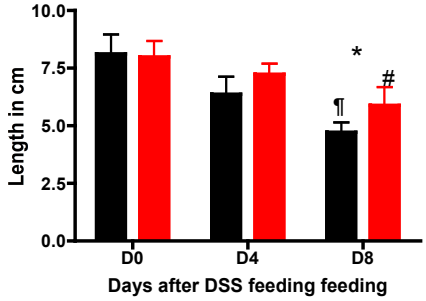

C

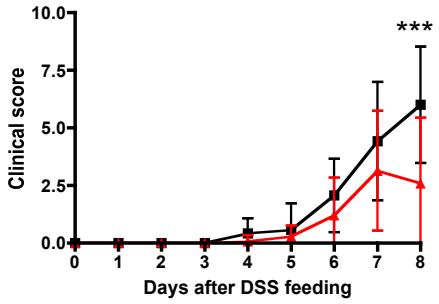

Figure 5.1. Role of CX3CR1 in DSS colitis. CX3CR1$^{GFP/GFP}$ (KO) and C57Bl/6 (WT) mice were given drinking water containing 2% DSS for 7-8 days and the progress of disease monitored by (A) percentage of the original weight loss, (B) colon shortening and clinical score (C). Results shown are the means ± 1 SD for three independent experiments with 3 mice/group. *p<0.05; ***p<0.001 WT or CX3CR1$^{GFP/+}$ vs KO; ¶p<0.001, WT D0 vs D8 DSS; $^{\#}$p<0.05, KO D0 vs DSS. Two-way ANOVA followed by Bonferroni's post-test.

5.3 CX3CR1^{+} cell distribution in bone marrow, blood and colon in steady state and inflammation

To examine whether the CX3CL1-CX3CR1 axis might be having more subtle effects on colitis, I went on to compare the inflammatory infiltrates in the colon, blood and BM of CX3CR1$^{GFP/+}$ (het) and CX3CR1$^{GFP/GFP}$ (KO) mice with DSS colitis. This also allowed me to determine if these various myeloid cell populations were altered by the absence of CX3CR1 in the steady state and during acute inflammation. Under resting conditions, both strains demonstrated the expected populations of CX3CR1^{hi}, CX3CR1^{int} and CX3CR1^{-} cells amongst the CD11b^{+} cells, with the CX3CR1^{hi} cells being in the majority (Figure 5.2 A & B top panels). As shown previously in the lab (Bain et al., 2013), after 4 days on DSS there was a substantial increase in the proportions of CX3CR1^{int} of cells in CX3CR1$^{GFP/+}$ mice (Figure 5.2 B bottom panels). Although these subsets were significantly higher as a proportion of total CD45^{+} leukocytes in CX3CR1 deficient mice compared with CX3CR1$^{GFP/+}$ mice with colitis, there were no differences between the strains in terms of absolute numbers (Figure 5.3). As expected from an acute inflammatory process, the frequency and absolute numbers of neutrophils increased in CX3CR1$^{GFP/+}$ mice with colitis, whereas only the numbers of neutrophils were significantly increased in CX3CR1 deficient mice with colitis (Figure 5.3 A & B). The numbers of CX3CR1^{hi} cells also increased, although their proportions decreased in parallel with marked rise in CX3CR1^{int} cells (Figure 5.3 E & F). Regardless of all these changes in cell distribution, no consistent differences between strains were seen during inflammation and therefore I did not analyse the CX3CR1-expressing populations further in terms of Ly6C or MHC II expression to identify the P1, P2, and P3 subsets described in earlier chapters.

To investigate if there were any intrinsic differences in the production of myeloid cells in CX3CR1 KO mice and to explore if they might be mobilised differently during inflammation, I examined the numbers of monocytes and granulocytes in BM and blood of CX3CR1$^{GFP/+}$ and KO mice in the resting state and in DSS colitis. Three populations of CD45^{+} CD11b^{+} cells were found in the BM, the largest of which was Ly6C^{int} CX3CR1^{-}, representing granulocytes. The

next biggest group comprised Ly6C^{hi} CX3CR1^{int} monocytes and there was a less well-defined group of Ly6C^{lo} CX3CR1^{+} monocytes (Figure 5.4 A). Steady state CX3CR1 deficient mice had a significantly lower proportion of granulocytes in the BM compared with resting CX3CR1$^{GFP/+}$ controls. However during DSS colitis the proportions of granulocytes in CX3CR1 KO BM rose to match the levels in CX3CR1$^{GFP/+}$ mice, which did not alter in colitis. (Figure 5.4 B). Concomitant with the changes in granulocytes, the proportion of Ly6C^{hi} monocytes was higher in steady state CX3CR1 KO mice compared with heterozygous controls but this decreased during inflammation, whilst again there was no change in this population in CX3CR1$^{GFP/+}$ mice during colitis (Figure 5.4 C). The low proportion of Ly6C^{lo} monocytes in CX3CR1$^{GFP/+}$ controls increased significantly during inflammation, while these were found at significantly higher levels in resting CX3CR1 KO BM, and did not change in colitis (Figure 5.4 D).

As expected, blood contained the same subsets of myeloid cells found in BM and there were no differences in the proportions of granulocytes between the strains in either steady state or during DSS colitis (Figure 5.5 A & B). However after 4 days on DSS the proportion of Ly6C^{hi} blood monocytes in CX3CR1 KO mice decreased, whereas they remained at the steady state level in CX3CR1$^{GFP/+}$ mice (Figure 5.5 C). Finally, the proportions of Ly6C^{lo} blood monocytes were higher in steady state CX3CR1 KO than in CX3CR1$^{GFP/+}$ controls, but this difference was not observed during DSS colitis (Figure 5.5 D).

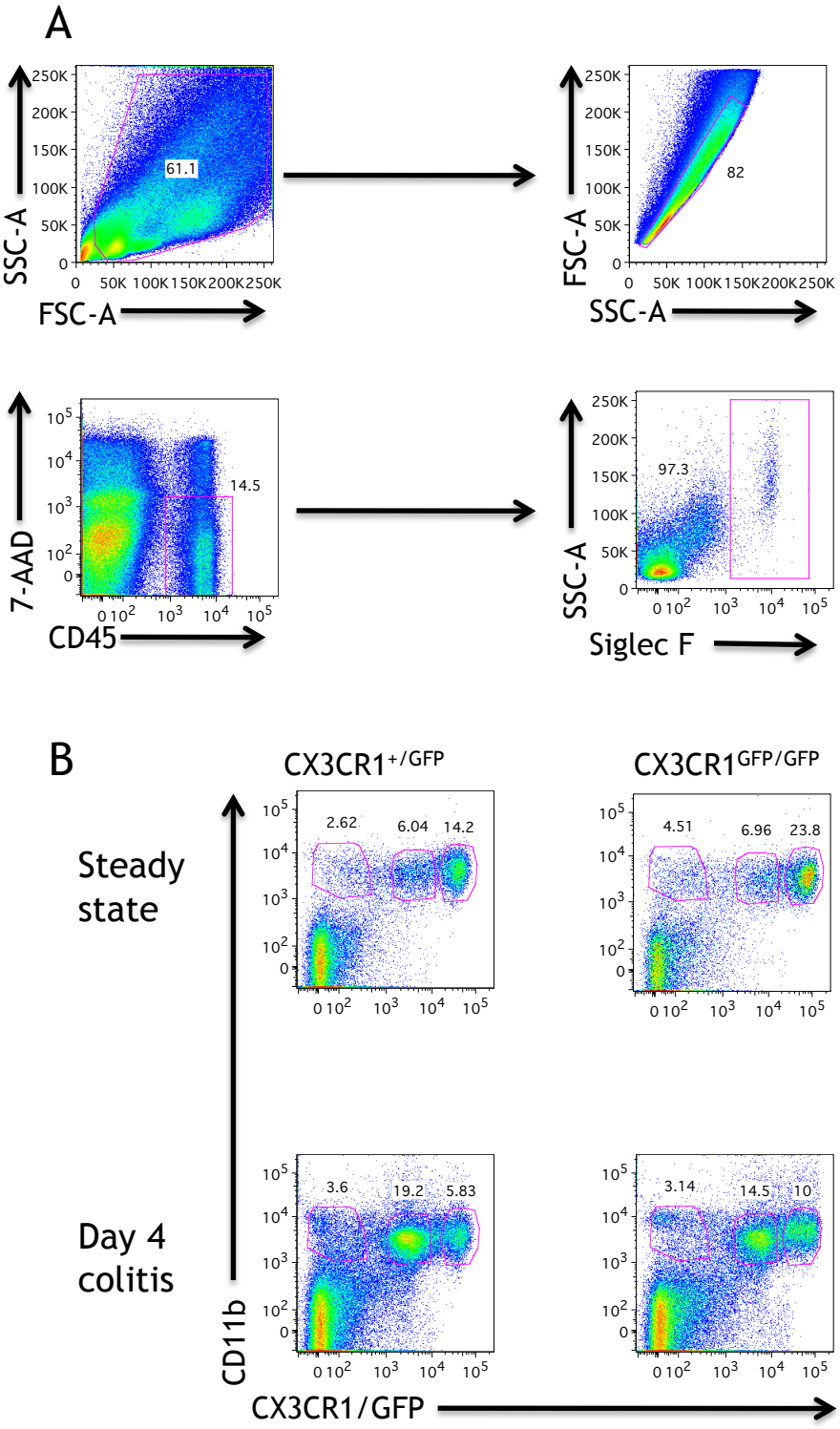

Figure 5.2. Role of CX3CR1 in leukocyte populations in colonic lamina propria of during steady state and in inflammation. (A) Gating strategy for the identification of colonic mφ. (B) CD11b and CX3CR1 expression by live gated CD45^{+} Siglec F^{-} cells from the colon of CX3CR1$^{GFP/+}$ (left) and CX3CR1$^{GFP/GFP}$ mice. Numbers represent the proportion of cells within each marked gate. Data are representative of two independent experiments.

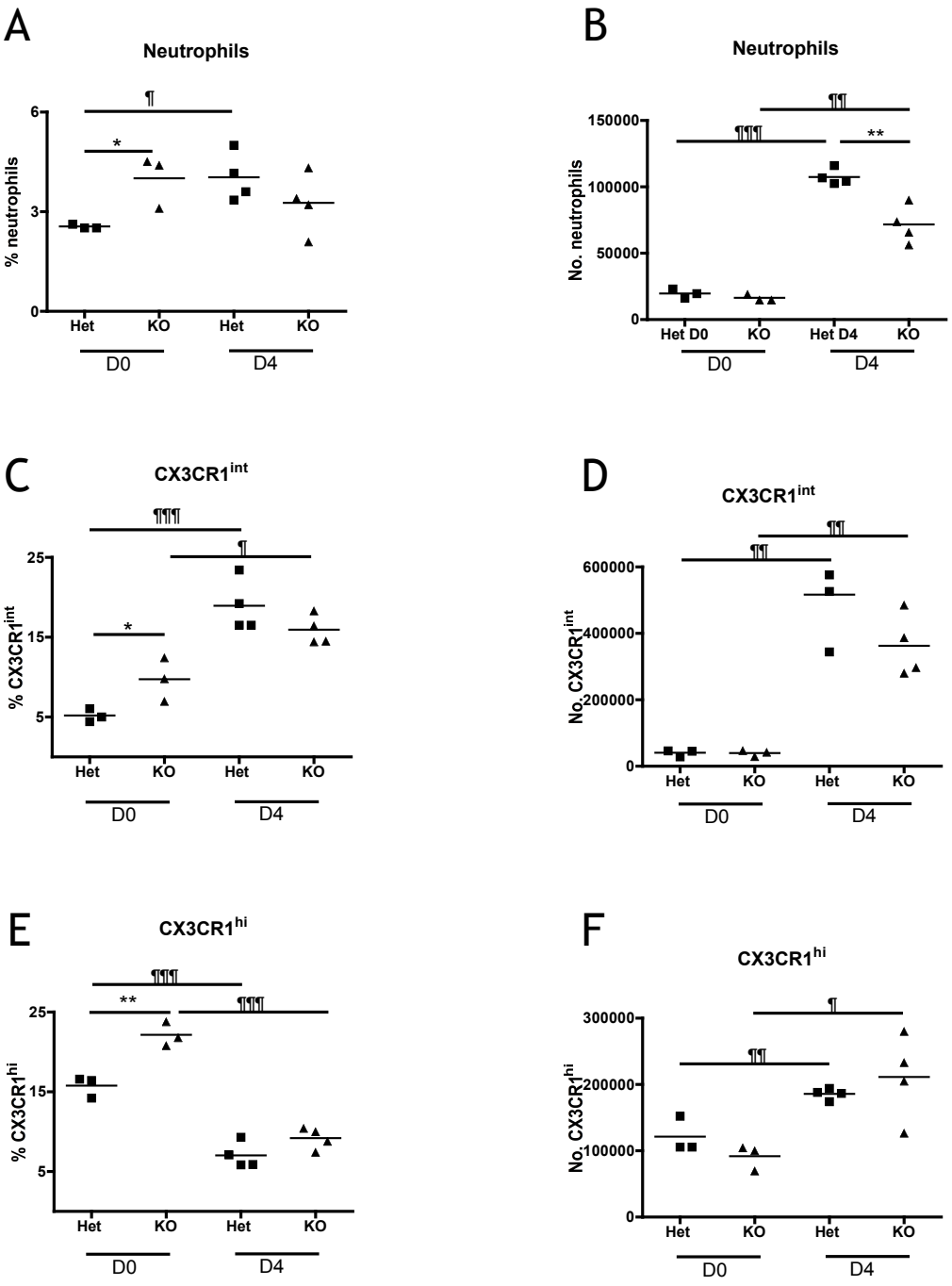

Figure 5.3. Role of CX3CR1 in leukocyte populations in colonic lamina propria of during steady state and in inflammation. Proportions (left panels) and absolute numbers (right panels) of neutrophils (A & B), CX3CR1^{int} (C & D) and CX3CR1^{hi} (E & F) cells amongst total live gated CD45^{+} Siglec F^{-} cells from the colon of CX3CR1$^{GFP/+}$ (het) and CX3CR1$^{GFP/GFP}$ mice. Data are representative of two independent experiments. *p<0.05, **p<0.01 CX3CR1$^{GFP/+}$ vs KO; ¶p<0.05, ¶¶p<0.01, ¶¶¶p<0.001 steady state vs inflammation. Student's t test.

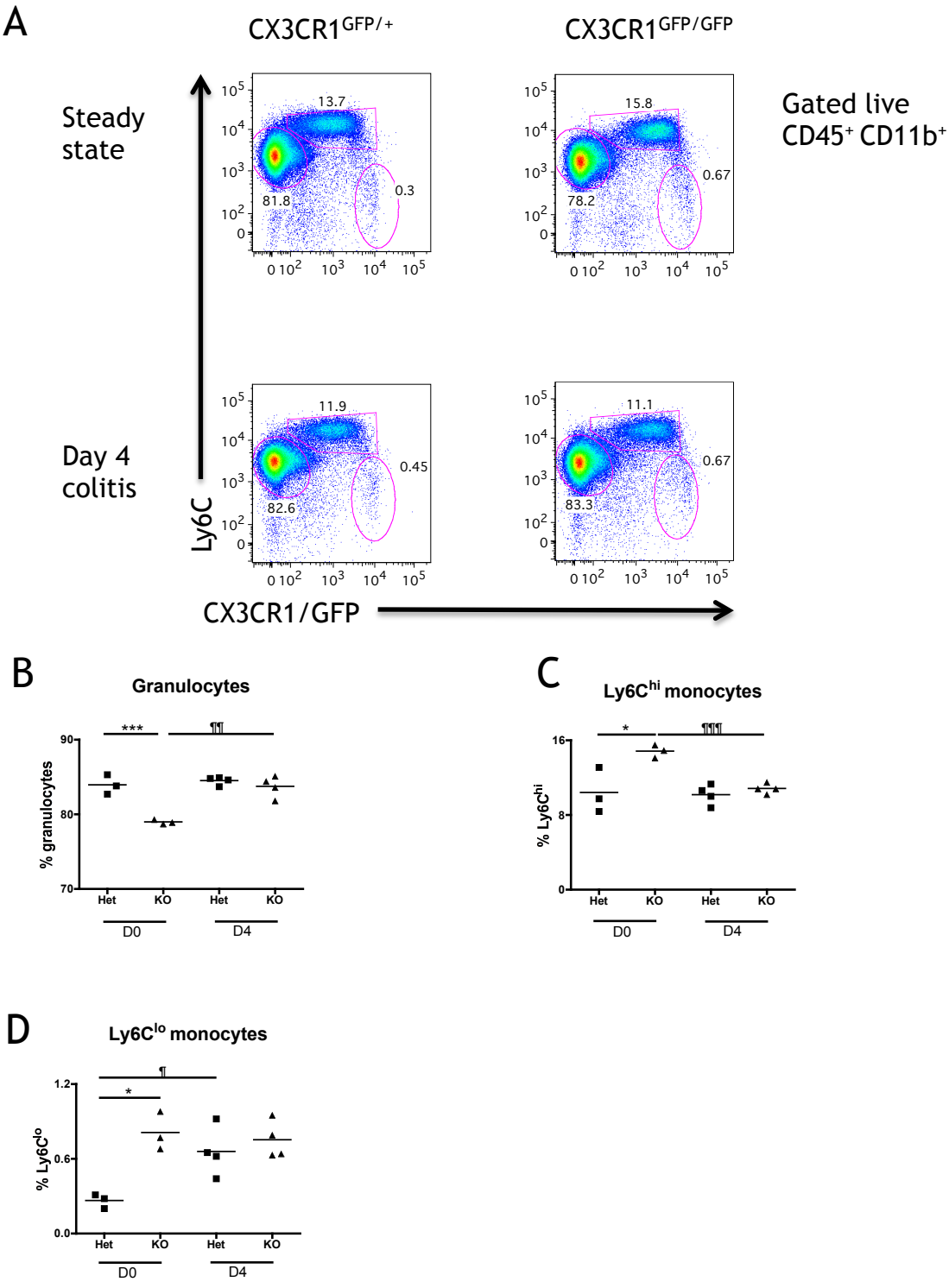

Figure 5.4. Role of CX3CR1 in leukocyte development in bone marrow during steady state and inflammation. (A) Expression of Ly6C and CX3CR1 by live gated CD45$^+$ CD11b$^+$ cells from BM of CX3CR1$^{GFP/+}$ (Het, left) and CX3CR1$^{GFP/GFP}$ (KO, right) mice showing granulocytes (Ly6C$^+$ CX3CR1$^-$), Ly6C^{hi} monocytes (Ly6C^{hi} CX3CR1^{lo}) and Ly6C^{lo} monocytes (Ly6C^{lo} CX3CR1$^+$). Frequencies of granulocytes (B), Ly6C^{hi} (C) and Ly6C^{lo} (D) monocytes. Data are representative of two independent experiments. *p<0.05, ***p<0.001 CX3CR1$^{GFP/+}$ vs KO; ¶p<0.05, ¶¶p<0.01, ¶¶¶p<0.001 steady vs inflammation. Student's t test.

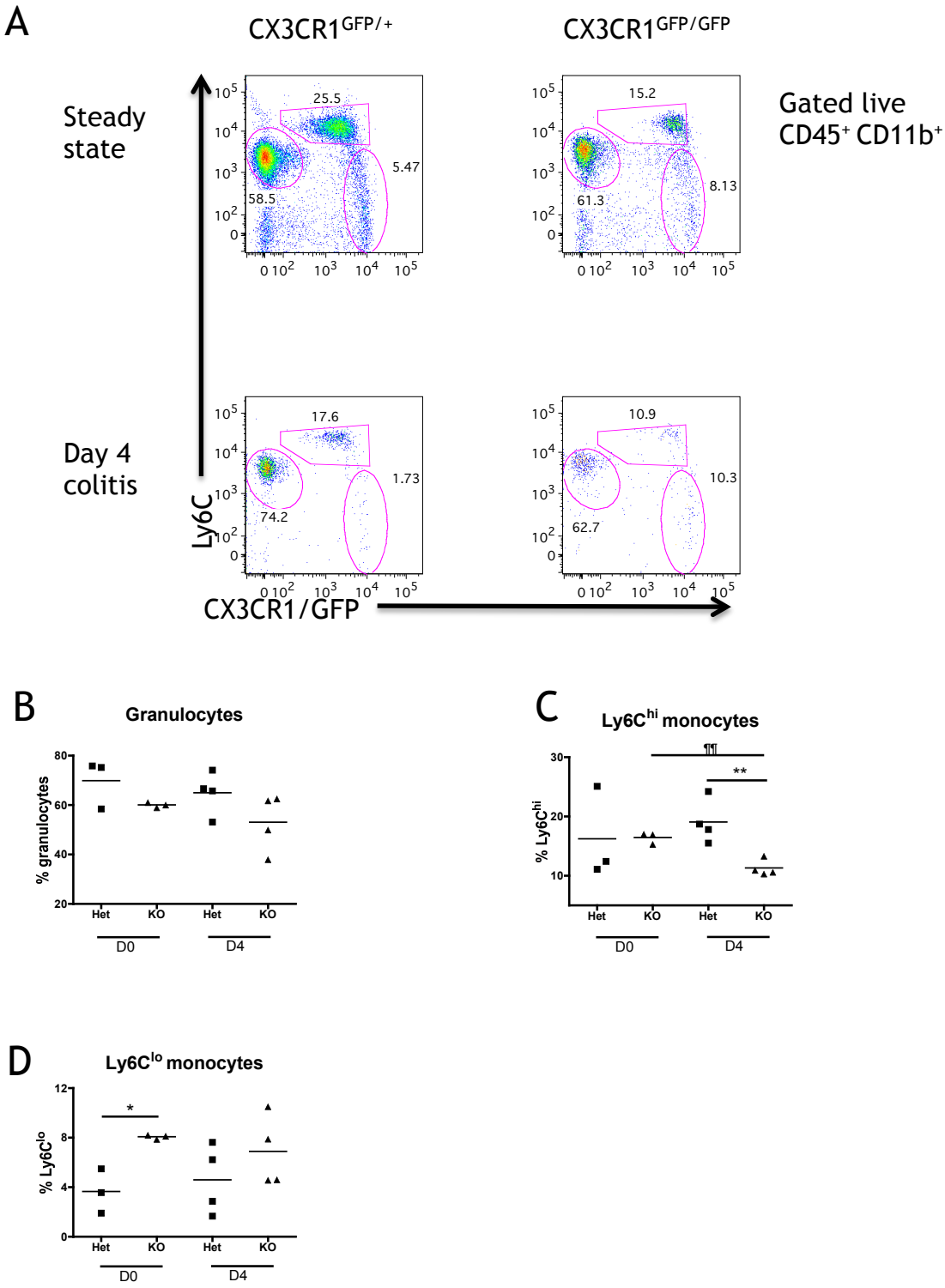

Figure 5.5. Leukocyte populations in blood of CX3CR1 KO and Het mice during steady state and inflammation. (A) Expression of Ly6C and CX3CR1 by live gated CD45$^+$ CD11b$^+$ cells from blood of CX3CR1$^{GFP/+}$ (left) and CX3CR1$^{GFP/GFP}$ (KO, right) mice showing granulocytes (Ly6C$^+$ CX3CR1$^-$), Ly6C^{hi} monocytes (Ly6C^{hi} CX3CR1^{lo}) and Ly6C^{lo} monocytes (Ly6C^{lo} CX3CR1$^+$). Frequencies of granulocytes (B), Ly6C^{hi} (C) and Ly6C^{lo} (D) monocytes. Data are representative of two independent experiments. *p<0.05, **p<0.01 CX3CR1$^{GFP/+}$ vs KO; ¶¶p<0.01 steady vs inflammation. Student's t test.

5.4 Oral priming in CX3CR1 deficient mice

To assess further the role of the CX3CL1-CX3CR1 axis in active immune responses in the intestine, I examined whether the reported defect in oral tolerance in CX3CR1$^{GFP/GFP}$ mice might have consequences for their susceptibility to be primed by this route. To do this, B6 WT and CX3CR1$^{GFP/GFP}$ animals were primed by oral gavage with either OVA and cholera toxin (CT), OVA alone or PBS, every 7 days for 3 weeks. Primary antigen-specific immune responses were then assessed by measuring the proliferative responses of MLN and splenic cells after restimulation with OVA *in vitro* and by measuring OVA-specific antibodies in serum and faeces (Figure 5.6 A).

As expected, splenocytes from WT mice that had been primed with OVA and CT showed significant proliferative responses when restimulated with OVA *in vitro* compared with PBS-fed control cells (Figure 5.6 B). In contrast splenocytes from WT mice fed OVA alone showed no increase in proliferation, confirming the need for CT as an adjuvant to induce priming. Splenocytes from CX3CR1 KO mice fed OVA+CT also had increased proliferative responses compared with PBS-fed controls after restimulation with OVA *in vitro*. However these responses were significantly lower than those of the primed WT spleen cells (Figure 5.6 B). Interestingly, CX3CR1 KO mice fed OVA alone also had significant proliferative responses in the spleen, perhaps consistent with their resistance to being tolerised by feeding antigen alone. This may also explain why MLN cells from CX3CR1 KO mice fed OVA+CT or OVA alone both showed equivalent and significant proliferative responses to stimulation *in vitro*, whereas no responses above the PBS fed background were found by MLN cells from the other groups of mice (Figure 5.6 C).

OVA-specific IgG1 responses were found in the serum of all WT and KO mice fed OVA, either alone or with CT, although these were highest in WT mice fed OVA+CT (Figure 5.7 A). WT mice fed OVA+CT were also the only group to show OVA-specific serum IgG2a antibodies above background (Figure 5.7 B). No OVA-specific IgA antibodies could be detected in either serum of faeces compared with WT mice (Figure 5.7 C, E). However there was an apparent

trend towards increased total IgA level in the faeces of CX3CR1 KO mice compared with WT controls (Figure 5.7 D).

Together these results suggest that in the absence of CX3CR1 oral priming may be partially impaired, from point of view of systemic immunity, as shown by the lack of T-cell proliferation in spleen but not in MLN. Moreover, this may be mirrored by the lower levels of OVA-specific IgG1 and IgG2a antibodies in CX3CR1 deficient mice, even in the presence of adjuvant.

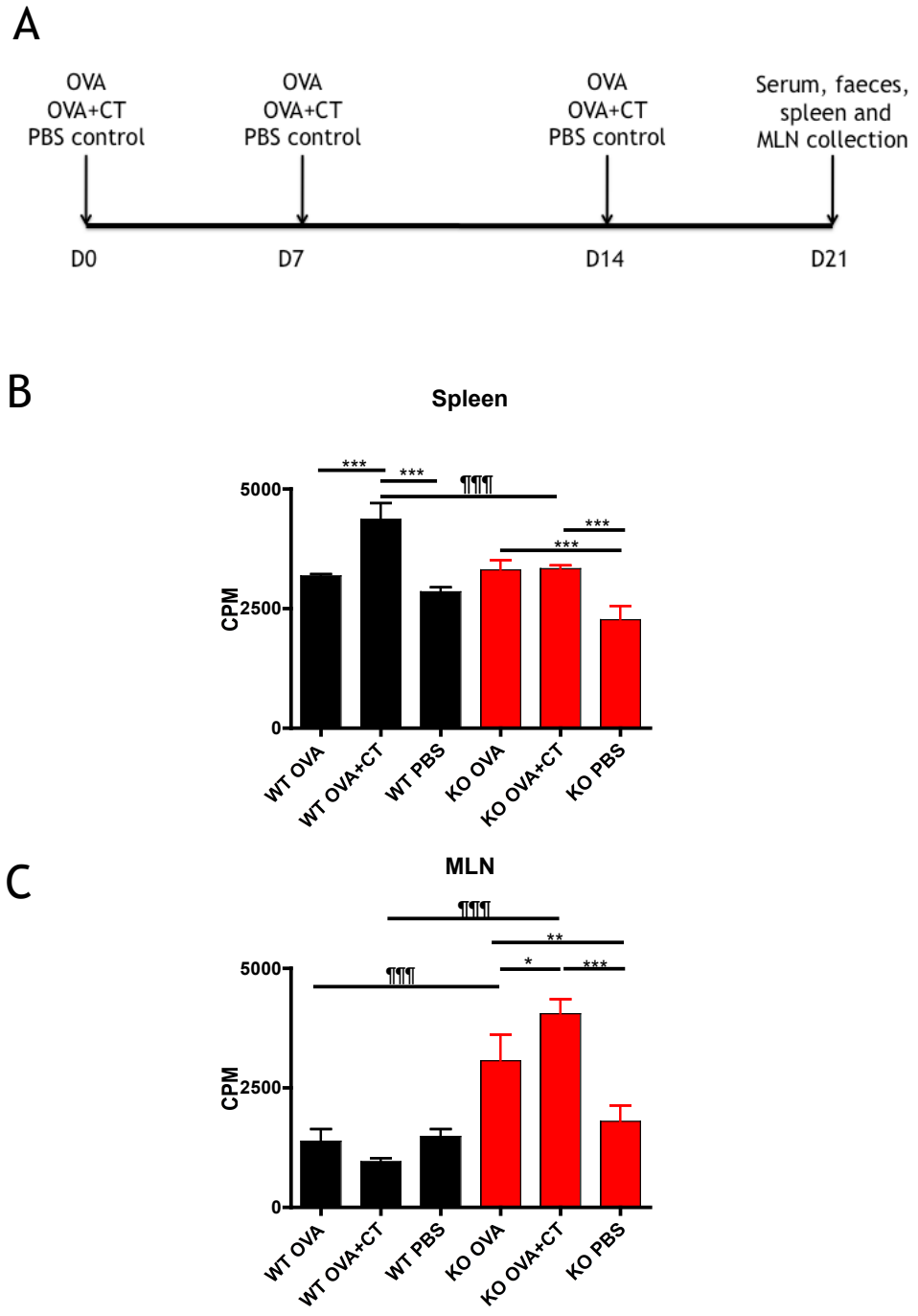

Figure 5.6. Role of CX3CR1 in OVA-specific oral priming. (A) C57Bl/6 (WT) and CX3CR1 KO mice were gavaged every 7 days for 3 weeks with 10mg OVA with or without 10µg cholera toxin as an adjuvant. At day 21, spleen, MLN, sera and faeces were collected. Spleen (B) and MLN cells (C) were restimulated with 500µg/ml OVA *in vitro* and proliferation assessed by measuring thymidine uptake after 3 days of culture. The data shown are means +1 SD from 6 individual mice/group. *p<0.05, **p<0.01, ***p<0.001 OVA vs OVA+CT vs PBS; ¶¶¶p<0.001 WT vs KO. One-way ANOVA followed by Bonferroni's post-test.

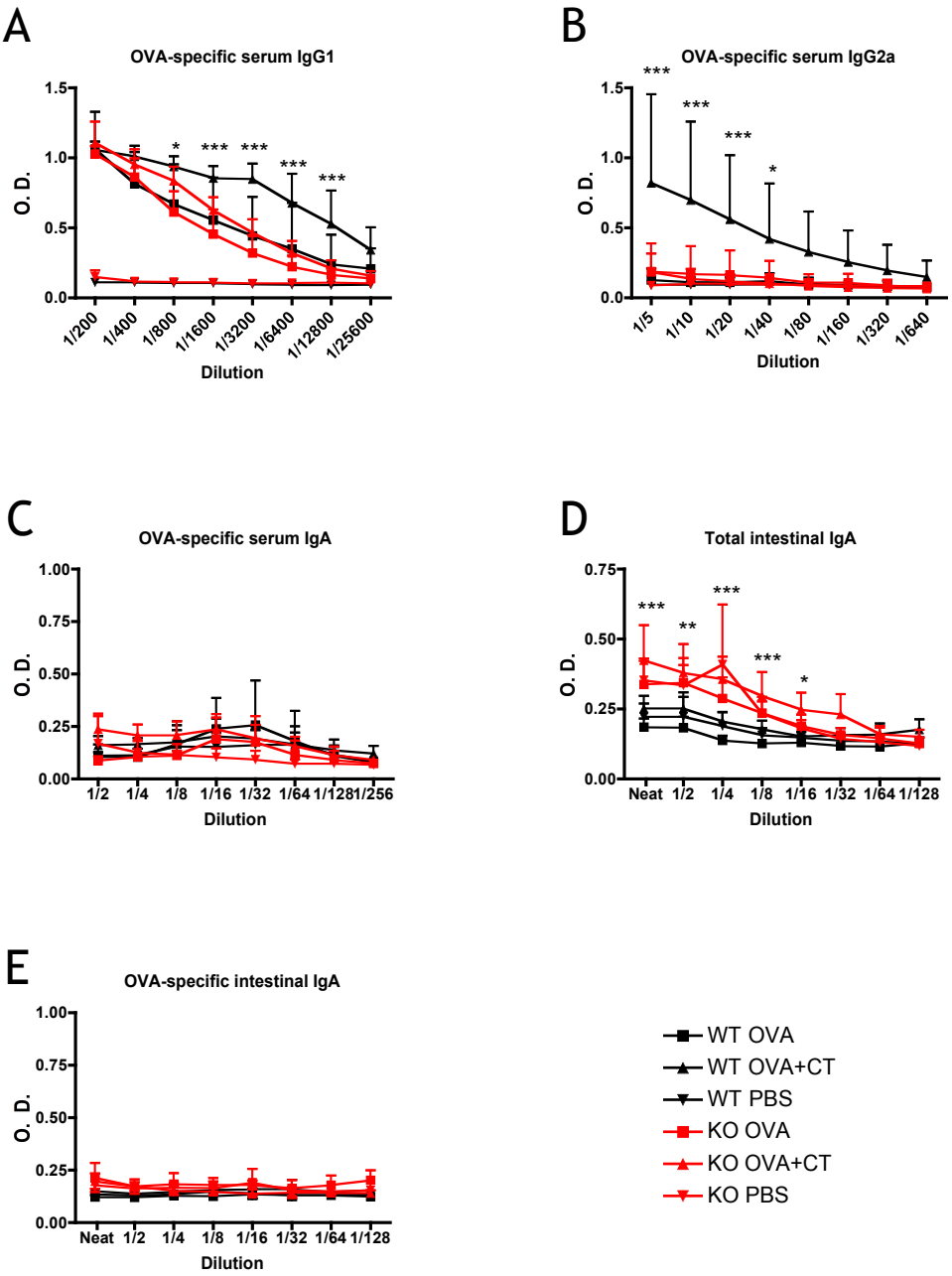

Figure 5.7. Role of CX3CR1 in OVA-specific oral priming. Serum OVA-specific IgG1, IgG2a and IgA antibodies (A-C). Total intestinal IgA (D) and OVA-specific IgA antibodies in faeces (E) assessed by ELISA were measured 7 days after the last of 3 feeds of OVA±CT and in PBS fed controls. The data shown are OD450 of 6 individual mice/group +1SD. *p<0.05, **p<0.01 and ***p<0.001 WT+CT vs KO+CT. Student's t test.

5.5 Effects of CX3CL1 on activation of macrophages *in vitro*

Together, although the results of my *in vivo* experiments were inconsistent, they did produce some evidence that intestinal immune responses may be dysregulated in the absence of CX3CR1. As previous studies had suggested this reflects abnormal mϕ function (Hadis et al., 2011), I decided to explore how the CX3CR1-CX3CL1 axis might influence mϕ activation, using TLR stimulation of bone marrow mϕ BMM *in vitro* as a model. First I determined the optimal concentration of LPS required for activating BMM. BMM from $CX3CR1^{GFP/+}$ mice were harvested after 6 days culture with M-CSF and stimulated overnight with increasing concentrations of LPS ranging from 100pg/ml to 1μg/ml (Figure 5.8). Mϕ activation was assessed by measuring the production of TNFα and IL6 using ELISA, while expression of MHC II and the costimulatory molecules CD40, CD80 and CD86 were assessed by flow cytometry. LPS stimulation caused a clear dose-dependent increase in IL6 production which was greatest using 1μg/ml LPS, while TNFα production reached a maximum at 100ng/ml LPS and above (Figure 5.8 F & G). LPS also led to increased expression of CD40 and CD86, with a similar dose effect to that seen with TNFα production (Figure 5.8 B & D). In contrast, LPS actually led to a dose dependent decrease in CD80 and MHC II expression (Figure 5.8 C & E). Importantly, the higher doses of LPS were associated with reduced viability of BMM as assessed by exclusion of $7\text{-}AAD^{+}$ cells (Figure 5.8 A) and on that basis, I decided to use 100ng/ml LPS for future experiments.

To explore the role of the CX3CL1-CX3CR1 axis, I first examined whether pre-incubation overnight with rCX3CL1 affected the response of WT BMM to LPS stimulation, using 3 different concentrations of rCX3CL1 which had been reported in a previous study (Mizutani et al., 2007). As before, stimulation with 100ng/ml LPS alone led to increased production of IL6 and TNFα by BMM, together with increased expression of CD40 and CD80, but had no effects on MHC II expression or viability (Figure 5.9 B). Pre-incubation with rCX3CL1 alone had no effects on any parameter at any concentration and had no effects on the stimulatory ability of LPS, apart from a small but significant decrease in LPS-induced CD80 expression after addition of 300ng/ml rCX3CL1. Significant decreases in viability were also seen when 3 or 300ng/ml rCX3CL1

was added to LPS. Due to the lack of a clear pattern in these experiments, I decided to rely on the middle dose reported in previous work.

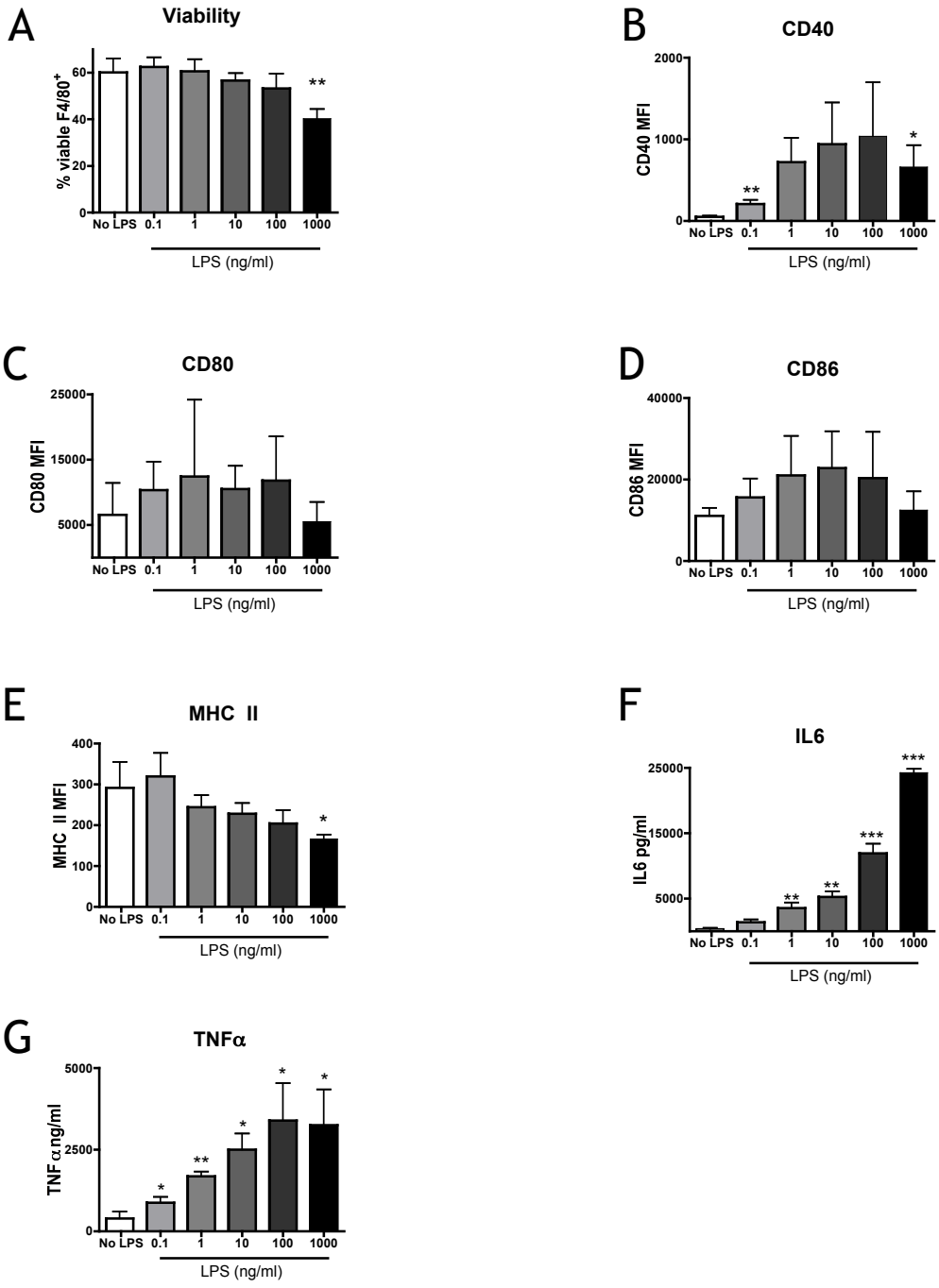

Figure 5.8. Dose dependent effects of LPS on BM macrophage activation. BMM from CX3CR1$^{GFP/+}$ mice were cultured for 6 days in M-CSF, harvested and cultured for a further 24h with increasing concentrations of LPS. Viability (A), CD40 (B), CD80 (C), CD86 (D) and MHC II (E) expression by F4/80^{+} BMM were assessed by flow cytometry, while IL6 (F) and TNFα (G) production were measured by ELISA. Data shown are expressed as pg/ml for cytokine production and MFI for surface markers and are means for 3 individual mice/ group +1SD and are representative of at least 3 independent experiments. *p<0.05, **p<0.01, ***p<0.001 vs unstimulated control. Student's t test.

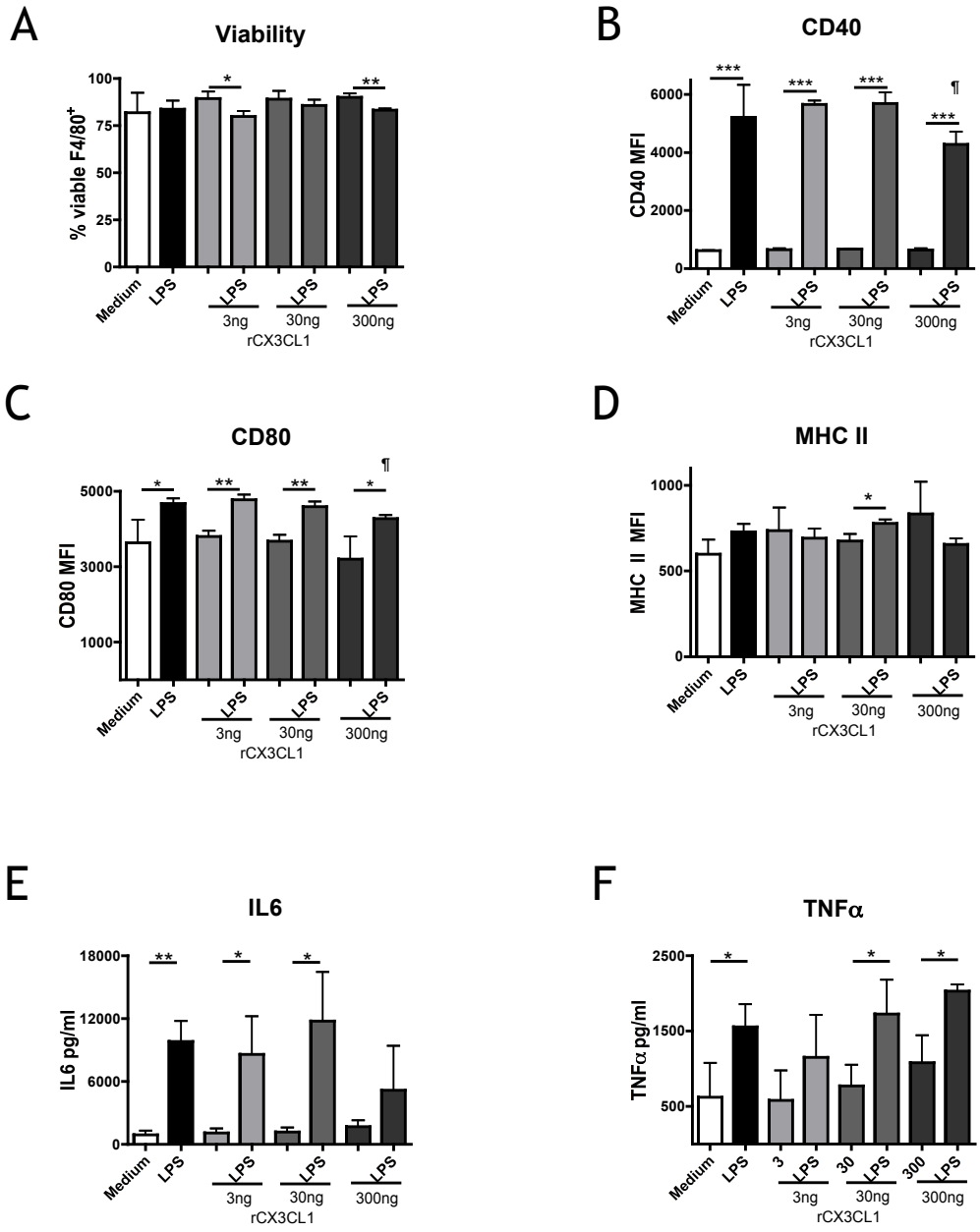

Figure 5.9. Effects of rCX3CL1 on LPS-induced activation of BM macrophages. BMM from CX3CR1$^{GFP/+}$ mice were cultured for 6 days in M-CSF, harvested and cultured for a further 24h with different amounts of rCX3CL1 (3, 30 and 300ng/ml) and 100ng/ml LPS. Viability (A), CD40 (B), CD80 (C), and MHC II (D) expression by F4/80^{+} BMM were assessed by flow cytometry, while IL6 (E) and TNFα (F) production were measured by ELISA. Data shown are expressed as pg/ml for cytokine production and MFI for surface markers and are means for 3 individual mice/group +1SD and are representative of at least 3 independent experiments. *p<0.05, **p<0.01, ***p<0.001 vs LPS stimulated in absence of rCX3CL1; ¶p<0.05 vs unstimulated BMM . Student's t test.

5.6 Effect of rCX3CL1 on CX3CR1 het and CX3CR1 KO BM macrophages

Next, I decided to repeat and extend the previous experiments using interferon gamma (IFNγ) as an additional stimulus for mϕ and also compared BMM from CX3CR1$^{GFP/+}$ and CX3CR1$^{GFP/GFP}$ (KO) mice. This was partly to examine how the lack of CX3CR1 might affect LPS responsiveness and partly to test if the effects of CX3CL1 I observed were truly CX3CR1 mediated.

As before, treatment of CX3CR1$^{GFP/+}$ BMM with 100ng/LPS induced increased production of IL6 and TNFα, as well as enhanced expression of CD40 and CD80. In this experiment CD86 expression was also increased by LPS (Figure 5.8). IFNγ alone had similar effects on all these parameters, except for IL6 production and also induced increased expression of MHC II (Figure 5.10). Stimulation with both IFNγ and LPS enhanced the production of IL6 and TNFα above that with either stimulus alone, but otherwise had similar or lesser effects to LPS alone (Figure 5.10 E, F). As I found previously, addition of 30ng/ml rCX3CL1 alone had no significant effect on any of these parameters using CX3CR1$^{GFP/+}$ BMM, while CX3CR1$^{GFP/GFP}$ BMM responded to LPS or IFNγ alone very similarly to their CX3CR1$^{GFP/+}$ counterparts, except when LPS+IFNγ were used together. Under these conditions, KO BMM expressed significantly more CD40 and CD80, but produced less IL6 and TNFα (Figure 5.10 B, C, E & F). However as this differential response by CX3CR1 KO BMM appeared to be abolished by addition of CX3CL1 despite the absence of its receptor, the significance of these results is unclear. None of the conditions had a significant effect on the viability of either het or KO BMM, although there was a trend towards lower viability when LPS+IFNγ were used together with both cell types (Figure 5.10 A). Overall, my results suggest that there are no consistent effects of deleting CX3CR1 or its ligand on mϕ responsiveness *in vitro*.

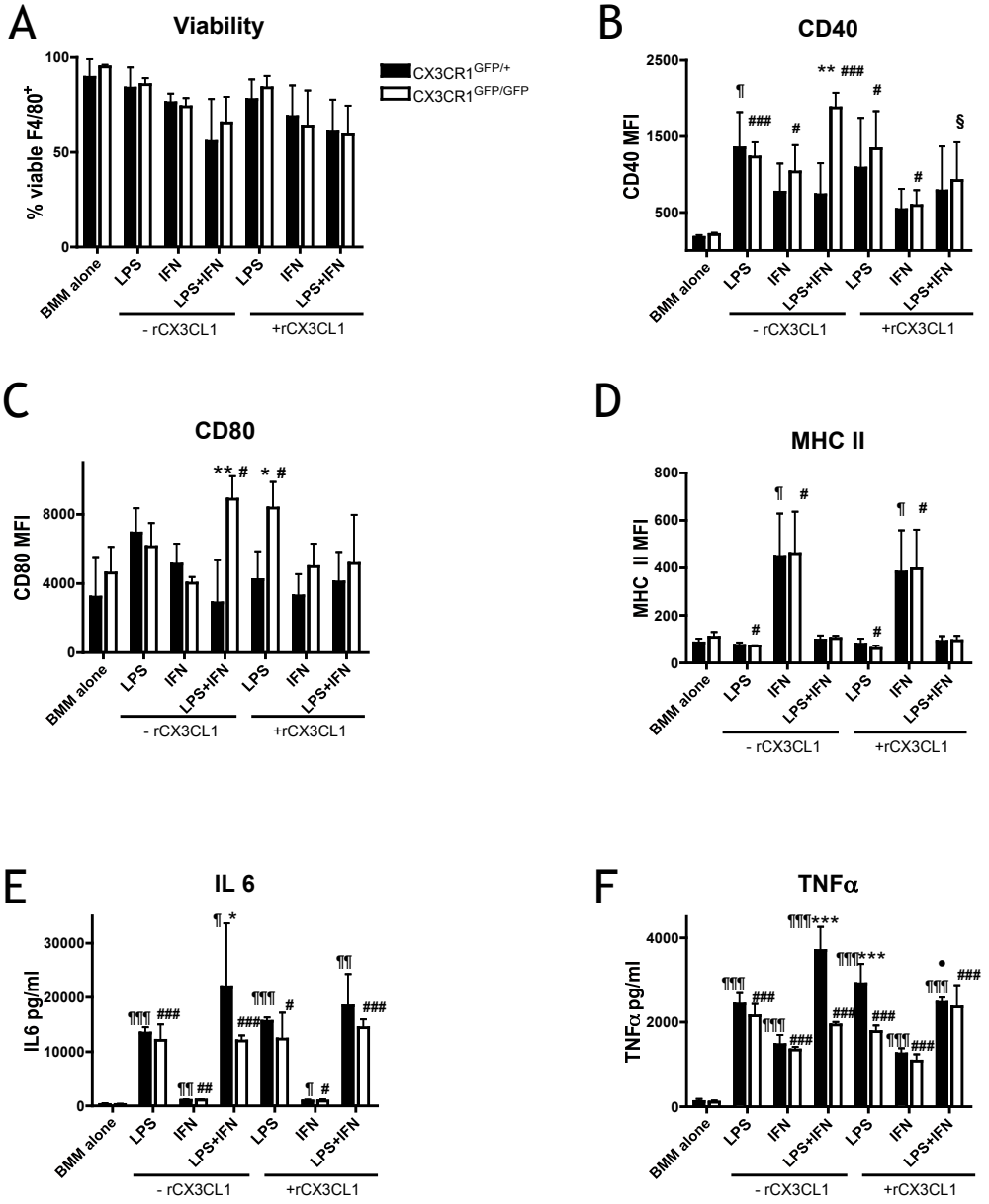

Figure 5.10. Effects of recombinant CX3CL1 on activation of BM macrophages. BMM from CX3CR1$^{GFP/+}$ and CX3CR1$^{GFP/GFP}$ mice were cultured for 6 days in M-CSF, harvested and cultured overnight with or without 30 ng/ml rCX3CL1 before being stimulated with 100ng/ml LPS ± 500ng/ml IFNγ for a further 24h Viability (A), CD40 (B), CD80 (C) and MHC II (D) expression were measured by flow cytometry, while IL6 (E) and TNFα (F) production were measured by ELISA. Data shown are expressed as pg/ml for cytokine production and MFI for surface markers and are means for 3 individual mice/group +1SD and are representative of at least 3 independent experiments. *p<0.05, **p<0.01, ***p<0.001 CX3CR1$^{+/GFP}$ vs CX3CR1$^{GFP/GFP}$, Two-way ANOVA followed by Bonferroni's post-test. ¶p<0.05, ¶¶p<0.01, ¶¶¶p<0.001, vs unstimulated CX3CR1$^{GFP/+}$ BMM; #p<0.05, ##p<0.01, ###p<0.001 vs CX3CR1$^{GFP/GFP}$ BMM; §p<0.05 vs CX3CR1$^{GFP/GFP}$+LPS+IFN in absence of rCX3CL1; •p<0.05 vs CX3CR1$^{GFP/+}$+LPS+IFN in absence of rCX3CL1. Student's t test.

5.7 Effect of CX3CL1-expressing epithelial cells on activation of BM macrophages

As these studies using soluble rCX3CL1 had not generated consistent results and CX3CL1 is expressed as a membrane bound protein *in vivo* (Bazan et al., 1997), I next attempted to mimic the natural environment of intestinal mϕ more closely by using human epithelial kidney cells (HEK293) that had been modified to express either membrane-bound (MB) or soluble (sol) CX3CL1. Untransfected HEK cells were used as control group, as well as BM mϕ alone, which were used as control for each condition. First I examined the effects of the different HEK cells by co-culturing them at a 1:1 ratio with BMM from WT B6, CX3CR1$^{GFP/+}$ and CX3CR1$^{GFP/GFP}$ mice for 24 hours before adding 100ng/ml LPS. Survival of BMM in the absence of LPS was generally low and only showed a significant increase when co-cultured with soluble CX3CL1 (Figure 5.11). Co-culture of BMM with HEK cells decreased expression of CD86 and MHC II (Figures 5.13 & 5.14) whilst it showed no significant effect on CD40 expression and IL6 and TNFα production (Figures 5.12, 5.15 & 5.16). As expected, addition of LPS to WT BMM induced the expression of CD40 (Figure 5.12), CD86 (Figure 5.13) and MHC II (Figure 5.14), as well as increased production of IL6 and TNFα (Figure 5.15 and 5.16) independently of the type of HEK cells used. Interestingly, CX3CR1 KO BMM cultured in presence of soluble CX3CL1 showed a significantly lower expression of CD40 (Figure 5.12C), CD86 (Figure 5.13C) and IL6 (Figure 5.14C), when compared to their WT BMM counterparts, however this results were the only clear indicators of an effect of the absence of CX3CR1 on BMM.

The effects of adding the epithelial cells on the individual parameters of activation were quite variable, but in general, the responses to LPS by all types of BMM were significantly inhibited in presence of HEK cells, irrespective of whether they expressed CX3CL1 or not. The only exception to this was TNFα production by most BMM types, where no significant differences were seen.

These effects could not be explained by differences in the viability of the different BMM cells co-cultured with the various HEK cells, as although there

was substantial variation in viability, no consistent patterns could be observed (Figures 5.11). It should also be noted that overall viability in this experiment was considerably lower than in my previous studies, perhaps reflecting the fact that these BMM cells were used after 8 days of culture in M-CSF, as opposed to 6 days previously.

Therefore, due to the lack of a clear or consistent pattern of results that could be attributed to the presence/absence of CX3CR1, I did not take these experiments further.

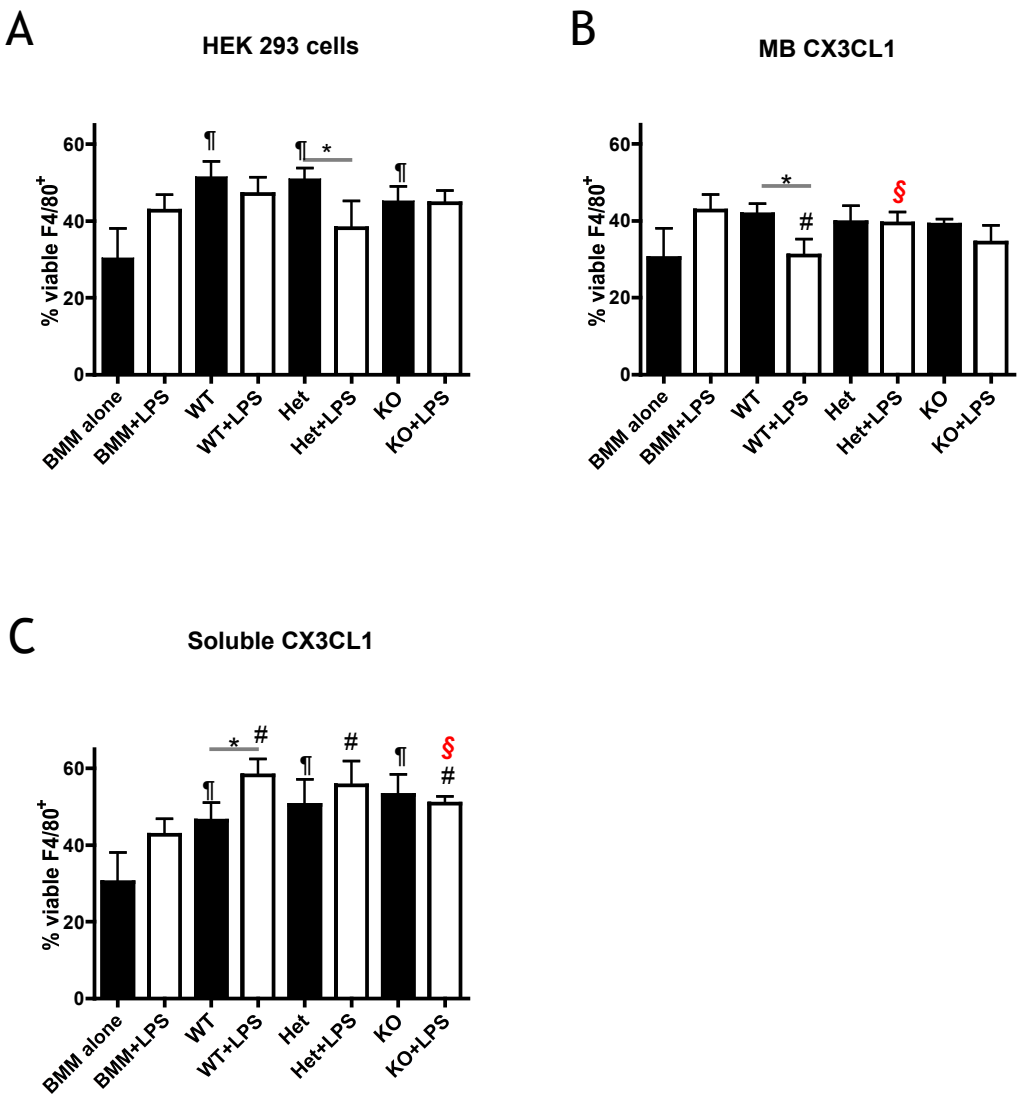

Figure 5.11. Effects of CX3CL1 expressing epithelial cells on viability by activated BM macrophages. BMM from C57Bl/6 (WT), CX3CR1$^{GFP/+}$ or CX3CR1$^{GFP/GFP}$ (KO) mice were cultured in M-CSF for 6 days, followed by 24 hours at a 1:1 ratio with control HEK293 cells (A) or HEK cells expressing membrane bound (MB) (B) or (C)) soluble CX3CL1 (sol) before 100ng/ml LPS was added for a further 24 hours. Viability was measured by flow cytometry. Data shown are expressed as frequency of viable (7-AAD$^-$) cells and shown as mean +1SD from 3 individual mice/group. Data are representative of at least 3 independent experiments. *p<0.05, unstimulated vs LPS-stimulated BMM; ¶p<0.05 vs unstimulated BMM alone; #p<0.05 vs LPS-stimulated BMM alone; §p<0.05 vs LPS-stimulated WT BMM. Student's t test.

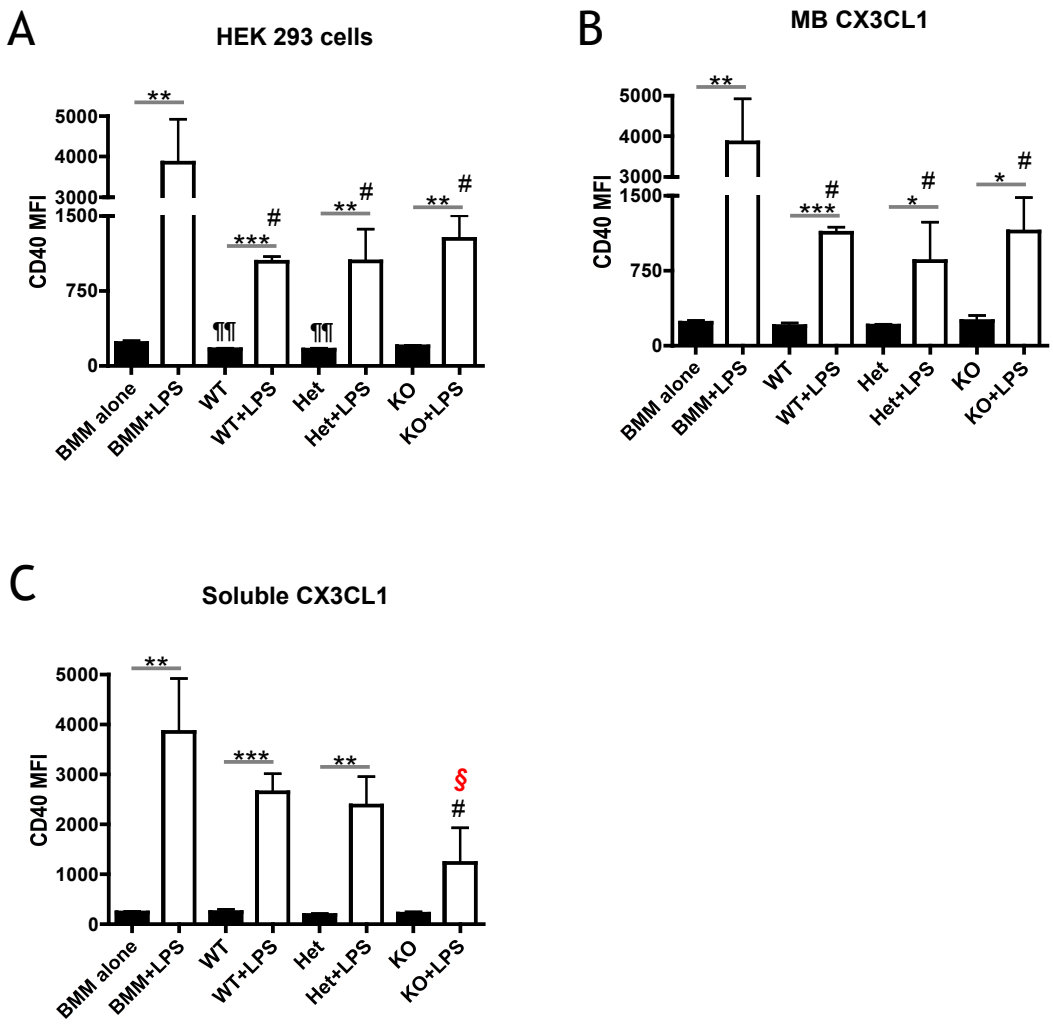

Figure 5.12. Effects of CX3CL1 expressing epithelial cells on CD40 expression by activated BM macrophages. BMM from C57Bl/6 (WT), CX3CR1$^{GFP/+}$ or CX3CR1$^{GFP/GFP}$ (KO) mice were cultured in M-CSF for 6 days, followed by 24 hours at a 1:1 ratio with control HEK293 cells (A) or HEK cells expressing membrane bound (MB) (B) or (C)) soluble CX3CL1 (sol) before 100ng/ml LPS was added for a further 24 hours. Viability was measured by flow cytometry. Data shown are expressed as frequency of viable (7-AAD$^-$) cells and shown as mean +1SD from 3 individual mice/group. Data are representative of at least 3 independent experiments. *p<0.05, **p<0.01, ***p<0.001 unstimulated vs LPS-stimulated BMM; ¶p<0.05, ¶¶p<0.01 vs unstimulated BMM alone; #p<0.05 vs LPS-stimulated BMM alone; §p<0.05 vs LPS-stimulated WT BMM. Student's t test.

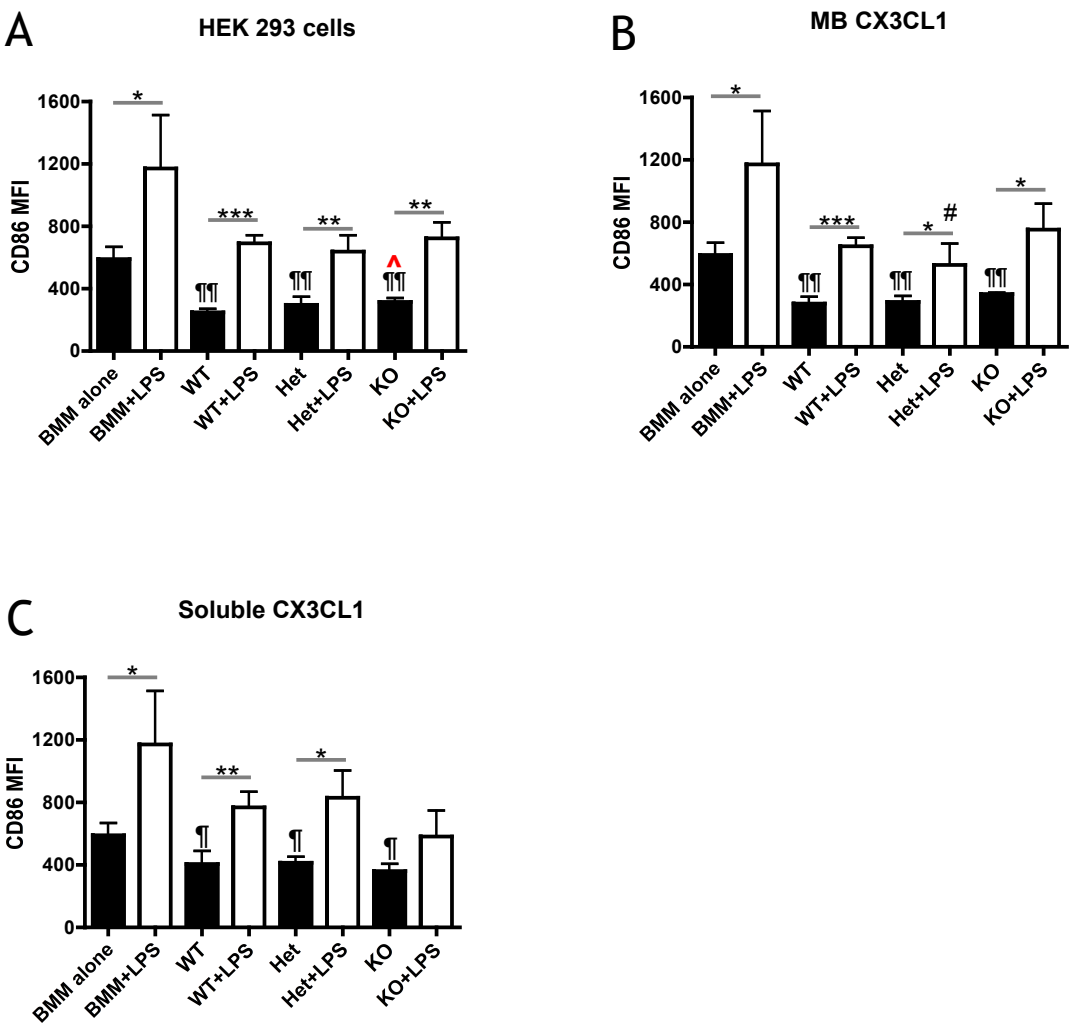

Figure 5.13. Effects of CX3CL1 expressing epithelial cells on CD86 expression by activated BM macrophages. BMM from C57Bl/6 (WT), CX3CR1$^{GFP/+}$ or CX3CR1$^{GFP/GFP}$ (KO) mice were cultured in M-CSF for 6 days, followed by 24 hours at a 1:1 ratio with control HEK293 cells (A) or HEK cells expressing membrane bound (MB) (B) or (C)) soluble CX3CL1 (sol) before 100ng/ml LPS was added for a further 24 hours. Viability was measured by flow cytometry. Data shown are expressed as frequency of viable (7-AAD$^-$) cells and shown as mean +1SD from 3 individual mice/group. Data are representative of at least 3 independent experiments. *p<0.05, **p<0.01, ***p<0.001 unstimulated vs LPS-stimulated BMM; ¶p<0.05, ¶¶p<0.01 vs unstimulated BMM alone; #p<0.05 vs LPS-stimulated BMM alone; ^p<0.05 vs unstimulated WT BMM. Student's t test.

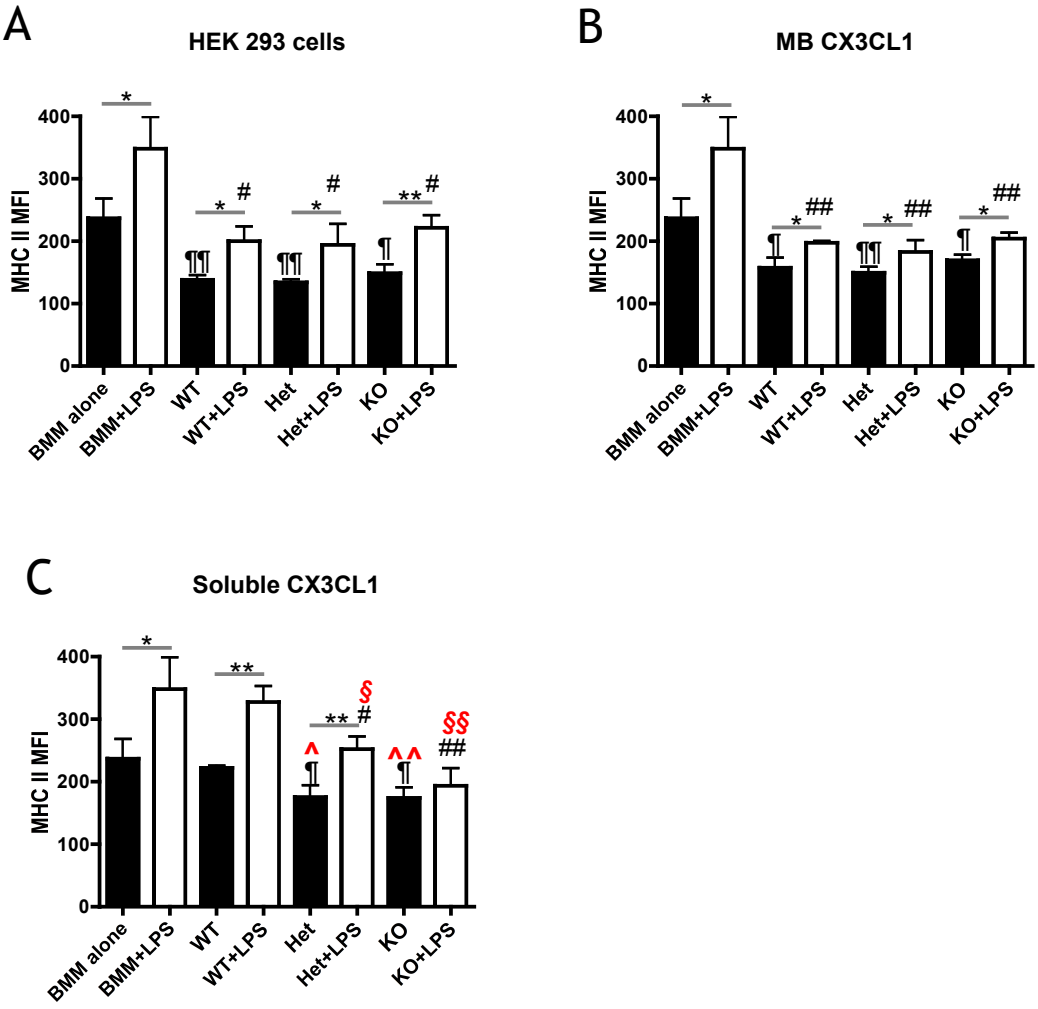

Figure 5.14. Effects of CX3CL1 expressing epithelial cells on MHC II expression by activated BM macrophages. BMM from C57Bl/6 (WT), CX3CR1$^{GFP/+}$ or CX3CR1$^{GFP/GFP}$ (KO) mice were cultured in M-CSF for 6 days, followed by 24 hours at a 1:1 ratio with control HEK293 cells (A) or HEK cells expressing membrane bound (MB) (B) or (C)) soluble CX3CL1 (sol) before 100ng/ml LPS was added for a further 24 hours. Viability was measured by flow cytometry. Data shown are expressed as frequency of viable (7-AAD$^-$) cells and shown as mean +1SD from 3 individual mice/group. Data are representative of at least 3 independent experiments. *p<0.05, **p<0.01, unstimulated vs LPS-stimulated BMM; ¶p<0.05, ¶¶p<0.01 vs unstimulated BMM alone; #p<0.05, ##p<0.01 vs LPS-stimulated BMM alone; ^p<0.05, ^^p<0.01 vs unstimulated WT BMM; §p<0.05, §§p<0.01 vs LPS-stimulated WT BMM. Student's t test.

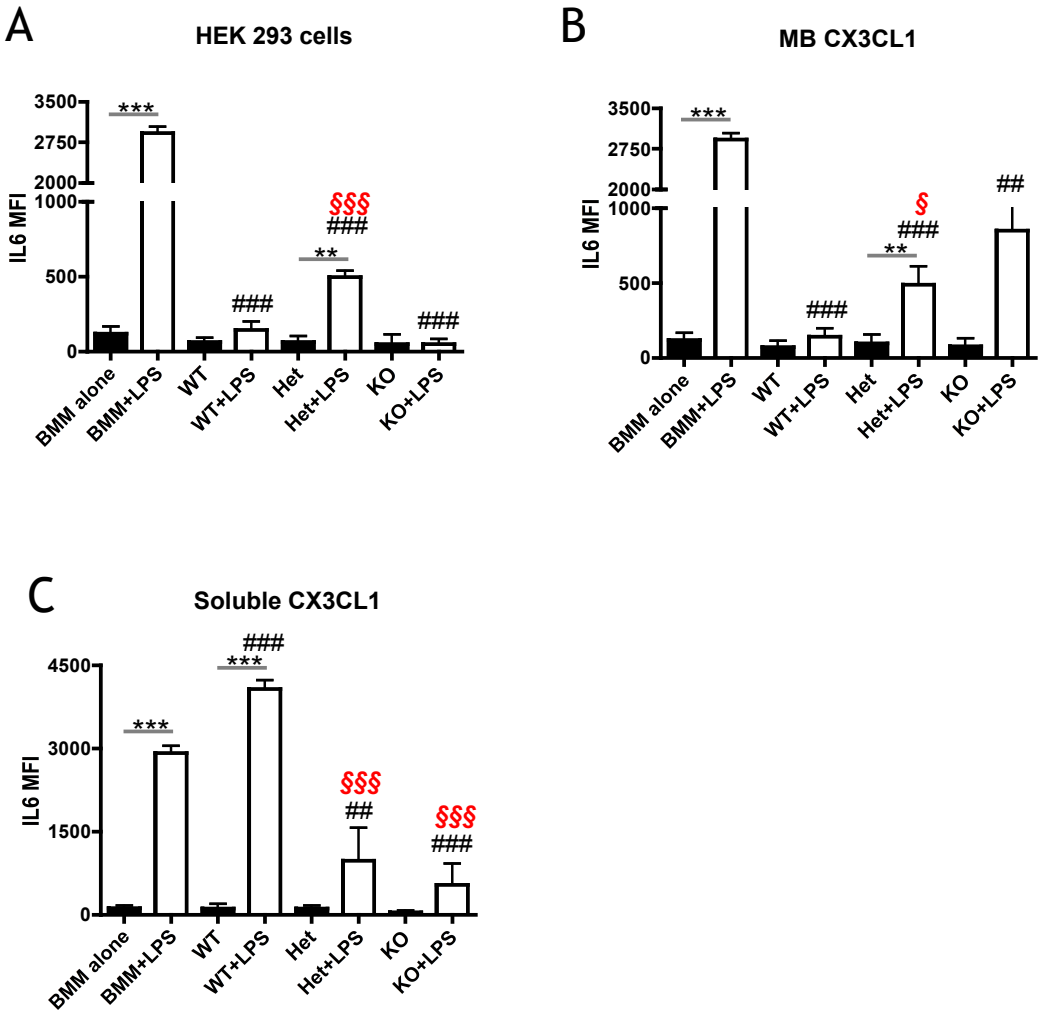

Figure 5.15. Effects of CX3CL1 expressing epithelial cells on IL6 production by activated BM macrophages. BMM from C57Bl/6 (WT), CX3CR1$^{GFP/+}$ or CX3CR1$^{GFP/GFP}$ (KO) mice were cultured in M-CSF for 6 days, followed by 24 hours at a 1:1 ratio with control HEK293 cells (A) or HEK cells expressing membrane bound (MB) (B) or (C)) soluble CX3CL1 (sol) before 100ng/ml LPS was added for a further 24 hours. Viability was measured by flow cytometry. Data shown are expressed as frequency of viable (7-AAD$^-$) cells and shown as mean +1SD from 3 individual mice/group. Data are representative of at least 3 independent experiments.**p<0.01, ***p<0.001 unstimulated vs LPS-stimulated BMM; ##p<0.01, ###p<0.001 vs LPS-stimulated BMM alone; §p<0.05, §§§p<0.01 vs LPS-stimulated WT BMM. Student's t test.

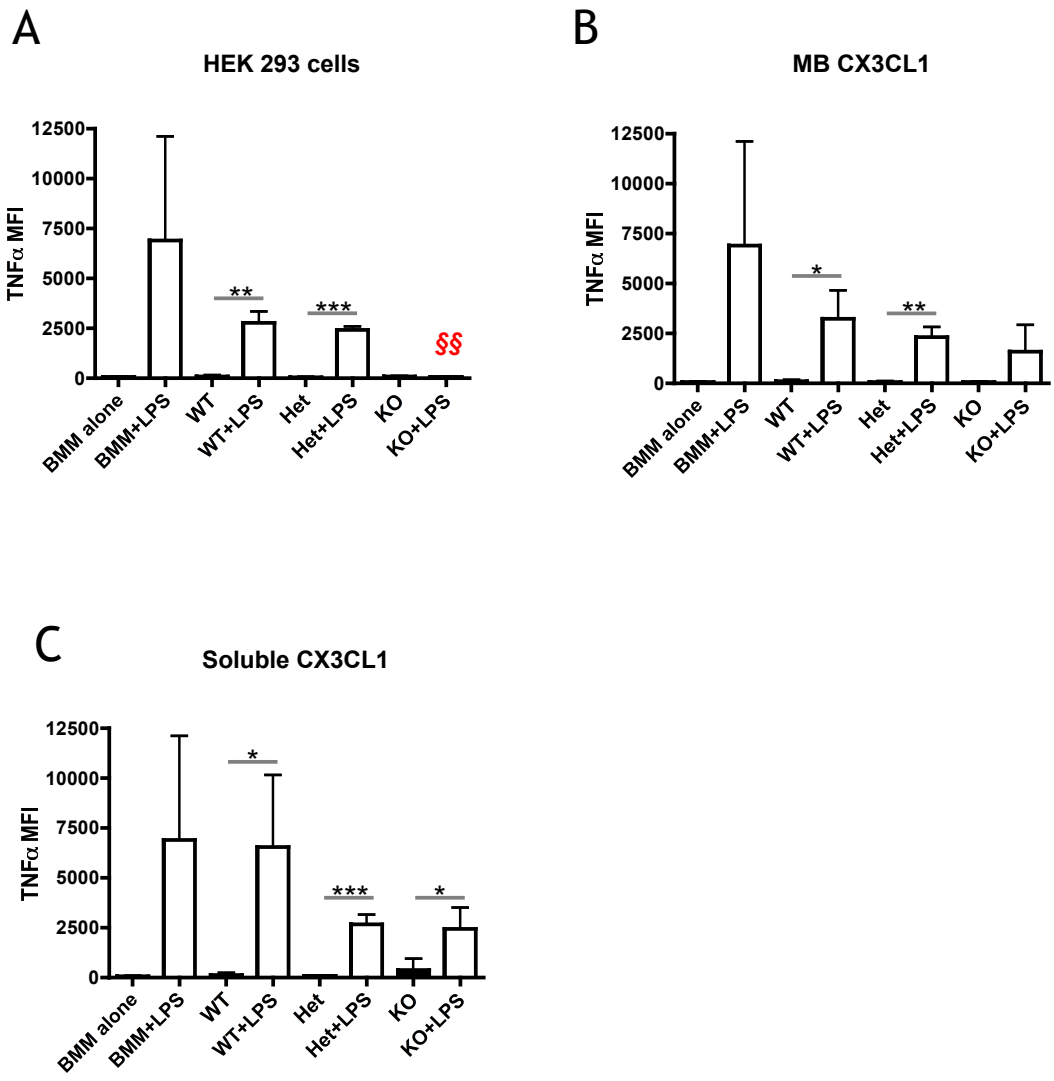

Figure 5.16. Effects of CX3CL1 expressing epithelial cells on TNFα production by activated BM macrophages. BMM from C57Bl/6 (WT), CX3CR1$^{GFP/+}$ or CX3CR1$^{GFP/GFP}$ (KO) mice were cultured in M-CSF for 6 days, followed by 24 hours at a 1:1 ratio with control HEK293 cells (A) or HEK cells expressing membrane bound (MB) (B) or (C)) soluble CX3CL1 (sol) before 100ng/ml LPS was added for a further 24 hours. Viability was measured by flow cytometry. Data shown are expressed as frequency of viable (7-AAD$^-$) cells and shown as mean +1SD from 3 individual mice/group. Data are representative of at least 3 independent experiments. *p<0.05, **p<0.01, ***p<0.001 unstimulated vs LPS-stimulated BMM; §§p<0.01 vs LPS-stimulated WT BMM. Student's t test.

5.8 Summary

The experiments in this chapter were designed to investigate the role of the CX3CL1-CX3CR1 axis on active intestinal immunity *in vivo* and on mϕ activation *in vitro*.

The results showed few consistent effects. Although my initial experiments seemed to support previous findings that CX3CR1 KO mice were partially protected from DSS colitis compared with B6 WT mice, this could not be reproduced in two repeat experiments using either B6 or CX3CR1$^{GFP/+}$ mice as controls. This applied to both systemic effects of DSS such as weight loss and myeloid cell recruitment, as well as inflammatory infiltrates of colon and colon shortening.

I did obtain some evidence that there may be intrinsic differences in the production of granulocytes and monocytes in the absence of CX3CR1, with an apparent reduction in granulocyte numbers. In addition, the proportions of Ly6C^{lo} monocytes were increased in the BM and bloodstream of CX3CR1 KO mice, perhaps reflecting decreased production. However these differences were overcome in colitis, consistent with normal recruitment to inflamed colon.

I next attempted to induce antigen specific immune responses in the intestine of WT and CX3CR1 KO mice by immunising orally with OVA together with CT as an adjuvant. These experiments revealed that there appeared to be a defect in systemic priming in KO mice as assessed by spleen cell responses to OVA restimulation *in vitro* and by serum IgG1 and IgG2a antibodies *in vivo*. In contrast I obtained some evidence to suggest that KO mice may be more susceptible to priming of local immune responses, even in the absence of adjuvant, as indicated by an increase in proliferative responses in the MLN. Total IgA levels also showed a trend towards being higher in KO intestine and together, these results could support previous findings of a defect in ability of CX3CR1 KO mice to be tolerised by feeding soluble protein (Hadis et al., 2011). However it is important to note that the

results of my experiments were very variable and I did not have sufficient time to repeat them.

My experiments on BMM *in vitro* showed no overall effect of the CX3CL1-CX3CR1 axis on mϕ activation. Although some effects of adding recombinant CX3CL1 on the responses of BMM to LPS and or IFNγ were observed, the results were not consistent between different parameters of activation and were not dependent on expression of CX3CR1 by the BMM. Similarly there were no consistent differences between the responses of CX3CR1 KO BMM from WT or het BMM. Finally, I examined the effects of co-culturing BMM with epithelial cells expressing soluble or membrane-bound CX3CR1. Unfortunately, all epithelial cells lines were found to typically inhibit the activation of BMM, irrespective of whether they expressed CX3CL1 or not. However there was some evidence that expression of soluble CX3CL1 could overcome some of these inhibitory effects in a CX3CR1 dependent manner, indicating that further experiments on this system might be interesting, but perhaps with a more physiologically relevant epithelial cell line.

Chapter 6
General discussion

6.1 Introduction

From the moment of birth, the intestinal tract is in perpetual contact with a wide range of antigens. In order to preserve homeostasis, the intestinal immune system has to identify and act against potentially dangerous microbes and substances, whilst tolerating the harmless materials that are beneficial to the host, such as commensal organisms and food proteins (Mowat, 2003). Macrophages play crucial roles in these processes and understanding their development and function was the principal aim of this project.

When I began my project, work in the lab had already developed rigorous multiparametric flow cytometry-based methods to analyse mϕ and DCs in adult mouse intestine and had described a number of subsets based on the expression of CX3CR1 and other markers. The majority of mϕ in healthy colon express high levels of CX3CR1 and are also F4/80^{hi} MHC II^{+}. Functionally, these cells have been shown to be hyporesponsive to TLR stimulation, produce copious amount of IL-10 and have high phagocytic activity (Bain et al., 2013). In addition to this subset, the steady state colon contains 3 transitional stages of macrophages, all of which are CX3CR1^{int}, but which can be distinguished from each other based on their expression of Ly6C and MHC II. These subsets represent sequential maturation stages between pro-inflammatory Ly6C^{hi} monocytes and resident mature mϕ. Further work has shown that these cells are replenished constantly by blood monocytes whose development into resident mϕ is driven by the local environment in the intestine. In my project I adopted the strategies developed in the earlier studies to explore how intestinal mϕ development was influenced by age, the microbiota and the CX3CR1 chemokine receptor.

6.2 Intestinal macrophages in early life

Although there has been a considerable amount of work exploring the development of the immune system in the neonate (Cope and Dilly, 1990; Haverson et al., 2007; Inman et al., 2010a; Maheshwari et al., 2011; Mulder et al., 2011; Schmidt et al., 2011; Stokes, 2004), there are only a limited number of studies focussing on intestinal antigen presenting cells under these

conditions, mainly dealing with DCs but not intestinal mϕ (Inman et al., 2012; Inman et al., 2010b). Therefore, my first experiments aimed to examine whether colonic mϕ in newborn mice have different phenotypic and functional characteristics to those in fully-grown animals.

For all the comparisons between adult mice and newborn I measured cell numbers as well as cell proportions. The importance of doing this is that even as the mouse grows it may be that the cell proportions do not vary very much, however the cell numbers may be increasing greatly, for instance at 3 weeks of age. A good example of this is the F4/80^{hi} CD11b^{int} cell population. In newborn mice, the proportion of these cells is the largest, although their numbers are small, whereas adult mice have a much larger number of F4/80^{hi} CD11b^{int} whilst their proportions are much smaller. Finally, for future experiments that may involve cell imaging, it would be important to quantify the mϕ expansion in the whole colon and compare it with the expansion of the rest of the cells that constitute the intestine. This may provide a very informative perspective to the phenomenon of mϕ expansion during development.

When I isolated LP cells from the colon of newborn mice and gated out granulocytes and DCs, it was immediately apparent that cells with the phenotypic features of resident intestinal mϕ were already present. Thus, I could identify significant numbers of cells expressing F4/80 and CD11b amongst CD45^{+} leukocytes, with the majority being F4/80^{hi} CD11b^{int}. This population was also CX3CR1^{hi}, as seen with their adult counterparts, but unlike adult intestine, only a small proportion of CX3CR1^{hi} F4/80^{hi} mϕ expressed MHC II at birth. Interestingly however, these neonatal cells expressed comparable levels of scavenger receptor and had similar phagocytic activity in adult and neonatal intestine. This is consistent with previous reports showing similar levels of phagocytosis and TLR hyporesponsiveness by CD14^{+} blood cells from human newborns and healthy adults (Gille et al., 2006). Thus these functions are important for processes that are common to the developing and mature intestine, such as phagocytosis of apoptotic cells (Wynn et al., 2013). On the other hand, my results showed that neonatal F4/80^{hi} mϕ produced higher amounts of TNFα constitutively than their adult counterparts, while their production of IL10

was lower, indicating that these properties may be defined by the nature of the local environment.

In our laboratory, phenotypical analysis of mϕ relied on the expression of CX3CR1, which allowed us to find clear mϕ subsets according to their maturation state. This characterisation approach has to be modified when identifying intestinal mϕ in non-CX3CR1-GFP mice. Therefore I decided that for most of this thesis I would define intestinal mϕ based on their expression of F4/80 and CD11b, with F4/80^{hi} CD11b^{int} being mostly equivalent to CX3CR1^{hi} cells and representing the fully mature mϕ subset. Conversely, F4/80^{lo} CD11b^{+} cells were mostly CX3CR1^{int}, similar to what is seen with the intermediary stages in adults.

One difference between the adult and neonatal intestine was that the F4/80^{lo} and F4/80^{hi} subsets were much more discrete in newborn mice. Additionally, the F4/80^{lo} numbers varied markedly at different times after birth, especially around the age of weaning. When the F4/80^{lo} subset was divided on the basis of Ly6C and MHC II, I found that at birth, the Ly6C^{hi} MHC II^{-} (P1) cells were the largest subset, but they quickly dropped to half after only 7 days. Interestingly Ly6C^{hi} MHC II^{+} (P2) cells were almost absent at birth and only started being clearly noticeable, in both proportions and numbers, after 14 days of life. Finally, Ly6C^{-} MHC II^{+} (P3) cells started with a low proportion that reached stable levels after 7 days of life, although in terms of absolute numbers they also showed their highest peak at 21 days of age. Thus I hypothesised that in newborn mice, the large number of Ly6C^{hi} MHC II^{-} monocyte-like cells, which are rare in adult intestine, could represent mϕ precursors derived from foetal liver. This would be consistent with other recent work suggesting that the FL is a major haematopoietic site at this age and that the progeny are F4/80^{lo} CD11b^{+} (Hoeffel et al., 2012). In contrast the numbers of Ly6C^{hi} MHC II^{+} cells were very low amongst F4/80^{lo} cells in newborn compared with adult intestine, while there were also reduced numbers of Ly6C^{-} MHC II^{+} thought to be the next stage in the differentiation continuum (Bain et al., 2013). Together these results could indicate that the normal maturation processes in the mϕ lineage have not yet begun at this early stage of life. Alternatively, the assumption that these phenotypic groups represent differentiation stages within the same lineage may not be

relevant in the newborn intestine and each population may actually be from distinct origins.

Interestingly, I detected a very small proportion of CX3CR1^{-} cells within the F4/80^{lo} CD11b^{+} subset of myeloid cells that could not be found in adult mice. I considered the possibility that these might be granulocytes contaminating the macrophage population in the neonate mice. Indeed, granulocytes such as eosinophils and neutrophils have been shown to express low levels of F4/80 (Narni-Mancinelli et al., 2011; Taylor et al., 2006). However these were excluded from my CD11b^{+} CX3CR1^{-} fraction of cells based on their expression of Siglec F and Ly6G. I have not found literature reporting any neonatal cell population with such characteristics. A final possibility is that they could be intestinal DC and if sufficient could be sorted, this could be tested by examining their expression of DCs-specific transcription factors, such as Zbtb46 (Meredith et al., 2012; Satpathy et al., 2012).

Unlike in adults, only a small proportion of the F4/80^{hi} CD11b^{int} CX3CR1^{hi} subset expressed MHC II at birth and this increased gradually with time. The lack of expression of MHC II on newborn intestinal mϕ is similar to what is seen with mature mϕ in other anatomical sites such as the peritoneum and spleen. However an important difference between these tissues and the maturing intestine is the increasing microbial colonisation of the gut. That this may play a major role in induction of MHC II was supported by my subsequent experiments in GF mice, where even adult mϕ showed delayed acquisition of MHC II. In addition, global gene analysis has shown that MHC expression decreases in small intestine and colon after treatment with broad-spectrum spectrum antibiotics (Schumann et al., 2005). Nevertheless it is clear that the microbiota are not entirely responsible for the expression of MHC II on intestinal mϕ. It has been reported that interaction with vascular endothelial cells may be sufficient to induce MHC II expression on blood monocytes as they enter tissues (Jakubzick et al., 2013). However this would not explain why the phenomenon is selective for the intestine, unless the vascular endothelium is different in this tissue. Ongoing studies in the lab have attempted to identify factors that might explain MHC II expression on intestinal mϕ and have excluded factors such as IFNγ, T cells, B cells and CSF2 (Bain, unpublished data).

Because of the gradual changes in MHC II expression after birth and the fact that the numbers of mϕ did not alter markedly until the 3rd week of life, it seems likely that these early changes reflected in situ differentiation of the cells that were already present. However I could not exclude the possibility that the increased numbers of MHC II^- mϕ reflected the arrival and maturation of small numbers of new monocyte-derived mϕ, as occurs in adults (Bain et al., 2013). However this would not be consistent with my findings that $Ly6C^{hi}$ MHC II^+ $F4/80^{lo}$ cell numbers were very low until weaning.

6.3 Origin and expansion of colonic macrophages after birth

The most dramatic feature of my studies of neonatal intestine was the large expansion in mϕ numbers around the time of weaning and I used a number of approaches to explore the reasons for this. An idea which was put forward during my project was that tissue resident mϕ might be derived from embryonic precursors in the YS or FL which self-renew throughout later life (Huber et al., 2004; Schulz et al., 2012). This was shown to be the case for alveolar mϕ, microglia, some splenic mϕ, liver Kupffer cells, pancreatic mϕ and Langerhans cell in the epidermis (Ginhoux et al., 2010; Lichanska and Hume, 2000; Naito et al., 1996; Schulz et al., 2012), but never explored in the intestine.

Therefore I thought it was important to examine this possibility, as the $F4/80^{hi}$ $CD11b^{int}$ and the $F4/80^{lo}$ $CD11b^+$ populations I found in neonatal intestine were phenotypically similar to the YS and FL derived subsets found in other tissues (Orkin and Zon, 2008; Schulz et al., 2012). To study this I visited Professor Frederic Geissmann's laboratory, where I used the reporter gene system he had developed to identify YS derived mϕ. Using this approach, I found CSF1-YFP^+ mϕ in 9 day old colon and these were uniformly $F4/80^{hi}$ $CD11b^{int}$, consistent with YS derived mϕ in other tissues. However, the frequency of CSF1-YFP^+ in the intestine was low compared with that in other tissues such as the brain (2% vs ~30%). Moreover, it has to be noted that even in tissues thought to be seeded exclusively from the YS, this system is not 100% efficient, meaning that the true level of YS derived intestinal mϕ may actually be higher. The reasons for this relative inefficiency are not known,

but may reflect the fact that the experiment involves a single pulse with tamoxifen to the pregnant dam at 8.5 of gestation, meaning that only a relatively small fraction of progenitors may be labelled in such a short period. It has also been suggested by others that the YS actually contributes little to tissue mϕ development and that even the F4/80^{hi} cells may be derived from FL (Ginhoux et al., 2010). However the authors of this paper only showed that there may be a later seeding of Langerhans cells precursors, but did not use any FL-specific marker to directly claim FL involvement in the process (Ginhoux et al., 2010). This lack of a reliable FL marker made impossible for me to replicate this approach and so I was unable to address the contribution of FL to the mϕ pool in neonatal mice. However its role in the postnatal accumulation and maturation of intestinal mϕ is likely to be limited, given that the BM takes over haematopoiesis soon after birth (Orkin and Zon, 2008), long before I found the most marked changes in the population to occur.

Throughout my experiments, a high variability between was noticed with each repeat. It was explained that due the low number of cells that can be isolated from young mice, and that for practical reasons, some experiments analysed mϕ from the same litter at different ages, whilst some other experiments used pups of different ages (consequently different litters) on the same day. An interesting observation suggested that by keeping track of the origin of the mϕ for each experiment could have showed a pattern regarding the high variability of the results, thus being able to control or reduce the variability between experiments. Indeed, this suggestion may be key and definitely will be considered for future experiments. Unfortunately for this thesis, the records I kept from the mice I used did not take this into consideration and are not useful for the data I present here.

The idea that self-renewal might contribute to the increasing number of mϕ in the first weeks of life was initially supported by my findings that a high percentage of F4/80^{hi} mϕ were dividing actively in neonatal mice. However this was most marked up to 2 weeks of life, when the population was not increasing greatly in size and it was already decreasing by 3 weeks of age, when the most dramatic accumulation of mϕ was seen. These findings suggest that the expansion of the intestinal mϕ pool is not due to the local

proliferation of existing cells, as it was previously thought (Chorro et al., 2009). Interestingly, the F4/80^{lo} CD11b^{+} monocyte-like cells were also Ki67^{+} when at various timepoints, suggesting that they are in active cell division throughout development. One explanation for this could be that monocytes recently released from the bone marrow and newly arrived in the tissue might carry residual levels of Ki67.

The lack of contribution of local self renewal to the intestinal mϕ is supported by the fact that the proportion of CSF1R-YFP^{+} cells amongst F4/80^{hi} mϕ was greatly decreased in adult intestine and indeed, the absolute numbers had also fallen. This contrasted markedly with other tissues such as the brain, skin and liver, where foetal precursor-derived cells remained present in approximately equal numbers (Schulz et al., 2012). Thus the intestine appears to be an exception to the new paradigm that all resident mϕ are derived from foetal progenitors. One additional finding that arose from my studies was that the relative expression of F4/80 and CD11b became increasingly unreliable as a means of defining the origin of mϕ in the intestine, as the F4/80^{hi} and F4/80^{lo} subsets were not as distinct in aged mice. This appeared to reflect the increased expression of both markers, so that most adult mϕ were F4/80^{hi} CD11b^{hi}. These results emphasise the difference between the intestine and other tissues and indicate that more definitive approaches are needed to identify the origins of gut mϕ.

Monocyte release from the BM is CCR2 dependent (Kurihara et al., 1997; Kuziel et al., 1997; Serbina and Pamer, 2006; Si et al., 2010; Tsou et al., 2007) and previous work in the lab had indicated that intestinal mϕ were at least partly deficient in adult CCR2 null mice (Bain et al., 2013). My results showed that this phenotype only became apparent after weaning and as I was writing up, subsequent studies revealed that the defect developed progressively until aged mice showed almost complete absence of mϕ (unpublished data). Despite considerable variability between individual mice and in the separate experiments I performed on weaning mice, it was evident that CCR2 null mice did not show the same degree of expansion in mϕ population as the wild type controls. This affected the F4/80^{lo} CD11b^{+} subset predominantly, whereas the F4/80^{hi} CD11b^{int} subset remained mostly intact.

The partial preservation of monocyte recruitment in CCR2 null mice at weaning raises questions about whether CCR2 is the only monocyte recruitment mechanism. Other possible chemokines involved could be CCR1 and CCR5, which are known to be involved in monocyte migration during inflammatory conditions such as arthritis, as well as in *in vitro* assays (Gouwy et al., 2013; Lebre et al., 2011). Finally, other mechanisms apart from chemokines have been reported to regulate monocyte migration to the LP including TGFβ and IL8 (Smythies et al., 2006), which can be produced by intestinal epithelial cells and mast cells.

An additional possibility is that the other subset of Ly6C^{lo} monocytes may play a role at weaning and not in adult intestine. Although it has been proven difficult to find evidence for these monocytes entering tissues and previous work in the laboratory could not find progeny of adoptively transferred Ly6C^{lo} monocytes in adult colon (Bain et al., 2013), their function has not been examined in early life. Thus it would be important to compare formally the mechanisms that might be involved in the recruitment of monocytes and mϕ in mice of different ages, perhaps by using mice deficient for other cytokine receptors such as CCR1 and CCR5.

It was clear from my experiments that the intestinal mϕ pool is relatively stable for the first 2 weeks of life and that dramatic changes occurred during the third week of life. This is the time of weaning in mice (and other species), when there are known to be major changes in intestinal physiology, cell populations and immune function (Bailey et al., 1992; Manzano et al., 2002). As well as the exposure to new food antigens, a novel range of bacterial strains appears, adding to the commensals that begin to colonise at birth (Bailey et al., 2005). In addition, withdrawal of maternal milk leads to the lack of exposure to immunomodulatory factors such as TGFβ (Maheshwari et al., 2011; Oddy and Rosales, 2010). In all my experiments, considerable variability was found when I examined mϕ numbers and subsets around the time of weaning, possibly because I usually used a fixed time point, whereas individual mice probably begin to sample solid food at different ages and in a continuous process. During my experiments, weaning was considered as the age when mice start eating solid food (day 14 onwards) rather than their withdrawal from the dam's milk, therefore I was not able to carry out

experiments in which the exact time of weaning was tightly controlled. It would important to do this for future experiments to prove that the rapid changes in mϕ populations are truly due to the effects of weaning, or simply reflect age-dependent alterations in e.g., haematopoiesis, mucosal physiology or monocyte development.

6.4 Functions of neonatal intestinal macrophages

The low number of mϕ obtainable from newborn mice meant that I could only perform limited functional studies. Nevertheless, I was able to show that F4/80^{hi} CD11b^{int} mϕ from neonates were fully capable of phagocytosis and expressed comparable levels of scavenger receptor CD163 to that found in their adult counterparts. Given the fact that the microbiota is virtually absent at this time, these features may indicate that the main role of intestinal mϕ in newborns is to participate in tissue remodelling process at the stage of intestinal development. Indeed, F4/80^{+} mϕ have been shown to participate in phagocytic clearing of naturally occurring programmed cell death in the remodelling interdigital zones of the developing limb buds (Hopkinson-Woolley et al., 1994). Thus by the time of birth mϕ are already well prepared to deal with removing apoptotic tissue (Hart et al., 2008; Mantovani et al., 2013; Schulz et al., 2012). Neonatal F4/80^{hi} CD11b^{int} mϕ were also already refractory to TLR4 ligation and failed to increase production of TNFa after LPS stimulation despite their constitutive production of this cytokine. In a similar fashion, albeit not to such an extent, F4/80^{hi} CD11b^{int} mϕ from adults showed an impaired responsiveness to LPS stimulation. These results are consistent with previously published findings that TLR unresponsiveness of human and mouse intestinal mϕ is already established in foetal life and is secondary to production of TGFβ by local stromal cells (Lotz et al., 2006; Maheshwari et al., 2011). An alternative source could be from the phagocytosis of apoptotic cells as this is known to drive TGFβ production (Henson and Bratton, 2013). This inertia contrasts with the similar TLR tolerance found in intestinal epithelial cells which involves exposure to microbial products during the birth process.

The inability of intestinal macrophages to mount inflammatory responses after LPS stimulation is in a stark contrast to blood monocytes that react

vigorously to TLR ligands. This inability of human and mouse intestinal macrophages to respond to LPS was explained by the apparent absence of the LPS receptor CD14 on their cell surface (Smythies et al., 2005) or markedly down-regulated adapter proteins MyD88 and TRIF (Smythies et al., 2010). Interestingly, greater susceptibility to infections in early life correlates with changes in innate TLR responses (Kollmann et al., 2012). Even though monocytes from neonates are capable, like adults, of recognising the presence of pathogens through TLR, several of their functions are impaired, including an inability to secrete cytokines or differentiate into macrophages (Dasari et al., 2011; Velilla et al., 2006).

Despite the similarities between newborn and adult intestinal macrophages, I also noted some important age-related differences. Namely, F4/80^{hi} CD11b^{int} mϕ from newborn intestine had lower levels of IL10 mRNA and intracellular cytokine compared with adult F4/80^{hi} CD11b^{int} mϕ, although these were still clearly higher than BMM used as a control for RNA expression. These findings are consistent with other reports that microbiota may be important in driving the high constitutive production of IL10 by resident intestinal mϕ (Rivollier et al., 2012). That the developing intestine itself can have significant effects on the maturation of intestinal mϕ is supported by the fact that F4/80^{hi} CD11b^{int} mϕ from newborn intestine also showed the constitutive production of significant amounts of TNFα seen in adult mϕ. Together with the high expression of CX3CR1 and some MHC II on the neonatal mϕ, these findings indicate that neonatal mucosa contains factors capable of conditioning the unique properties of intestinal mϕ, although these are still to be identified.

6.5 Effects of the microbiota on intestinal mϕ development

Although there is a considerable amount known about the effects of the microbiota on immune function (Atarashi et al., 2011; Cummins and Thompson, 2002), relatively few studies have examined intestinal mϕ specifically and none have investigated this in early life. Moreover, because of the dramatic changes I observed in gut mϕ populations in developing mice, particularly at weaning, I decided to investigate if the microbiota was involved in this phenomenon.

My first approach was to administer broad-spectrum antibiotics to adult mice, using regimes shown previously to modify innate immune responses *in vivo* (Abt et al., 2012; Rath et al., 2001). Initially I treated mice for 21 days with a mixture of meropenem and vancomycin, but the only effect I observed was a marginal increase in the frequency of CX3CR1^{hi} mϕ in the ABX treated animals, perhaps consequent on the parallel decrease in CX3CR1^{int} cells. The numbers of granulocytes, total leukocytes and CX3CR1^{int} mϕ were not altered by the ABX regime. There was a trend towards higher TNFα mRNA expression by ABX treated CX3CR1^{hi} cells, but a shorter regime had no effect on intracellular TNFα or IL10 production. The reasons for the apparent increase in CX3CR1^{hi} (F4/80^{hi}) mϕ are unknown, particularly in view of the lack of any overall effect of this regime, which contrasted with an earlier report using this cocktail to protect mice from intestinal inflammation (Rath et al., 2001). Although it has to be noted that I used C57Bl/6 mice, whereas Rath *et al*. used rats and BALB/c mice, there are no reports supporting strain or species differences in the efficacy of these particular antibiotics. Therefore I decided to try an alternative regime that contained a cocktail of ampicillin, gentamicin, metronidazole, neomycin and vancomycin that had been shown to reduce innate and adaptive immune responses to lymphocytic choriomeningitis virus (LCMV), including decreased TNFα production by peritoneal and splenic mϕ (Abt et al., 2012). In my hands, this regime had an obvious effect that was evident to the naked eye, with treated mice developing an enlarged caecum similar to what I found subsequently in GF mice. Despite this, there were few cellular changes amongst the colonic mϕ populations, apart from modest increases in total CD11b^{+} cells and granulocytes. There were no significant changes in the various populations of F4/80^{lo} or F4/80^{hi} mϕ, including Ly6C^{hi} monocytes, consistent with the findings of Abt and colleagues, who found no effects of this regime on the phenotype of splenic and peritoneal mϕ. However, in contrast to their studies, I did not find a decrease in TNFα mRNA expression by F4/80^{hi} CD11b^{int} mϕ from ABX treated intestine. In fact, there was a trend towards increased TNFα expression in these cells, similar to what I found with CX3CR1^{hi} cells in the first experiments. Unfortunately, I was unable to FACS purify enough F4/80^{lo} cells in this second series of experiments to obtain good quality RNA for analysis of cytokine gene expression.

The lack of effects of these antibiotic regimes on mϕ seemed surprising in view of the previous reports that similar regimes can prevent colitis, downregulate MHC II gene expression, and alter the balance between Th17 and Treg in LP (Ivanov et al., 2008; Lamouse-Smith et al., 2011; Schumann et al., 2005; Videla et al., 1994), especially in view of the clear effects of the second regime on caecal size. However, it should be noted that earlier work suggested that this phenomenon was due to direct effects of penicillin-related compounds on tissue osmolarity (Savage and Dubos, 1968; Savage and McAllister, 1971), rather than to changes in bacteria composition. In this regard, it is important to note that I was unable to carry out analysis of the microbiota to confirm directly what effects the antibiotic regimes had had. Nevertheless, other work going on in the lab while I was working showed that the same cocktail of ampicillin, gentamicin, neomycin, vancomycin and metronidazole reduced the frequency of Th17 cells in the small intestine (Scott C, unpublished data), suggesting that this regime was capable of modulating function in the intestine. One explanation for these discrepant findings could be that the short term treatment we used may be insufficient to influence the behaviour of longer lived cells such as intestinal mϕ, which are thought to have a lifespan of several weeks (Zigmond and Jung, 2013). Furthermore, work in our lab and others indicate that these cells are unable to change their functions once fully mature (Bain et al., 2013; Zigmond and Jung, 2013). However, as these cells appear to be replenished continuously from monocytes in a process that takes a week or less (Bain et al., 2013), it is surprising that the earliest stages of differentiation continuum were not affected by my antibiotic treatment. Unfortunately, I was unable to study the function of the various stages of differentiation directly using CX3CR1$^{GFP/+}$ mice, as the permeabilisation and fixation needed to assess intracellular cytokine staining alters GFP in such way that its fluorescence activity reduces, meaning that the CX3CR1^{int} populations become more difficult to define accurately (Kusser and Randall, 2003). Thus, in order to get a deeper insight to the effects of antibiotics it would be interesting to study their effect on each monocyte/mϕ populations by other methods such as qPCR or microarray analysis of sorted cells. It has been shown that a discrete but significant decrease in type I interferon expression can be elicited by antibiotic treatment (Abt et al., 2012; Ganal et al., 2012). This strategy

might be worth considering because it would provide a more focused and sensitive observation of the cell subsets involved and therefore, any subtle change could be easier to detect.

Finally, my results may suggest that antibiotic regimes have a minimal effect on the mϕ populations in the colon. A reason for this could be that the mϕ populations of conventional mice have already been conditioned by previous exposure to commensals and therefore their response to antibiotics is more difficult to quantify. In order to overcome this, it might be feasible to use a more intensive antibiotic regime such as that in which pregnant mice are given antibiotics and their pups continued on this after birth. This has been shown to modify antibody responses and tolerance to orally administered antigens (Kusser and Randall, 2003; Lamouse-Smith et al., 2011) and it might show a clearer effect of the antibiotics treatment.

6.6 Macrophage populations in germ free mice

As the experiments using antibiotics were inconclusive, I took the opportunity to visit Dr David Artis's laboratory in Philadelphia to study GF mice, which are known to have profound differences in immune functions (Eberl and Lochner, 2009; Ivanov and Honda, 2012; Kosiewicz et al., 2011; Molloy et al., 2012; Reading and Kasper, 2011; Round and Mazmanian, 2009).

The effects of the GF condition were shown clearly by the slightly longer colon and considerably larger caecum, confirming earlier findings (Savage and McAllister, 1971). In addition, adult GF mice had fewer F4/80^{hi} Ly6C^{-} mϕ compared with the conventionally reared controls, as well as reduced expression of MHC II by these cells, similar to the absence of MHC II on the F4/80^{hi} cells in neonatal intestine. These differences were even more pronounced in 3 week old GF mice, despite the fact that the total numbers of these cells were normal at this time. Interestingly however, F4/80^{hi} CD11b^{int} mϕ from 7 day old GF mice had equivalent levels of MHC II to their conventional counterparts, confirming my initial conclusions that a significant amount of mϕ differentiation in the early neonatal period is independent of the microbiota. However, the total numbers of F4/80^{hi} CD11b^{int} mϕ were also

lower in 7 days old GF pups, perhaps suggesting that primitive precursors of these early mϕ may be dependent on the presence of the microbiota.

As these experiments were carried out in non CX3CR1-GFP mice, I had to use the F4/80^{lo} population as a surrogate for analysing how monocytes and the intermediary subsets behaved in GF mice. Using this approach, I found that the total number of F4/80^{lo} cells only showed a significant difference between GF and CNV mice at 3 weeks of age, when they were decreased in GF colon. However, more detailed analysis of this population showed that the Ly6C^{hi} MHC II^{-} subset was significantly decreased in both 3 week old and in adult GF mice, while the Ly6C^{hi} MHC II^{+} (P2) subset was reduced in GF mice regardless of their age.

Together these results could support the idea that in the first week of life, the majority of intestinal mϕ is derived from foetal precursors, whose recruitment is mostly independent of the microbiota (Orkin and Zon, 2008). Moreover, my findings could suggest that while some myelopoiesis in the YS may be influenced by microbial colonisation, YS derived mϕ develop independently of the microbiota once they have arrived in the mucosa (Maheshwari et al., 2011). The normal numbers of Ly6C^{hi} MHC II^{-} monocytes in 7 day old GF mice may support the idea that these are FL derived at this time, although to my knowledge, the expression of Ly6C by FL monocytes has not been explored. The decreased numbers of Ly6C^{hi} MHC II^{+} (P2) in neonatal GF intestine and delayed acquisition of MHC II and upregulation of F4/80 in GF mice indicate these processes are dependent on the microbiota. Studying the ontogeny of intestinal mϕ in GF lineage tracker mice and/or developing adoptive transfer techniques for use in neonatal animals may allow these ideas to be explored directly.

At weaning, both the recruitment and maturation of BM derived Ly6C^{hi} monocytes become highly dependent on the microbiota and this defective recruitment and maturation persist into adult life. The fact that the differences between GF and CNV mice become so marked at this time emphasises what a crucial role weaning plays in the development of the intestinal mϕ pool (Mulder et al., 2011; Russell et al., 2013). Despite these effects on monocyte recruitment, it is interesting to note that substantial

numbers of mϕ were present in adult GF mice, indicating that factors other than the microbiota such as dietary components may be able to compensate for some of the effects normally provided by the microbiota. Previous studies of the effects of the microbiota on intestinal mϕ populations have produced conflicting results, with some suggesting that their numbers are reduced in GF intestine (Atarashi et al., 2008; Niess and Adler, 2010), while others have reported no difference (Rivollier et al., 2012). Although my results support the idea of a defect in the total mϕ pool in GF mice, they also show that the exact nature of this abnormality may depend on the stage of differentiation within the monocyte-mϕ continuum, as well as the age of the animal and the origin of the mϕ precursors. In this respect, it is important to note that none of the previous studies of intestinal mϕ in GF mice analysed neonatal and adult mϕ. A further factor which needs to be taken into account is that whereas there is contradictory evidence on the number of mϕ in GF intestine, there has been consensus on the fact that functions such as IL10 production may depend on the presence of microbiota (Kayama et al., 2012; Rivollier et al., 2012). Unfortunately, there were insufficient mice available for me to carry out direct functional analyses of GF mice during my visit to Philadelphia. Although I did isolate mRNA from F4/80^{hi} mϕ I sorted from these mice with the aim of performing microarray analysis, no meaningful results were obtained due to poor cell yield and low RNA quality. Therefore further experiments are now planned to correlate alterations in the mϕ subsets I observed in GF mice with functional indices.

6.7 Regulation of macrophage function by CX3CR1

One of the most characteristic features of resident intestinal mϕ is the acquisition of high levels of the CX3CR1 chemokine receptor during their differentiation from CX3CR1$^{lo/int}$ monocytes (Bain et al., 2013). One possibility raised by these findings is that CX3CR1 may play a role in controlling the differentiation or function of the mature mϕ via its ligand CX3CL1 that is expressed by epithelial cells and vascular endothelial cells in the intestine (D'Haese et al., 2010; Kim, 2011; Umehara et al., 2004). However, previous studies had produced contradictory results on the immunoregulatory effects of the CX3CL1-CX3CR1 axis. Although it has been suggested that CX3CL1 promotes intestinal inflammation, as shown by

increased CX3CL1 production in cases of Crohn's disease (D'Haese et al., 2010), and less severe DSS and T cell dependent colitis in CX3CR1 deficient mice (Kim, 2011; Kostadinova et al., 2010; Niess and Adler, 2010), others have reported anti-inflammatory effects. Indeed, CX3CR1 may be required for oral tolerance via the production of IL10 by intestinal mϕ (Dagkalis et al., 2009; Hadis et al., 2011). Therefore I decided to explore further the role of CX3CR1 in intestinal mϕ function.

First I examined the outcome of DSS colitis in $CX3CR1^{GFP/GFP}$ (KO) mice, but obtained inconsistent results, ranging from reduced susceptibility to a complete lack of effect. An example of this situation was noticed on one occasion, which suggested that the absence of CX3CR1 actually had a protective role, a trend could be observed in the 2nd and 3rd time I performed this experiment. During the discussion of results, it was suggested to pool the results from the three repeats and to perform a repeated-measures general linear model test, in order to increase the statistical power of the analysis. This analysis was not possible due to the lack of an even number of mice assessed at each timepoint, therefore it was substituted with a two way ANOVA. As expected, after pooling the experiments, a more robust data set is generated, however this was enough only to show significant differences in colon length and clinical score after 8 days on colitis.

The reasons for this high variability and for the discrepancy with the previous reports are unclear. However, as noted above, it is not the first time that opposing results have been published regarding the proinflammatory *versus* anti-inflammatory role of the CX3CL1-CX3CR1 axis (D'Haese et al., 2012; Kayama et al., 2012; Medina-Contreras et al., 2011; Niess and Adler, 2010). One possibility could be that the model of DSS colitis I used was too severe to be modified by the absence of CX3CR1 and that differences in the microbiota between different laboratories might determine the CX3CR1 dependency of colitis, which is known to be driven by local bacteria (Denning et al., 2011; Elsheikh et al., 2012; Ivanov et al., 2009; Wu et al., 2010). If correct, these findings indicate that CX3CR1 is not absolutely required for intestinal inflammation, but may only modulate certain aspects and/or forms.

Despite the fact that CX3CR1 is known to influence monocyte recruitment to tissues (Ancuta et al., 2003; Aspinall et al., 2010; Fong et al., 1998; Imaizumi et al., 2004), I could not find any difference in the numbers or proportions of myeloid subsets in steady state or inflamed intestine from CX3CR1 KO mice. These results suggest that this receptor is not required for the entry, maturation or survival of any of the CX3CR1^{+} mϕ and DCs in the mucosa. Whether it controls the anatomical location of these cells once in the intestine, as might be suggested by the inability of CX3CR1 KO mϕ to form TEDs (Niess et al., 2005), remains to be determined using immunohistology.

CX3CR1$^{GFP/GFP}$ mice did show some subtle differences in myeloid cell populations in the BM and bloodstream. Thus the BM of CX3CR1$^{GFP/GFP}$ mice had higher frequencies of Ly6C^{hi} and Ly6C^{lo} monocytes with a concomitant decrease in granulocytes compared with CX3CR1$^{GFP/+}$ controls. During DSS colitis, there was a decrease in the frequency of Ly6C^{hi} monocytes in CX3CR1 KO BM which did not occur in control mice, suggesting that CX3CR1 may normally act to inhibit release of monocytes from BM. Alternatively, as the frequency of Ly6C^{hi} monocytes were also decreased in the blood of CX3CR1 KO mice with colitis, it could be that there is actually enhanced recruitment of these cells to the inflamed mucosa in the KO mice. However, this would not be consistent with the lack of effect of CX3CR1 on the inflammatory infiltrate of the mucosa itself. A very recent study has shown that there are enhanced migration of Ly6C^{hi} monocytes into the spleen of CX3CR1 KO mice after chemotherapeutic ablation *in vivo* which was associated with reduced numbers (Jacquelin et al., 2013), similar to my findings in mice with DSS colitis. Although I found no difference in Ly6C^{hi} monocytes in the blood of steady state CX3CR1$^{GFP/GFP}$ mice, the proportions of Ly6C^{lo} monocytes were increased in these animals, which would appear to contradict a recent suggestion that soluble CX3CL1 is needed for the intravascular survival of these cells (Kim, 2011). As Ly6C^{lo} monocytes are now thought to be the progeny of Ly6C^{hi} monocytes (Ramachandran et al., 2012)), together these findings indicate that further studies are warranted to explore the role of CX3CR1 in the homeostasis of monocytes in steady state and inflammation.

6.8 CX3CL1-CX3CR1 axis in oral priming

Oral tolerance has been extensively studied in laboratory rodents, but also in several other species such as pigs and dogs (Deplazes et al., 1995; Miller et al., 1984; Stokes, 1987; Stokes et al., 1987). The phenomenon of oral tolerance can be defined as a state of immunological unresponsiveness to antigens that can be induced by oral administration of non-invasive antigen such as proteins. Intestinal mϕ are considered to be key in the regulation of mucosal immunity and their remarkable expression of CX3CR1 has been described by our group and others (Bain et al., 2013; Kayama et al., 2012; Zigmond and Jung, 2013), however no investigations have been conducted in order to define the role of this chemokine receptor in oral tolerance.

A recent report has shown that intestinal mϕ from CX3CR1 deficient mice had defective production of IL10, leading to reduced expansion of $Foxp3^+$ Treg cells in the LP and a subsequent defect in systemic tolerance induced by feeding ovalbumin (Hadis et al., 2011). To explore if this reflected a wider role for CX3CR1 in regulating all aspects of adaptive immunity in the intestine, I primed mice by feeding them OVA with or without cholera toxin as an adjuvant. After feeding OVA alone, CX3CR1 deficient, but not WT mice showed evidence of T cell priming in the MLN. In parallel, oral administration of CT adjuvant had a greater ability to enhance T cell responses in CX3CR1 deficient MLN compared with WT MLN, while $CX3CR1^{GFP/GFP}$ mice had increased total IgA levels in faecal extracts. Although it should be noted that the differences I found were modest and therefore need confirmation, they could indicate that local tolerance mechanisms may indeed be impaired by the absence of CX3CR1. This would be consistent with the lack of IL10 production by intestinal mϕ in $CX3CR1^{GFP/GFP}$ mice (Hadis et al., 2011). Although the IL10 producing cells studied in this and other laboratories have found there is also a *bona fide* population of $CX3CR1^{int}$ DCs, which could be implicated in these processes (Cerovic et al., 2013; Zigmond and Jung, 2013), cell specific KO mice could help resolve these issues.

I also found a rather different pattern of systemic immune responses in $CX3CR1^{GFP/GFP}$ mice, as these animals had lower T cell priming in the spleen and lower serum antibodies after feeding OVA+CT than WT mice. No

differences were observed in the very limited responses seen after feeding OVA alone. Again these results need to be confirmed, especially as they appear to conflict with the earlier report of defective systemic consequences of OVA-specific oral tolerance in CX3CR1$^{GFP/GFP}$ mice (Hadis et al., 2011). However my results could indicate that CX3CR1 may play distinct roles in determining whether tolerance or active immunity are generated in the mucosal and systemic immune systems. Alternatively it may have a role in controlling the systemic dissemination of whatever response is initiated in the intestine, be it tolerance or priming. Again the cells involved and exact consequences need to be explored. For instance it would be of interest to examine whether the absence of CX3CR1 alters the migration of DCs from LP to MLN, the cellular process that is central to the induction of oral tolerance (Worbs et al., 2006).

Finally, it is known that defects in oral tolerance are more common during infancy and weaning. Reports have shown that animals which received antigen during the first 1 or 2 days of life showed systemic priming when challenged parenterally as adults (Peng et al., 1989; Strobel and Ferguson, 1984), and interestingly this has been shown not only in neonate mice, but also in piglets (Miller et al., 1984; Stokes et al., 1987). Thus, even though the evidence from my oral priming experiments was not robust, it would be interesting to compare the efficiency to develop oral priming by CX3CR1 deficient mice at early age.

6.9 Role of the CX3CL1-CX3CR1 axis in macrophage function *in vitro*

My final experiments investigated how CX3CL1 might influence mϕ function directly and my initial plan was to study intestinal mϕ *in vitro*. However this proved impossible due to the poor viability of the mature CX3CR1^{hi} mϕ that could be purified from the intestine, while only low numbers of the intermediary CX3CR1^{int} subsets could be obtained. Therefore I decided to use BM-derived mϕ as a means of establishing the system, with the intention of moving on to intestinal mϕ once the technical issues had been overcome.

First I compared cytokine release and co-stimulatory molecule expression of CX3CR1 KO and WT BMM that had been stimulated with IFNγ or LPS+IFNγ in

the presence or absence of recombinant CX3CL1. As expected, WT BMM responded to LPS stimulation by upregulating the costimulatory molecules CD40 and CD80, together with increased production of TNFα and IL6. Although addition of recombinant CX3CL1 seemed to enhance the production of TNFα by CX3CR1$^{GFP/+}$ BMM, this had no consistent effect on costimulatory molecule expression. In general, CX3CR1 KO BMM responded equivalently, except for some increase in CD40 and CD80 and lower production of IL6 and TNFα when stimulated with LPS+IFNγ. However these effects were modest and inconsistent.

As the effects of recombinant CX3CL1 were inconclusive, I acquired epithelial cell lines expressing either the soluble or membrane bound forms of CX3CL1, in the hope this would mimic the physiological situation more accurately, where the transmembrane form is expressed by epithelial cells and endothelial cells (Andrzejewski et al., 2010). Again, the results were mostly inconclusive, with only modest effects of the soluble CX3CL1-expressing HEK cells on the viability and expression of costimulatory molecules by LPS stimulated CX3CR1 KO BMM when compared with their WT and CX3CR1$^{GFP/+}$ counterparts. On the other hand, the effects of HEK cells expressing membrane bound CX3CL1 were almost identical to those found using by untransfected HEK cells. Interestingly, there were some differences between WT and CX3CR1 KO BMM in certain parameters such as costimulatory molecules when cultured with soluble CX3CL1, however due to the lack of a clear pattern, these differences could not be related to the presence/absence of CX3CR1. Previously, these CX3CL1-expressing HEK cells had only be used to analyse structural properties of CX3CL1 (Andrzejewski et al., 2010) and not in cellular co-cultures *in vitro*. Therefore it seems that more work will be required to optimise this model. Furthermore it may be necessary to develop the method to use monocytes with the capacity for plasticity, or tissue mϕ that express more CX3CR1 than BMM.

Together my results suggest that there may be a role for the CX3CL1-CX3CR1 axis in modulating the balance between the local and systemic effects of mucosal immune responses *in vivo*. However the results from my *in vitro* experiments were not consistent enough to dissect the cellular mechanisms involved.

6.10 Concluding remarks

The results presented here show that although mϕ derived from primitive precursors are present in the colon before birth and can self renew for 1-2 weeks, they are replaced by an influx of conventional monocytes around the time of weaning. As described in other tissues, both YS and FL appear to contribute to the mϕ present in early neonatal intestine (Figure 6.1). The recruitment of monocytes at weaning is highly dependent on CCR2 and constant replenishment by CCR2-dependent monocytes then becomes the only source of mϕ in adult intestine. The recruitment of monocytes is only partly dependent on the microbiota and interestingly, the mϕ present at birth already have many characteristics of the fully mature mϕ found in adult intestine, including the expression of high levels of CX3CR1 and scavenger receptors, phagocytic activity and hyporesponsiveness to TLR ligation, together with some constitutive production of IL10 and TNFα. However the full expression of MHC II and production of IL10 are not acquired until adult life and may be driven by the microbiota.

These findings indicate that factors other than the commensal bacteria can contribute to the tissue specific maturation of monocytes after their arrival in the mucosa, but their identity remains to be determined. The mechanisms involved in the recruitment at weaning are also poorly defined. Although I attempted to explore the role of the CX3CL1-CX3CR1 axis in intestinal mϕ function, my experiments were not conclusive and more work is needed to identify these mechanisms.

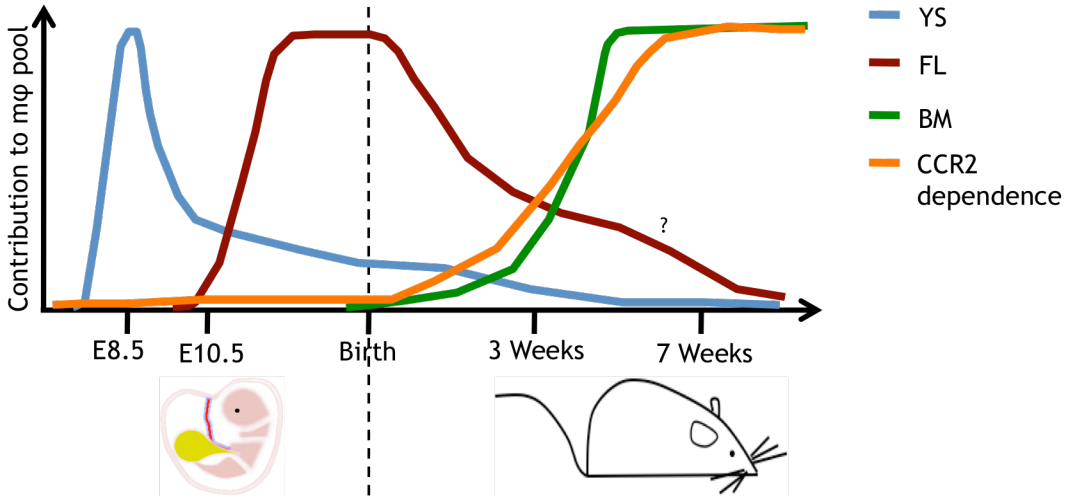

Figure 6.1. Development of the intestinal mϕ pool in mice. In early embryonic life (E8.5), yolk sac (YS) generates mϕ precursors before being superadded by the foetal liver (FL) around E10.5. Production of bone marrow (BM) monocytes begins becoming the exclusive source of monocytes around 3 weeks of age.

References

Abraham, C., and Medzhitov, R. (2011). Interactions between the host innate immune system and microbes in inflammatory bowel disease. Gastroenterology *140*, 1729-1737.

Abrams, G.D., Bauer, H., and Sprinz, H. (1963). Influence of the normal flora on mucosal morphology and cellular renewal in the ileum. A comparison of germ-free and conventional mice. Lab Invest *12*, 355-364.

Abreu, M.T. (2010). Toll-like receptor signalling in the intestinal epithelium: how bacterial recognition shapes intestinal function. Nat Rev Immunol *10*, 131-144.

Abt, M.C., Osborne, L.C., Monticelli, L.A., Doering, T.A., Alenghat, T., Sonnenberg, G.F., Paley, M.A., Antenus, M., Williams, K.L., Erikson, J., *et al*. (2012). Commensal bacteria calibrate the activation threshold of innate antiviral immunity. Immunity *37*, 158-170.

Ancuta, P., Rao, R., Moses, A., Mehle, A., Shaw, S.K., Luscinskas, F.W., and Gabuzda, D. (2003). Fractalkine preferentially mediates arrest and migration of CD16+ monocytes. J Exp Med *197*, 1701-1707.

Anderson, K.L., Smith, K.A., Conners, K., McKercher, S.R., Maki, R.A., and Torbett, B.E. (1998). Myeloid development is selectively disrupted in PU.1 null mice. Blood *91*, 3702-3710.

Andre, F., Cabioglu, N., Assi, H., Sabourin, J.C., Delaloge, S., Sahin, A., Broglio, K., Spano, J.P., Combadiere, C., Bucana, C., *et al*. (2006). Expression of chemokine receptors predicts the site of metastatic relapse in patients with axillary node positive primary breast cancer. Ann Oncol *17*, 945-951.

Andrzejewski, M.G., Koelsch, A., Kogel, T., Dreymueller, D., Schwarz, N., and Ludwig, A. (2010). Distinct role of the intracellular C-terminus for

subcellular expression, shedding and function of the murine transmembrane chemokine CX3CL1. Biochem Biophys Res Commun *395*, 178-184.

Anthony, R.M., Rutitzky, L.I., Urban, J.F., Jr., Stadecker, M.J., and Gause, W.C. (2007). Protective immune mechanisms in helminth infection. Nat Rev Immunol *7*, 975-987.

Artis, D. (2008). Epithelial-cell recognition of commensal bacteria and maintenance of immune homeostasis in the gut. Nat Rev Immunol *8*, 411-420.

Aspinall, A.I., Curbishley, S.M., Lalor, P.F., Weston, C.J., Liaskou, E., Adams, R.M., Holt, A.P., and Adams, D.H. (2010). CX(3)CR1 and vascular adhesion protein-1-dependent recruitment of CD16(+) monocytes across human liver sinusoidal endothelium. Hepatology *51*, 2030-2039.

Atarashi, K., Nishimura, J., Shima, T., Umesaki, Y., Yamamoto, M., Onoue, M., Yagita, H., Ishii, N., Evans, R., Honda, K., and Takeda, K. (2008). ATP drives lamina propria T(H)17 cell differentiation. Nature *455*, 808-812.

Atarashi, K., Tanoue, T., Oshima, K., Suda, W., Nagano, Y., Nishikawa, H., Fukuda, S., Saito, T., Narushima, S., Hase, K., *et al.* (2013). Treg induction by a rationally selected mixture of Clostridia strains from the human microbiota. Nature *500*, 232-236.

Atarashi, K., Tanoue, T., Shima, T., Imaoka, A., Kuwahara, T., Momose, Y., Cheng, G., Yamasaki, S., Saito, T., Ohba, Y., *et al.* (2011). Induction of colonic regulatory T cells by indigenous Clostridium species. Science *331*, 337-341.

Auffray, C., Fogg, D., Garfa, M., Elain, G., Join-Lambert, O., Kayal, S., Sarnacki, S., Cumano, A., Lauvau, G., and Geissmann, F. (2007). Monitoring of blood vessels and tissues by a population of monocytes with patrolling behavior. Science *317*, 666-670.

Auffray, C., Fogg, D.K., Narni-Mancinelli, E., Senechal, B., Trouillet, C., Saederup, N., Leemput, J., Bigot, K., Campisi, L., Abitbol, M., *et al.* (2009).

CX3CR1+ CD115+ CD135+ common macrophage/DC precursors and the role of CX3CR1 in their response to inflammation. J Exp Med *206*, 595-606.

Bachem, A., Hartung, E., Guttler, S., Mora, A., Zhou, X., Hegemann, A., Plantinga, M., Mazzini, E., Stoitzner, P., Gurka, S., *et al.* (2012). Expression of XCR1 Characterizes the Batf3-Dependent Lineage of Dendritic Cells Capable of Antigen Cross-Presentation. Front Immunol *3*, 214.

Bailey, M., Clarke, C.J., Wilson, A.D., Williams, N.A., and Stokes, C.R. (1992). Depressed potential for interleukin-2 production following early weaning of piglets. Vet Immunol Immunopathol *34*, 197-207.

Bailey, M., and Haverson, K. (2006). The postnatal development of the mucosal immune system and mucosal tolerance in domestic animals. Vet Res *37*, 443-453.

Bailey, M., Haverson, K., Inman, C., Harris, C., Jones, P., Corfield, G., Miller, B., and Stokes, C. (2005). The development of the mucosal immune system pre- and post-weaning: balancing regulatory and effector function. Proc Nutr Soc *64*, 451-457.

Bain, C.C., and Mowat, A.M. (2011). Intestinal macrophages - specialised adaptation to a unique environment. Eur J Immunol *41*, 2494-2498.

Bain, C.C., Scott, C.L., Uronen-Hansson, H., Gudjonsson, S., Jansson, O., Grip, O., Guilliams, M., Malissen, B., Agace, W.W., and Mowat, A.M. (2013). Resident and pro-inflammatory macrophages in the colon represent alternative context-dependent fates of the same Ly6C(hi) monocyte precursors. Mucosal Immunol *6*, 498-510.

Banchereau, J., and Steinman, R.M. (1998). Dendritic cells and the control of immunity. Nature *392*, 245-252.

Barnich, N., and Darfeuille-Michaud, A. (2007). Adherent-invasive Escherichia coli and Crohn's disease. Curr Opin Gastroenterol *23*, 16-20.

Bartelmez, S.H., Bradley, T.R., Bertoncello, I., Mochizuki, D.Y., Tushinski, R.J., Stanley, E.R., Hapel, A.J., Young, I.G., Kriegler, A.B., and Hodgson, G.S. (1989). Interleukin 1 plus interleukin 3 plus colony-stimulating factor 1 are essential for clonal proliferation of primitive myeloid bone marrow cells. Exp Hematol *17*, 240-245.

Bauer, H., Horowitz, R.E., Levenson, S.M., and Popper, H. (1963). The response of the lymphatic tissue to the microbial flora. Studies on germfree mice. Am J Pathol *42*, 471-483.

Bazan, J.F., Bacon, K.B., Hardiman, G., Wang, W., Soo, K., Rossi, D., Greaves, D.R., Zlotnik, A., and Schall, T.J. (1997). A new class of membrane-bound chemokine with a CX3C motif. Nature *385*, 640-644.

Benveniste, J., Lespinats, G., Adam, C., and Salomon, J.C. (1971). Immunoglobulins in intact, immunized, and contaminated axenic mice: study of serum IgA. J Immunol *107*, 1647-1655.

Blaschke, S., Koziolek, M., Schwarz, A., Benohr, P., Middel, P., Schwarz, G., Hummel, K.M., and Muller, G.A. (2003). Proinflammatory role of fractalkine (CX3CL1) in rheumatoid arthritis. J Rheumatol *30*, 1918-1927.

Bogunovic, M., Ginhoux, F., Helft, J., Shang, L., Hashimoto, D., Greter, M., Liu, K., Jakubzick, C., Ingersoll, M.A., Leboeuf, M., *et al.* (2009). Origin of the lamina propria dendritic cell network. Immunity *31*, 513-525.

Boring, L., Gosling, J., Chensue, S.W., Kunkel, S.L., Farese, R.V., Jr., Broxmeyer, H.E., and Charo, I.F. (1997). Impaired monocyte migration and reduced type 1 (Th1) cytokine responses in C-C chemokine receptor 2 knockout mice. J Clin Invest *100*, 2552-2561.

Bouskra, D., Brezillon, C., Berard, M., Werts, C., Varona, R., Boneca, I.G., and Eberl, G. (2008). Lymphoid tissue genesis induced by commensals through NOD1 regulates intestinal homeostasis. Nature *456*, 507-510.

Brand, S., Hofbauer, K., Dambacher, J., Schnitzler, F., Staudinger, T., Pfennig, S., Seiderer, J., Tillack, C., Konrad, A., Goke, B., *et al*. (2006). Increased expression of the chemokine fractalkine in Crohn's disease and association of the fractalkine receptor T280M polymorphism with a fibrostenosing disease Phenotype. Am J Gastroenterol *101*, 99-106.

Brasier, A.R. (2006). The NF-kappaB regulatory network. Cardiovasc Toxicol *6*, 111-130.

Bryant, C.E., and Monie, T.P. (2012). Mice, men and the relatives: cross-species studies underpin innate immunity. Open Biol *2*, 120015.

Butcher, E.C., and Picker, L.J. (1996). Lymphocyte homing and homeostasis. Science *272*, 60-66.

Cario, E. (2010). Toll-like receptors in inflammatory bowel diseases: a decade later. Inflamm Bowel Dis *16*, 1583-1597.

Cecchini, M.G., Dominguez, M.G., Mocci, S., Wetterwald, A., Felix, R., Fleisch, H., Chisholm, O., Hofstetter, W., Pollard, J.W., and Stanley, E.R. (1994). Role of colony stimulating factor-1 in the establishment and regulation of tissue macrophages during postnatal development of the mouse. Development *120*, 1357-1372.

Cerovic, V., Houston, S.A., Scott, C.L., Aumeunier, A., Yrlid, U., Mowat, A.M., and Milling, S.W. (2013). Intestinal CD103(-) dendritic cells migrate in lymph and prime effector T cells. Mucosal Immunol *6*, 104-113.

Cerutti, A., and Rescigno, M. (2008). The biology of intestinal immunoglobulin A responses. Immunity *28*, 740-750.

Chappert, P., Bouladoux, N., Naik, S., and Schwartz, R.H. (2013). Specific gut commensal flora locally alters T cell tuning to endogenous ligands. Immunity *38*, 1198-1210.

Chiodini, R.J. (1989). Crohn's disease and the mycobacterioses: a review and comparison of two disease entities. Clin Microbiol Rev *2*, 90-117.

Chorro, L., Sarde, A., Li, M., Woollard, K.J., Chambon, P., Malissen, B., Kissenpfennig, A., Barbaroux, J.B., Groves, R., and Geissmann, F. (2009). Langerhans cell (LC) proliferation mediates neonatal development, homeostasis, and inflammation-associated expansion of the epidermal LC network. J Exp Med *206*, 3089-3100.

Clevers, H.C., and Bevins, C.L. (2013). Paneth cells: maestros of the small intestinal crypts. Annu Rev Physiol *75*, 289-311.

Cope, E.M., and Dilly, S.A. (1990). Kupffer cell numbers during human development. Clin Exp Immunol *81*, 485-488.

Cummings, J.H., Macfarlane, G.T., and Macfarlane, S. (2003). Intestinal bacteria and ulcerative colitis. Curr Issues Intest Microbiol *4*, 9-20.

Cummins, A.G., and Thompson, F.M. (2002). Effect of breast milk and weaning on epithelial growth of the small intestine in humans. Gut *51*, 748-754.

D'Haese, J.G., Demir, I.E., Friess, H., and Ceyhan, G.O. (2010). Fractalkine/CX3CR1: why a single chemokine-receptor duo bears a major and unique therapeutic potential. Expert Opin Ther Targets *14*, 207-219.

D'Haese, J.G., Friess, H., and Ceyhan, G.O. (2012). Therapeutic potential of the chemokine-receptor duo fractalkine/CX3CR1: an update. Expert Opin Ther Targets *16*, 613-618.

Dagkalis, A., Wallace, C., Hing, B., Liversidge, J., and Crane, I.J. (2009). CX3CR1-deficiency is associated with increased severity of disease in experimental autoimmune uveitis. Immunology *128*, 25-33.

Dahan, S., Roth-Walter, F., Arnaboldi, P., Agarwal, S., and Mayer, L. (2007). Epithelia: lymphocyte interactions in the gut. Immunol Rev *215*, 243-253.

Dasari, P., Zola, H., and Nicholson, I.C. (2011). Expression of Toll-like receptors by neonatal leukocytes. Pediatr Allergy Immunol *22*, 221-228.

De Calisto, J., Villablanca, E.J., and Mora, J.R. (2012). FcgammaRI (CD64): an identity card for intestinal macrophages. Eur J Immunol *42*, 3136-3140.

Denning, T.L., Norris, B.A., Medina-Contreras, O., Manicassamy, S., Geem, D., Madan, R., Karp, C.L., and Pulendran, B. (2011). Functional specializations of intestinal dendritic cell and macrophage subsets that control Th17 and regulatory T cell responses are dependent on the T cell/APC ratio, source of mouse strain, and regional localization. J Immunol *187*, 733-747.

Durkan, A.M., Alexander, R.T., Liu, G.Y., Rui, M., Femia, G., and Robinson, L.A. (2007). Expression and targeting of CX3CL1 (fractalkine) in renal tubular epithelial cells. J Am Soc Nephrol *18*, 74-83.

Eberl, G., and Lochner, M. (2009). The development of intestinal lymphoid tissues at the interface of self and microbiota. Mucosal Immunol *2*, 478-485.

Elsheikh, W., Flannigan, K.L., McKnight, W., Ferraz, J.G., and Wallace, J.L. (2012). Dextran sulfate sodium induces pan-gastroenteritis in rodents: implications for studies of colitis. J Physiol Pharmacol *63*, 463-469.

Elson, C.O., Cong, Y., McCracken, V.J., Dimmitt, R.A., Lorenz, R.G., and Weaver, C.T. (2005). Experimental models of inflammatory bowel disease reveal innate, adaptive, and regulatory mechanisms of host dialogue with the microbiota. Immunol Rev *206*, 260-276.

Engberg, N., Kahn, M., Petersen, D.R., Hansson, M., and Serup, P. (2010). Retinoic acid synthesis promotes development of neural progenitors from mouse embryonic stem cells by suppressing endogenous, Wnt-dependent nodal signaling. Stem Cells *28*, 1498-1509.

Engel, D.R., Maurer, J., Tittel, A.P., Weisheit, C., Cavlar, T., Schumak, B., Limmer, A., van Rooijen, N., Trautwein, C., Tacke, F., and Kurts, C. (2008). CCR2 mediates homeostatic and inflammatory release of Gr1(high) monocytes from the bone marrow, but is dispensable for bladder infiltration in bacterial urinary tract infection. J Immunol *181*, 5579-5586.

Ewaschuk, J.B., Diaz, H., Meddings, L., Diederichs, B., Dmytrash, A., Backer, J., Looijer-van Langen, M., and Madsen, K.L. (2008). Secreted bioactive factors from Bifidobacterium infantis enhance epithelial cell barrier function. Am J Physiol Gastrointest Liver Physiol *295*, G1025-1034.

Fagundes, C.T., Souza, D.G., Nicoli, J.R., and Teixeira, M.M. (2011). Control of host inflammatory responsiveness by indigenous microbiota reveals an adaptive component of the innate immune system. Microbes Infect *13*, 1121-1132.

Farache, J., Koren, I., Milo, I., Gurevich, I., Kim, K.W., Zigmond, E., Furtado, G.C., Lira, S.A., and Shakhar, G. (2013). Luminal bacteria recruit CD103+ dendritic cells into the intestinal epithelium to sample bacterial antigens for presentation. Immunity *38*, 581-595.

Feterowski, C., Mack, M., Weighardt, H., Bartsch, B., Kaiser-Moore, S., and Holzmann, B. (2004). CC chemokine receptor 2 regulates leukocyte recruitment and IL-10 production during acute polymicrobial sepsis. Eur J Immunol *34*, 3664-3673.

Fong, A.M., Robinson, L.A., Steeber, D.A., Tedder, T.F., Yoshie, O., Imai, T., and Patel, D.D. (1998). Fractalkine and CX3CR1 mediate a novel mechanism of leukocyte capture, firm adhesion, and activation under physiologic flow. J Exp Med *188*, 1413-1419.

Franchi, L., Warner, N., Viani, K., and Nunez, G. (2009). Function of Nod-like receptors in microbial recognition and host defense. Immunol Rev *227*, 106-128.

Frank, D.N., St Amand, A.L., Feldman, R.A., Boedeker, E.C., Harpaz, N., and Pace, N.R. (2007). Molecular-phylogenetic characterization of microbial community imbalances in human inflammatory bowel diseases. Proc Natl Acad Sci U S A *104*, 13780-13785.

Fujimoto, K., Karuppuchamy, T., Takemura, N., Shimohigoshi, M., Machida, T., Haseda, Y., Aoshi, T., Ishii, K.J., Akira, S., and Uematsu, S. (2012). A new subset of CD103+CD8alpha+ dendritic cells in the small intestine expresses TLR3, TLR7, and TLR9 and induces Th1 response and CTL activity. J Immunol *186*, 6287-6295.

Gaboriau-Routhiau, V., Rakotobe, S., Lecuyer, E., Mulder, I., Lan, A., Bridonneau, C., Rochet, V., Pisi, A., De Paepe, M., Brandi, G., *et al*. (2009). The key role of segmented filamentous bacteria in the coordinated maturation of gut helper T cell responses. Immunity *31*, 677-689.

Ganal, S.C., Sanos, S.L., Kallfass, C., Oberle, K., Johner, C., Kirschning, C., Lienenklaus, S., Weiss, S., Staeheli, P., Aichele, P., and Diefenbach, A. (2012). Priming of natural killer cells by nonmucosal mononuclear phagocytes requires instructive signals from commensal microbiota. Immunity *37*, 171-186.

Ganz, T. (2003). Defensins: antimicrobial peptides of innate immunity. Nat Rev Immunol *3*, 710-720.

Garton, K.J., Gough, P.J., Blobel, C.P., Murphy, G., Greaves, D.R., Dempsey, P.J., and Raines, E.W. (2001). Tumor necrosis factor-alpha-converting enzyme (ADAM17) mediates the cleavage and shedding of fractalkine (CX3CL1). J Biol Chem *276*, 37993-38001.

Gay, N.J., Gangloff, M., and O'Neill, L.A. (2011). What the Myddosome structure tells us about the initiation of innate immunity. Trends Immunol *32*, 104-109.

Geissmann, F., Jung, S., and Littman, D.R. (2003). Blood monocytes consist of two principal subsets with distinct migratory properties. Immunity *19*, 71-82.

Geissmann, F., Manz, M.G., Jung, S., Sieweke, M.H., Merad, M., and Ley, K. (2010). Development of monocytes, macrophages, and dendritic cells. Science *327*, 656-661.

Gekas, C., Dieterlen-Lievre, F., Orkin, S.H., and Mikkola, H.K. (2005). The placenta is a niche for hematopoietic stem cells. Dev Cell *8*, 365-375.

Gille, C., Spring, B., Tewes, L., Poets, C.F., and Orlikowsky, T. (2006). A new method to quantify phagocytosis and intracellular degradation using green fluorescent protein-labeled Escherichia coli: comparison of cord blood macrophages and peripheral blood macrophages of healthy adults. Cytometry A *69*, 152-154.

Ginhoux, F., Greter, M., Leboeuf, M., Nandi, S., See, P., Gokhan, S., Mehler, M.F., Conway, S.J., Ng, L.G., Stanley, E.R., *et al.* (2010). Fate mapping analysis reveals that adult microglia derive from primitive macrophages. Science *330*, 841-845.

Gordon, S. (2007). The macrophage: past, present and future. Eur J Immunol *37 Suppl 1*, S9-17.

Gordon, S., and Taylor, P.R. (2005). Monocyte and macrophage heterogeneity. Nat Rev Immunol *5*, 953-964.

Gouwy, M., Struyf, S., Leutenez, L., Portner, N., Sozzani, S., and Van Damme, J. (2013). Chemokines and other GPCR ligands synergize in receptor-mediated migration of monocyte-derived immature and mature dendritic cells. Immunobiology.

Grainger, J.R., Wohlfert, E.A., Fuss, I.J., Bouladoux, N., Askenase, M.H., Legrand, F., Koo, L.Y., Brenchley, J.M., Fraser, I.D., and Belkaid, Y. (2013). Inflammatory monocytes regulate pathologic responses to commensals during acute gastrointestinal infection. Nat Med *19*, 713-721.

Greter, M., Lelios, I., Pelczar, P., Hoeffel, G., Price, J., Leboeuf, M., Kundig, T.M., Frei, K., Ginhoux, F., Merad, M., and Becher, B. (2012). Stroma-derived interleukin-34 controls the development and maintenance of langerhans cells and the maintenance of microglia. Immunity *37*, 1050-1060.

Guarner, F., and Malagelada, J.R. (2003). Role of bacteria in experimental colitis. Best Pract Res Clin Gastroenterol *17*, 793-804.

Gujral, N., Freeman, H.J., and Thomson, A.B. (2012). Celiac disease: prevalence, diagnosis, pathogenesis and treatment. World J Gastroenterol *18*, 6036-6059.

Hadis, U., Wahl, B., Schulz, O., Hardtke-Wolenski, M., Schippers, A., Wagner, N., Muller, W., Sparwasser, T., Forster, R., and Pabst, O. (2011). Intestinal tolerance requires gut homing and expansion of FoxP3+ regulatory T cells in the lamina propria. Immunity *34*, 237-246.

Hamann, I., Unterwalder, N., Cardona, A.E., Meisel, C., Zipp, F., Ransohoff, R.M., and Infante-Duarte, C. (2011). Analyses of phenotypic and functional characteristics of CX3CR1-expressing natural killer cells. Immunology *133*, 62-73.

Hammer, G.E., and Ma, A. (2013). Molecular control of steady-state dendritic cell maturation and immune homeostasis. Annu Rev Immunol *31*, 743-791.

Hans, W., Scholmerich, J., Gross, V., and Falk, W. (2000). The role of the resident intestinal flora in acute and chronic dextran sulfate sodium-induced colitis in mice. Eur J Gastroenterol Hepatol *12*, 267-273.

Hart, S.P., Dransfield, I., and Rossi, A.G. (2008). Phagocytosis of apoptotic cells. Methods *44*, 280-285.

Haverson, K., Rehakova, Z., Sinkora, J., Sver, L., and Bailey, M. (2007). Immune development in jejunal mucosa after colonization with selected commensal gut bacteria: a study in germ-free pigs. Vet Immunol Immunopathol *119*, 243-253.

Henson, P.M., and Bratton, D.L. (2013). Antiinflammatory effects of apoptotic cells. J Clin Invest *123*, 2773-2774.

Hettinger, J., Richards, D.M., Hansson, J., Barra, M.M., Joschko, A.C., Krijgsveld, J., and Feuerer, M. (2013). Origin of monocytes and macrophages in a committed progenitor. Nat Immunol *14*, 821-830.

Hoeffel, G., Wang, Y., Greter, M., See, P., Teo, P., Malleret, B., Leboeuf, M., Low, D., Oller, G., Almeida, F., *et al.* (2012). Adult Langerhans cells derive predominantly from embryonic fetal liver monocytes with a minor contribution of yolk sac-derived macrophages. J Exp Med *209*, 1167-1181.

Hooper, L.V., and Gordon, J.I. (2001). Commensal host-bacterial relationships in the gut. Science *292*, 1115-1118.

Hopkinson-Woolley, J., Hughes, D., Gordon, S., and Martin, P. (1994). Macrophage recruitment during limb development and wound healing in the embryonic and foetal mouse. J Cell Sci *107 (Pt 5)*, 1159-1167.

Huber, T.L., Kouskoff, V., Fehling, H.J., Palis, J., and Keller, G. (2004). Haemangioblast commitment is initiated in the primitive streak of the mouse embryo. Nature *432*, 625-630.

Hume, D.A., Monkley, S.J., and Wainwright, B.J. (1995). Detection of c-fms protooncogene in early mouse embryos by whole mount in situ hybridization indicates roles for macrophages in tissue remodelling. Br J Haematol *90*, 939-942.

Hundhausen, C., Misztela, D., Berkhout, T.A., Broadway, N., Saftig, P., Reiss, K., Hartmann, D., Fahrenholz, F., Postina, R., Matthews, V., *et al.* (2003). The disintegrin-like metalloproteinase ADAM10 is involved in constitutive cleavage of CX3CL1 (fractalkine) and regulates CX3CL1-mediated cell-cell adhesion. Blood *102*, 1186-1195.

Hwang, Y.Y., and McKenzie, A.N. (2013). Innate lymphoid cells in immunity and disease. Adv Exp Med Biol *785*, 9-26.

Imai, T., Hieshima, K., Haskell, C., Baba, M., Nagira, M., Nishimura, M., Kakizaki, M., Takagi, S., Nomiyama, H., Schall, T.J., and Yoshie, O. (1997). Identification and molecular characterization of fractalkine receptor CX3CR1, which mediates both leukocyte migration and adhesion. Cell *91*, 521-530.

Imaizumi, T., Yoshida, H., and Satoh, K. (2004). Regulation of CX3CL1/fractalkine expression in endothelial cells. J Atheroscler Thromb *11*, 15-21.

Inman, C.F., Haverson, K., Konstantinov, S.R., Jones, P.H., Harris, C., Smidt, H., Miller, B., Bailey, M., and Stokes, C. (2010a). Rearing environment affects development of the immune system in neonates. Clin Exp Immunol *160*, 431-439.

Inman, C.F., Laycock, G.M., Mitchard, L., Harley, R., Warwick, J., Burt, R., van Diemen, P.M., Stevens, M., and Bailey, M. (2012). Neonatal colonisation expands a specific intestinal antigen-presenting cell subset prior to CD4 T-cell expansion, without altering T-cell repertoire. PLoS One *7*, e33707.

Inman, C.F., Singha, S., Lewis, M., Bradley, B., Stokes, C., and Bailey, M. (2010b). Dendritic cells interact with CD4 T cells in intestinal mucosa. J Leukoc Biol *88*, 571-578.

Ivanov, II, Atarashi, K., Manel, N., Brodie, E.L., Shima, T., Karaoz, U., Wei, D., Goldfarb, K.C., Santee, C.A., Lynch, S.V., *et al.* (2009). Induction of intestinal Th17 cells by segmented filamentous bacteria. Cell *139*, 485-498.

Ivanov, II, Frutos Rde, L., Manel, N., Yoshinaga, K., Rifkin, D.B., Sartor, R.B., Finlay, B.B., and Littman, D.R. (2008). Specific microbiota direct the differentiation of IL-17-producing T-helper cells in the mucosa of the small intestine. Cell Host Microbe *4*, 337-349.

Ivanov, II, and Honda, K. (2012). Intestinal commensal microbes as immune modulators. Cell Host Microbe *12*, 496-508.

Jacquelin, S., Licata, F., Dorgham, K., Hermand, P., Poupel, L., Guyon, E., Deterre, P., Hume, D.A., Combadiere, C., and Boissonnas, A. (2013). CX3CR1 reduces Ly6Chigh-monocyte motility within and release from the bone marrow after chemotherapy in mice. Blood *122*, 674-683.

Jakubzick, C., Gautier, E.L., Gibbings, S.L., Sojka, D.K., Schlitzer, A., Johnson, T.E., Ivanov, S., Duan, Q., Bala, S., Condon, T., *et al*. (2013). Minimal differentiation of classical monocytes as they survey steady-state tissues and transport antigen to lymph nodes. Immunity *39*, 599-610.

Jiang, H.Q., Thurnheer, M.C., Zuercher, A.W., Boiko, N.V., Bos, N.A., and Cebra, J.J. (2004). Interactions of commensal gut microbes with subsets of B- and T-cells in the murine host. Vaccine *22*, 805-811.

Johansson-Lindbom, B., Svensson, M., Pabst, O., Palmqvist, C., Marquez, G., Forster, R., and Agace, W.W. (2005). Functional specialization of gut CD103+ dendritic cells in the regulation of tissue-selective T cell homing. J Exp Med *202*, 1063-1073.

Johnson, Z., Proudfoot, A.E., and Handel, T.M. (2005). Interaction of chemokines and glycosaminoglycans: a new twist in the regulation of chemokine function with opportunities for therapeutic intervention. Cytokine Growth Factor Rev *16*, 625-636.

Jung, C., Hugot, J.P., and Barreau, F. (2010). Peyer's Patches: The Immune Sensors of the Intestine. Int J Inflam *2010*, 823710.

Jung, S., Aliberti, J., Graemmel, P., Sunshine, M.J., Kreutzberg, G.W., Sher, A., and Littman, D.R. (2000). Analysis of fractalkine receptor CX(3)CR1 function by targeted deletion and green fluorescent protein reporter gene insertion. Mol Cell Biol *20*, 4106-4114.

Kasama, T., Wakabayashi, K., Sato, M., Takahashi, R., and Isozaki, T. (2010). Relevance of the CX3CL1/fractalkine-CX3CR1 pathway in vasculitis and vasculopathy. Transl Res *155*, 20-26.

Kaser, A., Zeissig, S., and Blumberg, R.S. (2010). Inflammatory bowel disease. Annu Rev Immunol *28*, 573-621.

Kayama, H., Ueda, Y., Sawa, Y., Jeon, S.G., Ma, J.S., Okumura, R., Kubo, A., Ishii, M., Okazaki, T., Murakami, M., *et al*. (2012). Intestinal CX3C chemokine receptor 1high (CX3CR1high) myeloid cells prevent T-cell-dependent colitis. Proc Natl Acad Sci U S A.

Kim, K.W.V.-E., A. Zigmond, E. Farache, J. Shezen, E. Shakhar, G. Ludwig, A. Lira, S. A. Jung, S. (2011). In vivo structure/function and expression analysis of the CX3C chemokine fractalkine. Blood *118*, e156-167.

Kim, T.S., Lim, H.K., Lee, J.Y., Kim, D.J., Park, S., Lee, C., and Lee, C.U. (2008). Changes in the levels of plasma soluble fractalkine in patients with mild cognitive impairment and Alzheimer's disease. Neurosci Lett *436*, 196-200.

Kollmann, T.R., Levy, O., Montgomery, R.R., and Goriely, S. (2012). Innate immune function by Toll-like receptors: distinct responses in newborns and the elderly. Immunity *37*, 771-783.

Kosiewicz, M.M., Zirnheld, A.L., and Alard, P. (2011). Gut microbiota, immunity, and disease: a complex relationship. Front Microbiol *2*, 180.

Kostadinova, F.I., Baba, T., Ishida, Y., Kondo, T., Popivanova, B.K., and Mukaida, N. (2010). Crucial involvement of the CX3CR1-CX3CL1 axis in dextran sulfate sodium-mediated acute colitis in mice. J Leukoc Biol *88*, 133-143.

Kurihara, T., Warr, G., Loy, J., and Bravo, R. (1997). Defects in macrophage recruitment and host defense in mice lacking the CCR2 chemokine receptor. J Exp Med *186*, 1757-1762.

Kusser, K.L., and Randall, T.D. (2003). Simultaneous detection of EGFP and cell surface markers by fluorescence microscopy in lymphoid tissues. J Histochem Cytochem *51*, 5-14.

Kuwahara, T., Ogura, Y., Oshima, K., Kurokawa, K., Ooka, T., Hirakawa, H., Itoh, T., Nakayama-Imaohji, H., Ichimura, M., Itoh, K., *et al*. (2011). The lifestyle of the segmented filamentous bacterium: a non-culturable gut-associated immunostimulating microbe inferred by whole-genome sequencing. DNA Res *18*, 291-303.

Kuziel, W.A., Morgan, S.J., Dawson, T.C., Griffin, S., Smithies, O., Ley, K., and Maeda, N. (1997). Severe reduction in leukocyte adhesion and monocyte extravasation in mice deficient in CC chemokine receptor 2. Proc Natl Acad Sci U S A *94*, 12053-12058.

Kvarnhammar, A.M., and Cardell, L.O. (2012). Pattern-recognition receptors in human eosinophils. Immunology *136*, 11-20.

Lamouse-Smith, E.S., Tzeng, A., and Starnbach, M.N. (2011). The intestinal flora is required to support antibody responses to systemic immunization in infant and germ free mice. PLoS One *6*, e27662.

Landsman, L., Bar-On, L., Zernecke, A., Kim, K.W., Krauthgamer, R., Shagdarsuren, E., Lira, S.A., Weissman, I.L., Weber, C., and Jung, S. (2009). CX3CR1 is required for monocyte homeostasis and atherogenesis by promoting cell survival. Blood *113*, 963-972.

Landsman, L., Varol, C., and Jung, S. (2007). Distinct differentiation potential of blood monocyte subsets in the lung. J Immunol *178*, 2000-2007.

Langhendries, J.P. (2005). Early colonisation of the intestine: why it matters. Ital. J. Pediatr *31*, 360-369.

Le, Y., Zhou, Y., Iribarren, P., and Wang, J. (2004). Chemokines and chemokine receptors: their manifold roles in homeostasis and disease. Cell Mol Immunol *1*, 95-104.

Lebre, M.C., Vergunst, C.E., Choi, I.Y., Aarrass, S., Oliveira, A.S., Wyant, T., Horuk, R., Reedquist, K.A., and Tak, P.P. (2011). Why CCR2 and CCR5 blockade failed and why CCR1 blockade might still be effective in the treatment of rheumatoid arthritis. PLoS One *6*, e21772.

Lesnik, P., Haskell, C.A., and Charo, I.F. (2003). Decreased atherosclerosis in CX3CR1-/- mice reveals a role for fractalkine in atherogenesis. J Clin Invest *111*, 333-340.

Lewis, M.C., Inman, C.F., Patel, D., Schmidt, B., Mulder, I., Miller, B., Gill, B.P., Pluske, J., Kelly, D., Stokes, C.R., and Bailey, M. (2012). Direct experimental evidence that early-life farm environment influences regulation of immune responses. Pediatr Allergy Immunol *23*, 265-269.

Ley, K., Laudanna, C., Cybulsky, M.I., and Nourshargh, S. (2007). Getting to the site of inflammation: the leukocyte adhesion cascade updated. Nat Rev Immunol *7*, 678-689.

Lichanska, A.M., Browne, C.M., Henkel, G.W., Murphy, K.M., Ostrowski, M.C., McKercher, S.R., Maki, R.A., and Hume, D.A. (1999). Differentiation of the mononuclear phagocyte system during mouse embryogenesis: the role of transcription factor PU.1. Blood *94*, 127-138.

Lichanska, A.M., and Hume, D.A. (2000). Origins and functions of phagocytes in the embryo. Exp Hematol *28*, 601-611.

Lotz, M., Gutle, D., Walther, S., Menard, S., Bogdan, C., and Hornef, M.W. (2006). Postnatal acquisition of endotoxin tolerance in intestinal epithelial cells. J Exp Med *203*, 973-984.

MacDermott, R.P., Sanderson, I.R., and Reinecker, H.C. (1998). The central role of chemokines (chemotactic cytokines) in the immunopathogenesis of ulcerative colitis and Crohn's disease. Inflamm Bowel Dis *4*, 54-67.

MacDonald, T.T., Monteleone, I., Fantini, M.C., and Monteleone, G. (2011). Regulation of homeostasis and inflammation in the intestine. Gastroenterology *140*, 1768-1775.

Macpherson, A.J., and Harris, N.L. (2004). Interactions between commensal intestinal bacteria and the immune system. Nat Rev Immunol *4*, 478-485.

Madan, J.C., Salari, R.C., Saxena, D., Davidson, L., O'Toole, G.A., Moore, J.H., Sogin, M.L., Foster, J.A., Edwards, W.H., Palumbo, P., and Hibberd, P.L. (2012). Gut microbial colonisation in premature neonates predicts neonatal sepsis. Arch Dis Child Fetal Neonatal Ed *97*, F456-462.

Maheshwari, A., Kelly, D.R., Nicola, T., Ambalavanan, N., Jain, S.K., Murphy-Ullrich, J., Athar, M., Shimamura, M., Bhandari, V., Aprahamian, C., *et al.* (2011). TGF-beta2 suppresses macrophage cytokine production and mucosal inflammatory responses in the developing intestine. Gastroenterology *140*, 242-253.

Maldonado-Contreras, A.L., and McCormick, B.A. (2011). Intestinal epithelial cells and their role in innate mucosal immunity. Cell Tissue Res *343*, 5-12.

Maloy, K.J., and Powrie, F. (2011). Intestinal homeostasis and its breakdown in inflammatory bowel disease. Nature *474*, 298-306.

Mantovani, A., Biswas, S.K., Galdiero, M.R., Sica, A., and Locati, M. (2013). Macrophage plasticity and polarization in tissue repair and remodelling. J Pathol *229*, 176-185.

Manzano, M., Abadia-Molina, A.C., Garcia-Olivares, E., Gil, A., and Rueda, R. (2002). Absolute counts and distribution of lymphocyte subsets in small intestine of BALB/c mice change during weaning. J Nutr *132*, 2757-2762.

Mazmanian, S.K., Round, J.L., and Kasper, D.L. (2008). A microbial symbiosis factor prevents intestinal inflammatory disease. Nature *453*, 620-625.

McKenna, H.J., Stocking, K.L., Miller, R.E., Brasel, K., De Smedt, T., Maraskovsky, E., Maliszewski, C.R., Lynch, D.H., Smith, J., Pulendran, B., *et al.* (2000). Mice lacking flt3 ligand have deficient hematopoiesis affecting hematopoietic progenitor cells, dendritic cells, and natural killer cells. Blood *95*, 3489-3497.

Medina-Contreras, O., Geem, D., Laur, O., Williams, I.R., Lira, S.A., Nusrat, A., Parkos, C.A., and Denning, T.L. (2011). CX3CR1 regulates intestinal macrophage homeostasis, bacterial translocation, and colitogenic Th17 responses in mice. J Clin Invest *121*, 4787-4795.

Medzhitov, R., and Janeway, C., Jr. (2000). Innate immunity. N Engl J Med *343*, 338-344.

Meredith, M.M., Liu, K., Darrasse-Jeze, G., Kamphorst, A.O., Schreiber, H.A., Guermonprez, P., Idoyaga, J., Cheong, C., Yao, K.H., Niec, R.E., and Nussenzweig, M.C. (2012). Expression of the zinc finger transcription factor zDC (Zbtb46, Btbd4) defines the classical dendritic cell lineage. J Exp Med *209*, 1153-1165.

Metchnikoff, E. (1989). The Nobel lectures in immunology. The Nobel prize for physiology or medicine, 1908, awarded to Elie Metchnikoff & Paul Ehrlich "in recognition of their work on immunity.". Scand J Immunol *30*, 383-398.

Mionnet, C., Buatois, V., Kanda, A., Milcent, V., Fleury, S., Lair, D., Langelot, M., Lacoeuille, Y., Hessel, E., Coffman, R., *et al.* (2010). CX3CR1 is required for airway inflammation by promoting T helper cell survival and maintenance in inflamed lung. Nat Med *16*, 1305-1312.

Mizutani, N., Sakurai, T., Shibata, T., Uchida, K., Fujita, J., Kawashima, R., Kawamura, Y.I., Toyama-Sorimachi, N., Imai, T., and Dohi, T. (2007). Dose-dependent differential regulation of cytokine secretion from macrophages by fractalkine. J Immunol *179*, 7478-7487.

Molloy, M.J., Bouladoux, N., and Belkaid, Y. (2012). Intestinal microbiota: shaping local and systemic immune responses. Semin Immunol *24*, 58-66.

Morganti, J.M., Nash, K.R., Grimmig, B.A., Ranjit, S., Small, B., Bickford, P.C., and Gemma, C. (2012). The soluble isoform of CX3CL1 is necessary for neuroprotection in a mouse model of Parkinson's disease. J Neurosci *32*, 14592-14601.

Mouchemore, K.A., and Pixley, F.J. (2012). CSF-1 signaling in macrophages: pleiotrophy through phosphotyrosine-based signaling pathways. Crit Rev Clin Lab Sci *49*, 49-61.

Mowat, A., Bain, CC. (2010). The curious case of the intestinal eosinophil. Mucosal Immunology *3*, 420-421.

Mowat, A.M. (2003). Anatomical basis of tolerance and immunity to intestinal antigens. Nat Rev Immunol *3*, 331-341.

Muehlhoefer, A., Saubermann, L.J., Gu, X., Luedtke-Heckenkamp, K., Xavier, R., Blumberg, R.S., Podolsky, D.K., MacDermott, R.P., and Reinecker, H.C. (2000). Fractalkine is an epithelial and endothelial cell-derived chemoattractant for intraepithelial lymphocytes in the small intestinal mucosa. J Immunol *164*, 3368-3376.

Mulder, I.E., Schmidt, B., Lewis, M., Delday, M., Stokes, C.R., Bailey, M., Aminov, R.I., Gill, B.P., Pluske, J.R., Mayer, C.D., and Kelly, D. (2011). Restricting microbial exposure in early life negates the immune benefits associated with gut colonization in environments of high microbial diversity. PLoS One *6*, e28279.

Muller, A.M., Medvinsky, A., Strouboulis, J., Grosveld, F., and Dzierzak, E. (1994). Development of hematopoietic stem cell activity in the mouse embryo. Immunity *1*, 291-301.

Murphy, K. (2012). Janeway's Immunobiology, 8th edn (New York: Garland Science, Taylor & Francis Group, LLC).

Naito, M., Umeda, S., Yamamoto, T., Moriyama, H., Umezu, H., Hasegawa, G., Usuda, H., Shultz, L.D., and Takahashi, K. (1996). Development, differentiation, and phenotypic heterogeneity of murine tissue macrophages. J Leukoc Biol *59*, 133-138.

Narni-Mancinelli, E., Soudja, S.M., Crozat, K., Dalod, M., Gounon, P., Geissmann, F., and Lauvau, G. (2011). Inflammatory monocytes and neutrophils are licensed to kill during memory responses in vivo. PLoS Pathog *7*, e1002457.

Natividad, J.M., Petit, V., Huang, X., de Palma, G., Jury, J., Sanz, Y., Philpott, D., Garcia Rodenas, C.L., McCoy, K.D., and Verdu, E.F. (2012). Commensal and probiotic bacteria influence intestinal barrier function and susceptibility to colitis in Nod1-/-; Nod2-/- mice. Inflamm Bowel Dis *18*, 1434-1446.

Niess, J.H. (2010). What are CX3CR1+ mononuclear cells in the intestinal mucosa? Gut Microbes *1*, 396-400.

Niess, J.H., and Adler, G. (2010). Enteric flora expands gut lamina propria CX3CR1+ dendritic cells supporting inflammatory immune responses under normal and inflammatory conditions. J Immunol *184*, 2026-2037.

Niess, J.H., Brand, S., Gu, X., Landsman, L., Jung, S., McCormick, B.A., Vyas, J.M., Boes, M., Ploegh, H.L., Fox, J.G., *et al.* (2005). CX3CR1-mediated dendritic cell access to the intestinal lumen and bacterial clearance. Science *307*, 254-258.

Nishimura, M., Kuboi, Y., Muramoto, K., Kawano, T., and Imai, T. (2009). Chemokines as novel therapeutic targets for inflammatory bowel disease. Ann N Y Acad Sci *1173*, 350-356.

Ochoa-Reparaz, J., Mielcarz, D.W., Wang, Y., Begum-Haque, S., Dasgupta, S., Kasper, D.L., and Kasper, L.H. (2010). A polysaccharide from the human commensal Bacteroides fragilis protects against CNS demyelinating disease. Mucosal Immunol *3*, 487-495.

Oddy, W.H., and Rosales, F. (2010). A systematic review of the importance of milk TGF-beta on immunological outcomes in the infant and young child. Pediatr Allergy Immunol *21*, 47-59.

Oldenburg, M., Kruger, A., Ferstl, R., Kaufmann, A., Nees, G., Sigmund, A., Bathke, B., Lauterbach, H., Suter, M., Dreher, S., *et al.* (2012). TLR13 recognizes bacterial 23S rRNA devoid of erythromycin resistance-forming modification. Science *337*, 1111-1115.

Onai, N., Obata-Onai, A., Schmid, M.A., Ohteki, T., Jarrossay, D., and Manz, M.G. (2007). Identification of clonogenic common Flt3+M-CSFR+ plasmacytoid and conventional dendritic cell progenitors in mouse bone marrow. Nat Immunol *8*, 1207-1216.

Orkin, S.H., and Zon, L.I. (2008). Hematopoiesis: an evolving paradigm for stem cell biology. Cell *132*, 631-644.

Ostman, S., Rask, C., Wold, A.E., Hultkrantz, S., and Telemo, E. (2006). Impaired regulatory T cell function in germ-free mice. Eur J Immunol *36*, 2336-2346.

Owlasiuk, P., Zajkowska, J.M., Pietruczuk, M., Pancewicz, S.A., and Hermanowska-Szpakowicz, T. (2009). [Fractalkine--structure, functions and biological activity]. Pol Merkur Lekarski *26*, 253-257.

Pabst, O., and Mowat, A.M. (2012). Oral tolerance to food protein. Mucosal Immunol *5*, 232-239.

Paidassi, H., Acharya, M., Zhang, A., Mukhopadhyay, S., Kwon, M., Chow, C., Stuart, L.M., Savill, J., and Lacy-Hulbert, A. (2012). Preferential expression

of integrin alphavbeta8 promotes generation of regulatory T cells by mouse CD103+ dendritic cells. Gastroenterology *141*, 1813-1820.

Pan, Y., Lloyd, C., Zhou, H., Dolich, S., Deeds, J., Gonzalo, J.A., Vath, J., Gosselin, M., Ma, J., Dussault, B., *et al.* (1997). Neurotactin, a membrane-anchored chemokine upregulated in brain inflammation. Nature *387*, 611-617.
Paun, A., and Pitha, P.M. (2007). The IRF family, revisited. Biochimie *89*, 744-753.

Pearson, C., Uhlig, H.H., and Powrie, F. (2012). Lymphoid microenvironments and innate lymphoid cells in the gut. Trends Immunol *33*, 289-296.

Pearson, J.P., and Brownlee, I.A. (2010). The interaction of large bowel microflora with the colonic mucus barrier. Int J Inflam *2010*, 321426.

Persson, E.K., Scott, C.L., Mowat, A.M., and Agace, W.W. (2013). Dendritic cell subsets in the intestinal lamina propria: Ontogeny and function. Eur J Immunol.

Pixley, F.J., and Stanley, E.R. (2004). CSF-1 regulation of the wandering macrophage: complexity in action. Trends Cell Biol *14*, 628-638.

Platt, A.M., Bain, C.C., Bordon, Y., Sester, D.P., and Mowat, A.M. (2010). An independent subset of TLR expressing CCR2-dependent macrophages promotes colonic inflammation. J Immunol *184*, 6843-6854.

Platt, A.M., and Mowat, A.M. (2008). Mucosal macrophages and the regulation of immune responses in the intestine. Immunol Lett *119*, 22-31.

Raetz, C.R., and Whitfield, C. (2002). Lipopolysaccharide endotoxins. Annu Rev Biochem *71*, 635-700.

Ramachandran, P., Pellicoro, A., Vernon, M.A., Boulter, L., Aucott, R.L., Ali, A., Hartland, S.N., Snowdon, V.K., Cappon, A., Gordon-Walker, T.T., *et al.* (2012). Differential Ly-6C expression identifies the recruited macrophage

phenotype, which orchestrates the regression of murine liver fibrosis. Proc Natl Acad Sci U S A *109*, E3186-3195.

Rath, H.C., Schultz, M., Freitag, R., Dieleman, L.A., Li, F., Linde, H., Scholmerich, J., and Sartor, R.B. (2001). Different subsets of enteric bacteria induce and perpetuate experimental colitis in rats and mice. Infection and immunity *69*, 2277-2285.

Reading, N.C., and Kasper, D.L. (2011). The starting lineup: key microbial players in intestinal immunity and homeostasis. Front Microbiol *2*, 148.

Reddy, K.V., Yedery, R.D., and Aranha, C. (2004). Antimicrobial peptides: premises and promises. Int J Antimicrob Agents *24*, 536-547.

Rivollier, A., He, J., Kole, A., Valatas, V., and Kelsall, B.L. (2012). Inflammation switches the differentiation program of Ly6Chi monocytes from antiinflammatory macrophages to inflammatory dendritic cells in the colon. J Exp Med *209*, 139-155.

Rollins, B.J., and Pober, J.S. (1991). Interleukin-4 induces the synthesis and secretion of MCP-1/JE by human endothelial cells. Am J Pathol *138*, 1315-1319.

Romagnani, S. (2004). The increased prevalence of allergy and the hygiene hypothesis: missing immune deviation, reduced immune suppression, or both? Immunology *112*, 352-363.

Rosenberg, H.F. (2003). Human neutrophils and TLRs: 2, 4, and plenty more. Blood *102*, 2319.

Rothenberg, M.E., and Hogan, S.P. (2006). The eosinophil. Annu Rev Immunol *24*, 147-174.

Round, J.L., and Mazmanian, S.K. (2009). The gut microbiota shapes intestinal immune responses during health and disease. Nat Rev Immunol *9*, 313-323.

Rowe, J., Macaubas, C., Monger, T.M., Holt, B.J., Harvey, J., Poolman, J.T., Sly, P.D., and Holt, P.G. (2000). Antigen-specific responses to diphtheria-tetanus-acellular pertussis vaccine in human infants are initially Th2 polarized. Infect Immun *68*, 3873-3877.

Russell, S.L., Gold, M.J., Willing, B.P., Thorson, L., McNagny, K.M., and Finlay, B.B. (2013). Perinatal antibiotic treatment affects murine microbiota, immune responses and allergic asthma. Gut Microbes *4*, 158-164.

Ryu, J., Lee, C.W., Hong, K.H., Shin, J.A., Lim, S.H., Park, C.S., Shim, J., Nam, K.B., Choi, K.J., Kim, Y.H., and Han, K.H. (2008). Activation of fractalkine/CX3CR1 by vascular endothelial cells induces angiogenesis through VEGF-A/KDR and reverses hindlimb ischaemia. Cardiovasc Res *78*, 333-340.

Sans, M., Danese, S., de la Motte, C., de Souza, H.S., Rivera-Reyes, B.M., West, G.A., Phillips, M., Katz, J.A., and Fiocchi, C. (2007). Enhanced recruitment of CX3CR1+ T cells by mucosal endothelial cell-derived fractalkine in inflammatory bowel disease. Gastroenterology *132*, 139-153.

Sartor, R.B. (2005). Does Mycobacterium avium subspecies paratuberculosis cause Crohn's disease? Gut *54*, 896-898.

Sartor, R.B. (2008). Microbial influences in inflammatory bowel diseases. Gastroenterology *134*, 577-594.

Satpathy, A.T., Kc, W., Albring, J.C., Edelson, B.T., Kretzer, N.M., Bhattacharya, D., Murphy, T.L., and Murphy, K.M. (2012). Zbtb46 expression distinguishes classical dendritic cells and their committed progenitors from other immune lineages. J Exp Med *209*, 1135-1152.

Savage, D.C., and Dubos, R. (1968). Alterations in the mouse cecum and its flora produced by antibacterial drugs. J Exp Med *128*, 97-110.

Savage, D.C., and McAllister, J.S. (1971). Cecal enlargement and microbial flora in suckling mice given antibacterial drugs. Infect Immun *3*, 342-349.

Schlitzer, A., McGovern, N., Teo, P., Zelante, T., Atarashi, K., Low, D., Ho, A.W., See, P., Shin, A., Wasan, P.S., *et al.* (2013). IRF4 transcription factor-dependent CD11b+ dendritic cells in human and mouse control mucosal IL-17 cytokine responses. Immunity *38*, 970-983.

Schmidt, B., Mulder, I.E., Musk, C.C., Aminov, R.I., Lewis, M., Stokes, C.R., Bailey, M., Prosser, J.I., Gill, B.P., Pluske, J.R., and Kelly, D. (2011). Establishment of normal gut microbiota is compromised under excessive hygiene conditions. PLoS One *6*, e28284.

Schulz, C., Gomez Perdiguero, E., Chorro, L., Szabo-Rogers, H., Cagnard, N., Kierdorf, K., Prinz, M., Wu, B., Jacobsen, S.E., Pollard, J.W., *et al.* (2012). A lineage of myeloid cells independent of Myb and hematopoietic stem cells. Science *336*, 86-90.

Schulz, O., Jaensson, E., Persson, E.K., Liu, X., Worbs, T., Agace, W.W., and Pabst, O. (2009). Intestinal CD103+, but not CX3CR1+, antigen sampling cells migrate in lymph and serve classical dendritic cell functions. J Exp Med *206*, 3101-3114.

Schumann, A., Nutten, S., Donnicola, D., Comelli, E.M., Mansourian, R., Cherbut, C., Corthesy-Theulaz, I., and Garcia-Rodenas, C. (2005). Neonatal antibiotic treatment alters gastrointestinal tract developmental gene expression and intestinal barrier transcriptome. Physiol Genomics *23*, 235-245.

Scott, C.L., Aumeunier, A.M., and Mowat, A.M. (2011). Intestinal CD103+ dendritic cells: master regulators of tolerance? Trends Immunol *32*, 412-419.

Seiderer, J., Elben, I., Diegelmann, J., Glas, J., Stallhofer, J., Tillack, C., Pfennig, S., Jurgens, M., Schmechel, S., Konrad, A., *et al.* (2008). Role of the novel Th17 cytokine IL-17F in inflammatory bowel disease (IBD): upregulated

colonic IL-17F expression in active Crohn's disease and analysis of the IL17F p.His161Arg polymorphism in IBD. Inflamm Bowel Dis *14*, 437-445.

Serbina, N.V., Jia, T., Hohl, T.M., and Pamer, E.G. (2008). Monocyte-mediated defense against microbial pathogens. Annu Rev Immunol *26*, 421-452.

Serbina, N.V., and Pamer, E.G. (2006). Monocyte emigration from bone marrow during bacterial infection requires signals mediated by chemokine receptor CCR2. Nat Immunol *7*, 311-317.

Serbina, N.V., Shi, C., and Pamer, E.G. (2012). Monocyte-mediated immune defense against murine Listeria monocytogenes infection. Adv Immunol *113*, 119-134.

Seth, A., Yan, F., Polk, D.B., and Rao, R.K. (2008). Probiotics ameliorate the hydrogen peroxide-induced epithelial barrier disruption by a PKC- and MAP kinase-dependent mechanism. Am J Physiol Gastrointest Liver Physiol *294*, G1060-1069.

Shale, M., Schiering, C., and Powrie, F. (2013). CD4(+) T-cell subsets in intestinal inflammation. Immunol Rev *252*, 164-182.

Shi, C., and Pamer, E.G. (2011). Monocyte recruitment during infection and inflammation. Nat Rev Immunol *11*, 762-774.

Shortman, K., and Liu, Y.J. (2002). Mouse and human dendritic cell subtypes. Nat Rev Immunol *2*, 151-161.

Si, Y., Tsou, C.L., Croft, K., and Charo, I.F. (2010). CCR2 mediates hematopoietic stem and progenitor cell trafficking to sites of inflammation in mice. J Clin Invest *120*, 1192-1203.

Siddiqui, K.R., Laffont, S., and Powrie, F. (2010). E-cadherin marks a subset of inflammatory dendritic cells that promote T cell-mediated colitis. Immunity *32*, 557-567.

Smith, K., McCoy, K.D., and Macpherson, A.J. (2007). Use of axenic animals in studying the adaptation of mammals to their commensal intestinal microbiota. Semin Immunol *19*, 59-69.

Smith, P.D., Smythies, L.E., Shen, R., Greenwell-Wild, T., Gliozzi, M., and Wahl, S.M. (2011). Intestinal macrophages and response to microbial encroachment. Mucosal Immunol *4*, 31-42.

Smythies, L.E., Maheshwari, A., Clements, R., Eckhoff, D., Novak, L., Vu, H.L., Mosteller-Barnum, L.M., Sellers, M., and Smith, P.D. (2006). Mucosal IL-8 and TGF-beta recruit blood monocytes: evidence for cross-talk between the lamina propria stroma and myeloid cells. J Leukoc Biol *80*, 492-499.

Smythies, L.E., Sellers, M., Clements, R.H., Mosteller-Barnum, M., Meng, G., Benjamin, W.H., Orenstein, J.M., and Smith, P.D. (2005). Human intestinal macrophages display profound inflammatory anergy despite avid phagocytic and bacteriocidal activity. J Clin Invest *115*, 66-75.

Smythies, L.E., Shen, R., Bimczok, D., Novak, L., Clements, R.H., Eckhoff, D.E., Bouchard, P., George, M.D., Hu, W.K., Dandekar, S., and Smith, P.D. (2010). Inflammation anergy in human intestinal macrophages is due to Smad-induced IkappaBalpha expression and NF-kappaB inactivation. J Biol Chem *285*, 19593-19604.

Sokol, H., Pigneur, B., Watterlot, L., Lakhdari, O., Bermudez-Humaran, L.G., Gratadoux, J.J., Blugeon, S., Bridonneau, C., Furet, J.P., Corthier, G., *et al.* (2008). Faecalibacterium prausnitzii is an anti-inflammatory commensal bacterium identified by gut microbiota analysis of Crohn disease patients. Proc Natl Acad Sci U S A *105*, 16731-16736.

Sonnenberg, G.F., Monticelli, L.A., Alenghat, T., Fung, T.C., Hutnick, N.A., Kunisawa, J., Shibata, N., Grunberg, S., Sinha, R., Zahm, A.M., *et al.* (2012). Innate lymphoid cells promote anatomical containment of lymphoid-resident commensal bacteria. Science *336*, 1321-1325.

Spits, H., Artis, D., Colonna, M., Diefenbach, A., Di Santo, J.P., Eberl, G., Koyasu, S., Locksley, R.M., McKenzie, A.N., Mebius, R.E., *et al.* (2013). Innate lymphoid cells--a proposal for uniform nomenclature. Nat Rev Immunol *13*, 145-149.

Staniland, A.A., Clark, A.K., Wodarski, R., Sasso, O., Maione, F., D'Acquisto, F., and Malcangio, M. (2010). Reduced inflammatory and neuropathic pain and decreased spinal microglial response in fractalkine receptor (CX3CR1) knockout mice. J Neurochem.

Steinman, R.M., and Cohn, Z.A. (1973). Identification of a novel cell type in peripheral lymphoid organs of mice. I. Morphology, quantitation, tissue distribution. J Exp Med *137*, 1142-1162.

Stokes, C.R., Bailey, M., Heverson, K., Harris, C., Jones, P., Inman, C., Pie, S., oswald, I. P., Williams, B. A., Akkermans, A. D. L., Sowa, E., Rothkötter, H., Miller, B. (2004). Postnatal development of intestinal immune system in piglets: implications for the process of weaning. Anim. Res. *53*, 325-334.

Strachan, D.P. (1989). Hay fever, hygiene, and household size. BMJ *299*, 1259-1260.

Struyf, S., Van Collie, E., Paemen, L., Put, W., Lenaerts, J.P., Proost, P., Opdenakker, G., and Van Damme, J. (1998). Synergistic induction of MCP-1 and -2 by IL-1beta and interferons in fibroblasts and epithelial cells. J Leukoc Biol *63*, 364-372.

Suurmond, J., Stoop, J.N., Rivellese, F., Bakker, A.M., Huizinga, T.W., and Toes, R.E. (2013). Activation of human basophils by combined toll-like receptor- and FcepsilonRI-triggering can promote Th2 skewing of naive T helper cells. Eur J Immunol.

Suzuki, F., Kubota, T., Miyazaki, Y., Ishikawa, K., Ebisawa, M., Hirohata, S., Ogura, T., Mizusawa, H., Imai, T., Miyasaka, N., and Nanki, T. (2012). Serum level of soluble CX3CL1/fractalkine is elevated in patients with polymyositis

and dermatomyositis, which is correlated with disease activity. Arthritis Res Ther *14*, R48.

Suzuki, F., Nanki, T., Imai, T., Kikuchi, H., Hirohata, S., Kohsaka, H., and Miyasaka, N. (2005). Inhibition of CX3CL1 (fractalkine) improves experimental autoimmune myositis in SJL/J mice. J Immunol *175*, 6987-6996.

Tamoutounour, S., Henri, S., Lelouard, H., de Bovis, B., de Haar, C., van der Woude, C.J., Woltman, A.M., Reyal, Y., Bonnet, D., Sichien, D., *et al.* (2012). CD64 distinguishes macrophages from dendritic cells in the gut and reveals the Th1-inducing role of mesenteric lymph node macrophages during colitis. Eur J Immunol *42*, 3150-3166.

Taylor, M.D., Harris, A., Nair, M.G., Maizels, R.M., and Allen, J.E. (2006). F4/80+ alternatively activated macrophages control CD4+ T cell hyporesponsiveness at sites peripheral to filarial infection. J Immunol *176*, 6918-6927.

Testro, A.G., and Visvanathan, K. (2009). Toll-like receptors and their role in gastrointestinal disease. J Gastroenterol Hepatol *24*, 943-954.

Tlaskalova-Hogenova, H., Stepankova, R., Kozakova, H., Hudcovic, T., Vannucci, L., Tuckova, L., Rossmann, P., Hrncir, T., Kverka, M., Zakostelska, Z., *et al.* (2011). The role of gut microbiota (commensal bacteria) and the mucosal barrier in the pathogenesis of inflammatory and autoimmune diseases and cancer: contribution of germ-free and gnotobiotic animal models of human diseases. Cell Mol Immunol *8*, 110-120.

Tokuyama, H., Ueha, S., Kurachi, M., Matsushima, K., Moriyasu, F., Blumberg, R.S., and Kakimi, K. (2005). The simultaneous blockade of chemokine receptors CCR2, CCR5 and CXCR3 by a non-peptide chemokine receptor antagonist protects mice from dextran sodium sulfate-mediated colitis. Int Immunol *17*, 1023-1034.

Tsou, C.L., Haskell, C.A., and Charo, I.F. (2001). Tumor necrosis factor-alpha-converting enzyme mediates the inducible cleavage of fractalkine. J Biol Chem *276*, 44622-44626.

Tsou, C.L., Peters, W., Si, Y., Slaymaker, S., Aslanian, A.M., Weisberg, S.P., Mack, M., and Charo, I.F. (2007). Critical roles for CCR2 and MCP-3 in monocyte mobilization from bone marrow and recruitment to inflammatory sites. J Clin Invest *117*, 902-909.

Tsuboi, N., Yoshikai, Y., Matsuo, S., Kikuchi, T., Iwami, K., Nagai, Y., Takeuchi, O., Akira, S., and Matsuguchi, T. (2002). Roles of toll-like receptors in C-C chemokine production by renal tubular epithelial cells. J Immunol *169*, 2026-2033.

Turnbull, E.L., Yrlid, U., Jenkins, C.D., and Macpherson, G.G. (2005). Intestinal dendritic cell subsets: differential effects of systemic TLR4 stimulation on migratory fate and activation in vivo. J Immunol *174*, 1374-1384.

Ueda, Y., Kayama, H., Jeon, S.G., Kusu, T., Isaka, Y., Rakugi, H., Yamamoto, M., and Takeda, K. (2010). Commensal microbiota induce LPS hyporesponsiveness in colonic macrophages via the production of IL-10. Int Immunol *22*, 953-962.

Umehara, H., Bloom, E.T., Okazaki, T., Nagano, Y., Yoshie, O., and Imai, T. (2004). Fractalkine in vascular biology: from basic research to clinical disease. Arterioscler Thromb Vasc Biol *24*, 34-40.

van der Flier, L.G., and Clevers, H. (2009). Stem cells, self-renewal, and differentiation in the intestinal epithelium. Annu Rev Physiol *71*, 241-260.

van Furth, R., and Cohn, Z.A. (1968). The origin and kinetics of mononuclear phagocytes. J Exp Med *128*, 415-435.

van Furth R, C.Z., Hirsch JG, Humphrey JH, Spector WG, Langevoort HL. (1972). The mononuclear phagocyte system: a new classification of

macrophages, monocytes, and their precursor cells. Bull World Health Organ. *46*, 845-852.

van Wijk, F., and Cheroutre, H. (2009). Intestinal T cells: facing the mucosal immune dilemma with synergy and diversity. Semin Immunol *21*, 130-138.

Varol, C., Landsman, L., Fogg, D.K., Greenshtein, L., Gildor, B., Margalit, R., Kalchenko, V., Geissmann, F., and Jung, S. (2007). Monocytes give rise to mucosal, but not splenic, conventional dendritic cells. J Exp Med *204*, 171-180.

Varol, C., Vallon-Eberhard, A., Elinav, E., Aychek, T., Shapira, Y., Luche, H., Fehling, H.J., Hardt, W.D., Shakhar, G., and Jung, S. (2009a). Intestinal lamina propria dendritic cell subsets have different origin and functions. Immunity *31*, 502-512.

Varol, C., Yona, S., and Jung, S. (2009b). Origins and tissue-context-dependent fates of blood monocytes. Immunol Cell Biol *87*, 30-38.

Velilla, P.A., Rugeles, M.T., and Chougnet, C.A. (2006). Defective antigen-presenting cell function in human neonates. Clin Immunol *121*, 251-259.

Videla, S., Vilaseca, J., Guarner, F., Salas, A., Treserra, F., Crespo, E., Antolin, M., and Malagelada, J.R. (1994). Role of intestinal microflora in chronic inflammation and ulceration of the rat colon. Gut *35*, 1090-1097.

Vivier, E., Raulet, D.H., Moretta, A., Caligiuri, M.A., Zitvogel, L., Lanier, L.L., Yokoyama, W.M., and Ugolini, S. (2011). Innate or adaptive immunity? The example of natural killer cells. Science *331*, 44-49.

Vivier, E., Tomasello, E., Baratin, M., Walzer, T., and Ugolini, S. (2008). Functions of natural killer cells. Nat Immunol *9*, 503-510.

Walker, J.A., Barlow, J.L., and McKenzie, A.N. (2013). Innate lymphoid cells--how did we miss them? Nat Rev Immunol *13*, 75-87.

Wang, Y., Szretter, K.J., Vermi, W., Gilfillan, S., Rossini, C., Cella, M., Barrow, A.D., Diamond, M.S., and Colonna, M. (2012). IL-34 is a tissue-restricted ligand of CSF1R required for the development of Langerhans cells and microglia. Nat Immunol *13*, 753-760.

Worbs, T., Bode, U., Yan, S., Hoffmann, M.W., Hintzen, G., Bernhardt, G., Forster, R., and Pabst, O. (2006). Oral tolerance originates in the intestinal immune system and relies on antigen carriage by dendritic cells. J Exp Med *203*, 519-527.

Wu, H.J., Ivanov, II, Darce, J., Hattori, K., Shima, T., Umesaki, Y., Littman, D.R., Benoist, C., and Mathis, D. (2010). Gut-residing segmented filamentous bacteria drive autoimmune arthritis via T helper 17 cells. Immunity *32*, 815-827.

Wynn, T.A., Chawla, A., and Pollard, J.W. (2013). Macrophage biology in development, homeostasis and disease. Nature *496*, 445-455.

Yamamoto, M., Sato, S., Hemmi, H., Uematsu, S., Hoshino, K., Kaisho, T., Takeuchi, O., Takeda, K., and Akira, S. (2003). TRAM is specifically involved in the Toll-like receptor 4-mediated MyD88-independent signaling pathway. Nat Immunol *4*, 1144-1150.

Yona, S., Jung, S. (2009). Monocytes: Subsets, origins, fates and functions. Current Opinion in Hematology *16*, 000-000.

Yoshida, H., Hayashi, S., Kunisada, T., Ogawa, M., Nishikawa, S., Okamura, H., Sudo, T., and Shultz, L.D. (1990). The murine mutation osteopetrosis is in the coding region of the macrophage colony stimulating factor gene. Nature *345*, 442-444.

Yrlid, U., Cerovic, V., Milling, S., Jenkins, C.D., Zhang, J., Crocker, P.R., Klavinskis, L.S., and MacPherson, G.G. (2006). Plasmacytoid dendritic cells do not migrate in intestinal or hepatic lymph. J Immunol *177*, 6115-6121.

Zigmond, E., and Jung, S. (2013). Intestinal macrophages: well educated exceptions from the rule. Trends Immunol *34*, 162-168.

Zimmerman, N.P., Vongsa, R.A., Wendt, M.K., and Dwinell, M.B. (2008). Chemokines and chemokine receptors in mucosal homeostasis at the intestinal epithelial barrier in inflammatory bowel disease. Inflamm Bowel Dis *14*, 1000-1011.

Zlotnik, A., and Yoshie, O. (2000). Chemokines: a new classification system and their role in immunity. Immunity *12*, 121-127.